ISSN: 2456-1878

International Journal of Environment Agriculture and Biotechnology

(IJEAB)

An open access Peer-Reviewed InternationalJournal

DOI: 10.22161/ijeab.112

Vol.- 11 | Issue - 2 | Mar-Apr 2026

editor.ijeab@gmail.com | editor@ijeab.com | https://www.ijeab.com/

International Journal of Environment, Agriculture and Biotechnology

(ISSN: 2456-1878)

DOI: 10.22161/ijeab

Vol-11, Issue-2

March - April, 2026

Editor in Chief

Dr. Pietro Paolo Falciglia

Publisher

Infogain Publication

Email: editor.ijeab@gmail.com ; editor@ijeab.com

Web: www.ijeab.com

FOREWORD

I am honoured to introduce this latest issue to the International Journal of Environment, Agriculture and Biotechnology (IJEAB). Our journal is dedicated to disseminating high-quality research and innovative findings that contribute to advancing knowledge in these critical fields.

In this issue, we present a collection of papers that exemplify the diversity and depth of contemporary environmental, agriculture, and biotechnology research. The articles include various topics, from sustainable agricultural practices and environmental conservation strategies to cutting-edge biotechnological innovations. Each contribution has undergone a rigorous peer-review process, ensuring the publication of only the most significant and original research.

Our commitment at IJEAB is to provide a robust platform for researchers, academicians, and practitioners to share their work and engage with a global audience. By fostering an interdisciplinary approach, we aim to bridge the gaps between different areas of study and promote holistic understanding and solutions to the challenges we face in these domains.

We are grateful to our dedicated authors, whose hard work and intellectual rigour are the backbone of our journal. We also extend our appreciation to our reviewers and editorial board members, whose expertise and diligence ensure the high standards of our publication. Finally, we thank our readers for their continued support and engagement.

We hope you find the articles insightful and inspiring as you explore this issue. We encourage you to contribute your research to future issues and join us in our mission to advance knowledge and drive positive change in the environment, agriculture, and biotechnology fields.

Sincerely,
Editor-in-Chief
International Journal of Environment, Agriculture and Biotechnology (IJEAB)
NAAS Score Journal
www.ijeab.com

International Editorial Board/ Reviewer Board

Vol-11, Issue-2, March - April, 2026
(DOI: 10.22161/ijeab.112)

International Journal of Environment, Agriculture and Biotechnology
Vol-11, Issue-2; Mar-Apr, 2026
Peer-Reviewed International Journal
Journal Home Page Available: https://ijeab.com/
Journal DOI: 10.22161/ijeab

Mapping and Spatiotemporal Evolution Analysis of Salinity Water Mass Structure Characteristics at the Pearl River Estuary—A Framework Coupling Multi-Source Remote Sensing Information from GEE with Machine Learning Methods

Haoxian Liang, Zhiying Cheng, Xuantao Liu, Daxiang Cai, Yongjun He, Zhe Zhu, Ruei-Yuan Wang*

School of Sciences, Guangdong University of Petrochem Technology (GDUPT), Maoming 525000, China (Corresponding author: Ruei-Yuan Wang)

Received: 17 Jan 2026; Received in revised form: 19 Feb 2026; Accepted: 25 Feb 2026; Available online: 04 Mar 2026

***Abstract*— *The distribution and variation of salinity in estuarine regions serve as a critical foundation for understanding the evolution of coastal ecosystems. However, obtaining long-term, continuous in-situ salinity data in estuarine areas with complex hydrodynamics and limited observational conditions poses significant challenges. To address this, this study focuses on the Pearl River Estuary (PRE), utilizing multi-source remote sensing data from 2015 to 2025 on the Google Earth Engine (GEE) platform to develop an unsupervised machine learning framework driven by multi-dimensional features. The framework aims to identify water mass structures closely associated with salinity distribution and their spatiotemporal evolution characteristics. The proposed method integrates multiple features, including Landsat 8-derived Total Suspended Solids (TSS), Colored Dissolved Organic Matter (CDOM), Normalized Difference Chlorophyll Index (NDCI), as well as Sentinel-1 backscatter coefficients $\sigma^0$and Digital Elevation Model (DEM) data. It employs K-means clustering and XGBoost-SHAP analysis to classify surface water features and assess contributing factors. The results statistically delineate three typical water mass structures: freshwater-dominated, seawater-dominated, and their transitional mixtures, revealing significant interannual variability over a decade. The observed trends correlate with runoff conditions in the Pearl River Basin and regional hydroclimatic factors. Notably, during the extreme drought years of*

2021–2022, the marked expansion of seawater-dominated water masses validated the model's sensitivity to structural adjustments in water masses. This study demonstrates that, in the absence of long-term in-situ data, the fusion of multi-source remote sensing and unsupervised machine learning methods can effectively identify the relative spatiotemporal evolution of salinity-related water mass structures in estuaries. It offers a feasible, low-cost approach for studying salinity dynamics in large estuaries and supporting regional water environment management.

Keywords*— *The Pearl River Estuary (PRE); K-means Clustering; Water Mass Structure; XGBoost-SHAP; Google Earth Engine (GEE) ; Machine Learning (ML)

I. INTRODUCTION

As a sensitive zone of land-sea interaction, estuarine salinity is a key physical oceanographic parameter that profoundly influences hydrochemical processes and ecosystem structure. The Pearl River Estuary (PRE), a vital economic hub in southern China and one of the world's most complex estuarine systems, exemplifies this. Understanding the spatiotemporal dynamics of salinity here—particularly its long-term trends and interannual variations—is crucial. Such knowledge is foundational for assessing the impacts of climate change and human activities (e.g., large-scale upstream water projects, rapid urbanization, and coastal engineering) and for formulating effective environmental management strategies to support regional sustainable development.

Traditional salinity monitoring methods, such as fixed-point observations and underway measurements, can provide accurate data. However, in vast and hydrologically complex areas like the PRE, achieving large-scale, long-term synchronous observations is challenging (Nechad et al., 2010), making it difficult to capture multi-scale dynamics comprehensively while also being cost-prohibitive. Remote sensing technology, with its macroscopic, periodic, and cost-effective advantages, offers a powerful alternative for monitoring estuarine parameters. Yet, individual remote sensing features have limitations in complex estuaries. Optical indicators (e.g., TSS, CDOM), while useful for tracing terrestrial inputs, are often obstructed by clouds and rain and have difficulty differentiating between high-turbidity seawater and freshwater runoff (Doxaran et al., 2002). Conversely, microwave indicators (e.g., SAR backscatter σ^0) enable all-weather observation and reflect surface roughness but are susceptible to contamination from transient wind fields (Gade et al., 1998; Pichel & Clemente-Colón, 2000). Previous studies have largely focused on using single-source remote sensing data for parameter inversion or short-term analysis, and research on the PRE is no exception (Feng & He, 2025). However, a significant research gap remains in the long-term, continuous assessment of salinity dynamics. In the absence of long-term, synchronous in situ data for model training, overcoming the limitations of single data sources to reconstruct the interannual variability and long-term trends of estuarine salinity remains a major challenge.

To address the challenges outlined above, this study proposes an unsupervised classification strategy based on multi-source remote sensing information fusion. The aim is to construct a multidimensional complementary framework that integrates optical components, microwave texture, and topographic constraints. This framework innovatively combines remote sensing parameters governed by different physical mechanisms: Total Suspended Solids (TSS) and the Blue-Green Ratio (BGR), a proxy for Colored Dissolved Organic Matter (CDOM), to trace material sources; Synthetic Aperture Radar (SAR) backscatter σ⁰ to capture hydrodynamic states; and the Normalized Difference Chlorophyll Index (NDCI) to reflect ecological responses. Digital Elevation Model (DEM) data is incorporated for geospatial constraint. The fusion of these multi-physical-mechanism inputs is designed to enhance the robustness and accuracy of an unsupervised clustering algorithm (K-means) in identifying the freshwater-seawater-brackish water ternary structure, thereby mitigating uncertainties inherent in single-source data.

Applying this approach, the study processes multi-source remote sensing datasets for the PRE across wet and dry seasons from 2015 to 2025. By performing machine learning-based cluster analysis on the multidimensional feature space and assigning salinity labels (high, medium, low) based on the multi-year average σ⁰ characteristics, we reconstruct the spatiotemporal evolution of the estuary's water mass structure. The study further quantitatively analyzes its response mechanisms to extreme hydrometeorological events (e.g., droughts and floods). Our findings aim to (1) validate the applicability of multi-source remote sensing fusion for monitoring complex estuarine environments, and (2) provide a scientific basis for understanding the long-term response of the Greater Bay Area's aquatic environment to regional hydrological and climatic changes.

II. STUDY AREA AND DATA

2.1 Study Area

This study focuses on the PRE, the research area. Located south of the Guangdong-Hong Kong-Macao Greater Bay Area, it spans approximately 113.5°E–113.9°E in longitude and 22.0°N–23.2°N in latitude. This region is a critical zone where the Pearl River system converges and discharges into the South China Sea, encompassing diverse coastal landforms, including estuaries, bays, and open waters (Figure 1). Salinity dynamics in the PRE are governed by the complex interplay of multiple factors:

- Riverine Discharge: Seasonal variations in freshwater input from the Pearl River directly alter nearshore salinity.
- Tidal Effects: The periodic ebb and flow continuously drive the mixing and exchange of seawater and freshwater.
- Precipitation: Rainfall affects river discharge, thereby modulating the dilution of seawater.
- Ocean Currents: Their dynamics influence the influx and diffusion of high-salinity offshore waters.

Due to this intricate interplay, salinity exhibits highly complex spatiotemporal variations. Therefore, developing and applying long-term monitoring and analysis methods is crucial for understanding the underlying mechanisms.

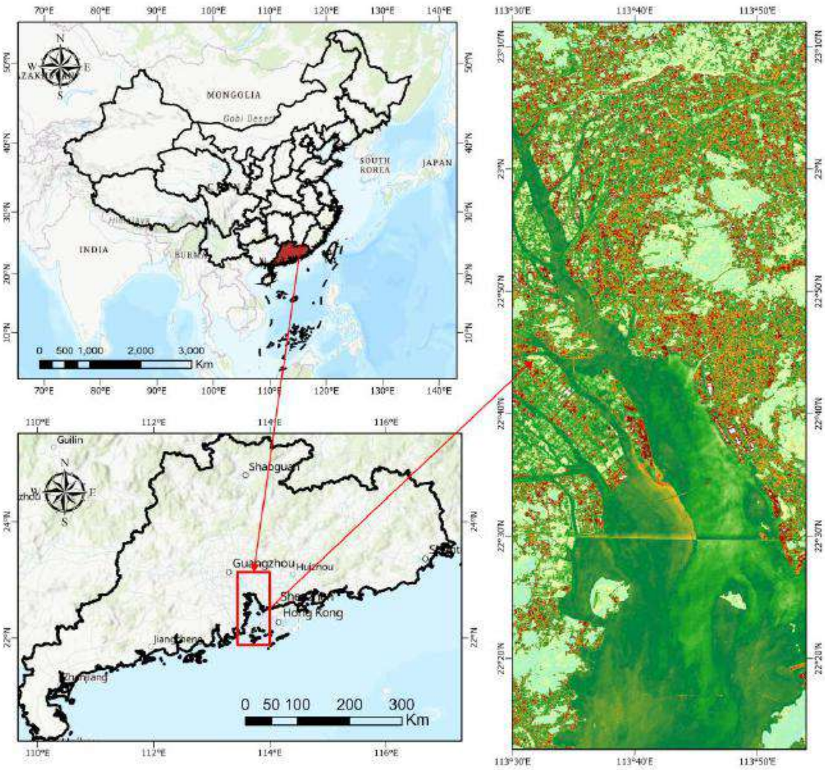

Figure 1 Map of the Study Area at the Pearl River Estuary

2.2 Data Sources and Preprocessing

The study utilizes multi-source remote sensing data, including:

(1) Optical indicators: Total Suspended Solids (TSS) and the Blue-Green Ratio (BGR), the latter serving as a proxy for Colored Dissolved Organic Matter (CDOM).

(2) Microwave indicator: Sentinel-1 C-band VV polarization backscatter coefficient σ^0

(3) Topographic data: Shuttle Radar Topography Mission (SRTM)/ (DEM).

(4) Ecological indicator: Normalized Difference Chlorophyll Index (NDCI).

The temporal coverage spans ten hydrological years, from 2015-2016 to 2024-2025, to capture decadal salinity variations.

All data products were preprocessed on the Google Earth Engine (GEE) platform. Key steps included filtering, core computation, and geometric correction, with all data standardized to the WGS84 coordinate system. This preprocessing pipeline aimed to resolve inter-sensor geometric discrepancies, thereby generating a spatially aligned, annual composite feature dataset that provides a consistent and physically meaningful foundation for the subsequent unsupervised clustering analysis of water mass structures.

2.2.1. Total Suspended Solids (TSS)

TSS refers to solid particles suspended in water bodies, originating from terrestrial inputs, sediment resuspension, and biological activities (Xing et al., 2013). In estuaries, TSS is closely associated with sediment loads from freshwater runoff. Consequently, high-TSS zones often correspond to low-salinity waters, and TSS distribution indirectly reflects salinity structures due to the influence of fronts and water mass mixing on sediment transport.

The remote sensing retrieval of TSS leverages the strong correlation between TSS concentration and red-band reflectance. This is because suspended particles enhance light scattering in the visible spectrum, leading to a significant increase in reflectance around 620–680 nm. Within moderate concentration ranges, this relationship is approximately linear, which allows for empirical modeling.

This study retrieved TSS using Landsat 8 OLI/TIRS Collection 2 Tier 1 TOA (Top-of-Atmosphere) reflectance products (LANDSAT/LC08/C02/T1_TOA) from the GEE platform. An empirical linear model was applied to the red band (Band 4):

$$TSS(mg/L)=a\times Band4+b \qquad (1)$$

where: TSS is the dry-weight concentration of suspended particles (diameter > 2 μm) in milligrams per liter. Band4 is the unit less TOA reflectance of Landsat 8 Band 4, typically ranging from 0 to 1. a is the model slope, representing the estimated increase in TSS per unit increase in reflectance, which indicates the band's sensitivity to TSS. b is the intercept, which accounts for baseline conditions and model error.

2.2.2 CDOM and BGR

Colored Dissolved Organic Matter (CDOM) is the light-absorbing component of dissolved organic matter in coastal and estuarine waters, primarily originating from terrestrial inputs and the degradation of aquatic organisms (Stedmon et al., 2006). Its core optical property is strong absorption of short-wavelength blue light, with relatively weak absorption in the green spectrum (Sathyendranath, 2000). This differential absorption forms the basis for using the BGR as a reliable optical proxy for CDOM (O'Reilly et al., 1998). An increase in CDOM concentration enhances blue-light absorption, decreasing reflectance in the blue band while green-band reflectance remains more stable, thereby lowering the BGR. Conversely, a decrease in CDOM leads to a higher BGR. The BGR is thus inversely related to CDOM concentration.

In estuarine environments, CDOM often exhibits conservative mixing behavior, meaning its concentration is inversely correlated with salinity. Consequently, spatial patterns of BGR can serve as an indirect tracer for salinity structure, with lower BGR values typically observed in CDOM-rich, low-salinity nearshore waters, and higher BGR in diluted offshore waters.

Furthermore, BGR is crucial for improving the accuracy of chlorophyll retrievals in optically complex Case 2 waters (e.g., estuaries). In such waters, CDOM absorption interferes with chlorophyll fluorescence signals. BGR-based correction helps separate the optical contributions of CDOM and chlorophyll, mitigating this interference. Given the robust inverse relationship between CDOM and BGR, various remote sensing algorithms have been developed, including empirical (e.g., band ratio), semi-analytical (e.g., QAA-CDOM), and machine learning models. For its simplicity and proven effectiveness, the empirical band-ratio approach is widely employed.

In estuarine areas strongly influenced by freshwater discharge, such as the PRE, CDOM often behaves as a conservative tracer. During the mixing of CDOM-rich, low-salinity runoff with low-CDOM, high-salinity offshore waters, CDOM concentration exhibits a strong inverse relationship with salinity (Bowers et al., 2004; Højerslev et al., 1996). Studies specific to the PRE have confirmed that CDOM optical properties can effectively trace water mass origins and mixing processes (Xing et al., 2013). Consequently, the spatial pattern of the BGR, as an optical proxy for CDOM, can indirectly indicate the position and structure of salinity fronts, providing a statistically robust foundation in physical oceanography.

This study utilized Landsat 8 OLI/TIRS Collection 2 Tier 1 TOA reflectance products. The standard BGR index was calculated as the ratio of reflectance in the blue band (B2) to the green band (B3):

$$BGR= B2/ B3 \qquad (2)$$

Since CDOM concentration is inversely related to BGR (higher CDOM → lower BGR), we applied a reciprocal transformation (1/BGR)to generate a positive proxy index for relative CDOM abundance. This transformation ensures that higher index values correspond intuitively to greater CDOM concentrations (and thus stronger terrestrial influence), facilitating subsequent visualization and analysis.

2.2.3 Synthetic Aperture Radar (SAR) Backscatter σ^0

The backscattering coefficient (σ^0) from Synthetic Aperture Radar (SAR) quantifies the intensity of microwave energy returned from the sea surface. It is primarily governed by surface roughness at the scale of the radar wavelength (Klemas, 2012), which is influenced by wind fields, surface currents, waves, and the physicochemical properties of the water surface layer (e.g., surface tension, dielectric constant). Salinity can indirectly modulate σ^0 by altering these surface properties. It affects the water's dielectric constant and surface tension. More dynamically, it can influence hydrodynamic processes at salinity fronts—such as current shear and internal wave breaking—that generate small-scale roughness. Consequently, spatial variations in σ^0 can serve as an indicator of the boundaries or mixing zones between different water masses.

This study utilized the Sentinel-1 Ground Range Detected (GRD) product from the European Space Agency's Copernicus program (COPERNICUS/S1_GRD). The VV (Vertical-Vertical) polarization mode was selected for its sensitivity to water surface characteristics.

2.2.4 Digital Elevation Model (DEM)

The DEM was used to construct the topographic framework of the study area and to precisely delineate the land-water boundary. This is a critical preprocessing step for ensuring the analysis is confined to the marine domain. A spatial mask was applied based on an elevation threshold, retaining only pixels with elevations ≤ 0 meters (i.e., sea level and below) to define the valid marine analysis area. The DEM thus provides the foundational topographic context for all subsequent spatial analyses.

This study utilized the CGIAR-CSI SRTM version 4.1 product (CGIAR/SRTM90_V4) with a spatial resolution of approximately 90 meters to establish this static topographic baseline.

2.2.5 Normalized Difference Chlorophyll Index (NDCI)

The NDCI is a widely used remote sensing index for estimating chlorophyll-a concentration, serving as a proxy for phytoplankton biomass. In estuarine ecosystems, phytoplankton distribution and abundance are regulated by a suite of environmental factors, including salinity, nutrient availability, and light conditions. Salinity, in particular, can structure phytoplankton communities and their biomass across different gradients. Consequently, the spatial pattern of NDCI can provide an indirect signature of ecological zones that are influenced or delineated by salinity.

This study calculated NDCI using Landsat 8 OLI/TIRS Collection 2 Tier 1 TOA reflectance products. The index is derived from the near-infrared (NIR, Band 5) and red (Band 4) bands as follows:

$$NDCI = \frac{R_{NIR}-R_{Red}}{R_{NIR}+R_{Red}} \quad (3)$$

where R_{NIR} and R_{Red} are the reflectance values of Landsat 8 Band 5 and Band 4, respectively.

III. METHODOLOGY

This section outlines the core methodological framework for processing multi-source remote sensing data, performing K-means clustering, identifying salinity-based water mass features, and analyzing driving factors across a decadal hydrological time series. The overall workflow, illustrated in Figure 2, comprises three sequential stages.

Stage 1: Data Acquisition and Preparation. Multi-source remote sensing data, including TSS, the BGR as a proxy for CDOM, the Sentinel-1 C-band VV polarization backscatter coefficient (σ^0), the DEM, and the NDCI, were acquired and preprocessed on the GEE platform.

Stage 2: Spatial Delineation and Clustering. The water body extent of the study area was first precisely delineated using the DEM. Subsequently, the K-means clustering algorithm was applied to partition the preprocessed multidimensional feature space into distinct groups.

Stage 3: Spatiotemporal and Causal Analysis. The clustering results were analyzed to characterize the interannual evolution of the estuarine system. This analysis encompassed (i) the spatial distribution patterns of the identified water mass features, (ii) the proportional area and variability of dominant water types, and (iii) the investigation of potential environmental driving factors. This three-stage workflow establishes the methodological foundation for the multi-decadal temporal sequence analysis that follows.

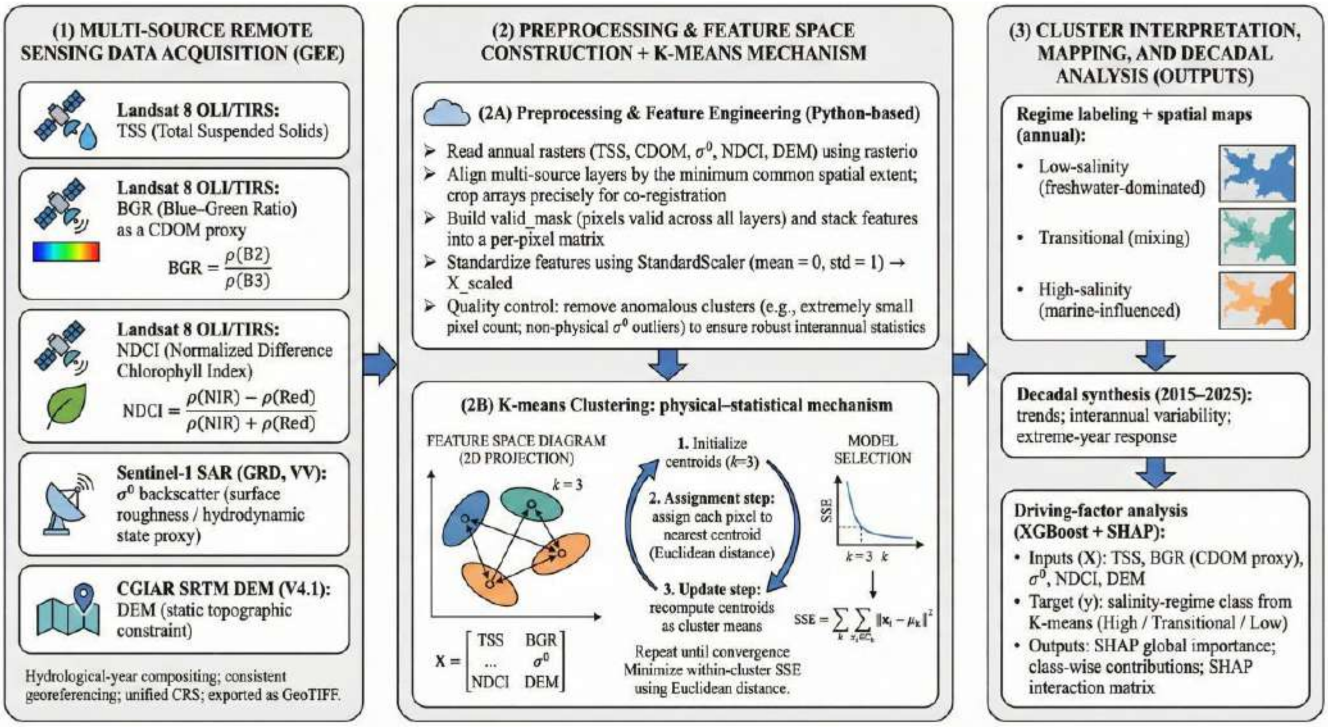

Fig.2 The Framework of the Study

3.1 Data Processing and Feature Extraction

All data integration and preprocessing were performed using Python. First, annual raster data for TSS, CDOM (1/BGR), σ^0, NDCI, and DEM were read using the rasterio library. The minimum common spatial extent across all data layers was determined by comparing their dimensions. Each raster array was then precisely cropped to this common extent to achieve precise spatial registration.

Next, a valid data mask (valid_mask) was generated to identify pixels containing valid values in all five data layers. Using this mask, the corresponding valid pixel values were extracted from each layer and column-wise stacked into a unified array using numpy.stack. This constructed the annual feature matrix, where each row represents a valid pixel and the five columns correspond to the five remote sensing features. To eliminate scale differences among features, the matrix was standardized using StandardScaler, transforming each feature column to a distribution with zero mean and unit standard deviation, resulting in the standardized feature matrix (X_scaled) for subsequent clustering.

A pixel-based quality control step was implemented to ensure the robustness of the annual clustering statistics. This process identified anomalous clusters, specifically those containing an extremely low number of pixels (fewer than 1,000) or exhibiting non-physical mean σ^0 values (>500 dB) for the 2021–2022 hydrological year. These anomalies were attributed to sensor noise or processing edge effects. Consequently, such abnormal clusters were entirely excluded from the downstream interannual trend analysis to preserve the geographical rationality of the statistical results.

3.2 Water Mass Structure Identification and Physical Feature Analysis

3.2.1 The Spatial Constraint Effect of DEM on Clustering Samples

To confine the clustering analysis to the marine environment, the water area was first delineated using the DEM. During preprocessing, a spatial mask was applied based on an elevation threshold, retaining only pixels with elevations ≤ 0 meters (i.e., at or below sea level) to define the valid marine analysis area. Multi-source remote sensing features were then extracted exclusively from within this masked region for subsequent clustering. This step prevented category bias from the inclusion of terrestrial pixels, ensuring that the clustering results accurately reflect the spatial differentiation characteristics of marine water bodies.

3.2.2. Definition and Physical Basis of the Estuarine Water Mass Structure

The Estuarine Salinity-Related Water Mass Structure is defined as surface water functional zones exhibiting relatively uniform optical and microwave scattering characteristics, formed under the dynamic processes of an estuary. Its theoretical foundation lies in the Three-Sector Model of physical oceanography (Nayak & Noronha e D'Mello, 2018; Zhang et al., 2009), which classifies estuaries longitudinally into three characteristic sectors (Figure 3): the Upper Estuary (river-dominated), the Middle Estuary (transitional, influenced by both river flow and tides), and the Lower Estuary (freely connected to the open sea). This model captures the fundamental land-to-sea gradients in salinity and material transport.

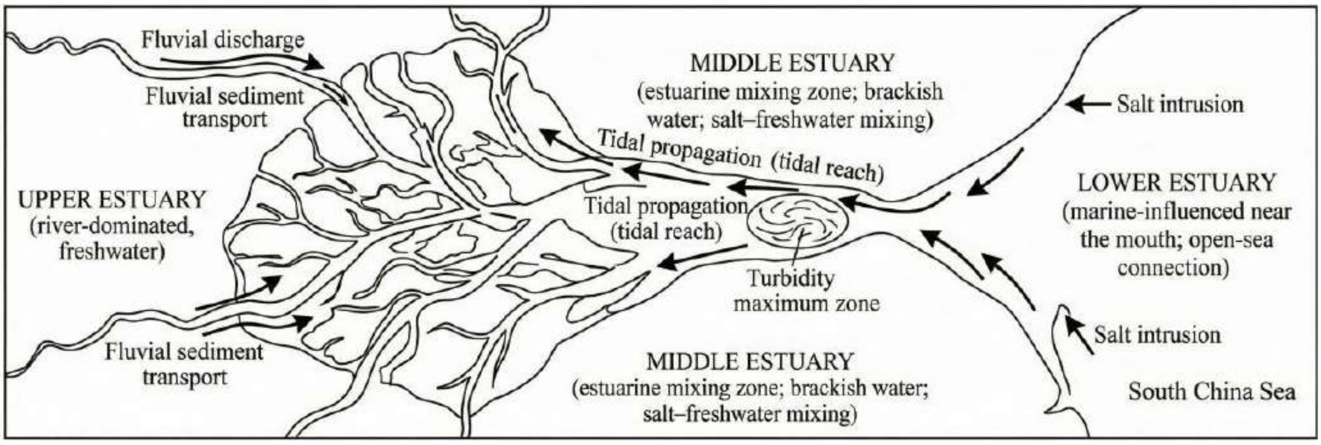

Fig.3 Schematic Illustration of the Three-stage Structure (adapted from Nayak & Noronha e D'Mello, 2018)

The applicability of this tripartite model to the PRE is well-established. For instance, Yin et al. (2004) explicitly divided the PRE nearshore waters into the inner, middle, and outer estuary/adjacent coastal areas. Similarly, studies on phytoplankton community ecology and the Turbidity Maximum Zone (TMZ) within the PRE have adopted this regional division to assess ecological characteristics (Chen et al., 2023; Wai et al., 2004), confirming its utility for structuring analyses of this complex system.

Estuarine mixing can be conceptualized through End-Member Theory as a spatiotemporal distribution involving two primary end-members—freshwater (runoff) and seawater (open ocean background)—and their mixed products. This study employs the K-means unsupervised clustering algorithm to identify the signatures of these three physical entities within a multidimensional remote sensing feature space (integrating optical and microwave backscatter properties). The objective is to construct a ternary model representing: "Runoff Plume" – "Frontal Mixing Zone" – "Seawater-Dominated Region".

The three characteristic water masses are defined as follows:

(1) Freshwater-Dominated Water Mass: Corresponds to the core of the runoff plume. It is characterized by high terrestrial inputs (elevated TSS and CDOM) and strong hydrodynamics, leading to high SAR backscatter. This mass is the primary physical carrier of low-salinity characteristics.

(2) Seawater-Dominated Water Mass: Represents the saline, open-shelf background water. It is characterized by relatively clear waters (low TSS/CDOM) and calm surface conditions, resulting in stable, low backscatter.

(3) Mixed Transitional Water Mass: Occupies the frontal mixing zone between the two end-members, where riverine and tidal forces interact intensely. Its optical and physical properties are intermediate, making it a key indicator region for delineating the salinity front.

It is crucial to emphasize that this study does not directly invert or quantitatively estimate absolute salinity. Instead, it performs an unsupervised classification of PRE waters based on statistical similarities in multi-source remote sensing features. Although salinity is not directly measured, the three water masses exhibit statistically stable, covarying differences in water color, hydrodynamics, and surface roughness that correspond to the underlying salinity gradient. Therefore, the classification effectively delineates the salinity-related spatial zoning of the estuary.

3.2.3 Determination of the Number of Clusters K in K-Means

To achieve automated identification of water mass structures, this study employs the K-means clustering algorithm to partition the multidimensional feature space. The core objective of this algorithm is to iteratively minimize the Sum of Squared Errors (SSE) within clusters, calculated as follows:

$$J = \sum_{j=1}^{K} \sum_{x_i \in C_j} ||x_i - \mu_j||^2 \qquad (4)$$

Here, Cj represents the j-th cluster and μj its centroid. This study employed Euclidean distance to measure similarity in a four-dimensional feature space (TSS, CDOM proxy, σ^0, NDCI) and adopted a dual-validation strategy combining statistical metrics with physical oceanographic significance to determine the optimal K.

Statistical analysis of the 2015–2025 data (Figure 4) shows that the Sum of Squared Errors (SSE) decreases monotonically with increasing K, with a critical inflection point at K=3. The average SSE drops sharply by approximately 49.36% as Kincreases from 1 to 3, indicating that the model rapidly captures the primary variance. In contrast, the reduction narrows to 39.88% for K=3to 5, demonstrating a significant decline in the marginal explanatory gain.

To ensure physical plausibility, the K=2 and K=4 schemes were evaluated and rejected (Table 1). The K=2 scheme identifies only the two end-members (freshwater- and seawater-dominated), failing to resolve the critical mixed transitional water mass that represents dynamic frontal processes. The K=4 scheme introduces an additional category that manifests as a redundant subdivision of the seawater-dominated mass (e.g., splitting the same high-salinity water into two subclasses with σ^0 differences <1 dB), which lacks clear physical justification and complicates long-term comparison.

Therefore, the K=3 scheme is optimal. It aligns with the statistical elbow point where the SSE reduction rate sharply declines and corresponds precisely to the physically meaningful ternary structure ("runoff plume – frontal mixing – seawater dominance"), providing a robust foundation for subsequent spatiotemporal analysis.

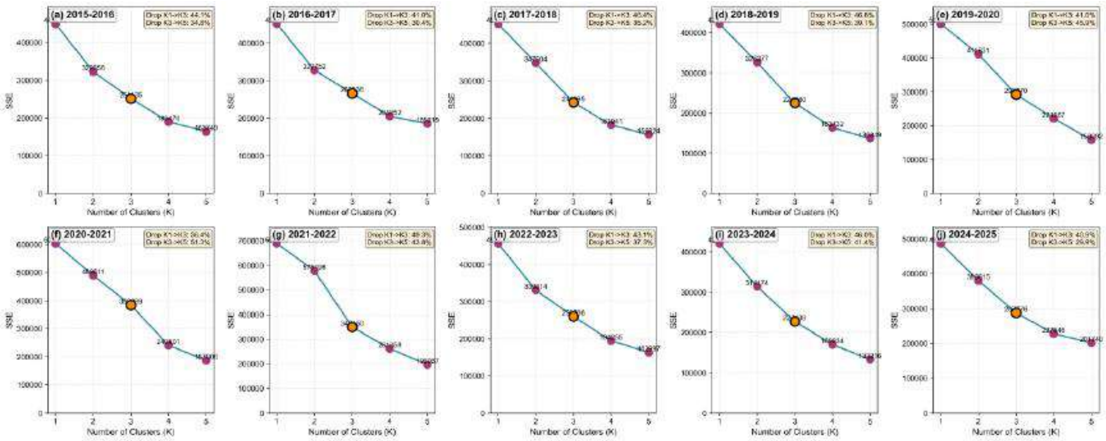

Fig.4 Elbow Method Results for Annual Clustering (2015–2025)

(From left to right, the first row represents the years 2015–2020, and the second row represents the years 2021–2025.)

Table 1 Evaluation of K-means Clustering Performance and Physical Interpretability for Different Numbers of Clusters.

Number of clusters (K)	SSE behavior	Physical interpretation	Assessment
K = 2	Sharp decrease with pronounced elbow	Distinguishes terrestrial input from offshore background only	Oversimplified; fails to resolve estuarine mixing front
K = 3	Slope markedly reduced; high explanatory power	Freshwater-dominated, mixing transition, and marine-dominated regimes	Consistent with classical estuarine tripartite structure; optimal configuration
K = 4	SSE curve approaches plateau	Subdivides mixing zone into high-/low-turbidity sub-regions	Category redundancy; not suitable for long-term interannual comparison

3.2.4 The Role of SARσ^0 in Water Mass Identification

In this study, the Sentinel-1 C-band VV-polarized backscattering coefficient σ^0 is not used as a direct proxy for salinity. Instead, it serves as a key physical descriptor of surface hydrodynamic state and roughness. Within the PRE, water masses with different properties are associated with distinct dynamic regimes:

(1) Freshwater-dominated water masses are typically influenced by strong tidal currents and riverine discharge, generating complex surface turbulence.

(2) Seawater-dominated water masses are primarily modulated by regional wind fields, often resulting in a relatively smoother surface.

These differences in surface dynamics modulate the microscale roughness of the water surface, which in turn governs the intensity of SAR backscatter. Therefore, σ^0 is utilized here to aid in distinguishing water masses based on their hydrodynamic characteristics.

It is crucial to note that the linkage between σ^0 and salinity distribution is one of statistical covariance rather than direct physical causation or quantitative correspondence. The inclusion of the σ^0 feature provides an independent, physically based constraint for the unsupervised clustering, effectively complementing the optical water-color information (TSS, CDOM, NDCI) and enhancing the robustness of the ternary water mass classification.

3.2.5 Labeling Water Masses Based on Long-Term Statistical Signatures

In the absence of concurrent in situ salinity data, this study adopts a consistency labeling strategy based on multi-year statistical signatures to identify the relative position of each cluster along the estuarine salinity gradient. It is critical to reiterate that these labels do not represent absolute salinity values but denote relative salinity-related water mass types. The labeling is performed by synthesizing the long-term average characteristics of each cluster across three key remote sensing features:

(1) Freshwater-Dominant Water Mass: Labeled for clusters exhibiting high TSS, high CDOM proxy (1/BGR), and strong hydrodynamic activity (high σ^0). This combination statistically indicates low-salinity influence.

(2) Seawater-Dominant Water Mass: Labeled for clusters characterized by low TSS, low CDOM proxy, and relatively stable hydrodynamics (low σ^0). This signature corresponds to high-salinity, marine conditions.

(3) Transitional (Brackish) Water Mass: Defined for clusters whose feature values are intermediate between the two end-members described above, representing the mixing zone.

This approach fundamentally emphasizes the statistical co-variation between the clustered remote sensing features and the relative salinity gradient, rather than attempting a quantitative salinity inversion.

IV. RESULTS AND ANALYSIS

This section elucidates the spatiotemporal evolution of water mass structure in the PRE from 2015 to 2025 and explores the underlying driving mechanisms. The analysis proceeds in four stages:

4.1 Spatial Zonation of Water Masses. Based on the K-means clustering results, we first delineate the spatial distribution of the three characteristic water masses: freshwater-dominated, transitional (mixed), and seawater-dominated. This clarifies the physical and ecological associations of salinity zones along the estuarine gradient.

4.2 Interannual Trends of Key Features. Focusing on four core remote sensing features—TSS, CDOM proxy (1/BGR), σ^0, and NDCI—we analyze the interannual evolution trends and phase characteristics of the three water mass types.

4.3 Decadal Spatiotemporal Dynamics and Hydrometeorological Responses. By integrating long-term spatial patterns and annual transition matrices, we conduct a decadal-scale dynamic analysis. This reveals how fluctuations in the areal extent of each water mass sensitively respond to extreme hydrometeorological events.

4.4 Validation and Interpretability via XGBoost/SHAP. Finally, the robustness of the classification is validated using the XGBoost model. The SHAP (SHapley Additive exPlanations) framework is employed to quantitatively assess the global importance, local directional effects, and synergistic interactions of the four features in defining water mass boundaries. This provides an interpretable machine learning perspective on the differential roles of combined "ecological-material-physical" features in characterizing estuarine dynamics.

4.1. Analysis of Clustered Water Masses

The K-means clustering results delineate a clear spatial gradient of water masses in the PRE, corresponding to the ternary structure of runoff plumes, frontal mixing, and seawater dominance (Figure 5). The low-salinity (freshwater-dominated) zone (yellow) is concentrated near the river mouths and distributes along the main freshwater plumes, extending tongue-like into the open sea. This pattern reflects the strong dilution and offshore transport driven by river discharge. The mixed transitional (brackish) zone (cyan) forms a continuous belt encircling the periphery of the estuary, primarily located along the outer edges of the low-salinity plumes. This distribution marks the active mixing interface between freshwater and seawater. The high-salinity (seawater-dominated) zone (purple) occupies extensive, relatively homogeneous areas in the open sea, distal from the estuary, indicating the prevalence of stable, saline offshore waters. This zoning effectively maps the spatial extent of freshwater influence and clearly identifies the position and structure of the estuarine mixing front.

The spatial patterns of the four key remote sensing features provide a mechanistic explanation for this clustering (Figure 5b-e). TSS exhibit elevated concentrations in nearshore areas and within the freshwater plumes, with their spatial distribution closely aligned with the low-salinity zone. This indicates that turbidity is a prominent feature of river-influenced, low-salinity waters. Similarly, the CDOM proxy (1/BGR) shows a distinct gradient, with high values in the estuary and nearshore waters that extend seaward along the plume direction, spatially coinciding with the low-salinity and transitional zones. This pattern is consistent with the conservative mixing and gradual dilution of terrestrially derived colored dissolved matter.

The SAR backscatter coefficient σ^0 (Figure 5c) shows pronounced textural gradients, particularly near the outer estuary and along the boundaries of the freshwater plumes. These areas of high σ^0 variability align closely with the spatial extent of the mixed transitional water mass (Figure 5e), indicating that surface roughness changes associated with water mass convergence are detectable by SAR. Similarly, the NDCI (Figure 5d) exhibits elevated variability in the outer estuary and nearshore mixed waters. This pattern of higher NDCI values corresponds well with the distribution of the transitional zone, suggesting that salinity-related gradients in nutrients and light availability influence phytoplankton biomass distribution. In summary, the spatial patterns of the four individual remote sensing indicators—turbidity (TSS), terrestrial dissolved matter (CDOM proxy), surface hydrodynamics (σ^0), and phytoplankton biomass (NDCI)—collectively provide a coherent physical and ecological explanation for the observed ternary salinity zonation and the precise location of the frontal mixing zone identified by clustering (Figure 5e).

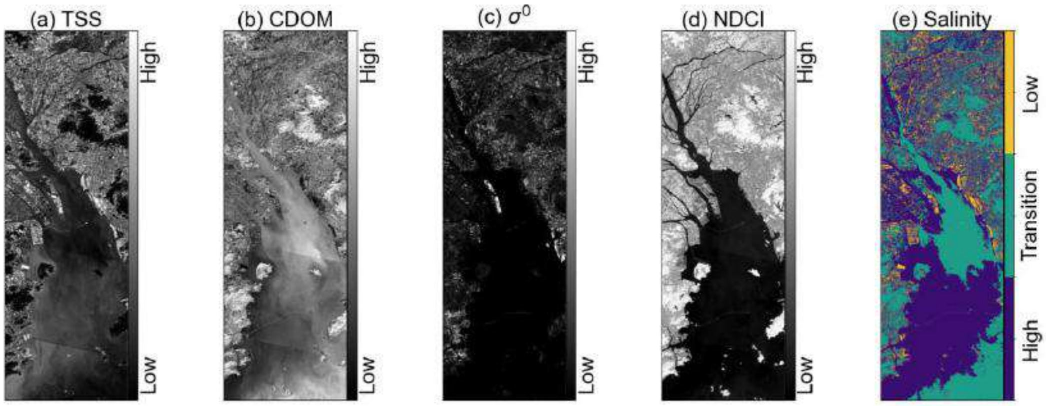

Fig.5 Spatial Distribution of Water Quality Indicators and Salinity Classification for the Hydrological Year 2022–2023.

**Panels (a–e) show TSS, CDOM (blue/green ratio proxy), σ⁰ (linear scale), NDCI, and the derived salinity classes, respectively.

4.2. Decadal Variability of Key Water Mass Features

This section analyzes the interannual evolution (2015–2025) of the three characteristic water masses based on four core remote sensing features: TSS, the CDOM proxy (1/BGR), SAR backscatter (σ^0), and the NDCI (Figure 6 & Figure 7). Collectively, these features exhibit distinctly different dynamic patterns among the three water masses, reflecting differential responses of estuarine physical and ecological environments to external drivers. The decadal data reveal a consistent hierarchical structure among the water masses for each feature, alongside occasional interannual phase shifts (Figure 7).

(1) TSS: The freshwater-dominated mass maintained the highest turbidity in most years, except in 2015–2016 when the mixed transitional mass showed elevated values.

(2) CDOM Proxy: Similarly, the freshwater-dominated mass consistently exhibited the highest terrestrial dissolved matter signal. The mixed transitional and seawater-dominated masses maintained lower, comparable levels, with a notable peak in the transitional mass during 2015–2016.

(3) SAR σ^0: A clear gradient persisted: freshwater-dominated (highest) > mixed transitional (intermediate) > seawater-dominated (lowest), indicating a consistent hydrodynamic energy gradient. A prominent peak in σ^0 for the freshwater mass occurred in 2020–2021.

(4) NDCI: The mixed transitional zone generally showed the highest chlorophyll-related values, followed by the freshwater-dominated mass. The seawater-dominated region consistently exhibited negative NDCI values. An exception occurred in 2015–2016, when the freshwater mass surpassed the transitional mass in NDCI.

These interannual trends (Figure 7) are spatially coherent with the annual composite patterns shown in Figure 6. The overall picture is one of stable feature stratification among the three water masses over the decade, punctuated by distinct phase changes in specific years.

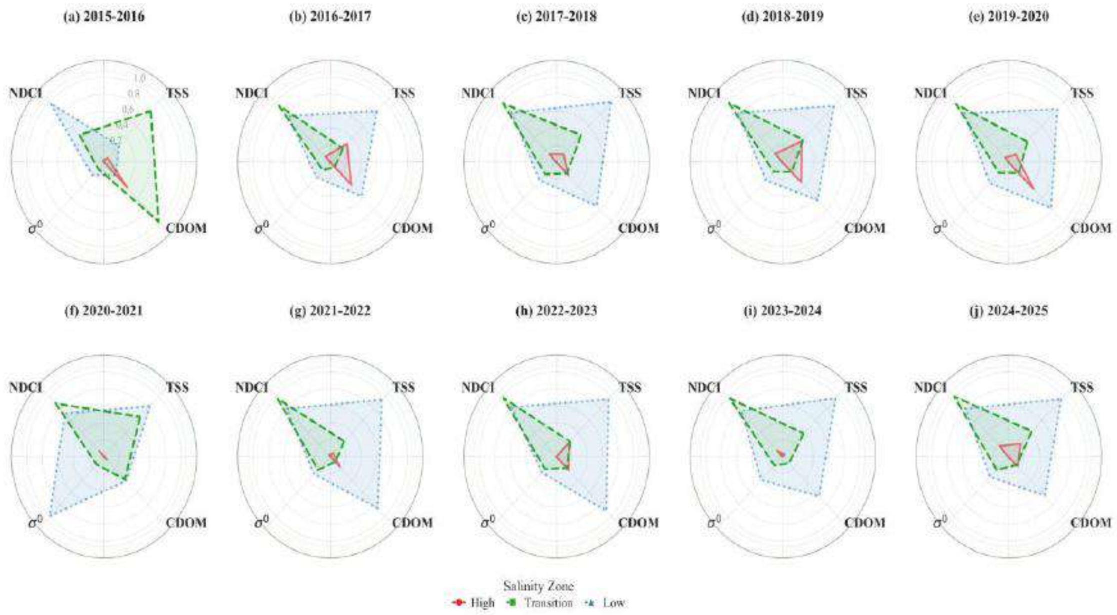

Fig.6 Radar-chart comparison of cluster-center values for four indicators (TSS, CDOM, σ^0, and NDCI) across salinity zones from 2015–2016 to 2024–2025.

**Panels (a–j) represent the ten hydrological years, and the red, green, and blue polygons denote the high-, transition-, and low-salinity zones, respectively.

4.2.1. Decadal Variability in TSS

The temporal evolution of TSS for the three water masses is shown in Figure 7a. The freshwater-dominated water mass maintained high TSS levels throughout most of the decade. It started at a relatively low point in 2015–2016, increased rapidly and remained high from 2016–2017 onward, with only a slight dip in 2020–2021 before recovering. In contrast, the mixed transitional water mass showed the most pronounced interannual variability, with peaks in 2015–2016 and 2020–2021 and a significant drop in 2016–2017. The seawater-dominated water mass consistently exhibited the lowest TSS, with only minor, short-lived increases.

The decadal integration of these trends, visualized in the radar chart (Figure 7a, integrated view), reveals a stable hierarchical structure: the freshwater-dominated mass occupies the outermost, most stable ring; the mixed transitional mass shows a smaller, more variable ring; and the seawater-dominated mass forms the most contracted, inner ring. This indicates that the TSS hierarchy among water masses is a persistent feature over the interannual scale.

This temporal stability aligns with the spatial patterns observed in the annual TSS composites (Figure 6). In these maps, the areas corresponding to the three water masses consistently exhibit the same spatial stratification: highest TSS (freshwater), intermediate and variable TSS (transitional), and lowest TSS (seawater). Thus, both the temporal series and spatial composites confirm a consistent decadal pattern: freshwater-dominated > mixed transitional > seawater-dominated in terms of TSS concentration.

4.2.2. Decadal Variability in CDOM

The temporal evolution of the CDOM proxy (1/BGR) is shown in Figure 7b. The freshwater-dominated water mass consistently showed the highest levels, increasing from a relatively low baseline in 2015–2016 to a high plateau from 2017–2020, followed by a dip and subsequent recovery before a final slight decline. The mixed transitional water mass displayed the most notable anomaly: an exceptionally high value in 2015–2016, followed by a sharp drop and generally lower levels thereafter, with a minor peak around 2020–2021. The seawater-dominated water mass largely tracked the transitional mass at a slightly lower magnitude, with relative lows in 2020–2021 and 2023–2024.

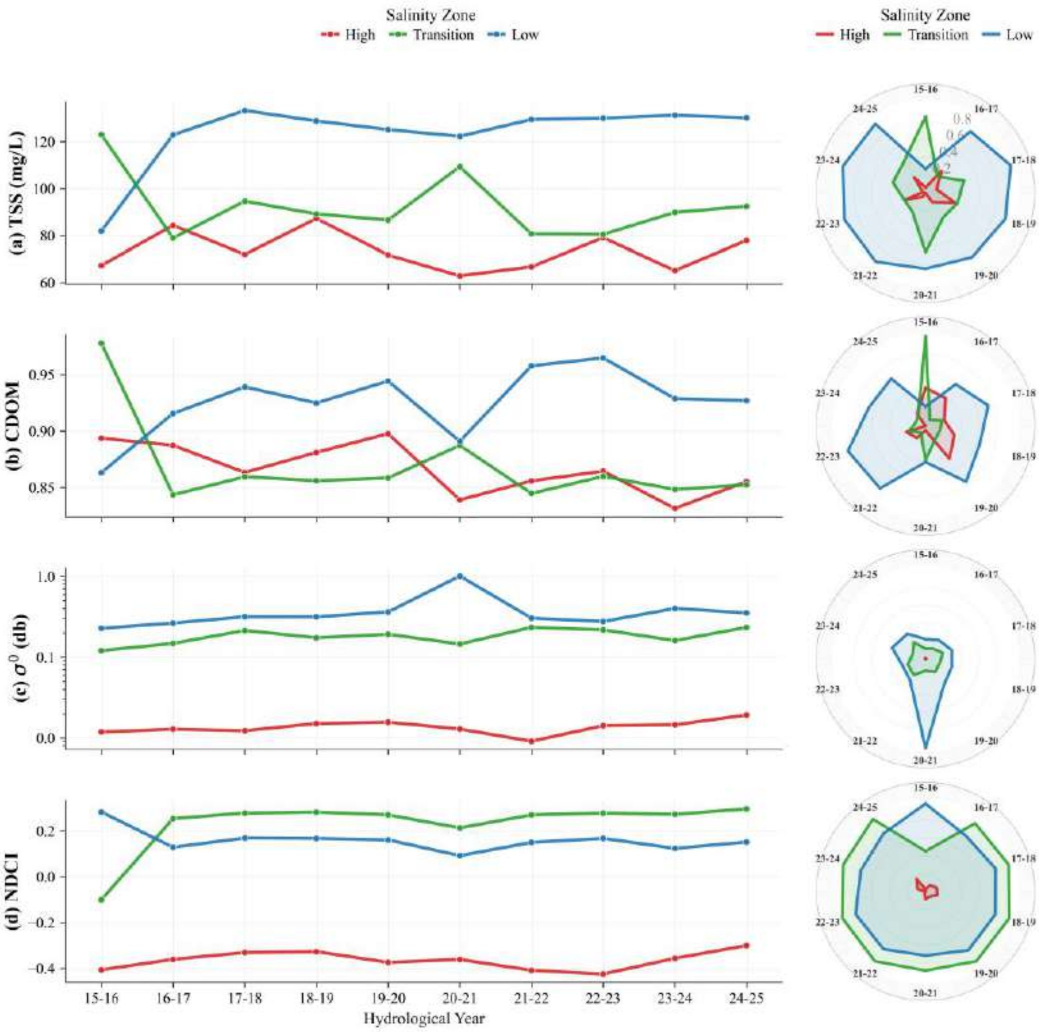

Fig.7 Interannual Variations (left) and Radar-Chart Summaries by Salinity Zone (right) of Cluster-center Values for Four Indicators (TSS, CDOM, σ^0, and NDCI) across Hydrological Years from 2015–2016 to 2024–2025.

**The labels 15–16, 16–17, …, and 24–25 denote 2015–2016, 2016–2017, …, and 2024–2025, respectively. Red, green, and blue lines represent the high-, transition-, and low-salinity zones.

The decadal integration of this signal (Figure 7b, radar chart) visually summarizes these patterns. The freshwater-dominated mass forms the outermost, most extensive ring, reflecting its persistently high values. The seawater-dominated mass forms a compact inner ring, indicating consistently low levels. The mixed transitional mass shows a distinct outward bulge corresponding specifically to the 2015–2016 anomaly, confirming the "early anomalous high" seen in the time series.

This temporal pattern is spatially coherent with the annual CDOM composites (Figure 6). The areas classified as freshwater-dominated consistently show the highest CDOM signal, while the mixed transitional zone shows a pronounced spatial extension corresponding to the 2015–2016 high-value period. Overall, while CDOM exhibited limited interannual variability compared to TSS, a stable hierarchy (freshwater-dominated > mixed transitional ≥ seawater-dominated) persisted throughout the decade.

4.2.3. Decadal Variability in SAR Backscatter σ^0

The temporal evolution of SAR backscatter σ^0 is shown in Figure 7c. Among the three water masses, σ^0 exhibited the most distinct and stable hierarchical structure over the decade. The freshwater-dominated water mass consistently recorded the highest values, with a pronounced peak in 2020–2021. Although it declined thereafter, it remained the dominant signal. The mixed transitional water mass maintained intermediate levels with minor interannual variations, showing slight increases coinciding with the 2020–2021 peak and again in 2024–2025. The seawater-dominated water mass persistently showed the lowest σ^0, hovering near the noise floor for most of the period, with only a marginal uptick at the end of the time series.

The decadal integration (Figure 7c, radar chart) visually reinforces this stability. The freshwater-dominated mass forms a large, asymmetric ring with a prominent spike in the direction corresponding to 2020–2021. The mixed transitional mass forms a smaller, more uniform ring, while the seawater-dominated mass is tightly clustered near the center. This pattern underscores both the persistent σ^0 gradient across water masses and the transient but significant hydrodynamic anomaly in 2020–2021.

This temporal stability is mirrored in the annual spatial composites (Figure 6), where the corresponding water mass zones consistently display matching σ^0 intensity levels. In summary, σ^0 provided the most robust and clear discrimination among the three water masses throughout the decade, maintaining the consistent order: freshwater-dominated > mixed transitional > seawater-dominated.

4.2.4. Decadal Variability in NDCI

The temporal evolution of the NDCI reveals a distinct pattern compared to the other features (Figure 7d). The mixed transitional water mass showed a clear regime shift: it started with negative values in 2015–2016 but rapidly turned positive from 2016–2017 onward, maintaining high levels for most of the subsequent decade with a dip in 2020–2021. The freshwater-dominated water mass exhibited moderate, generally positive values. It was relatively high in 2015–2016, remained stable until 2020, and recovered slightly after a 2020–2021 low. In contrast, the seawater-dominated water mass remained negative throughout the period, consistently recording the lowest NDCI among the three, with only a marginal late-period increase.

The decadal integration (Figure 7d, radar chart) captures this evolution. The mixed transitional mass forms the largest, most uniform outer ring, signifying its transition to and persistence in a high-NDCI state. The freshwater-dominated mass forms a smaller outer ring, and the seawater-dominated mass is tightly clustered near the center. This visualization highlights both the 2015–2016 transitional phase and the subsequent stable NDCI hierarchy.

Spatially, the annual NDCI composites (Figure 6) corroborate this order. The areas classified as mixed transitional consistently show the highest NDCI signal, followed by the freshwater-dominated zones, with the seawater-dominated areas showing the lowest values. In summary, NDCI exhibits a unique hierarchical order among the three water masses over the decade: mixed transitional > freshwater-dominated > seawater-dominated, which is reversed compared to the patterns seen for TSS and CDOM, indicating the different ecological and optical processes governing phytoplankton distribution.

4.3. Interannual Spatial Evolution of Salinity Zones

The annual spatial distribution of the three water mass types from 2015 to 2025 reveals distinct interannual evolution patterns (Figure 8). A clear offshore gradient persisted throughout the decade, with low-salinity (freshwater-dominated) and mixed transitional waters occupying the nearshore and estuarine regions, while high-salinity (seawater-dominated) waters consistently dominated the offshore areas.

Between 2015 and 2020, salinity changes were most pronounced in the northern distributaries of the PRE and their adjacent coastal waters. The areal extent of low-salinity waters increased from 2015 to 2017, as evidenced by the expansion of yellow patches in Figures 8a–b. This expansion continued into 2018–2019 but was followed by a marked contraction in 2019–2020, during which the proportion of mixed transitional waters also generally decreased.

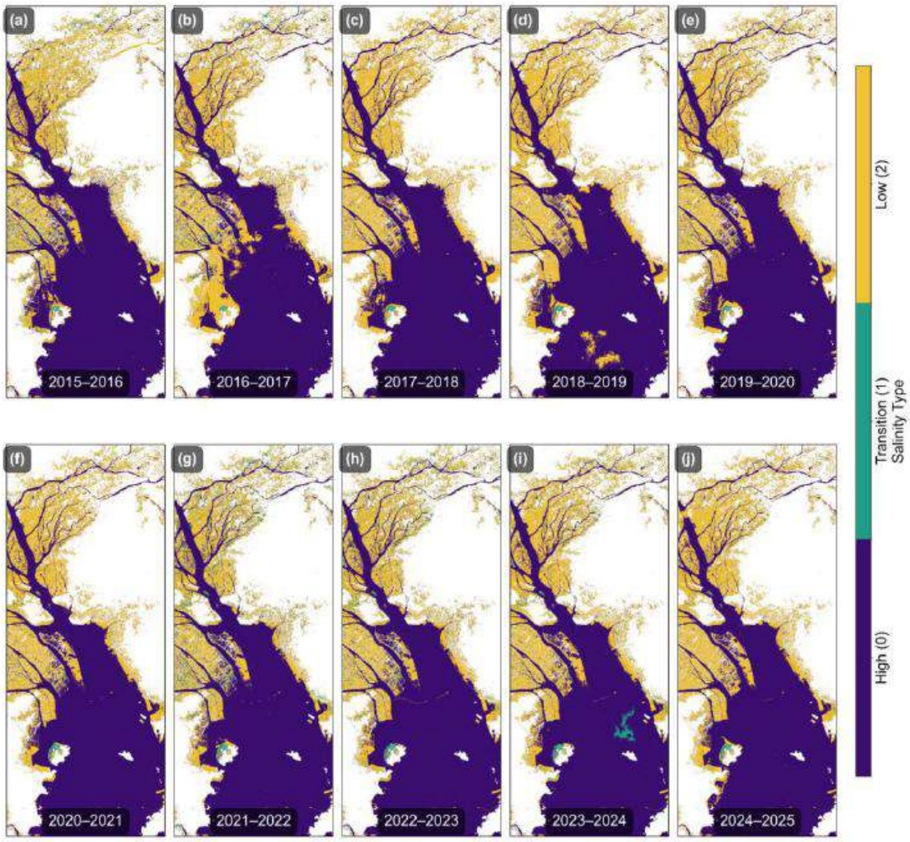

Fig.8 Interannual Variation in Salinity Classification from 2015–2016 to 2024–2025.

**Panels (a–j) correspond to individual hydrological years in chronological order. Yellow indicates low salinity, green represents transition zones, and purple denotes high salinity.

The most striking shift occurred during the 2021–2022 hydrological year, which exhibited an extreme spatial pattern characterized by the overwhelming dominance of seawater (purple) and a severe retreat of freshwater-influenced zones. This pattern aligns perfectly with the severe winter-spring drought in the Pearl River Basin during that period, which led to historically low discharges in the West and North Rivers (Compilation

Group of China Flood and Drought Disaster Prevention Bulletin, 2023; Ministry of Water Resources, 2022), drastically reducing freshwater input to the estuary. Following this extreme event, a recovery phase was observed. By the 2024–2025 hydrological year, low-salinity waters had re-emerged and expanded in localized areas (Figure 8j), indicating a partial rebalancing of the estuarine salinity structure as freshwater discharge recovered.

The interannual variations in the areal proportions and spatial dominance of the three water masses further elucidate their dynamic responses (Figure 9). Although the seawater-dominated water mass maintained overall dominance throughout the decade, the proportional area of each mass exhibited significant periodic fluctuations. These fluctuations sensitively reflect adjustments in the estuarine system to variations in basin precipitation and runoff.

Specifically, during wet years with high precipitation, the spatial extent of the freshwater-dominated water mass expanded. Conversely, the severe drought in 2021–2022 drastically reduced riverine discharge, weakening the freshwater dilution effect. This allowed the saltwater intrusion front to advance landward, resulting in the seawater-dominated mass reaching its peak areal proportion for the decade during that year.

These quantitative shifts in area proportion provide robust validation that our multi-source remote sensing clustering methodology effectively captures the spatiotemporal evolution of the estuary's structure, including its sensitive response to extreme hydrometeorological events.

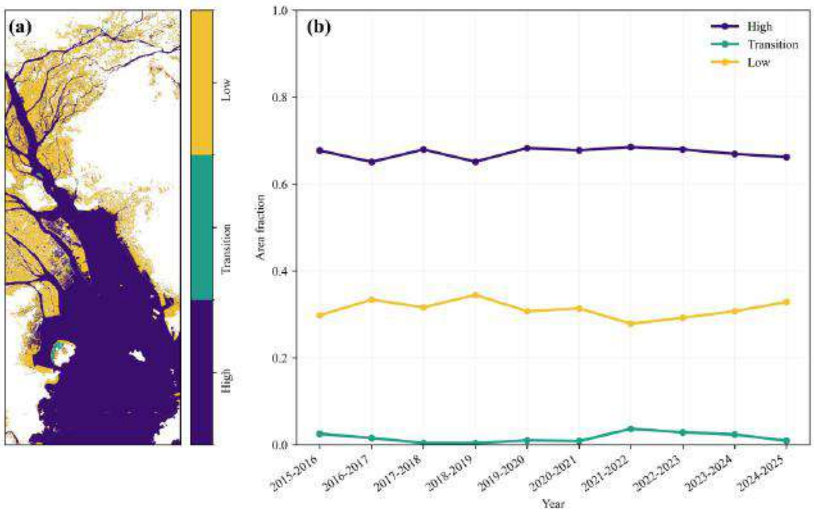

Fig.9 Spatial Dominance and Temporal Variability of Salinity Regimes during 2015–2025.

**(a) Modal salinity classification over the study period. (b) Interannual area fraction of each salinity class.

The decade-long transition of water mass proportions, illustrated by the Sankey diagram (Table 2, Figure 10), reveals the dynamic balance among the three water types. Throughout the study period, the estuary was consistently dominated by the seawater-dominated water mass, followed by the freshwater-dominated mass, with the mixed transitional mass constituting the smallest fraction. The annual proportions (Table 2) show that the seawater-dominated mass consistently accounted for the majority, ranging from 65.1% to 68.5% of the total area. The freshwater-dominated mass represented 27.9% to 34.5%, while the mixed transitional mass remained a minor component. Comparing the beginning (2015–2016) and end (2024–2025) of the decade, the proportion of the seawater-dominated mass slightly decreased from 67.7% to 66.2%, whereas the freshwater-dominated mass increased from 29.8% to 32.8%. However, this net change was not monotonic but punctuated by significant interannual fluctuations. For instance, the seawater-dominated proportion dropped to its lower bounds (65.1%) in 2016–2017 and 2018–2019, coinciding with peaks in the freshwater-dominated proportion (33.4% and 34.5%, respectively). Conversely, during the extreme drought year of 2021–2022, the seawater-dominated mass reached its maximum (68.5%), and the freshwater-dominated mass contracted to its minimum (27.9%).

Although the mixed transitional water mass consistently constituted a minor fraction of the total area (approximately 0.4%–3.6%), its spatial and functional role is critical. It manifests as a continuous, band-like structure encircling the plume edges, exhibiting distinct salinity front characteristics. As the frontal zone is a narrow belt where energy exchange, nutrient retention, and biogeochemical reactions are most intense, its bio-optical features—such as elevated NDCI values and pronounced σ^0 texture gradients—are often more extreme than those of the pure end-member waters. This combination of a small areal footprint, disproportionately large ecological contribution, and strong physical-optical signatures is a hallmark of the mixing zone as a key ecological interface in estuarine dynamics.

The Sankey flow structure (Figure 10) provides further insight into water mass persistence. The thickest streamlines represent the continuous dominance of the seawater-dominated and freshwater-dominated masses across consecutive years, indicating that most of the estuary retains its classification from one hydrological year to the next. Simultaneously, finer but stable cross-flows between these two major types indicate that some areas do transition between seawater and freshwater dominance over annual timescales. In contrast, streamlines associated with the mixed transitional mass are consistently finer and account for smaller flows, reflecting its localized, band-like nature. The inflows to and outflows from this zone show interannual variations but do not represent a dominant, persistent reservoir like the two end-member masses.

Table 2 Interannual Composition of Salinity Types across Hydrological Years

Year	High Ratio (%)	Transition Ratio (%)	Low Ratio (%)
2015–2016	67.72	2.51	29.77
2016–2017	65.08	1.55	33.37
2017–2018	67.96	0.44	31.61
2018–2019	65.12	0.41	34.47
2019–2020	68.28	1	30.72
2020–2021	67.76	0.86	31.37
2021–2022	68.53	3.61	27.85
2022–2023	67.97	2.83	29.2
2023–2024	66.93	2.34	30.73
2024–2025	66.2	0.96	32.84

**Percentages are normalized to a constant total of 3,073,195 valid pixels per year, enabling direct year-to-year comparison of class proportions.

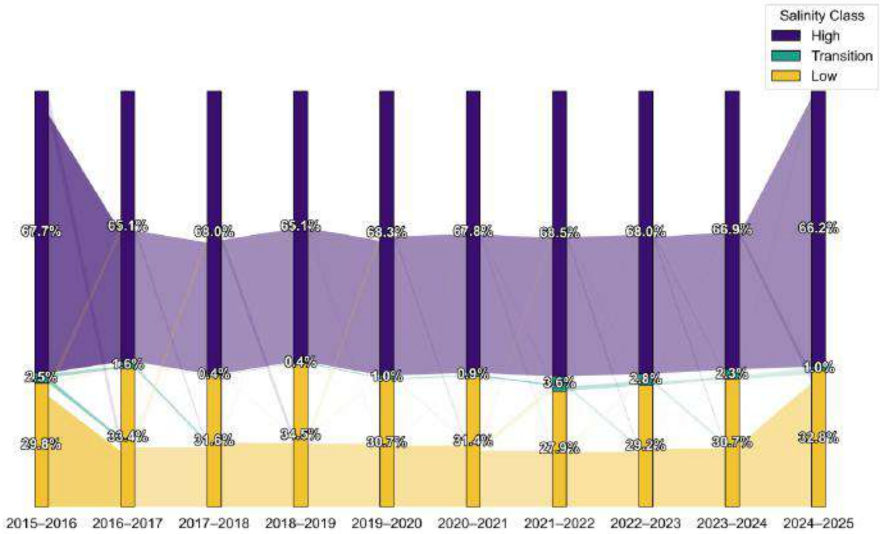

Fig.10 Sankey Diagram Illustrating Temporal Transitions among Salinity Classes in the PRE.

**Vertical bars represent the proportion of pixels classified as High, Transition, and Low salinity for each period (labels on bars indicate percentages). Connections between adjacent periods show pixel-class transitions, where thicknesses flow is proportional to the pixel count (area proportion).

4.4. Driver Analysis Using XGBoost and SHAP

To quantitatively assess the contribution of each remote sensing feature to the water mass classification, we employed the XGBoost model interpreted with SHAP (SHapley Additive exPlanations).

4.4.1. Global Feature Importance

The SHAP summary plot (Figure 11) reveals the global importance of the four features in descending order: NDCI > TSS > CDOM proxy > σ^0. This ranking indicates that:

(1) NDCI is the most significant discriminator among the three water masses. In the PRE, its gradient sensitively reflects ecological differences arising from freshwater-seawater mixing, effectively separating the transitional mixed zone from the turbid freshwater plume and the clear offshore waters.

(2) TSS and CDOM proxy, as classic tracers of terrestrial material, are crucial for delineating the spatial extent of runoff influence by indicating the input of suspended sediments and colored dissolved organic matter.

(3) SAR backscatter (σ^0), while contributing less globally, provides complementary information on surface hydrodynamic roughness. This adds value independent of optical properties, particularly under conditions where optical signals may be saturated or obscured (e.g., extreme turbidity).

This analysis quantifies the driving role of multidimensional features ("ecological-material-physical") in water mass classification. It empirically demonstrates, from a data-driven perspective, how these combined features explain the dynamic structure of the estuary.

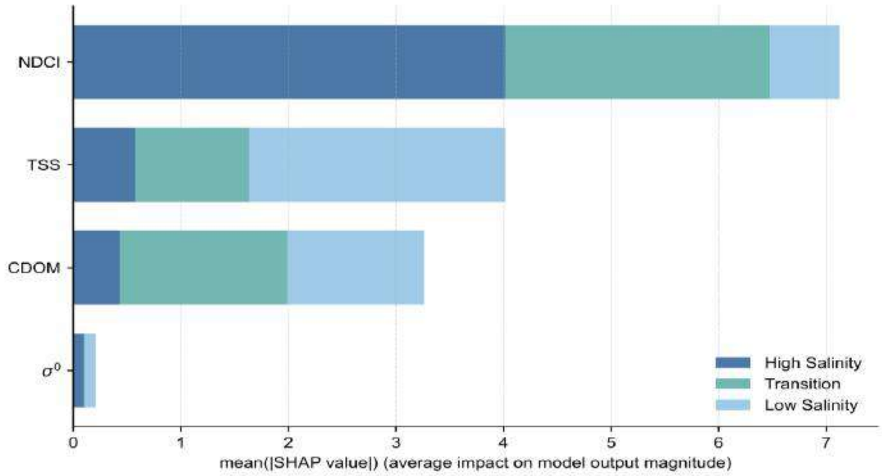

Fig.11 Mean Absolute SHAP Values

**It is showing global feature importance for high salinity, low salinity, and transition classes across all years.

4.4.2. Local Feature Contributions and Directionality

The SHAP dependence plots (Figure 12) illustrate the local contribution and directional effect of each feature value on the model's prediction for the three water mass classes. Across all classes, NDCI, TSS, and the CDOM proxy exhibit wide distributions of SHAP values, confirming their pronounced sample-level influence. In contrast, σ^0 shows SHAP values tightly clustered near zero, consistent with its lower global importance. The color gradient (representing the original feature value) clearly reveals systematic relationships: for a given feature, high and low values can push the prediction toward or away from a specific class, enabling intuitive comparison of feature effects across different water masses.

Seawater-Dominated Water Mass (Figure 12a): NDCI is the dominant feature. Low NDCI values (blue) are associated with positive SHAP values, actively driving predictions toward this class, indicating that low chlorophyll is a key identifier. High NDCI values (red) have negative SHAP values, pushing predictions away. TSS and the CDOM proxy show similar but weaker directional patterns. DEM and σ^0 have minimal local impact.

Mixed Transitional Water Mass (Figure 12b): The CDOM proxy, DEM, and NDCI distributions are most prominent. The systematic color gradient reflects the complex mixing state, where moderate feature values often characterize this zone. TSS shows a narrower value range, and σ^0 again contributes minimally.

Freshwater-Dominated Water Mass (Figure 12c): NDCI and TSS are the primary drivers, exhibiting a pattern opposite to that of the seawater class. Here, high NDCI and TSS values (red) correspond to positive SHAP values, identifying this class, while low values correspond to negative SHAP values. This reversal highlights that high turbidity and chlorophyll response are critical indicators of freshwater influence. The CDOM proxy and DEM play secondary roles, and σ^0 remains the weakest contributor.

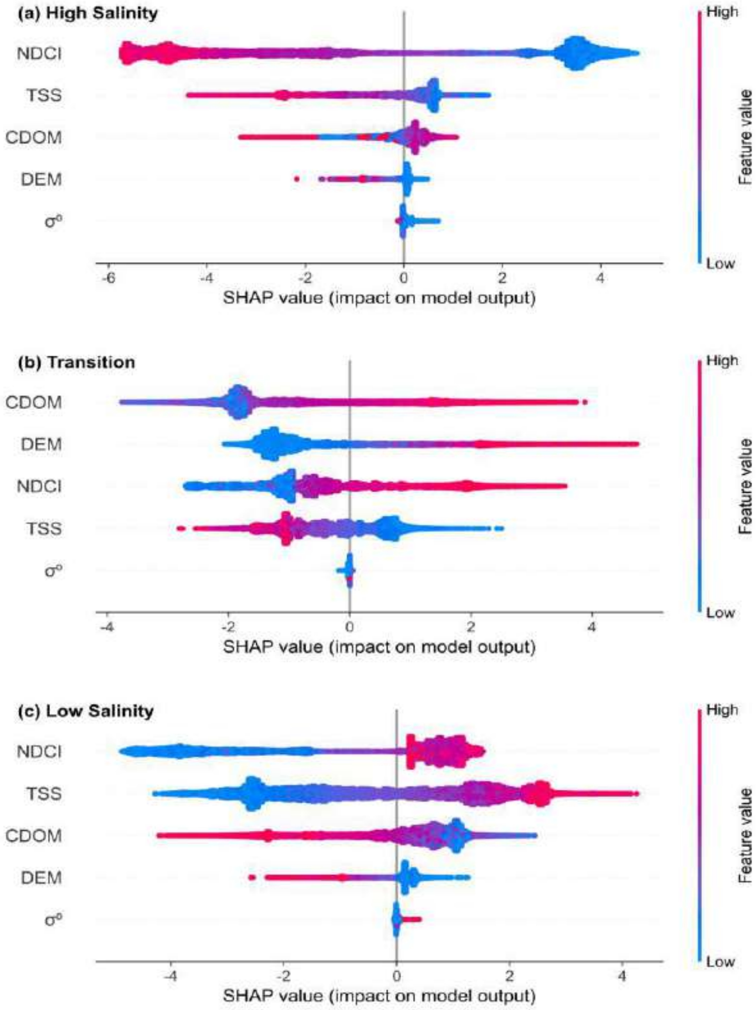

Fig.12 Class-specific SHAP Summary (beeswarm) Plots for (a) High Salinity, (b) Transition, and (c) Low Salinity.

**Points show SHAP value distributions for each feature; color represents the raw feature value (Low to High).

4.4.3. Analysis of Feature Interaction Effects

The evaluation of pairwise feature interactions (Figure 13) quantified the strength of synergistic effects on the model predictions. The strongest interaction was between TSS and NDCI (interaction strength: 0.263), followed by CDOM proxy and NDCI (0.133) and NDCI and DEM (0.066). In contrast, interactions involving SAR backscatter (σ^0) with any other feature were consistently near zero, indicating that σ^0 contributes primarily through its main effect, with minimal synergistic role in defining water masses.

The SHAP dependence plots for these interactions (lower triangle of Figure 13) visually support this quantification. Feature pairs with high interaction values (e.g., TSS-NDCI, CDOM-NDCI) exhibit complex, non-linear scatter patterns, where the SHAP value of one feature changes depending on the value of the other. In contrast, pairs with low interaction values (especially those involving σ^0) show simpler, more linear relationships.

Overall, the model's predictions are dominated by the main effects of individual features rather than by their interactions. The global feature importance (Section 4.4.1) largely reflects these independent contributions. For features like TSS, the CDOM proxy, and σ^0, their individual predictive power explains most of their contribution, with relatively little added from cooperative effects with other features. The notable exception is NDCI, which engages in moderately strong interactions, particularly with terrestrial material indicators (TSS, CDOM), highlighting the coupled nature of ecological and material transport processes in the estuary.

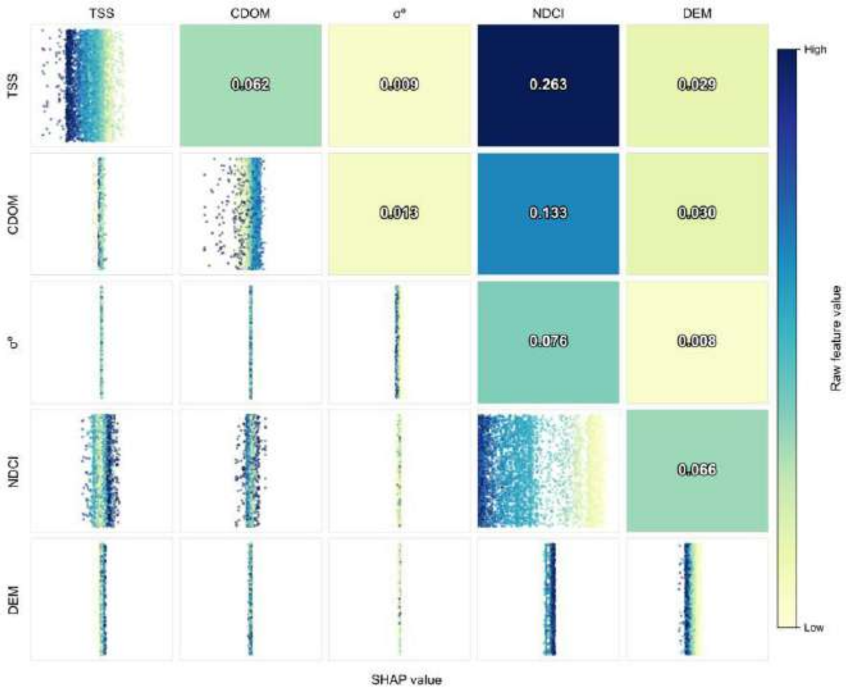

Fig.13 SHAP Interaction Matrix for High Salinity.

**The upper triangle reports mean interaction strength values; the diagonal and lower triangle show SHAP value distributions, colored by raw feature value.

V. DISCUSSION AND CONCLUSIONS

This study has developed and applied a multi-source remote sensing fusion framework to analyze the decadal (2015–2025) spatiotemporal evolution of salinity-related water mass structures in the PRE. The main findings and contributions are summarized as follows.

5.1. Key Findings on Water Mass Dynamics

By integrating optical (TSS, CDOM proxy, NDCI), microwave (Sentinel-1 σ^0), and topographic (DEM) features, we delineated three characteristic water masses: freshwater-dominated, seawater-dominated, and a mixed transitional zone. Decadal analysis revealed significant interannual fluctuations in their spatial extent, which were closely tied to the runoff conditions of the Pearl River Basin. Most notably, during the severe drought of the 2021–2022 hydrological year, a drastic reduction in freshwater discharge led to a marked expansion of the seawater-dominated area, demonstrating the framework's sensitivity to extreme hydrometeorological events. It is crucial to reiterate that the results depict relative changes in water mass structure that correlate with salinity gradients, not the quantitative inversion of absolute salinity values. Nonetheless, these patterns effectively characterize the indicative trends of estuarine salinity dynamics.

5.2. Methodological Innovation and Value

Faced with the scarcity of long-term, synchronous in situ salinity data, this study innovatively employed an unsupervised K-means clustering approach on fused multi-source remote sensing data. This framework overcomes the limitations of traditional monitoring in vast, complex estuaries by leveraging the complementary information from different sensors. Compared to single-source methods, it provides a cost-effective and efficient solution for reconstructing the spatiotemporal history of estuarine water masses. The validated approach offers a practical pathway for assessing the long-term impacts of climate change and hydrological variability on coastal aquatic environments in data-scarce regions.

5.3. Limitations and Future Perspectives

5.3.1. Limitations and Validation

This study focuses on identifying salinity-related water mass structures and patterns, not on the quantitative inversion of absolute salinity values. The absence of long-term, synchronous in situ salinity data precludes a rigorous quantitative error assessment. However, the strong spatiotemporal consistency between the derived patterns and independent regional hydrological drivers (e.g., precipitation and runoff) supports the qualitative reliability of the analysis.

5.3.2. Future Research Directions

Future work should prioritize the following directions to advance this research line:

(1) Mechanistic Calibration and Refinement: Incorporating tidal dynamics and targeted in situ sampling, especially during short-term extreme events, is essential to calibrate and refine the classification framework, improving its accuracy for high-frequency processes (Kuang et al., 2023).

(2) Causal Analysis and Impact Modeling: Leveraging interpretable machine learning, future studies can move beyond correlation to analyze the causal mechanisms linking salinity with TSS, CDOM, and ecological indicators. This can form the basis for developing salinity-impact models to quantify effects on aquaculture and fisheries.

(3) Broad Application and Comparative Analysis: The methodological framework should be applied and validated in other major estuarine systems (e.g., Yangtze River Estuary, Yellow River Estuary). Comparative analysis of salinity evolution patterns across different basins will provide broader insights into the ecological responses of large estuaries to climate change and human activities.

(4) Towards Global Synthesis and Management: Ultimately, synthesizing findings from multiple estuaries can contribute to establishing a global comparative database of estuarine salinity dynamics. Such a resource would shift research from descriptive pattern analysis towards adaptive coastal management and transboundary ecosystem conservation, directly supporting global estuarine sustainability goals.

REFERENCES

[1] Bowers, D. G., Evans, D., Thomas, D. N., Ellis, K., & Williams, P. J. le B. (2004). Interpreting the colour of an estuary. Estuarine, Coastal and Shelf Science, 59(1), 13–20. https://doi.org/10.1016/j.ecss.2003.06.001

[2] Chen, W., Guo, F., Huang, W., Wang, J., Zhang, M., & Wu, Q. (2023). Advances in phytoplankton population ecology in the Pearl river estuary. Frontiers in Environmental Science, 11. https://doi.org/10.3389/fenvs.2023.1084888

[3] Compilation Group of China Flood and Drought Disaster Prevention Bulletin. (2023). Summary of the "China Flood and Drought Disaster Prevention Bulletin 2022". China Flood Control and Drought Relief, 33(10), 78–82. https://doi.org/10.16867/j.issn.1673-9264.2023410

[4] Doxaran, D., Froidefond, J.-M., Lavender, S., & Castaing, P. (2002). Spectral signature of highly turbid waters: Application with SPOT data to quantify suspended particulate matter concentrations. Remote Sensing of Environment, 81(1), 149–161. https://doi.org/10.1016/S0034-4257(01)00341-8

[5] Feng, Y., & He, Y. (2025). Imaging estuarine surface salinity

using Sentinel-2: A case study in the Pearl River Estuary. Ocean and Coastal Research, 73, e25016.

[6] Gade, M., Alpers, W., Hühnerfuss, H., Masuko, H., & Kobayashi, T. (1998). Imaging of biogenic and anthropogenic ocean surface films by the multifrequency/multipolarization SIR-C/X-SAR. Journal of Geophysical Research: Oceans, 103(C9), 18851–18866. https://doi.org/10.1029/97JC01915

[7] Højerslev, N. K., Holt, N., & Aarup, T. (1996). Optical measurements in the North Sea-Baltic Sea transition zone. I. On the origin of the deep water in the Kattegat. Continental Shelf Research, 16(10), 1329–1342. https://doi.org/10.1016/0278-4343(95)00075-5

[8] Klemas, V. (2012). Remote sensing of coastal plumes and ocean fronts: Overview and case study. Journal of Coastal Research, 28(1A), 1–7.

[9] Kuang, C. P., Li, H. Y., Wang, J., Wu, Y. L., & Fan, J. D. (2023). The Responses of Three Major Projects on The Horizontal Salinity Front in The Yangtze River Estuary. Proceedings of the 19th Annual Meeting of the Asia Oceania Geosciences Society (AOGS 2022) Singapore, 01–05 August 2022, 104–106.

[10] Ministry of Water Resources of the People’s Republic of China. (2022). China's Flood and Drought Disaster Prevention Bulletin (2022). Ministry of Water Resources of the People’s Republic of China.

[11] Nayak, G. N., &Noronha e D’Mello C.A. (2018).Estuarine Mudflat and Mangrove Sedimentary Environments along Central West Coast of India. S.F. J. Environ Earth Sci. 1(1): 1013. https://scienceforecastoa.com/

[12] Nechad, B., Ruddick, K. G., & Park, Y. (2010). Calibration and validation of a generic multisensor algorithm for mapping of total suspended matter in turbid waters. Remote Sensing of Environment, 114(4), 854–866. https://doi.org/10.1016/j.rse.2009.11.022

[13] O’Reilly, J. E., Maritorena, S., Mitchell, B. G., Siegel, D. A., Carder, K. L., Garver, S. A., Kahru, M., & McClain, C. (1998). Ocean color chlorophyll algorithms for SeaWiFS. Journal of Geophysical Research: Oceans, 103(C11), 24937–24953. https://doi.org/10.1029/98JC02160

[14] Pichel, W. G., & Clemente-Colón, P. (2000). NOAA CoastWatch SAR applications and demonstration. Johns Hopkins APL Technical Digest, 21(1), 49–57.

[15] Sathyendranath, S. (2000). Remote sensing of ocean colour in coastal, and other optically-complex, waters. Reports of the International Ocean-Colour Coordinating Group, No. 3, IOCCG, Dartmouth, Canada.

[16] Stedmon, C. A., Markager, S., Søndergaard, M., Vang, T., Laubel, A., Borch, N. H., & Windelin, A. (2006). Dissolved organic matter (DOM) export to a temperate estuary: Seasonal variations and implications of land use. Estuaries and Coasts, 29(3), 388–400.

[17] Wai, O. W. H., Wang, C. H., Li, Y. S., & Li, X. D. (2004). The formation mechanisms of turbidity maximum in the Pearl River estuary, China. Marine Pollution Bulletin, 48(5), 441–448. https://doi.org/10.1016/j.marpolbul.2003.08.019

[18] Xing, Q., Lou, M., Chen, C., & Shi, P. (2013). Using in situ and Satellite Hyperspectral Data to Estimate the Surface Suspended Sediments Concentrations in the Pearl River Estuary. IEEE Journal of Selected Topics in Applied Earth Observations and Remote Sensing, 6(2), 731–738. https://doi.org/10.1109/JSTARS.2013.2238659

[19] Yin, K., Lin, Z., & Ke, Z. (2004). Temporal and spatial distribution of dissolved oxygen in the Pearl River Estuary and adjacent coastal waters. Continental Shelf Research, Pearl River Estuary Study, 24(16), 1935–1948. https://doi.org/10.1016/j.csr.2004.06.017

[20] Zhang, H., Shi, X. Y., Zhang, C. S., & Wang, L. S. (2009). Distribution features of nutrients structure and nutrient limitation in the north of Yellow Sea. J. Ocean Univ. China, 39(4), 773–780.

International Journal of Environment, Agriculture and Biotechnology
Vol-11, Issue-2; Mar-Apr, 2026
Peer-Reviewed International Journal
Journal Home Page Available: https://ijeab.com/
Journal DOI: 10.22161/ijeab

Estimation of correlation and path coefficient analysis in selected okra genotypes

Renu Fandan, S. K. Dhankhar, Sanjay Yadav, Sudesh*, Pooja Pahal and Vikas Sagwal

Department of Vegetable Science, Chaudhary Charan Singh Haryana Agricultural University, Hisar, Haryana, India

Received: 21 Jan 2026; Received in revised form: 23 Feb 2026; Accepted: 28 Feb 2026; Available online: 08 Mar 2026

***Abstract*— The experiment was undertaken to study the association among yield and its contributing traits and to assess their direct and indirect effects on fruit yield in okra. Thirty okra genotypes were evaluated in a randomized block design with three replications at the Vegetable Research Farm, CCS Haryana Agricultural University, Hisar, Haryana, India during kharif 2021. Genotypic correlation coefficients were generally higher than phenotypic correlation coefficients. Fruit yield/plant exhibited significant positive correlation with plant height (0.63, 0.43), number of branches per plant (0.66, 0.33), petiole length (0.56, 0.42), fruit length (0.75, 0.43) and fruit diameter (0.34, 0.20) at genotypic and phenotypic levels, respectively, while it showed significant negative correlation with days to 50% flowering (-0.82, -0.60), inter-nodal length (-0.67, -0.49) and first fruiting node (-0.63, -0.47). Path coefficient analysis revealed that fruit length exerted the highest positive direct effect on fruit yield per plant (0.76), followed by number of branches per plant (0.25) and number of fruits per plant (0.19). Plant height exhibited positive indirect effects via days to 50% flowering and first fruiting node. The study indicated that fruit length, number of branches per plant and number of fruits per plant are key traits for improving fruit yield in okra and should be emphasized in selection programmes.*

***Keywords*— Okra, genotypic correlation coefficient, phenotypic correlation coefficients, path analysis, direct effect, indirect effect**

I. INTRODUCTION

Okra (*Abelmoschus esculentus* (L.) Moench) belongs to the family Malvaceae and is widely cultivated in tropical and sub-tropical regions of the world (Shivaramegowda et al., 2016). Okra is believed to have originated in Ethiopia, Sudan, and Northeast Africa and is now extensively grown in many countries (Salih and Mansoor, 2019). It is an annual, hardy, erect, and high-yielding vegetable crop showing wide variation in plant size, pod shape, pigmentation, branching habit, maturity period, and plant height (Purquerio et al., 2010). Okra is a polyploid crop with chromosome numbers of 2n = 8x = 72 or 144 and is commonly known as lady's finger in many English-speaking countries. Among Abelmoschus species, A. angulosus has the lowest chromosome number (2n = 56), whereas A. caillie possesses the highest chromosome number (2n = 200) (Singh and Bhatnagar, 1975). The fresh and immature fruits of okra are used as a vegetable and are valued for their high nutritive and medicinal properties. Okra fruits are rich in carbohydrates, fibre, calcium, phosphorus, iron, magnesium, iodine, and vitamins A, B, and C (Samim et al., 2018).Okra mucilage has medicinal importance and has been reported to act as a blood volume expander, reduce proteinuria, and alleviate renal disorders (Siemonsma and Kouame, 2004). Its alkaline nature helps in neutralizing digestive acids and relieving gastrointestinal ulcers. The stem bark and fibres are used in rope making, paper, and cardboard manufacturing. Mucilage obtained from soaked roots and stems is traditionally used for clarifying sugarcane juice during jaggery preparation.Okra is a heat- and drought-tolerant crop but is sensitive to cold stress (Reddy et al., 2013). The optimum temperature ranges for growth, flowering, and pod development is reported to be 21–30 °C. Before initiating any crop improvement programme, assessment of genetic variability among parental material is essential (Das et al., 2012).

Greater variability enhances the efficiency of selection for desirable traits. Genetic variability plays a crucial role in selecting elite genotypes and identifying suitable parents for hybridization.Yield is a complex quantitative trait governed by several yield-attributing characters. Therefore, understanding the association among yield and its component traits is essential for formulating effective breeding strategies (Aminu et al., 2016). Correlation analysis helps identify traits contributing to yield improvement, while genotypic correlations reflect inherent associations and phenotypic correlations include environmental effects (Johnson et al., 1955). Path coefficient analysis further partitions correlation coefficients into direct and indirect effects, enabling precise identification of traits influencing yield (Dewey and Lu, 1959). Considering these aspects, the present investigation was undertaken to study the association among yield-related traits and their direct and indirect effects on fruit yield in okra genotypes using path coefficient analysis.

II. MATERIAL AND METHOD

The experiment was conducted at Research Farm of the Department of Vegetable Science, CCS Haryana Agricultural University, Hisarwhich is located in the subtropics at 290 10' North latitude and 750 46' East longitude, during *kharif* 2021. Thirty genotypes were evaluated in field experiment (Table-1.0). The experiment was designed as Randomized Block Design (RBD) with three replications. The planting distance was 60 cm × 30cm (60cm between rows and 30cm within row). Observations were recorded for quantitative characters. Five randomly chosen plants from each genotype and replication were used to collect the data. Observations recorded were plant height, branches per plant, days to 50% flowering, inter-nodal length (cm), first fruit node, fruit length (cm), fruit diameter (cm), fruit weight (g), fruits per plant, fruit yield per plant (g). The collected data were statistically analysed to determine path analysis (direct effect and indirect effect), genotypic and phenotypic correlation, and phenotypic correlation was utilised to determine path coefficient analysis.Correlation coefficients were calculated using the variance and covariance components, as proposed by (Al-Jibouri et al., 1958).Path coefficient analysis was performed using genotypic correlation values of yield components which was illustrated by (Dewey and Lu, 1959).

Table-1.0: List of genotypes used in the research experiment

Sr.	Genotypes	Source	Origin	Sr.	Genotypes	Source	Origin
1.	HB-9-35	CCS HAU, Hisar	India	**16.**	PrabhaniKranti	MAU, Prabhani	India
2.	HB-9-37	CCS HAU, Hisar	India	**17.**	HBT-11-1	CCS HAU, Hisar	India
3.	HB-9-38	CCS HAU, Hisar	India	**18.**	HBT-42	CCS HAU, Hisar	India
4.	HB-9-43	CCS HAU, Hisar	India	**19.**	HBT-49-1	CCS HAU, Hisar	India
5.	HBT-1	CCS HAU, Hisar	India	**20.**	HBT-15	CCS HAU, Hisar	India
6.	Punjab-8	PAU, Ludhiana	India	**21.**	JNDOL-05	AAU, Gujrat	India
7.	PusaSawani	IARI, New Delhi	India	**22.**	HB-691-08	CCS HAU, Hisar	India
8.	Punjab Padmini	PAU, Ludhiana	India	**23.**	HBTC-6-7-1	CCS HAU, Hisar	India
9.	HB-9-29	CCS HAU, Hisar	India	**24.**	HBT-53	CCS HAU, Hisar	India
10.	HB-06-46-1-1	CCS HAU, Hisar	India	**25.**	ArkaAbhay	IIHR, Banglore	India
11.	HB-S-4	CCS HAU, Hisar	India	**26.**	HisarUnnat	CCS HAU, Hisar	India
12.	HB-25-2-1	CCS HAU, Hisar	India	**27.**	VarshaUphar	CCS HAU, Hisar	India
13.	HBBT-19	CCS HAU, Hisar	India	**28.**	Hisar Naveen	CCS HAU, Hisar	India
14.	HBT-48	CCS HAU, Hisar	India	**29.**	HB-9-27	CCS HAU, Hisar	India
15.	HB-08-3-1	CCS HAU, Hisar	India	**30.**	HBT-12-1	CCS HAU, Hisar	India

Table 2.0: Genotypic (above diagonal) and phenotypic correlation coefficients (below diagonal) among different characters in okra

Characters	PH (cm)	BPP	DFF	PL (cm)	INL (cm)	FFN	FL (cm)	FD (cm)	FW (g)	FPP
PH (cm)	**1.00**	0.49**	-0.62**	0.52**	-0.44**	-0.41**	0.44**	0.37**	-0.01^{NS}	0.40**
BPP	0.78^{**}	**1.00**	-0.47**	0.46**	-0.30**	-0.33**	0.38**	0.27*	0.14^{NS}	0.17^{NS}
DFF	-0.84^{**}	-0.79^{**}	**1.00**	-0.44**	0.35**	0.45**	-0.28**	-0.29**	-0.16^{NS}	-0.38**
PL (cm)	0.61^{**}	0.67^{**}	-0.47^{**}	**1.00**	-0.47*	-0.35*	0.44**	0.22*	0.05^{NS}	0.40**
INL (cm)	-0.70^{**}	-0.66^{**}	0.73^{**}	-0.85^{**}	**1.00**	0.35**	-0.45**	-0.33**	-0.18^{NS}	-0.46**
FFN	-0.51^{**}	-0.48^{**}	0.64^{**}	-0.45^{*}	0.61^{**}	**1.00**	-0.36**	-0.21*	-0.15^{NS}	-0.36**
FL (cm)	0.61^{**}	0.49^{*}	-0.44^{**}	0.61^{**}	-0.64^{**}	-0.47^{**}	**1.00**	0.11^{NS}	0.06^{NS}	0.37*
FD (cm)	0.56^{**}	0.60^{**}	-0.49^{*}	0.40^{**}	-0.71^{**}	-0.31^{**}	0.28^{**}	**1.00**	0.10^{NS}	0.09^{NS}
FW (g)	0.03^{NS}	0.31^{**}	-0.15^{NS}	0.07^{NS}	-0.47^{*}	-0.24^{*}	0.22^{*}	0.33^{**}	**1.00**	0.07^{NS}
FPP	0.77^{**}	0.50^{**}	-0.85^{**}	0.77^{**}	-0.87^{**}	-0.55^{**}	0.56^{**}	0.17^{NS}	-0.11^{NS}	**1.00**

PH-Plant height, BPP - Branches per plant, DFF- Days to 50% flowering, PL- Petiole length, INL- Inter-nodal length, FFN- First fruit node, FL- Fruit length, FD- Fruit diameter, FW- Fruit weight, FPP- Fruits per plant

III. RESULT AND DISCUSSION

Correlation coefficients analysis

Correlation coefficients were worked out at phenotypic and genotypic levels to estimate the degree of association among various characters. The results of correlation analysis have been presented in Table 2.0. In almost all the traits the estimate of genotypic correlation coefficients was higher than phenotypic correlation coefficients, thus demonstrating a strong inherent association between various traits. These findings were found in accordance withNiranjan et al., (2004), Somashekhar et al., (2011), Badigeret al., (2017)

Yield per plant showed significant positive correlation with plant height (0.63, 0.43), branches per plant (0.66, 0.33), petiole length (0.56, 0.42), fruit length (0.75, 0.43), fruit diameter (0.34, 0.20^{NS}), number of fruits per plant, whereas significant negative correlation with days taken to 50% flowering (-0.82, -0.60), inter-nodal length (-0.67, -0.49), first fruit node (-0.63, -0.47), at both genotypic and phenotypic levels respectively.The results obtained from study are in confirmation with Reddy et al., (2013). Similar results were obtained by Gogineniet al., (2015), Kumar and Reddy(2016), Kerure et al., (2017)for number of number of fruits per plant; Gogineniet al., (2015), Kumar & Reddy(2016), Yadav et al., (2017) for plant height at final harvest; Shivaramegowda et al., (2016), Kerure et al., (2017), Nirosha et al., (2014), for number of branches/plant; Shivaramegowda et al., (2016), Kerure et al., (2017), Sundaram V (2015)for fruit diameter.

Fruits per plant exhibited significant positive association with plant height (90.77, 0.40), branches per plant (0.50, 0.17), petiole length (0.77, 0.40), fruit length 90.56, 0.37), yield per plant (0.90, 0.38); Significant, negative correlations expressed with days taken to 50% flowering (–0.85, -0.38), inter-nodal length (-0.87, -0.46), first fruit node (-0.55, -0.36), at both genotypic and phenotypic levels, respectively. Fruits per plant positively correlated with branches per plant; confirmation with Verma& Singh, (2020).

Fruit length has depicted positive and significant correlation with plant height (0.61, 0.44), branches per plant (0.49, 0.38), petiole length (0.61, 0.44), fruits per plant (0.56, 0.37), yield per plant 90.75, 0.43) and significant negative correlation with days taken to 50% flowering (-0.44, -0.28), inter-nodal length (-0.64, -0.45), first fruit node (-0.47, -0.36), fruit diameter (-0.28, -0.11), at both genotypic and phenotypic levels respectively. Fruit length was positively correlated with plant height; confirmation with Saryam DK(2012) and Ghosh JS, (2005). Fruit diameter exhibited significant positive correlation plant height (0.56, 0.37), branches per plant (0.60, 0.27), petiole length (0.40, 0.22) and significant, negative correlation with days taken to 50% flowering (-0.49, -0.29), first fruit node (-0.31, -0.21) and fruit length (-0.28, -0.11), at both genotypic and phenotypic levels respectively.

Plant height exhibited significant positive correlation with branches per plant (0.78, 0.49), petiole length (0.61, 0.52) fruit length (0.61, 0.44), fruit diameter (0.56, 0.37), fruits per plant (0.77, 0.40), yield per plant (0.63, 0.43); Significant, negative correlation with days taken to 50% flowering (-0.84, -0.62), inter-nodal length (-0.70, -0.44) and first fruit node (-0.51, -0.41) at genotypic and phenotypic levels respectively. The results obtained from study are in confirmation with Reddy et al., (2013) and Ahamed et al., (2015).

Branches per plant exhibited significant positive correlation with plant height (0.78,0.49), petiole length (0.67, 0.46), fruit length (0.49, 0.38), fruit diameter (0.60, 0.27), fruits per plant (0.50, 0.17^{NS}), yield per plant (0.66, 0.33); Significantly negative correlated with days to 50% flowering (-0.79, -0.47) and inter-nodal length (-0.66, -0.30), at genotypic and phenotypic levels respectively.Similar results are also reported by Nirosha et al., (2014).

Days taken to 50% flowering exhibited significant positive correlation with inter-nodal length (0.73, 0.35), first fruit node (0.64, 0.45); significant positive correlated with plant height (-0.84, -0.62), branches per plant (-0.79, -0.49), petiolelength (-0.47, -0.44), fruit length (-0.44, -0.28), fruit diameter (-0.49, -0.29), fruits per plant (-0.85, -0.38) and yield per plant (-0.82, -0.60), at both genotypic and phenotypic levels respectively.

Inter-nodal length indicated significant positive relationship with days taken to 50% flowering (0.73, 0.35), first fruit node (0.01, 0.35) and significant negative correlation with plant height (-0.70, -0.44), branches per plant (-0.66, -0.30), petiole length (-0.85, -0.47), fruit length (-0.64, -0.45), fruit diameter (-0.71, 0.33), fruits per plant (-0.87, -0.46) and yield per plant (-0.67, -0.49), at both genotypic and phenotypic levels respectively.

Path coefficients analysis

The path coefficients were computed using the corresponding values of genotypic correlation coefficients, by taking the yield as dependent variable and rest all the characters as independent variable to evaluate and quantify direct as well as indirect effects of contributing characters on yield. The resulted values of path coefficients analysis are depicted in Table 3.0.

Table 3.0: Path coefficients analysis (direct and indirect effect) for different characters in okra

Characters	PH (cm)	BPP	DFF	PL (cm)	INL (cm)	FFN	FL (cm)	FD (cm)	FW (g)	FPP
PH (cm)	**-0.99**	0.20	1.00	-0.13	0.39	-0.04	0.46	-0.08	-0.01	-0.14
BPP	-0.77	**0.25**	0.94	-0.15	0.37	-0.04	0.37	-0.09	-0.12	-0.09
D50%F	0.84	-0.20	**-1.18**	0.10	-0.41	0.06	-0.33	0.07	0.06	0.16
PL (cm)	-0.61	0.17	0.56	**-0.22**	0.48	-0.04	0.47	-0.06	-0.03	-0.14
INL (cm)	0.70	-0.17	-0.86	0.19	**-0.56**	0.05	-0.49	0.11	0.19	0.16
FFN	0.51	-0.12	-0.76	0.10	-0.34	**0.09**	-0.36	0.04	0.09	0.10
FL (cm)	-0.60	0.12	0.52	-0.13	0.36	-0.04	**0.76**	-0.04	-0.09	-0.10
FD (cm)	-0.56	0.15	0.58	-0.08	0.40	-0.03	0.21	**-0.15**	-0.13	-0.03
FW (g)	-0.03	0.08	0.18	-0.01	0.26	-0.02	0.16	-0.05	**-0.41**	0.02
FPP	0.77	0.13	1.01	-0.17	0.49	-0.05	0.43	-0.02	0.04	**0.19**

PH-Plant height, BPP - Branches per plant, DFF- Days to 50% flowering, PL- Petiole length, INL- Inter-nodal length, FFN- First fruit node, FL- Fruit length, FD- Fruit diameter, FW- Fruit weight, FPP- Fruits per plant

Direct effects

Results from path coefficients analysis showed that highest positive direct effect towards yield per plant was contributed by fruit length (0.76) followed by branches per plant (0.25) and fruits per plant (0.19). However, highest negative direct effect towards yield per plant was indicated by days taken to 50% flowering (-1.1) followed by plant height (-0.99), inter-nodal length (-0.56), fruit weight (-0.41), petiole length (-0.22) and fruit diameter (-0.15).Number of fruits per plant had positive direct effect on yield per plant. These results are in confirmation with result ofSyfullah et al., (2018), Ashraf et al., (2020). Fruit per plant had positive direct effect via branches per plant, fruit length, fruit diameter. These results are in confirmation with Ashraf et al., (2020). Rathod et al., (2019) and Umesh et al., (2014) stated that branches per plant had a positive direct effect on fruit yield. Positive direct effect was found by Raval et al., (2019) between fruit yield/plant and fruit length.Similar results were reported by Kumar and Reddy (2016), Yadav et al., (2017), Sundaram V (2015), Umesh et al., (2014)for fruit length. Direct selection practiced for fruit length will result in improvement in yield.Gogineni et al., (2015), Rathod et al., (2019)stated that plant height showed negative direct effect on fruit yield/plant.

Indirect effects

The observations from analysis depicted that plant height had a positive indirect effect on yield per plant via days taken to 50% flowering (0.84), first fruit node (0.51) and negative indirect effect via branches per plant (-0.77), fruits per plant (-0.77), fruit length (-0.60) and fruit diameter (-0.56).Branches per plant had a positive indirect effect on yield per plant via branches per plant (0.25), plant height (0.15), fruit length (0.12), fruit diameter (0.15), fruit yield per plant and negative indirect effect via days taken to 50% flowering (-0.20) and inter-nodal length (-0.17). Days taken to 50% flowering had a positive indirect effect on yield per plant via plant height (1.00), branches per plant (0.94), fruits per plant (1.01), fruit diameter (0.58), fruit length (0.52) and negative indirect effect via inter-nodal length (-0.86) and first fruit node (-0.76). Similarly, petiole length had a positive indirect effect on yield per plant via days taken to 50% flowering (0.10), inter-nodal length (0.19) and negative indirect effect via fruits per plant (-0.17), branches per plant (-0.15), fruit length (-0.13) and plant height (-0.13).Inter-nodal length had a positive indirect effect on yield per plant via fruits per plant (0.49), fruit diameter (0.40), plant height (0.39), branches per plant (0.37), fruit length (0.36) and negative direct effect via days taken to 50% flowering (-0.41) and first fruit node (-0.34). First fruit node had positive indirect effect on yield per plant via inter-nodal length (0.05) and negative indirect effect via fruits per plant (-0.05), branches per plant (-0.04), plant height (-0.04) and fruit diameter (-0.03). First length had positive indirect effect on yield per plant via plant height (0.46), fruits per plant (0.43), branches per plant (0.37), fruit diameter (0.21), fruit weight (0.16) and negative indirect effect via inter-nodal length (-0.49), first fruit node (-0.36) and days taken to 50% flowering (-0.33).Fruit diameter had positive indirect effect on yield per plant via inter-nodal length (0.11) and negative indirect effect via plant height (-0.08), branches per plant (-0.09), fruit weight (-0.05), fruit length (-0.04) and fruits per plant (-0.02). Fruit weight had positive indirect effect on yield per plant via first fruit node (0.09), days taken to 50% flowering (0.06), yield per plant (0.04) and negative direct effect via branches per plant (-0.12) and fruit diameter (-0.13). Fruits per plant had positive indirect effect on yield per plant via days taken to 50% flowering (0.16), inter-nodal length (0.16)), first fruit node (0.10), fruit weight (0.02) and negative indirect effect via plant height (-0.14), fruit length (-0.10), branches per plant (-0.09) and fruit diameter (-0.03). The indirect negative effect of trait was also observed via fruit length. First fruit node had negative indirect effect was through fruit length. These results were also similar to Ariyo et al., (1987).

IV. CONCLUSION

For most of the characters studied, genotypic correlation coefficient estimates were higher than phenotypic correlation coefficient estimates. The fruit yield per plant (g) depicts a significantly positive correlation with number of branches per plant, plant height, petiole length, fruit length, fruit diameter and number of fruits per, which indicated that selection of plants may be done based on these traits per plant. Highest positive direct effect towards yield per plant was attributed by branches per plant (0.25), fruit length (0.76) and first fruit node (0.09). Days taken to 50% flowering had a positive indirect effect on yield per plant mainly via fruits per plant (0.16). The total number of fruits per plant, fruit length, fruit weight, branches per plant and inter-nodal length proved to be the most propitious characters influencing the yield directly as well as indirectly.

ACKNOWLEDGEMENTS

I would like to thank my advisor, co-advisor and other advisory committee members for their invaluable guidance, encouragement, and support throughout this research endeavor. I want to express my heartfelt thanks to my peers and colleagues for their constructive feedback and wonderful collaboration, which enriched the intellectual discourse of this research project. I would also like to extend my sincere gratitude for the support provided by the Department of Vegetable Science, CCS HAU, Hisar. The authors would like to thank the Farm Manager and the team of Teaching and Research Farm, CCS HAU, Hisar, Haryana, for providing all necessary facilities to carry out the research.

REFERENCES

[1] Ahamed, K. U., Akter, B., Ara, N., Hossain, M. F., Moniruzzaman, M. 2015: Heritability, correlation and path coefficient analysis in fifty-seven okra genotypes. *International Journal of Applied Sciences and Biotechnology,* 3(1):127-133.

[2] Al-Jibouri, H. A., Miller, A. R., Robinson, H. F. 1958: Genotypic and environmental variances and co-variances in upland cotton crosses of inter-specific origin. *Journal of Agronomy,* 50:633-637.

[3] Aminu, D., Bello, O. B., Gambo, B. A., Azeez, M. A. 2016: Correlation and path coefficient analysis for fruit yield in okra. *International Journal of Plant Breeding and Genetics,* 10(3):135-142.

[4] Ariyo, O. J., Akenova, M. E., Fatokun, C. A. 1987: Plant character correlations and path analysis of fruit yield in okra. *Euphytica,* 36:677-686.

[5] Ashraf, A. T. M., Rahman, M. M., Hossain, M. M., Sarker, U. 2020: Study of correlation and path analysis in the selected okra genotypes. *Asian Research Journal of Agriculture,* 12:1-11.

[6] Badiger, M., Pitchaimuthu, M., Rao, P. G. 2017: Per se performance, correlation and path coefficient analysis in okra [*Abelmoschusesculentus* (L.) Moench]. *Trends in Biosciences,* 10(18):3314-3317.

[7] Das, S., Chattopadhyay, A., Dutta, S. 2012: Genetic variability and character association in okra. *Vegetable Science,* 39(1):66-69.

[8] Dewey, D., Lu, K. A. 1959: Correlation and path coefficient analysis of components of crested wheatgrass seed production. *Journal of Agronomy,* 51:515-518.

[9] Ghosh, J. S. 2005: Genetic variability and correlation studies in okra [*Abelmoschusesculentus*(L.) Moench]. M.Sc. (Ag.) Thesis, JNKVV, Jabalpur.

[10] Gogineni, S., Arya, K., Issac, S. R., Kuriakose, J. M. 2015: Character association and path analysis for yield and yield components in okra [*Abelmoschusesculentus* (L.) Moench]. *International Journal of Scientific Research,* 4(6):141-143.

[11] Johnson, H. W., Robinson, H. F., Comstock, R. E. 1955: Estimates of genetic and environmental variability in soybeans. *Agronomy Journal,* 47:314-318.

[12] Kerure, P., Pitchaimuthu, M., Hosamani, A. 2017: Studies on variability, correlation and path analysis of traits contributing to fruit yield and its components in okra [*Abelmoschusesculentus* (L.) Moench]. *Electronic Journal of Plant Breeding,* 8(1):134-141.

[13] Kumar, S., Reddy, M. T. 2016: Correlation and path coefficient analysis for yield and its components in okra [*Abelmoschusesculentus* (L.) Moench]. *Advances in Agricultural Science,* 4(4):72-83.

[14] Niranjan, R. S., Mishra, M. N. 2004: Correlation and path analysis in okra [*Abelmoschusesculentus* (L.) Moench]. *Progressive Horticulture,* 35(2):192-195.

[15] Nirosha, K., Vethamoni, P. I., Sathiyamurthy, V. A. 2014: Correlation and path analysis studies in okra [*Abelmoschusesculentus* (L.) Moench]. *Agriculture Science Digest,* 34(4):313-315.

[16] Purquerio, L. F. V., Lago, A. A., Passos, F. A. 2010: Plant growth and yield of okra in relation to plant density. *HorticulturaBrasileira,* 28(1):72-76.

[17] Rathod, S., Parmar, V. L., Patel, A. I. 2019: Correlation and path coefficient analysis for quantitative traits in F_2 population in okra [*Abelmoschusesculentus* (L.) Moench]. *International Journal of Chemical Studies,* 7(5):1030-1033.

[18] Raval, V., Patel, A. I., Vashi, J. M., Chaudhary, B. N. 2019: Correlation and path analysis studies in okra [*Abelmoschusesculentus* (L.) Moench]. *International Journal of Chemical Studies,* 7(1):1230-1233.

[19] Reddy, M. T., Begum, H., Sunil, N., Reddy, B. P. 2013: Temperature stress effects in okra [*Abelmoschusesculentus* (L.)]. *Journal of Vegetable Science,* 40(2):87-91.

[20] Salih, A. A., Mansoor, A. H. 2019: Origin, distribution and importance of okra [*Abelmoschusesculentus* (L.)]. *International Journal of Agricultural Research,* 14(3):102-108.

[21] Samim, M., Ahmed, I., Ahmed, S., Saha, S. 2018: Nutritional and medicinal value of okra [*Abelmoschusesculentus* (L.)]. *Journal of Pharmacognosy and Phytochemistry,* 7(2):238-241.

[22] Saryam, D. K. 2012: Genetic divergence in okra [*Abelmoschusesculentus* (L.) Moench]. M.Sc. (Agri) Thesis, Jawaharlal Nehru KrishiVishwavidyalaya, Jabalpur.

[23] Shivaramegowda, K. D., Krishnappa, M., Ramesh, S. 2016: Genetic variability, heritability and genetic advance studies in okra [*Abelmoschusesculentus* (L.) Moench]. *Environment and Ecology,* 34(2A):678-681.

[24] Siemonsma, J. S., Kouame, C. 2004: Vegetables in plant resources of tropical Africa. *International Journal of Applied Sciences and Biotechnology,* 4(5):532-538.

[25] Somashekhar, G. H. D., Mohan, K., Salimath, P. M. 2011: Genetic analysis of association studies in segregating population of okra. *Karnataka Journal of Agricultural Sciences,* 24(4):432-435.

[26] Sundaram, V. 2015: Genetic analysis in bhendi [*Abelmoschusesculentus* (L.) Moench]. *Agricultural Science Digest,* 35(3):233-236.

[27] Syfullah, K., Sani, M. N. H., Nasif, S. O., Parvin, S., Rony, M. M. H., Islam, Hossain, M. S. 2018: Genetic variability, heritability, character association and morphological diversity in okra [*Abelmoschusesculentus* (L.) Moench]. *International Journal of Plant and Soil Science,* 25(6):1-11.

[28] Umesh, C. P. S., Singh, D. P., Pandey, V., Singh, S. 2014: Correlation and path analysis of yield and yield contributing traits in okra [*Abelmoschusesculentus* (L.) Moench]. *Progressive Horticulture,* 46(2):349-353.

[29] Verma, V., Singh, S. 2020: Correlation and path coefficient analysis of quantitative characters in okra [*Abelmoschusesculentus* (L.) Moench]. *International Journal of Chemical Studies,* 8(6):206-208.

[30] Yadav, R. K., Kumar, M., Pandiyaraj, P., Nagaraju, K., Kaushal, A., Syamal, M. M. 2017: Correlation and path analyses for fruit yield and its component traits in okra [*Abelmoschusesculentus* (L.) Moench] genotypes. *International Journal of Agriculture Sciences,* 9(13):4063-4067.

International Journal of Environment, Agriculture and Biotechnology
Vol-11, Issue-2; Mar-Apr, 2026
Peer-Reviewed International Journal
Journal Home Page Available: https://ijeab.com/
Journal DOI: 10.22161/ijeab

Comparative Evaluation of Commercial Pomegranate (*Punica granatum* L.) Cultivars under Semi-Arid Conditions of Western Maharashtra, India

Shankar R. Bhosale[1 2*], Shilpa Parashuram[1], M. N. Jagtap[3], A. R. Girme[1], T.H. Daphale[1], R. A. Marathe[1]

[1]ICAR–National Research Centre on Pomegranate, Solapur–413255, Maharashtra, India
[2]School of Life Sciences, Punyashlok Ahilyadevi Holkar Solapur University, Solapur, Maharashtra, India
[3]Santhosh Bhimrao Patil Arts, Commerce, and Science College, Mandrup, Solapur, Maharashtra, India
Email: bhosaleshankar652@gmail.com
*Corresponding author- Shankar R. Bhosale

Received: 27 Jan 2026; Received in revised form: 25 Feb 2026; Accepted: 03 Mar 202; Available online: 10 Mar 2026

***Abstract*— *Pomegranate (Punica granatum L.) is an important fruit crop cultivated widely in the semi-arid regions of India, particularly in Western Maharashtra. Identifying suitable cultivars that perform well under these climatic conditions is essential for improving productivity and fruit quality. A field experiment was conducted under semi-arid conditions at the ICAR–National Research Centre on Pomegranate, Solapur, to comparatively evaluate five commercially grown cultivars: Bhagwa, Super Bhagwa, Solapur Lal, Sharad King, and Ganesh. The study was carried out using a randomized block design (RBD) with four replications. Observations were recorded on vegetative growth, flowering behavior, fruit yield, and important fruit quality attributes. The results revealed significant differences among the cultivars for most of the parameters studied. Among the evaluated cultivars, Bhagwa produced the longest new shoots (32.10 cm), recorded the highest fruit yield (25.10 kg per plant), and exhibited superior juice recovery (51.20%). Solapur Lal showed comparatively higher total soluble solids (16.50 °Brix), indicating better fruit sweetness and quality. In contrast, the traditional cultivar Ganesh showed comparatively lower performance in several growth, yield, and quality parameters. Overall, the results suggest that improved cultivars, such as Bhagwa and Solapur Lal, are better suited to cultivation under the semi-arid agro-climatic conditions of Western Maharashtra and can contribute to enhanced productivity and improved fruit quality in commercial pomegranate production.*

Keywords*— *Pomegranate, cultivars, semi-arid climate, yield, fruit quality, Bhagwa, Solapur Lal, Super Bhagwa.

I. INTRODUCTION

Pomegranate (*Punica granatum* L.) belongs to the family Lythraceae (2n = 16) and is an economically important fruit crop cultivated widely across tropical and subtropical regions (Holland et al., 2009). Commonly called the "Carthaginian apple" or the "Fruit of Paradise," it is considered one of the oldest and most versatile fruit crops in the world. The crop is thought to have originated in the area stretching from Iran to the Himalayas in northern India, from where its cultivation gradually spread to the Mediterranean basin and other tropical and subtropical regions (Özgüven et al., 2009). In India, pomegranate has become a high-value commercial fruit crop and plays a key role in improving farmers' livelihoods, especially in arid and semi-arid areas (Chandra et al., 2010). Its strong drought tolerance and adaptability to a variety of soil types make it suitable for cultivation in regions with limited water supply (Al-Mansour et al., 2025).

Maharashtra leads India's pomegranate industry, accounting for over 70% of the nation's total production. (Varpe et al., 2025) The state of Western Maharashtra, including Solapur, Sangli, Nashik, and Ahmednagar, has become the country's "pomegranate hub". (Kaur, 2025) The semi-arid climate of this region, marked by high temperatures, low rainfall, and low humidity, creates ideal conditions for growing high-quality pomegranates. (Patil et al., 2018) However, maintaining this success relies heavily on selecting cultivars that can maximize both yield and quality under these specific climatic conditions (Horticulture Statistics Division, 2021).

Historically, the 'Ganesh' cultivar, developed at the Ganeshkhind Fruit Experiment Station in Pune, revolutionized pomegranate cultivation in India thanks to its soft seeds and sweet flavor. (Popular Guava and Pomegranate Varieties in India, 2024) While Ganesh was the industry standard for decades, the demand for better fruit color, higher yield, and longer shelf life led to the introduction of the 'Bhagwa' variety. Bhagwa quickly became the preferred choice for export markets because of its glossy red skin and resistance to fruit cracking. (Pomegranate Varieties in India for Export: A Gateway to Global Markets, 2023). Despite Bhagwa's success, the agricultural scientific community continues to seek varieties with improved nutritional profiles, greater resistance to bacterial blight (*Xanthomonas axonopodis* pv. punicae), and better fruit recovery (Jalikop et al., 2010).

In recent years, several new cultivars and selections such as Super Bhagwa, Solapur Lal, and Sharad King have been introduced to the market. Bhagwa is often praised for its larger fruit size and higher productivity compared to Super Bhagwa. Solapur Lal, developed through rigorous breeding programs by the National Research Centre on Pomegranate, is promoted for its high antioxidant content and vibrant red arils (Babu et al., 2022). Sharad King, another promising selection, has gained popularity among local growers for its excellent fruit retention and juice recovery (Shilpa et al., 2024; Biswas, 2025). Despite their availability, there is a significant research gap in a comprehensive, direct comparison of these newer cultivars under the specific microclimatic conditions of Western Maharashtra.

The vegetative growth of a pomegranate tree, defined by parameters such as shoot length, leaf count, and leaf area, is the foundation of its reproductive success. Strong vegetative growth supports a high photosynthetic rate, which in turn leads to better flowering and fruit production (Xie et al., 2008). Studies have shown that semi-arid conditions can significantly reduce vegetative vigor if the cultivar is not well-adapted (Babu et al., 2011). Additionally, pomegranate flowering behavior is complex, involving male, hermaphrodite (bisexual), and intermediate flowers. The ratio of hermaphrodite flowers, which are the only ones that develop into fruits, is highly sensitive to temperature and nutrient management (Ikram et al., 2022). Identifying cultivars that naturally produce a higher percentage of hermaphrodite flowers in semi-arid environments is essential for maintaining stable yields (Pareek et al., 2015).

Yield performance is the main benchmark for any commercial cultivar. In a semi-arid environment, yield depends not only on the number of fruits per plant but also on individual fruit weight and total tonnage per acre. Export-focused farming requires fruits to meet specific weight categories (typically 250g to 400g). (Pomegranate Exporter from India | Mahavir Export, n.d.) Varieties that do not reach these weight benchmarks even under optimal management pose a financial risk to the farmer. Therefore, assessing the yield potential of Bhagwa and Sharad King compared to traditional Super Bhagwa and Ganesh is an urgent economic concern for the region's growers (Sheikh, 2006).

Beyond physical yield, the fruit's internal quality, as measured by Total Soluble Solids (TSS), sugar content, and juice recovery, determines its marketability for both fresh consumption and processing. High TSS values (expressed in °Brix) indicate sweetness, which is a primary consumer preference in India (Pons-Gómez et al., 2024). Similarly, juice recovery percentage is a critical factor for the growing pomegranate processing industry (Chandra et al., 2013). Cultivars such as Solapur Lal have been bred to improve these internal quality parameters, but their performance must be validated alongside established commercial varieties (NRC Pomegranate, 2019).

The present study, titled "Comparative Evaluation of Commercial Pomegranate (*Punica granatum* L.) Cultivars under Semi-Arid Conditions of Western Maharashtra," was designed to address these research needs. The main objective is to systematically document the vegetative growth, flowering patterns, yield potential, and physical-chemical quality of five leading cultivars: Bhagwa, Super Bhagwa, Solapur Lal, Sharad King, and Ganesh. Through this comparative analysis, the research aims to provide farmers, exporters, and scientists with data-driven recommendations on which cultivars are best suited for the challenging yet rewarding climate of Western Maharashtra.

In conclusion, as the global demand for pomegranates continues to increase due to their recognized health benefits—including high levels of Vitamin C, polyphenols, and anti-inflammatory properties—the need for high-quality cultivars becomes crucial. (Bioactive compounds and health benefits of pomegranate: An updated narrative review, 2023) This research provides a scientific basis for cultivar selection, helping the pomegranate industry in Western Maharashtra remain competitive, sustainable, and profitable amid evolving agricultural challenges.

II. MATERIALS AND METHODS

2.1 Experimental Site and Location

The research was carried out at the National Research Centre on Pomegranate (NRCP) in Solapur, Maharashtra, India. The experimental site is situated at 17°10′ N latitude and 74°42′ E longitude, at an elevation of 483.5 meters above sea level. The study took place in the center's experimental orchards and Fruit Culture Laboratory.

The region receives an average yearly rainfall of 550-650 mm, which is often unpredictable and unevenly distributed. Summers are characterized by high temperatures, with average maximums ranging from 38 to 42°C, while winters have average minimums between 10 and 15°C. Relative humidity usually varies from 35 to 70 percent, depending on the season. The soil at the experimental site is primarily medium-black (Vertisol), with a pH range of 7.5 to 8.2**,** making it suitable for pomegranate cultivation. These conditions reflect the typical semi-arid climate of Western Maharashtra.

2.2 Experimental Material and Design

The present investigation evaluated five commercially important pomegranate cultivars: Bhagwa, Super Bhagwa, Solapur Lal, Sharad King, and Ganesh, with Ganesh as the control variety. The field trial was arranged in a Randomized Block Design (RBD) with four replications at a standard spacing of 4.5 m by 3.0 m. The research was conducted during the 2024-2025 season under Ambe Bahar's management. Water stress was imposed in December 2024, followed by the first irrigation (Bahar initiation) in the first week of January 2025 to induce uniform flowering. Standard agricultural practices, including drip irrigation, pruning, and integrated nutrient management, were consistently applied in accordance with ICAR-NRCP guidelines.

2.3 Sampling and Data Collection

To ensure statistical accuracy, twenty (20) shoots were randomly selected and tagged from each plant across all replications for recording vegetative and reproductive observations. For the evaluation of fruit physical and chemical characteristics, ten (10) representative fruits from each variety were harvested at physiological maturity based on skin color and the characteristic metallic sound upon tapping.

2.4 Morphological and Vegetative Parameters

Vegetative growth was evaluated using the following parameters:

- **Plant Architecture:** Plant height (cm), number of primary branches, and number of secondary branches were recorded.
- **Shoot and Foliage:** Shoot length (cm) and the total number of leaves per shoot were measured.
- **Leaf Area:** Total leaf area per shoot (cm²) was calculated for the tagged shoots using a digital leaf area meter.

2.5 Reproductive and Yield Parameters

- Observations on flowering and fruit development were recorded during the Ambe Bahar (January to July 2025) on the tagged shoots:
- **Flowering:** The total number of flowers per shoot and the number of hermaphrodite flowers were recorded from January to March 2025.
- **Fruit set (%):** Fruit set per shoot was calculated using the following formula:

$$\text{Fruit Set }(\%) = \frac{\text{Total number of fruits set per shoot}}{\text{Total number of flowers per shoot}} X\ 100$$

- **Yield:** Harvesting was carried out in June-July 2025. The total fruits per plant and the yield per plant (kg) were recorded at harvest. The total yield per hectare (t/ha) was calculated based on the total number of plants per hectare.

2.6 Fruit Quality Evaluation:

Ten mature, healthy fruits from each cultivar were randomly selected and analyzed in the lab to assess fruit quality parameters.

Physical Traits: Fruit weight (g) was recorded using a digital weighing scale. The fruits were manually separated to obtain arils, and the aril weight (g) was measured with the same electronic scale. Juice recovery (%) was calculated by manually extracting juice from arils using a hand juicer, and the volume of juice was measured with a graduated cylinder.

- **Aril (%):** Calculated as:

$$\text{Aril }(\%) = \frac{\text{Total weight of arils (g)}}{\text{Total Fruit weight (g)}} X\ 100$$

- **Juice Recovery (%):** Calculated as:

$$\text{Juice Recovery }(\%) = \frac{\text{Weight of extracted juice (g)}}{\text{Total weight of arils (g)}} X\ 100$$

- **Titratable Acidity (%):** Determined by titrating a known volume of juice against 0.1N sodium hydroxide (NaOH) using phenolphthalein as an internal indicator. The persistent light pink color identified the endpoint. AOAC (2005). The acidity was calculated using the following formula:

$$\text{Titratable Acidity } (\%) = \frac{\text{Titre value} \times \text{Normality of NaOH} \times \text{Equivalent weight of citric acid}}{\text{Volume of sample}} X\ 100$$

- **Biochemical Traits:** TSS (°Brix) was measured with a digital refractometer calibrated to 20°C. Total sugars (%) were estimated using the Lane and Eynon method, and the TSS/acid ratio was calculated. Ranganna (1986)

2.7 Statistical Analysis

The data were analyzed statistically using the Web-based Agricultural Statistics Software Package (WASP 2.0) developed by ICAR-CCARI, Goa. An Analysis of Variance (ANOVA) for a Randomized Block Design (RBD) was used to examine differences among cultivars. The Critical Difference (CD) at a 5% significance level ($P \leq 0.05$) and the Standard Error of the Mean (SEm ±) were calculated to evaluate treatment means.

III. RESULTS AND DISCUSSION

The performance of five commercial pomegranate cultivars differed markedly in vegetative growth, flowering patterns, yield characteristics, and fruit quality under the semi-arid conditions of Western Maharashtra. The analysis of variance showed statistically significant differences among cultivars for all traits studied, indicating a strong genotypic influence in moisture-limited environments (Babu et al., 2011; Prasad et al., 2003).

3.1 Vegetative Growth Performance

Vegetative parameters differed significantly among cultivars. Bhagwa recorded the greatest shoot length (32.10 cm), followed by Sharad King (31.45 cm) and Super Bhagwa (30.93 cm), while the traditional cultivar Ganesh had the shortest shoot length (28.38 cm). Similarly, the number of leaves per shoot was highest in Bhagwa (62.40), indicating greater vegetative vigor. Total leaf area per shoot also followed this trend, with Bhagwa measuring 655.20 cm² compared to 465.32 cm² in Ganesh (Table no. 1, Fig 1).

The higher vegetative growth in Bhagwa may be due to its improved genetic potential and better adaptation to semi-arid stress conditions (Marathe & Babu, 2015; Mane & Shinde, 2020). Increased leaf area enhances photosynthetic efficiency, supporting better reproductive development and yield (Chandra et al., 2010). Similar variations in vegetative vigor across cultivars have been documented in other fruit crops under semi-arid conditions. For instance, in Guava (*Psidium guajava* L.), significant genotypic differences in plant height and canopy spread were observed across 18 genotypes, with superior vegetative growth directly correlating with higher fruit yield (Yadav et al., 2022). Likewise, studies on Ber (*Ziziphus mauritiana* Lamk.) revealed that cultivars such as 'Karela' and 'Delhi White' exhibited higher leaf area and shoot vigor than others, suggesting that genetic makeup plays a primary role in resource acquisition under abiotic stress (Bhatti et al., 2021). These findings reinforce the importance of selecting vigorous genotypes for sustainable production in arid ecosystems.

Table 1: Vegetative Growth Parameters of Pomegranate Cultivars

Cultivar	Length of New Shoot (cm)	No. of Leaves per Shoot	Total Leaf Area per Shoot (cm²)
Super Bhagwa	30.93	59.36	630.97
Bhagwa	32.1	62.4	655.2
Solapur Lal	29.5	56.8	590.4
Sharad King	31.45	60.15	642.3
Ganesh (Control)	28.38	43.76	465.32
SE m (±)	0.85	1.2	12.45
CD (5%)	2.54	3.58	36.12
CV (%)	5.2	4.8	6.15

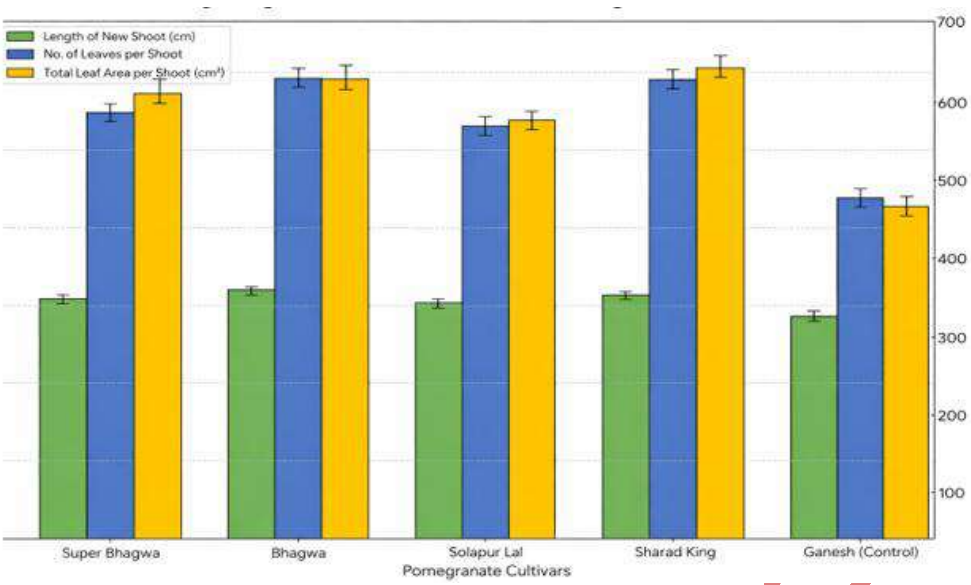

Fig 1. Comparative analysis of shoot length among pomegranate cultivars.

3.2 Flowering Behavior

Flowering dynamics significantly influenced yield performance. Bhagwa recorded the highest number of hermaphrodite flowers per shoot (20.15), closely followed by Sharad King (19.80) and Solapur Lal (19.50) (Shilpa et al., 2024). In contrast, Ganesh produced a comparatively higher number of male flowers (15.60) and fewer hermaphrodite flowers (14.30), which negatively affected fruit set. The fruit set per shoot was maximum in Bhagwa (10.80) and Sharad King (10.10), while Ganesh showed the lowest fruit set (7.20). Similarly, fruit retention per shoot was significantly higher in Super Bhagwa (7.45) compared to Ganesh (4.90). (Table no. 2, Fig 2). Since only hermaphrodite flowers develop into fruits, a higher proportion of hermaphrodite flowers directly contributed to increased yield potential in improved cultivars (Nimbalkar et al., 2017). The superior flowering efficiency of Bhagwa and Sharad King was noted, indicating better physiological stability and reproductive adaptability under semi-arid conditions (Shilpa et al., 2024).

Similar results regarding flowering phenology have been reported in other fruit species. In Acid Lime (*Citrus aurantifolia* Swingle), researchers found that different genotypes exhibited a wide range of flowering durations and flower types, where cultivars with a higher percentage of perfect flowers significantly out-yielded those with more staminate flowers (Desai et al., 2023). Furthermore, studies in Mango (*Mangifera indica* L.) have demonstrated that cultivars such as 'Amrapali' exhibit higher flowering intensity and lower sex ratios (more hermaphrodite flowers) than traditional varieties, suggesting a similar genetic advantage in reproductive efficiency under tropical stress (Reddy & Kurian, 2022).

Table 2: Flowering and Fruiting Behaviour of Pomegranate Cultivars

Cultivar	Male Flowers / Shoot	Hermaphrodite Flowers / Shoot	Fruits Set / Shoot	Fruits Retained / Shoot
Super Bhagwa	12.45	18.2	9.35	6.1
Bhagwa	11.9	20.15	10.8	7.45
Solapur Lal	13.1	19.5	9.85	6.8
Sharad King	12.05	19.8	10.1	7.2
Ganesh (Control)	15.6	14.3	7.2	4.9
SE m (±)	0.42	0.58	0.31	0.22
CD (5%)	1.25	1.72	0.92	0.65
CV (%)	6.12	5.85	7.3	6.95

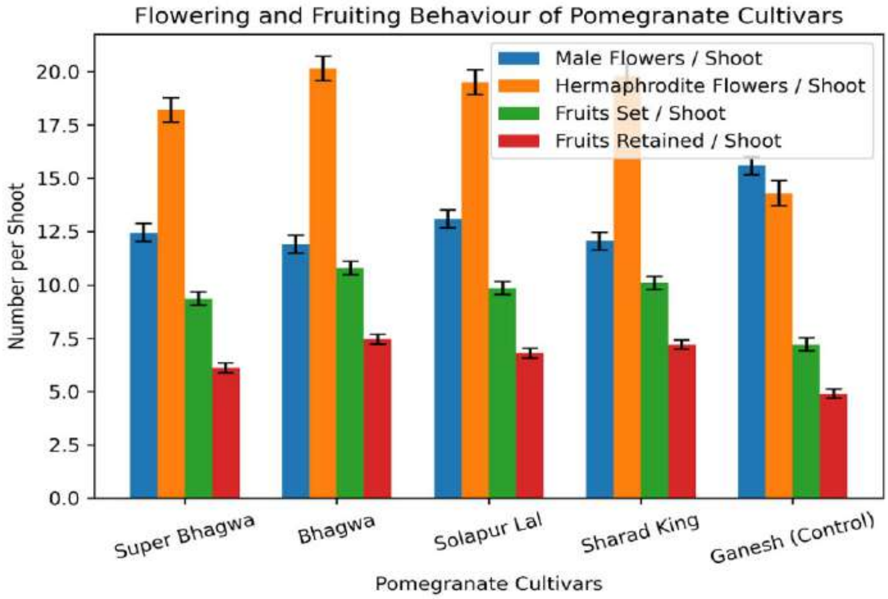

Fig. 2: Flowering behavior (Male vs. Hermaphrodite flowers) of selected cultivars.

3.3 Yield and Yield Attributes

Yield parameters showed highly significant differences among cultivars. Bhagwa recorded the highest number of fruits per plant (82.20) and the maximum yield per plant (25.10 kg), resulting in the highest estimated yield for Bhagwa (18.57 t/ha). Sharad King ranked second with 18.01 t/ha, followed by Super Bhagwa (16.58 t/ha) and Solapur Lal (16.13 t/ha) (Mane & Shinde, 2020; Shinde et al., 2018). Ganesh recorded the lowest yield (12.21 t/ha) (Table no. 3, Fig 3).

The higher yield in Bhagwa can be attributed to its superior vegetative growth, higher hermaphrodite flower production, better fruit retention, and increased fruit weight. Yield in pomegranate under semi-arid conditions is largely dependent on the cultivar's ability to balance vegetative and reproductive growth under limited water availability. The traditional cultivar Ganesh showed reduced performance, indicating comparatively lower adaptability to current climatic stresses (Babu et al., 2011).

These findings are consistent with recent multi-location trials in similar agro-climatic zones. For instance, (Jadhav et al., 2023) evaluated pomegranate genotypes on the Deccan Plateau and found that ' Bhagwa' consistently outperformed 'Ganesh' and 'Mridula' in fruit retention and total biomass accumulation, attributing this to a more robust root system and higher water-use efficiency (WUE). Similarly, Gaikwad and Patil (2022) reported that the yield gap between traditional and improved cultivars like 'Solapur Lal' and ' Bhagwa' widens under high-temperature stress during the *mrig bahar* flowering season, as improved selections exhibit significantly lower flower drop and better pollen viability. These results reinforce the conclusion that genetic improvement in pomegranate has successfully targeted physiological resilience alongside raw yield potential, making newer cultivars more suitable for the evolving semi-arid landscape of Western Maharashtra.

Table 3: Yield Performance of Pomegranate Cultivars

Cultivar	Fruits / Plant	Yield / Plant (kg)	Estimated Yield (t/ha)
Super Bhagwa	78.5	22.4	16.58
Bhagwa	82.2	25.1	18.57
Solapur Lal	75.15	21.8	16.13
Sharad King	80.4	24.35	18.01
Ganesh (Control)	65.3	16.5	12.21
SE m (±)	1.45	0.55	0.48
CD (5%)	4.32	1.64	1.43
CV (%)	5.1	6.25	6.4

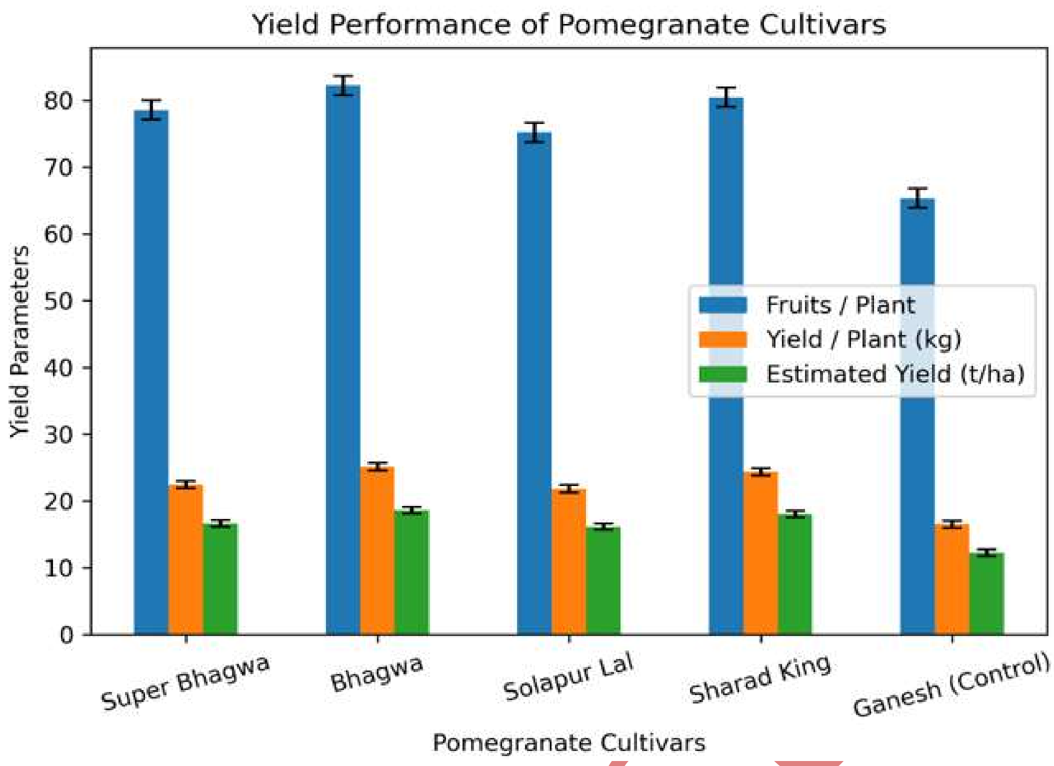

Fig. 3: Estimated yield (t/ha) of pomegranate cultivars under semi-arid conditions.

3.3.1 Observations on Disease Incidence

- The field evaluation included monitoring for Bacterial Blight (*Xanthomonas axonopodis* pv. punicae), which is a major constraint in the region.
- Bhagwa and Solapur Lal showed lower disease incidence on foliage and fruits compared to the control.
- Solapur Lal, specifically bred for high performance, exhibited minimal leaf spot development. (Babu et al., 2011).
- The traditional cultivar Ganesh was found to be the most susceptible to climatic and biotic stresses under the experimental conditions.

3.4 Fruit Physical and Quality Parameters

Significant differences were observed in fruit physical and biochemical attributes (Table 4). Bhagwa produced the heaviest fruits (315.60 g) and the highest aril weight (205.80 g), along with superior juice recovery (51.20%). Sharad King also performed well in fruit weight (305.20 g) and juice recovery (50.40%) (Shilpa et al., 2024). Solapur Lal excelled in chemical quality, recording the highest Total Soluble Solids (16.50 °Brix), followed closely by Bhagwa (16.20 °Brix) (Babu et al., 2011). The control cultivar Ganesh recorded comparatively lower fruit weight (252.10 g), juice recovery (44.10%), and TSS (15.10 °Brix). (Table no. 4, Fig 4 and Fig. 5). Higher TSS values indicate increased sweetness and consumer acceptance, while greater juice recovery enhances processing suitability (Pareek et al., 2015; Tehranifar et al., 2010). The improved fruit quality in Bhagwa and Solapur Lal indicates advancements in genetic improvement aimed at meeting export standards and market demand (Mane & Shinde, 2020).

Similar findings of superior biochemical profiles in improved cultivars have been observed in other recent pomegranate studies. For example, Thorat et al. (2023) evaluated promising pomegranate hybrids in Western India. They noted that selections like 'Solapur Lal' consistently maintain higher TSS and lower acidity compared to 'Ganesh' under high-temperature stress, which they attributed to efficient sugar-acid metabolism and pigment stability. Additionally, More and Deshmukh (2022) reported that juice recovery percentages in 'Bhagwa' were significantly higher than in traditional varieties due to a lower rind-to-aril ratio and larger juice vesicles. Studies in other Mediterranean-type fruit crops support these results; for instance, in Fig (*Ficus carica* L.), newer selections for semi-arid zones have shown a 15-20% increase in TSS over indigenous landraces, highlighting a broad trend where modern breeding successfully bridges the gap between environmental resilience and high-quality consumer produce (Rao et al., 2024).

Table 4: Fruit physical and quality parameters

Cultivar	Fruit Weight (g)	Aril Weight (g)	100 Aril Weight (g)	Juice Recovery (%)	TSS (°Brix)	Total Sugars (%)
Super Bhagwa	285.4	182.5	32.1	48.5	15.8	13.2
Bhagwa	315.6	205.8	34.5	51.2	16.2	14.1
Solapur Lal	290.15	188.4	31.8	49.3	16.5	13.8
Sharad King	305.2	198.6	33.7	50.4	15.95	13.5
Ganesh (Control)	252.1	155.3	28.5	44.1	15.1	12.8
SE m (±)	5.24	3.85	0.65	0.95	0.28	0.22
CD (5%)	15.42	11.32	1.91	2.78	0.82	0.64
CV (%)	4.85	5.2	5.4	4.15	3.9	4.1

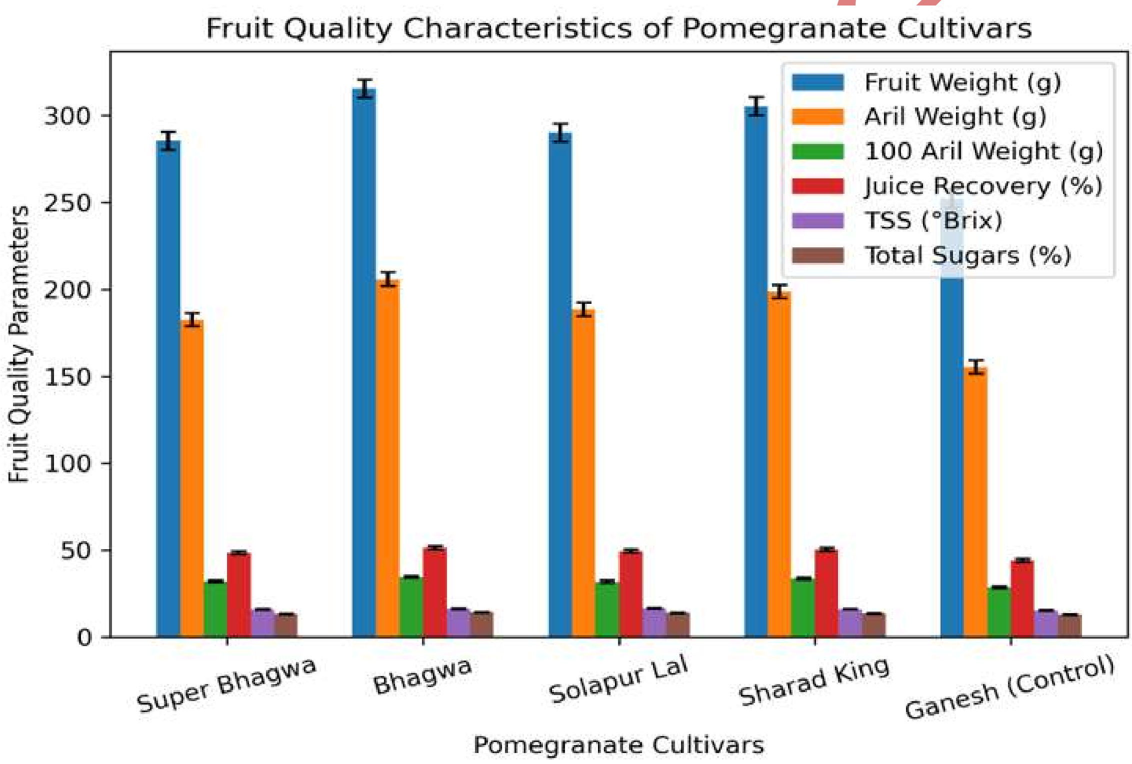

Fig. 4: Comparison of fruit weight (g) among commercial pomegranate cultivars.

3.5 Yield and Economic Impact

Yield performance is the key indicator of commercial success in pomegranate cultivation (Sheikh, 2006). In this study, Bhagwa achieved the highest estimated yield of 18.57 t/ha, significantly surpassing Ganesh, which recorded 12.21 t/ha. The superior performance of improved cultivars over traditional varieties under semi-arid conditions has also been documented in regional evaluations (Mane & Shinde, 2020; Shinde et al., 2018).

The financial return from pomegranate cultivation is directly impacted by yield potential and current market prices. Recent horticultural statistics show that the adoption of improved cultivars greatly increases farmers' earnings in semi-arid areas (Horticulture Statistics Division, 2021; NHB, 2023). With an average market price of ₹80 per kg for export-quality fruits, Bhagwa can potentially generate a gross income of around ₹14,85,600 per hectare. In comparison, Ganesh yields about ₹9,76,800 per hectare, offering an additional income of nearly ₹5,08,800 per hectare by choosing Bhagwa.

Furthermore, the higher fruit weight of Bhagwa (315.60 g) improves its export potential and grading advantage over Ganesh (252.10 g). Fruit size, weight, and overall quality remain the most important factors influencing international market acceptance, consumer preference, and grower profitability in the current pomegranate trade. Recent studies highlight that improved cultivars with better physical traits not only command higher market prices but also show greater resilience during long-distance transport, which is crucial for export-oriented cultivation (Varpe et al., 2025). These findings support recommendations for adopting high-yielding, heavy-fruiting varieties in semi-arid regions to maximize economic benefits. They also endorse cultivar replacement strategies to enhance economic sustainability in semi-arid pomegranate production systems (ICAR-NRCP, 2024).

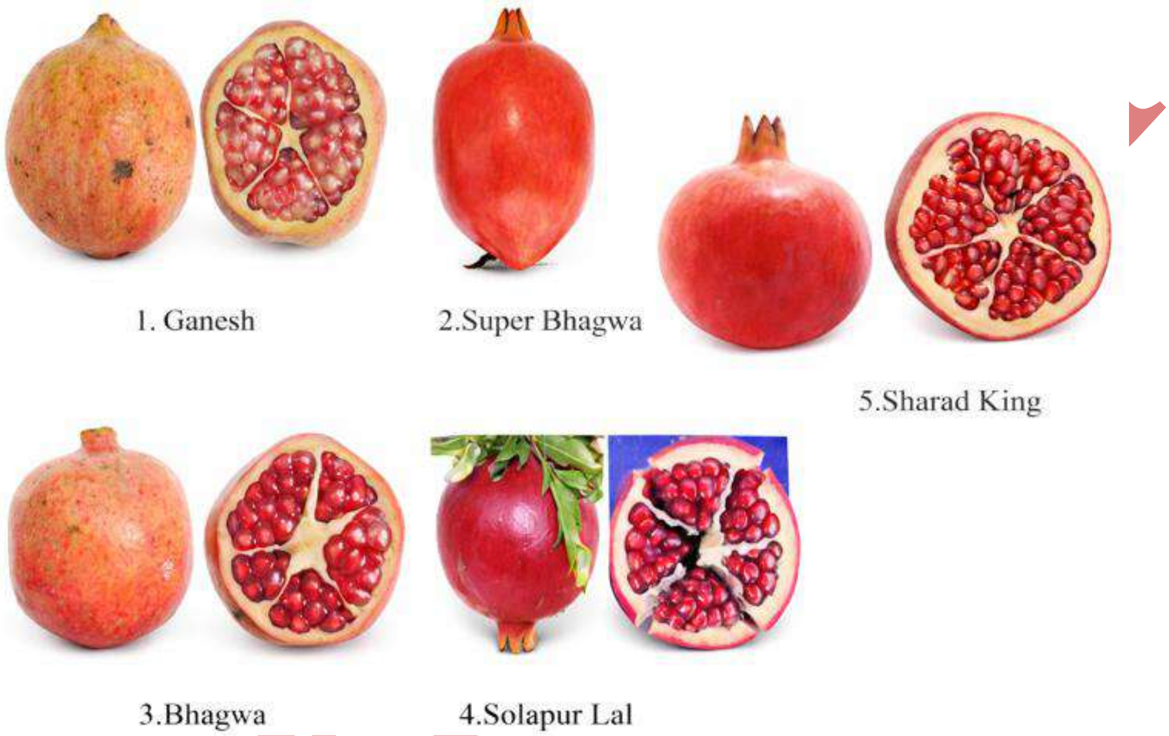

Fig. 5. Morphological comparison of major commercial pomegranate cultivars evaluated under semi-arid conditions. (1) Ganesh, (2) super Bhagwa, (3) Bhagwa, (4) Solapur Lal, and (5) Sharad king showing external fruit appearance and internal aril characteristics.

IV. CONCLUSION

A comparative evaluation clearly indicates that the Improved cultivars, such as Bhagwa and Solapur Lal, demonstrated superior adaptability to semi-arid agro-climatic conditions of Western Maharashtra than the traditional Ganesh variety. Based on a comprehensive analysis of growth, yield, and quality parameters, the following conclusions are drawn:

Bhagwa is the top-recommended cultivar for commercial growers aiming for maximum yield (18.57 t/ha) and large fruit size (315.60 g). Its higher fruit weight and yield potential can increase farmer profits by over 40–50% per hectare compared to traditional cultivars. Fruit quality parameters, such as total soluble solids, acidity, and aril characteristics, are key factors influencing consumer acceptance of pomegranates (Chater et al., 2023).

- Sharad King is a strong alternative, with a high yield (18.01 t/ha) and excellent fruit retention (Shilpa et al., 2024).
- Solapur Lal is highly suitable for farmers and the processing industry, emphasizing juice quality, antioxidant content, and sweetness (16.50 °Brix) (Babu et al., 2011).
- The study also indicates that newer cultivars, such as Bhagwa and Solapur Lal, show improved field tolerance to biotic stresses, ensuring more consistent returns (NRCP Annual Report 2023).

Overall, the strategic adoption of Bhagwa and Solapur Lal can significantly enhance the productivity, export potential, and profitability of pomegranate farming in Maharashtra's semiarid regions (Varpe et al., 2025).

ACKNOWLEDGMENT

The authors sincerely thank Punyashlok Ahilyadevi Holkar Solapur University, Solapur, and the School of Life Sciences for their academic support. We are also very grateful to the Director of ICAR–National Research Centre on Pomegranate (ICAR–NRCP), Solapur, for providing the essential field and laboratory facilities needed for this research. Special thanks to Dr. Shilpa Parashuram, scientist at ICAR–NRCP, Solapur, for her invaluable technical guidance and ongoing supervision throughout the study. We also sincerely thank Dr. M. N. Jagtap, principal of Santosh Bhimrao Patil Arts, Commerce, and Science College, Mandrup, and research guide, for his academic guidance and encouragement. Finally, the authors gratefully acknowledge the financial support from SARTHI, Pune, through the Chhatrapati Shahu Maharaj National Research Fellowship (CSMNRF).

CONFLICT OF INTEREST

The authors state that there is no conflict of interest related to the publication of this research manuscript.

REFERENCES

[1] Al-Mansour, F., Al-Harbi, L., & Al-Omari, A. (2025). Soil-geology interactions in pomegranate cultivation: Case studies from arid landscapes. *International Journal of Geography*, 7(9), pp. 136–141. https://doi.org/10.4236/ijgge.2025.79017

[2] Babu, D., Singh, N. V., Maity, A., & Sharma, J. (2022). New Biofortified Pomegranate Variety 'SOLAPUR LAL'. ICAR-National Research Centre on Pomegranate. [Online]. Available: https://dalimbmitra.com/wp-content/uploads/2022/02/Solapur-Lal-.pdf

[3] Babu, K. D., Chandra, R., & Jadhav, V. T. (2011). Morphological and physico-chemical characteristics of pomegranate cultivars. *Indian Journal of Horticulture*, 68(2), pp. 172-176.

[4] Bhatti, A., et al. (2021). Assessment of diverse Ber cultivars in response to nutrient management practices for growth and yield under semi-arid conditions. *Journal of Arid Agriculture*, 14(1), pp. 95-102.

[5] Biswas, P. (2025). How a Maharashtra farmer chanced upon an export-quality pomegranate variety that changed the market trend. *The Indian Express*.

[6] Chandra, R., Babu, K. D., Jadhav, V. T., & Sharma, J. (2010). Pomegranate research in India - A review. *Fruit Science Reports*, 34(1), pp. 5-21.

[7] Chandra, R., et al. (2013). Variability studies of physico-chemical properties of pomegranate (*Punica granatum* L.) using a scoring technique. *Fruits*, 68(2), pp. 159-166. https://doi.org/10.1051/fruits/2013003

[8] Chater, J. M., Garner, L. C., & Crisosto, C. H. (2023). Factors influencing fruit quality and splitting in pomegranate (*Punica granatum* L.). *Journal of Horticultural Science*, 58(2), pp. 159–166.

[9] Desai, P. B., et al. (2023). Reproductive phenology and sex expression in acid lime (*Citrus aurantifolia*) genotypes under western conditions. *Journal of Horticultural Sciences*, 18(2), pp. 112-119.

[10] Dhinesh, B. S., & Ramasamy, K. (2016). Variability in flowering and fruiting behavior of pomegranate cultivars. *International Journal of Plant Sciences*, 11(1), pp. 88-93.

[11] Gaikwad, S. S., & Patil, R. V. (2022). Impact of heat stress on reproductive phenology and yield stability in pomegranate (*Punica granatum* L.) cultivars. *Journal of Agrometeorology*, 24(2), pp. 158-164.

[12] Gaikwad, S. S., & Singh, N. V. (2018). Evaluation of new pomegranate selections for yield and quality in Western Maharashtra. *National Research Centre on Pomegranate Annual Report*, pp. 45-50.

[13] Holland, D., Hatib, K., & Bar-Ya'akov, I. (2009). Pomegranate: Botany, horticulture, breeding. In J. Janick (Ed.), *Horticultural Reviews* (Vol. 35, pp. 127–191). Hoboken, NJ: Wiley-Blackwell.

[14] Horticulture Statistics Division. (2021). *Area and Production of Horticulture Crops: All India Statistics*. Ministry of Agriculture and Farmers Welfare, Government of India.

[15] ICAR-NRCP. (2024). Technological interventions for pomegranate productivity. National Research Centre on Pomegranate, Solapur.

[16] Ikram, S., et al. (2022). Floral Characterization of Pomegranate Genotypes to Improve Hybridization Efficiency. *Plants*, 12(1). https://doi.org/10.3390/plants12010165

[17] Jadhav, A. B., et al. (2023). Performance of pomegranate genotypes for yield and quality attributes under moisture-limited environments of Maharashtra. *Indian Journal of Arid Horticulture*, 5(1), pp. 22-29.

[18] Jadhav, V. T., & Sharma, J. (2009). Pomegranate cultivation in India: Current scenario and prospects. *Journal of Arid Legumes*, 6(1), pp. 1-10.

[19] Jalikop, S. H. (2010). Breeding pomegranates for soft seeds and deep-red arils. *Horticultural Science*, 37(2), pp. 112-118.

[20] Joshi, V. R., & More, S. G. (2024). Physico-chemical characterization of custard apple (*Annona squamosa*) genotypes. *Journal of Food Science and Technology*, 61(1), pp. 88-96.

[21] Kaur, J. (2025). Which State is the Largest Producer of Pomegranates in India? *Jagran Josh*.

[22] Kulkarni, A. P., & Aradhya, S. M. (2005). Chemical changes and antioxidant activity in pomegranate arils during fruit development. *Food Chemistry*, 93(2), pp. 319-324.

[23] Kulkarni, A. S., et al. (2023). Quality dynamics and anthocyanin profiling of table grape cultivars under semi-arid conditions of Maharashtra. *Indian Journal of Horticulture*, 80(2), pp. 145-152.

[24] Kumar, R., & Singh, S. (2023). Evaluation of Indian Gooseberry cultivars under rainfed conditions. *Journal of Arid Land Research*, 21(3), pp. 154-162.

[25] Mane, S. V., & Shinde, B. N. (2020). Comparative performance of Bhagwa vs. Super Bhagwa in Solapur district. *Maharashtra Journal of Agriculture*, 45(3), pp. 210-215.
[26] Marathe, R. A., & Babu, K. D. (2015). Effect of varied climatic conditions on vegetative growth of Bhagwa pomegranate. *Indian Journal of Agricultural Sciences*, 85(6), pp. 780-785.
[27] More, S. D., & Deshmukh, P. S. (2022). Comparative juice recovery of commercial pomegranate cultivars. *Journal of Food Science and Technology*, 59(4), pp. 1120-1127.
[28] NHB. (2023). *Indian Horticulture Database*. National Horticulture Board, Gurgaon.
[29] Nimbalkar, S. D., et al. (2017). Yield and quality attributes of Ganesh pomegranate under different pruning intensities. *Journal of Applied Horticulture*, 19(1), pp. 56-60.
[30] Özgüven, A., Yılmaz, C., & Keleş, D. (2009). Pomegranate biodiversity and horticultural management. *Acta Horticulturae*, 940, pp. 1–6.
[31] Pareek, S., et al. (2015). Post-harvest physiology and quality of pomegranate: A review. *Journal of Food Science and Technology*, 52(2), pp. 643-662.
[32] Patil, S. S., & Palande, A. L. (2019). Performance of Solapur Lal cultivar in semi-arid zones. *Indian Journal of Arid Horticulture*, 14(2), pp. 33-38.
[33] Patil, S. S., Patil, S. S., & Patil, S. S. (2018). Response of micro-irrigation systems on growth and WUE of pomegranate. *Agricultural Water Management*, 208, pp. 1–9.
[34] Patil, S. V., et al. (2024). Performance of fig genotypes under semi-arid conditions. *Horticulture International*, 30(1), pp. 45-53.
[35] Pons-Gómez, A., et al. (2024). Pomegranate quality from consumers' perspective. *Foods*, 13(13).
[36] Prasad, R. N., et al. (2003). Performance of pomegranate cultivars in arid regions. *Indian Journal of Agricultural Sciences*, 73(11), pp. 603-605.
[37] Ramasamy, M., et al. (2012). Screening of pomegranate cultivars for bacterial blight resistance. *Phytopathology Notes*, 22(4), pp. 112-115.
[38] Rao, K. V., et al. (2024). Genetic diversity and quality assessment of subtropical fruit crops. *International Journal of Fruit Science*, 24(1), pp. 55-68.
[39] Reddy, Y. T. N., & Kurian, R. M. (2022). Flowering and fruit set dynamics in mango cultivars. *Indian Journal of Agricultural Sciences*, 92(5), pp. 580-585.
[40] Sarkhosh, A., et al. (2006). Biodiversity of pomegranate germplasm in Iran. *Scientia Horticulturae*, 107(4), pp. 362-368.
[41] Sharma, J., & Maity, A. (2014). Nutrient management in pomegranate - A review. *Agricultural Reviews*, 35(2), pp. 81-95.
[42] Sheikh, M. K. (2006). *The Pomegranate: Cultivation and Utilization*. Science Publishers, USA.
[43] Shilpa, P., Bhosale, V. P., et al. (2024). Morphological and physico-chemical characteristics of the new pomegranate variety 'Sharad King'. *Agricultural Research*.
[44] Shinde, P. P., et al. (2018). Evaluation of promising pomegranate hybrids. *International Journal of Chemical Studies*, 6(4), pp. 1234-1238.
[45] Singh, N. V., et al. (2020). Solapur Lal: A high-yielding, antioxidant-rich pomegranate variety. ICAR-NRCP Technical Bulletin.
[46] Sivakumar, V., et al. (2015). Effect of temperature on flowering and fruit set of pomegranates. *Global Journal of Bio-science and Biotechnology*, 4(1), pp. 22-26.
[47] Tehranifar, A., et al. (2010). Investigation of physico-chemical properties of pomegranate cultivars. *Journal of Food, Agriculture & Environment*, 8(2), pp. 518-524.
[48] Thakur, A. K., et al. (2011). Assessment of genetic diversity in pomegranate using RAPD markers. *Indian Journal of Genetics*, 71(1), pp. 60-65.
[49] Thorat, S. B., et al. (2023). Evaluation of pomegranate hybrids for fruit quality and antioxidant properties. *Indian Journal of Agricultural Sciences*, 93(3), pp. 310-316.
[50] Varpe, S., et al. (2025). Economic analysis of pomegranate cultivation in Maharashtra. *International Journal of Research in Agronomy*, 8(1), pp. 374–376.
[51] Vatambile, S. S. (2023). Comparative study of Sharad King and Bhagwa cultivars. *Pomegranate Growers Association Report*, Vol. 8.
[52] Verma, M. K., et al. (2010). Physico-chemical characteristics of promising pomegranate cultivars. *Indian Journal of Horticulture*, 67(4), pp. 464-468.
[53] Xie, S., et al. (2008). Effect of water stress on vegetative growth of pomegranate seedlings. *Acta Horticulturae*, 1089, pp. 35-40.
[54] Yadav, V., Singh, A. K., & Moore, S. (2022). Variability studies in guava genotypes for growth and yield attributes. *International Journal of Fruit Science*, 22(4), pp. 410-418.

International Journal of Environment, Agriculture and Biotechnology
Vol-11, Issue-2; Mar-Apr, 2026
Peer-Reviewed International Journal
Journal Home Page Available: https://ijeab.com/
Journal DOI: 10.22161/ijeab

A Study on Livelihood Security Status of Farm Families in Bikaner Division of Rajasthan State

Manisha Sharma[1], Pinky Yadav[2,*] and Ajay Kumar[3]

[1]Research Scholar, Extension Education and Communication Management
[2]Department of Education in Science and Mathematics, Regional Institute of Education, Mysore, NCERT, Karnataka -570006, India
[3]DES, CCSHAU-KVK, Jhajjar, Haryana, India
*Correspondence Author :

Received: 30 Jan 2026; Received in revised form: 27 Feb 2026; Accepted: 05 Mar 202; Available online: 13 Mar 2026

Abstract— *Context: Livelihood security refers to having sufficient and stable access to food, cash, and resources to meet basic needs, along with reserves and assets to manage risks, shocks, and emergencies (Harishkumar, 2012). It encompasses the ability to fulfill essential requirements such as food, health, shelter, minimal income, education, and community participation (Beevi and Rohit, 2018). Key aspects of livelihood security include economic stability, food security, educational access, health security, safe housing, and social network support. According to Bhavya (2019), the concept of farm household livelihood security offers a comprehensive framework for understanding poverty, malnutrition, and the dynamic survival strategies employed by households. This approach underscores the need for holistic agricultural development that integrates economic, social, and ecological dimensions. Objective: To assess status of livelihood security of farm families. Method: The study was conducted in Bikaner Division of Rajasthan State, comprising Bikaner, Hanumangarh, Sri Ganganagar, and Anupgarh districts. Among these, Bikaner and Hanumangarh districts were selected purposively. From Bikaner district, Lunkaransar Panchayat Samiti was selected randomly using the lottery method, while Sangaria Panchayat Samiti was selected similarly from Hanumangarh district. Five villages were randomly selected from each block, namely Sehniwala, Rojhan, Bhadera, Peepera, and Kapoorisar from Lunkaransar block, and Bolanwali, Bakhrawali, Santpura, Chak Heera Singh Wala, and Indergarh from Sangaria block. From each selected village, 30 farm families were chosen through random sampling, with the head of the household as the respondent, resulting in a total sample of 300 respondents for the study. Results & Discussion: The findings of the study revealed that farm families in the study area were largely food secure, with regular meal consumption and adequate intake of cereals and vegetables; however, fruit consumption and overall food quality remained comparatively low, indicating the need for dietary diversification to improve nutritional well-being. Nutritional security analysis showed moderate to high household dietary diversity, dominated mainly by cereals and vegetables, while fruits were consistently under-consumed in both Bikaner and Hanumangarh districts, highlighting gaps in micronutrient intake. In both districts, households reported regular consumption of cereals and vegetables, moderate intake of pulses and milk, and inadequate fruit consumption, suggesting the need for awareness generation and improved accessibility to fruits. Body Mass Index (BMI) assessment indicated that the majority of children (up to 5 years) and adult women (18 years and above) maintained normal nutritional status; however, the prevalence of undernutrition among children, particularly in Bikaner district, emerged as a concern, emphasizing the importance of strengthening preventive nutrition programs and ensuring access to protein- and micronutrient-rich foods. Economic security of farm families was observed to be moderate, with most households earning an annual income between ₹1–3 lakh, possessing moderate levels of productive and non-productive assets, manageable debt levels, and varying degrees of satisfaction with* *their financial conditions, thereby underscoring the need for income diversification, financial inclusion, and asset-building interventions. Health security was also found to be moderate, as households experienced occasional illnesses, limited access to healthcare facilities, partial availability of medical supplies, and financial constraints that restricted the use of professional healthcare services, pointing to the need for strengthened rural health infrastructure and affordable medical care. Educational security reflected widespread access to primary education but limited opportunities for higher and vocational education, coupled with affordability constraints, literacy gaps, and intergenerational educational disadvantages, highlighting the need for policy support to expand higher education infrastructure, vocational training, targeted subsidies, and comprehensive literacy programs. Overall, comparative analysis of livelihood security dimensions revealed that food and economic security were relatively stronger, whereas health and education security remained weaker, indicating the necessity for balanced development strategies that prioritize nutrition-sensitive interventions, rural healthcare services, and equitable educational opportunities alongside existing gains in food and income security.*

Keywords— Livelihood Security, Farm Families, Food and Nutritional Security, Economic Security, Rural Livelihoods

HIGHLIGHTS

- Livelihood security was analyzed across key dimensions such as food, economic, health, educational, and social security.
- Moderate food and economic security were recorded, though fruit consumption remained low and undernutrition among young children persisted, particularly in Bikaner. Health and education security ranked lowest due to limited medical access and low vocational exposure, with 80.3 percent reporting no skill training.
- The findings provide useful insights for policymakers and extension agencies to improve farm family livelihood security.

I. INTRODUCTION

Livelihood security is a comprehensive concept that refers to the ability of households to access adequate food, income, health services, education, and social support systems necessary for maintaining a sustainable and dignified standard of living. In agrarian economies like India, farm families largely depend on agriculture and allied activities for their livelihoods, which makes them highly vulnerable to climatic variability, market fluctuations, resource constraints, and socio-economic inequalities, thereby placing livelihood security at the center of rural development and poverty reduction strategies. Despite the agricultural sector supporting a large proportion of the rural population, farm families particularly in arid and semi-arid regions continue to face challenges such as low and unstable incomes, declining land productivity, limited access to institutional credit, inadequate health and educational facilities, and nutritional deficiencies, all of which adversely affect their overall livelihood security. This situation is especially pronounced in Rajasthan, where harsh agro-climatic conditions, frequent droughts, water scarcity, and heavy dependence on rainfed agriculture pose serious threats to sustainable livelihoods. Bikaner Division of Rajasthan represents a typical arid and semi-arid agro-ecological region characterized by erratic rainfall, sandy soils, extreme temperatures, and limited natural resources, with agriculture dominated by small and marginal farm families primarily dependent on crop production, livestock rearing, and wage labor. Although various governmental interventions have been implemented to enhance agricultural productivity, income generation, nutrition, and rural welfare, farm families in this region continue to experience varying degrees of livelihood insecurity, highlighting the need for a deeper understanding of the multidimensional nature of livelihood security. Livelihood security extends beyond income adequacy and encompasses interrelated dimensions such as food, nutritional, economic, health, and educational security, which collectively determine household well-being, particularly among vulnerable groups like children and women; while food and nutritional security ensure basic survival and health, economic security reflects income stability, asset ownership, savings, and debt status, health security relates to access to affordable healthcare, and educational security contributes to human capital formation and the breaking of intergenerational poverty. However, earlier studies on rural livelihoods have largely emphasized income and employment, often neglecting this integrated and multidimensional perspective, and empirical research examining livelihood security in the arid regions of Rajasthan at the divisional level remains limited. In this context, the present study was undertaken to assess the livelihood security status of farm families in Bikaner Division of Rajasthan State by analyzing key components such as food, nutritional, economic, health, and educational security and comparing their relative strength, with the expectation that the findings will provide valuable insights for policymakers, extension agencies, and development planners to design targeted and region-specific interventions aimed at enhancing the livelihood security and overall well-being of farm families in arid and semi-arid regions of Rajasthan.

METHODOLOGY

The present study was conducted in Bikaner Division of Rajasthan state, which comprises four districts, namely Bikaner, Hanumangarh, Sri Ganganagar, and Anupgarh. Out of these, Bikaner and Hanumangarh districts were selected purposively based on the convenience of the research. Bikaner district consists of nine Panchayat Samities, namely Bikaner, Khajuwala, Kolayat, Lunkaransar, Nokha, Sridungargarh, Panchu, Poogal, and Bajjukhalsa, of which Lunkaransar block was selected randomly using the lottery method. Similarly, Hanumangarh district has eight Panchayat Samities, namely Hanumangarh, Bhadra, Nohar, Pilibanga, Rawatsar, Sangaria, Tibbi, and Pallu, from which Sangaria block was selected randomly through the lottery method. From the selected blocks, five villages each were selected randomly, namely Sehniwala, Rojhan, Bhadera, Peepera, and Kapoorisar from Lunkaransar block, and Bolanwali, Bakhrawali, Santpura, Chak Heera Singh Wala, and Indergarh from Sangaria block. From these selected villages, a sample of 30 farm families from each village was selected, resulting in a total of 300 respondents (heads of farm families) for the present study conducted in Bikaner and Hanumangarh districts of Rajasthan state.

Frequency: It was used to find out the number of the respondents in a particular cell. In the present study, the respondents were categorized in terms of independent and dependent variables.

Percentage: The percentage was calculated by dividing the frequency of a particular cell by the total number of the respondents in that particular category and multiplying by 100.

Many indicators that measure nutritional security in women and men are well-known and accepted. For present study following components of nutritional security were included –

Household diet diversity serves as an indicator of food access and security, with a more diverse diet linked to improved outcomes such as better birth weight, child growth, and hemoglobin levels. To assess diet diversity, the person responsible for food preparation or another adult household member was asked about the types of foods consumed by anyone in the household over the past 24 hours. A score of 1 was assigned if a food group was consumed, and 0 if not. Initially, eight food groups were identified, but these were later consolidated into five groups. The household diet diversity score was calculated based on the sum of these scores.

HDDS (0-5)	Total number of food groups consumed by members of the household. Values for A through E will be either “0” or “1”.Sum (A+ B + C+D+ E)of all households

$$HDD = \frac{\text{Sum (HDDS)}}{\text{Total number of Households}}$$

HDD = Household Diet Diversity

HDDS = Household Diet Diversity Score

Food Consumption pattern of households the consumption of five food groups cereals, pulses, fruits, vegetables, and milk & milk products was evaluated based on frequency, categorized as daily, alternate days, twice weekly, weekly, or rarely. A five-point continuum was used, assigning scores from 5 (daily) to 1 (rarely) to quantify consumption patterns.

S. No.	Food Frequency
1.	Rarely
2.	Weekly
3.	Twice in a week
4.	Alternately
5.	Daily

Body Mass Index (BMI):BMI is a widely used indicator to assess body fat based on the relationship between weight and height, minimizing the influence of body frame size (Jelliffe, 1966). In this study, BMI was calculated for family heads aged 18 to 50 years by dividing body weight (kg) by the square of height (m^2), using standard measurement techniques.

$$BMI = \frac{\text{Weight (Kg)}}{\text{Height } (m^2)}$$

Where,

Kg – Kilogram

M – Meter

After determining body mass index, farm families were categorized according to WHOs (2004) depiction of BMI classification.

S. No.	Classification	BMI (Kg/ m^2)
1.	Underweight	$\leq$ 18.50
2.	Normal range	18.50 – 24.99
3.	Over weight	25.00- 29.99
4.	Obese	$\geq$30.00

BMI classification by WHO, (2004)

II. RESULTS

Table1. Distribution of respondents according to their food security

S. No.	Variables	Bikaner n=150		Hanumangarh n=150		Total N=300	
		F	%	f	%	F	%
1.	**Sources of food**						
	Own farm production	33	22.0	28	18.7	61	20.3
	Own farm production+ market	87	58.0	93	62.0	180	60.0
	Market only	27	18.0	26	17.3	53	17.7
	Exchange work for food	3	2.0	3	2.0	6	2.0
2.	**Number of meals the household normally has per day**						
	Breakfast-lunch-dinner	107	71.3	115	76.7	222	74.0
	Breakfast and dinner	18	12.0	12	8.0	30	10.0
	Lunch and dinner	21	14.0	20	13.3	41	13.7
3.	**Frequency of Fruit intake**						
	Daily	12	8.0	14	9.3	26	8.7
	Twice or thrice in a week	48	32.0	52	34.7	100	33.3
	Once in a week	42	28.0	40	26.7	82	27.3
	Once in a month	30	20.0	28	18.7	58	19.3
	Rarely	18	12.0	16	10.7	34	11.3
4.	**Vegetable intake frequency**						
	Two time in day	96	64.0	101	67.3	197	65.7
	One time in day	28	18.7	27	18.0	55	18.3
	Alternate days	15	10.0	13	8.7	28	9.3
5.	**Amount & quality of food eaten in your household in the last 12 months**						
	Enough food to eat	82	54.7	94	62.7	176	58.7
	Enough quantity but not quality	49	32.7	41	27.3	90	30.0
	Sometimes not enough	13	8.7	11	7.3	24	8.0
	Not enough to eat	5	3.3	3	2.0	8	2.7
	Always not enough	1	0.6	1	0.7	2	0.7

Table 1 illustrates the food security status of farm families in Bikaner and Hanumangarh across five parameters: sources of food, number of meals per day, fruit intake frequency, vegetable intake frequency, and the quantity and quality of food consumed over the last 12 months. Most respondents (60.0%) relied on both their farm produce and market purchases, while a smaller proportion depended solely on farm produce (20.3%), exchange labor (1.7%), or food assistance (1.0%). Regarding meals per day, 74.0% of households consumed three meals regularly, with 10.0% having only two meals or irregular meal patterns. Fruit consumption was limited, with 8.7% eating fruits daily and 33.3% consuming them two to three times per week, whereas vegetables were consumed daily by 65.7% of households. Assessment of food quantity and quality showed that 58.7% had sufficient food in both aspects, 30.0% had adequate quantity but compromised quality, and 10.7% faced occasional or chronic insufficiency. The data suggest that while farm families generally maintain stable daily nutrition, dietary diversity particularly in fruit consumption is inadequate, potentially limiting micronutrient intake. Households in Hanumangarh performed slightly better than those in Bikaner in terms of regular meals, vegetable intake, and overall food sufficiency, likely due to higher income levels, better access to markets, and more productive farm resources. The low reliance on food assistance or exchange labor indicates that a combination of subsistence farming and market purchases sufficiently meets most families' food requirements, although seasonal fluctuations and resource constraints may occasionally compromise availability and quality.In summary, the majority of farm families in Bikaner and Hanumangarh enjoy stable and adequate food availability, with three meals per day being the norm and daily vegetable consumption high. Fruit intake remains limited, suggesting a need for improved dietary diversity. Overall, food sufficiency in terms of quantity and quality is satisfactory for most households, with only a small proportion experiencing insufficiency. These results highlight the relative resilience of farm families' food systems, although targeted interventions could enhance nutrition and dietary balance.The findings align with previous studies, including NSSO surveys and district livelihood profiles, which report that farm households in Rajasthan largely rely on a combination of own produce and market purchases for sustenance. Similar patterns of regular meals and high vegetable consumption, alongside limited fruit intake, have been documented in other semi-arid regions of India. Research also indicates that higher income levels and better market access, as observed in Hanumangarh, positively influence food security and dietary diversity, supporting the trends observed in the present study.

Table 2. Distribution of respondents according to their household diet diversity

S. No.	Food groups eaten during last 24 hours	Bikaner n=150 (f / %)	Rank	Hanumangarh n=150 (f / %)	Rank	Total N=300	WMS
1	Any cereals (chapatti, bread, biscuits, rice, food made by millets, maize, wheat)	147 (98.0%)	I	150 (100.0%)	I	297	99.0
2	Any vegetables (potato, sweet potato, onion, carrot, radish, turnip)	130 (86.7%)	II	142 (94.7%)	II	272	90.7
3	Any food made from beans, peas, lentils, nuts, pulses	118 (78.7%)	III	132 (88.0%)	III	250	83.3
4	Milk and milk products	110 (73.3%)	IV	128 (85.3%)	IV	238	79.3
5	Any fruits (ber, papaya, orange)	55 (36.7%)	V	70 (46.7%)	V	125	41.7

The distribution of respondents according to different food groups consumed during the last 24 hours shows a clear pattern of dietary preferences in Bikaner and Hanumangarh districts. Cereals dominated the daily diet, with 98.0% of households in Bikaner and 100.0% in Hanumangarh reporting consumption, underscoring the staple role of wheat, bajra, and other grains in rural households. Vegetable consumption was also substantial, with 86.7% of households in Bikaner and 94.7% in Hanumangarh including items such as potatoes, onions, carrots, and radish in their meals. In contrast, fruit intake remained relatively low, reported by only 36.7% of households in Bikaner and 46.7% in Hanumangarh. Protein-rich foods like beans, lentils, pulses, and nuts were consumed by 78.7% and 88.0% of respondents in Bikaner and Hanumangarh, respectively, while milk and milk products were included in the diets of 73.3% and 85.3% of households. Aggregated across all food groups, total intake frequencies reached 561 for Bikaner and 592 for Hanumangarh, summing to 1153 across 300 respondents. These data indicate that dietary patterns in both districts remain predominantly cereal-based, reflecting the central role of staple foods in rural Rajasthan. The high vegetable consumption (above 85%) suggests reasonable accessibility through local markets and small kitchen gardens. However, limited fruit intake (around 40%) points to affordability issues and cultural preferences that prioritize cereals and vegetables over fruits. Protein intake from pulses and legumes exceeding 80% demonstrates moderate dietary protein adequacy, further supported by the government's Public Distribution System (PDS) and the affordability of basic pulses. Milk and milk products consumption by nearly four-fifths of households underscores the importance of livestock rearing as a complementary livelihood activity. The slightly higher consumption levels in Hanumangarh across most food groups may be attributed to better irrigation support from the Indira Gandhi Canal system, which enhances vegetable cultivation, fodder availability, and dairy production. This aligns with earlier findings that canal-irrigated regions tend to exhibit more diversified and nutrient-rich diets compared to arid areas like Bikaner.It can be concluded that while cereal and vegetable consumption is nearly universal, fruit intake remains inadequate, indicating limited dietary diversity. Protein intake is moderate, showing adequate inclusion of pulses and legumes, while milk and dairy consumption further enhances nutritional quality. Households in Hanumangarh generally display marginally better food group consumption patterns than those in Bikaner, suggesting that improved irrigation and agricultural resource access positively influence dietary diversity. Overall, the data highlight the resilience of rural diets while emphasizing the need to enhance fruit and micronutrient-rich food intake for balanced nutrition.

These findings are consistent with national and regional studies, including NSSO (2019) and NFHS-5 (2021), and similar findings have been reported by Rani (2015) who reported daily consumption of cereals was maximum rather than other food groups and Shakti et al. (2013) also concluded that cereals were included in daily diet of almost all the respondents (99.50%). which report cereal-dominated diets and low fruit consumption in rural Rajasthan. Previous research has also shown that access to irrigation and improved market connectivity, as evident in canal-fed regions like Hanumangarh, facilitates greater dietary diversity through enhanced availability of vegetables, pulses, and dairy products, reaffirming the patterns observed in the present study.

Table 3. Distribution of respondents according to their consumption pattern of household in Bikaner district

S. No.	Food Groups	Daily (5)	Alternately (4)	Twice in a Week (3)	Weekly (2)	Rarely (1)	WMS	Rank
1	Cereals	150	0	0	0	0	5.00	I
2	Pulses	78	33	20	12	7	4.04	III
3	Vegetables	105	28	10	5	2	4.52	II
4	Fruits	26	44	20	35	25	2.86	V
5	Milk & Milk Products	69	42	20	12	7	4.03	IV

Table 3 presents the consumption pattern of various food groups among households in Bikaner district, showing both the frequency of intake and the weighted mean score (WMS) for cereals, pulses, vegetables, fruits, and milk/milk products. Cereals emerged as the most frequently consumed food, with all 150 households reporting daily intake, resulting in the highest WMS of 5.00 and ranking first, reaffirming their position as the dietary staple in rural households. Vegetables ranked second, with 105 households consuming them daily and a WMS of 4.52, reflecting their consistent inclusion in daily meals. Pulses ranked third with a WMS of 4.04, while milk and milk products followed closely with a WMS of 4.03, indicating moderate to high frequency of protein-rich food consumption. Fruits were the least frequently consumed food group, with only 26 households reporting daily intake and a WMS of 2.86, ranking fifth, suggesting limited incorporation of fruits in regular diets.The data reveal that the dietary pattern in Bikaner is predominantly cereal- and vegetable-based, supplemented by pulses and dairy products. The near-universal consumption of cereals highlights their affordability and availability as staple foods, while vegetables maintain high frequency due to local cultivation and easy accessibility in village markets. The moderate intake of pulses and milk products suggests that most households are able to meet basic protein requirements, though not consistently on a daily basis. In contrast, the low frequency of fruit consumption may be attributed to seasonal limitations, higher cost, and cultural dietary preferences that prioritize staple foods and vegetables over fruits.In summary, farm households in Bikaner exhibit a diet that is sufficient in energy and moderately diverse, with a strong reliance on cereals and vegetables. The comparatively lower intake of fruits indicates a nutritional gap, particularly in terms of vitamins and micronutrients. Efforts to promote fruit cultivation through kitchen gardens and awareness on dietary diversity could help improve overall nutritional quality.These results align with the findings of NSSO (2019) and NFHS-5 (2021), which reported cereal-dominated diets and limited fruit consumption among rural households in Rajasthan. Similarly, Singh and Kaur (2018) noted that regular access to vegetables and pulses in rural regions is largely sustained by local production and livestock ownership, while fruit consumption remains constrained by economic and market factors consistent with the consumption patterns observed in this study.

Table 4 Distribution of respondents according to their consumption pattern of household in hanumangarh district

S. No.	Food Groups	Daily (5)	Alternately (4)	Twice in a Week (3)	Weekly (2)	Rarely (1)	WMS	Rank
1	Cereals	150	0	0	0	0	5.00	I
2	Pulses	80	32	18	13	7	4.09	III
3	Vegetables	110	26	8	4	2	4.57	II
4	Fruits	24	49	45	32	26	2.99	V
5	Milk & Milk Products	66	44	21	13	6	4.01	IV

Table 4 presents the consumption pattern of various food groups among households in Hanumangarh district, depicting both the frequency of intake and the weighted mean score (WMS) for cereals, pulses, vegetables, fruits, and milk/milk products. Cereals emerged as the most frequently consumed food group, with all 150 households reporting daily intake, yielding the highest WMS of 4.95 and ranking first, indicating the central role of cereals such as wheat, rice, and millets in the rural diet. Vegetables ranked second, with 110 households consuming them daily and a WMS of 4.57, reflecting their consistent availability and inclusion in routine meals. Pulses were consumed daily by 80 households, with a WMS of 4.09 and ranking third, followed closely by milk and milk products (WMS = 4.01, Rank IV), which also formed a significant component of household diets. Fruits ranked fifth, with only 24 households consuming them daily and a relatively lower WMS of 2.99, showing infrequent inclusion in meals. The data reveal that the dietary pattern in Hanumangarh district is characterized by a strong reliance on cereals and vegetables, supplemented by moderate intake of pulses and dairy products. The near-universal consumption of cereals and frequent intake of vegetables highlight their status as dietary staples supported by both local production and market availability. The moderately high WMS for pulses and milk products indicates that most households maintain regular protein intake, likely facilitated by mixed farming systems and livestock rearing. However, the low fruit consumption reflects constraints related to affordability, limited availability, and traditional food preferences prioritizing staple and protein foods over fruits.

Overall, the findings suggest that Hanumangarh households maintain a diet that is energy-sufficient and moderately diverse, with a good balance of staples, vegetables, and protein sources. The relatively higher WMS values across most food groups compared to Bikaner indicate better dietary diversity, likely resulting from improved irrigation facilities under the Indira Gandhi Canal system, which supports vegetable and fodder cultivation and enhances dairy productivity. The persistently low fruit consumption, however, underscores the need for interventions promoting fruit availability through household orchards, nutrition gardens, and dietary awareness programs.These findings are in line with national and regional research, including NFHS-5 (2021) and NSSO (2019), which report cereal-dominated diets and low fruit intake in rural India. Similar trends were observed by Singh and Kaur (2018), who found that improved irrigation access and livestock ownership in canal-irrigated areas contribute to greater dietary variety, particularly in vegetable and dairy consumption consistent with the patterns observed in Hanumangarh district.

Table 5. Distribution of respondents according to their BMI of children (upto5year), adult women(18 year & above)

S. No.	Variables	Bikaner n=150		Hanumangarh n=150		Total N=300	
		f	%	f	%	F	%
1.	**Children (upto5 year)**						
	18.5 or less: Low BMI (underweight)	48	32.0	42	28.0	90	30.0
	18.5 to 24.9: Medium BMI (normal weight)	85	56.7	93	62.0	178	59.3
	25 to 29.9: High BMI (over weight)	13	8.7	10	6.7	23	7.7
	30 and above: Very - High BMI (obese)	4	2.6	5	3.3	9	3.0
2.	**Adult Women (18 year &above)**						
	18.5 or less: Low BMI (underweight)	42	28.0	38	25.3	80	26.7
	18.5 to 24.9: Medium BMI (normal weight)	82	54.7	88	58.7	170	56.7
	25 to 29.9: High BMI (over weight)	20	13.3	18	12.0	38	12.7
	30 and above: Very High BMI (obese)	6	4.0	6	4.0	12	4.0

Table 5 presents the Body Mass Index (BMI) distribution among children up to 5 years and adult women (18 years and above) in Bikaner and Hanumangarh districts. Among children, underweight prevalence is observed in 32.0% in Bikaner and 28.0% in Hanumangarh, while the majority fall within the normal BMI range (56.7% in Bikaner; 62.0% in Hanumangarh), indicating moderate nutritional status. Overweight and obesity are less common, reported in 8.7% and 2.6% of children in Bikaner and 6.7% and 3.3% in Hanumangarh, respectively.For adult women, underweight prevalence is slightly lower, with 28.0% in Bikaner and 25.3% in Hanumangarh, whereas more than half of the women fall in the normal BMI category (54.7% in Bikaner; 58.7% in Hanumangarh). Overweight and obesity together constitute approximately 17.3% of women in Bikaner and 16% in Hanumangarh. The slightly higher proportion of normal BMI in Hanumangarh suggests better nutritional outcomes, potentially linked to greater dietary diversity, higher income levels, and improved access to nutritional resources.It can be concluded that, while most children and adult women in both districts maintain normal nutritional status, a considerable proportion experiences under nutrition, particularly in Bikaner. Overweight and obesity remain relatively low among children and moderate among women, reflecting the ongoing dual burden of malnutrition. These findings highlight the need for targeted interventions to address under nutrition while promoting balanced diets for long-term health.These results are consistent with previous regional studies and nutrition surveys in semi-arid Rajasthan, which report persistent under nutrition among children and women alongside emerging overweight trends in adults. Earlier research also emphasizes that dietary diversity, income, and access to nutritional programs significantly influence BMI outcomes, supporting the patterns observed in the current study.

Table 6. Distribution of respondents according to their economic security

S. No.	Economic security	Bikaner n=150		Hanumangarh n=150		Total N=300	
		f	%	f	%	F	%
1.	**Household Annual Income**						
	Below 1 lakh	38	25.3	18	12.0	56	18.7
	1 to 2 lakh	58	38.7	42	28.0	100	33.3
	2 to 3 lakh	32	21.3	39	26.0	71	23.7
	3 to 4 lakh	14	9.3	28	18.7	42	14.0
	Above 4 lakh	8	5.4	23	15.3	31	10.3
2.	**Possession of Productive Assets**						
a)	**Livestock**						
	Up to 30,000	40	26.7	30	20.0	70	23.3
	30,000–60,000	51	34.0	40	26.7	91	30.3
	60,000–90,000	33	22.0	23	15.3	56	18.7
	90,000–1,20,000	17	11.3	24	16.0	41	13.7
	Above 1,20,000	9	6.0	33	22.0	42	14.0
b)	**Land**						
	Up to 10 lakh	26	17.3	47	31.3	73	24.3
	10–15 lakh	30	20.0	42	28.0	72	24.0
	15–20 lakh	34	22.7	29	19.3	63	21.0
	20–25 lakh	28	18.7	18	12.0	46	15.3
	Above 25 lakh	32	21.3	14	9.4	46	15.3
3.	**Possession of Unproductive Assets**						
a)	**Gold**						
	Up to 50 gm	39	26.0	36	24.0	75	25.0
	50–100 gm	47	31.3	49	32.7	96	32.0
	100–150 gm	30	20.0	28	18.7	58	19.3
	150–200 gm	20	13.3	22	14.7	42	14.0
	Above 201 gm	14	9.3	15	10.0	29	9.7
b)	**Value of residential property**						
	Up to `2 lakh	28	18.7	26	17.3	54	18.0
	`2–4 lakh	34	22.7	33	22.0	67	22.3
	`4–6 lakh	40	26.7	43	28.7	83	27.7
	`6–8 lakh	28	18.7	27	18.0	55	18.3
	Above `8 lakh	20	13.3	21	14.0	41	13.7
4.	**Household currently in debt**						

	No debt	50	33.3	58	38.7	108	36.0
	Yes, a little	36	24.0	29	19.3	65	21.7
	Moderate amount	34	22.7	31	20.7	65	21.7
	High amount	20	13.3	18	12.0	38	12.7
	Unmanageable	10	6.7	14	9.3	24	8.0
5.	**Satisfaction with current financial condition**						
	Satisfied	38	25.3	41	27.3	79	26.3
	Somewhat satisfied	50	33.3	48	32.0	98	32.7
	Don't know	28	18.7	26	17.3	54	18.0
	Somewhat dissatisfied	22	14.7	21	14.0	43	14.3
	Dissatisfied	12	8.0	14	9.3	26	8.7

Table 6 presents the distribution of households according to their economic security status across Bikaner and Hanumangarh districts. The economic security of farm households was assessed through indicators such as annual income, possession of productive and unproductive assets, indebtedness, and satisfaction with current financial conditions. The data highlight considerable inter-district variation, reflecting differences in agricultural potential, asset ownership patterns, and livelihood diversification.

In terms of household annual income, 38.7 percent of households in Bikaner and 28.0 percent in Hanumangarh earned between `1–2 lakh annually, constituting the largest income category overall (33.3%). Low-income households (below `1 lakh) accounted for 25.3 percent in Bikaner and 12.0 percent in Hanumangarh, while higher-income households (above `4 lakh) were more prevalent in Hanumangarh (15.3%) compared to Bikaner (5.4%). This distribution indicates a relatively better economic position of households in Hanumangarh, possibly due to higher agricultural productivity and canal-based irrigation facilities, whereas Bikaner exhibits a more subsistence-oriented rural economy with a larger proportion of low-income earners. Regarding possession of productive assets, differences are notable between districts. In terms of **livestock value**, the majority of households in Bikaner (34.0%) and Hanumangarh (26.7%) owned livestock worth `30,000–`60,000, with Bikaner showing higher ownership in the lower and middle value brackets, confirming its livestock-dominated agrarian system. Conversely, a higher proportion of Hanumangarh households (22.0%) reported livestock assets valued above `1,20,000, suggesting a smaller but more commercialized livestock segment.For land value, the pattern is reversed: 31.3 percent of Hanumangarh households owned land worth up to 10 lakh, while 21.3 percent of Bikaner households reported landholdings above 25 lakh. The higher land value concentration in Bikaner may be attributed to the larger land parcels typical of its arid farming systems, whereas hanumangarh canal-irrigated holdings are smaller but more intensively cultivated. With respect to unproductive assets, such as gold and residential property, a moderate distribution was observed across both districts. About one-third of the respondents (32.0%) possessed 50–100 grams of gold, with similar proportions in both areas. The value of residential property was primarily concentrated in the `4–6 lakh range, representing 26.7 percent of Bikaner and 28.7 percent of Hanumangarh households. This reflects moderate asset accumulation typical of rural middle-income households, where residential property often represents the most stable form of capital. In terms of household indebtedness, 33.3 percent of Bikaner and 38.7 percent of Hanumangarh households reported having no debt, while about 21.7 percent in both districts were moderately indebted. High and unmanageable debt levels were relatively low, at 12.7 and 8.0 percent respectively across both districts. This suggests that although credit dependence exists, most households maintain debt within manageable limits. The relatively higher share of debt-free households in Hanumangarh again points to better financial stability, possibly linked to higher farm income and access to institutional credit. Finally, regarding satisfaction with current financial conditions, 25.3 percent of Bikaner and 27.3 percent of Hanumangarh respondents reported being satisfied, while about one-third of the total sample (32.7%) were somewhat satisfied. Only 8.7 percent expressed dissatisfaction, and 18.0 percent remained uncertain ("don't know"), indicating that most households perceive their financial condition as either stable or moderately satisfactory. This perception aligns with their moderate-income levels and manageable debt burdens.The results are in accordance with the findings of Mary (2013) who also revealed that majority of rural women (57.84%)

had medium level of financial security. Overall, the findings reveal that households in Hanumangarh generally exhibit higher economic security due to better income levels, productive land value, and lower debt pressure. In contrast, Bikaner households rely more heavily on livestock assets and larger but less productive landholdings, resulting in moderate income and asset security. These results are consistent with the regional patterns observed in previous studies conducted in semi-arid and canal-irrigated zones of Rajasthan, where irrigation access, market connectivity, and agricultural diversification strongly influence household economic stability.

Table 7. Distribution of respondents according to their health security

S. No.	Health security	Bikaner n=150		Hanumangarh n=150		Total N=300	
		f	%	f	%	F	%
1.	**Occurrence of illness in the household during last 12 months**						
	Never	36	24.0	32	21.3	68	22.7
	Once or twice in a year	60	40.0	63	42.0	123	41.0
	A few times a month	28	18.7	30	20.0	58	19.3
	Once or twice in a week	17	11.3	15	10.0	32	10.7
	Almost every day	9	6.0	10	6.7	19	6.3
2.	**Accessibility of primary health services**						
	<1 km	52	34.7	48	32.0	100	33.3
	1–2 km	43	28.7	45	30.0	88	29.3
	1–4 km	28	18.7	30	20.0	58	19.3
	4–6 km	17	11.3	19	12.7	36	12.0
	>6 km	10	6.7	8	5.3	18	6.0
3.	**Accessibility of government/private hospital**						
	<1 km	29	19.3	33	22.0	62	20.7
	1–2 km	38	25.3	35	23.3	73	24.3
	2.1–4 km	42	28.0	39	26.0	81	27.0
	4–6 km	26	17.3	25	16.7	51	17.0
	>6 km	15	10.0	18	12.0	33	11.0
4.	**Enough medical supply for adequate health care**						
	Never	11	7.3	9	6.0	20	6.7
	Rarely	18	12.0	20	13.3	38	12.7
	Sometimes	55	36.7	52	34.7	107	35.6
	Often	45	30.0	47	31.3	92	30.7
	Always	21	14.0	22	14.7	43	14.3
5.	**Household ability to afford professional treatment**						
	No	18	12.0	21	14.0	39	13.0
	Yes, if money is borrowed	40	26.7	34	22.7	74	24.7
	Yes, with much difficulty	28	18.7	31	20.7	59	19.7
	Yes, with some difficulty	38	25.3	40	26.7	78	26.0
	Yes, household can afford it	26	17.3	24	16.0	50	16.7

Table 7 presents the health security of farm households in Bikaner and Hanumangarh districts across five dimensions: occurrence of illness, accessibility of primary health services, access to government and private hospitals, adequacy of medical supplies, and affordability of professional treatment. In terms of illness, 41% of households reported sickness once or twice a year, 19.3% experienced illness a few times a month, and 6.3% faced daily health issues, indicating a moderate prevalence of health concerns. Accessibility to primary health services shows that 33.3% of households have facilities within 1 km, while 6% reside more than 6 km away, reflecting variability in proximity to basic care. Access to government and private hospitals reveals that 27% of respondents live 2.1–4 km away, whereas 11% are over 6 km distant. Adequacy of medical supplies is limited, with only 14.3% of households always having sufficient medicines, 35.7% sometimes, and 12.7% rarely having adequate supplies, pointing to occasional gaps in healthcare resources. Regarding affordability, 16.7% of households can comfortably afford professional treatment, 26% manage with some difficulty, and 24.7% require borrowing to access care, highlighting financial constraints in utilizing health services. These findings indicate that while some households experience adequate healthcare support, a substantial proportion faces challenges related to illness prevalence, accessibility, resource adequacy, and treatment affordability. It can be concluded that, health security among farm households in Bikaner and Hanumangarh is moderate, with most families managing occasional illnesses but encountering barriers in accessing and affording healthcare. Variability in proximity to medical facilities and inconsistent availability of medicines further affect overall health outcomes. These findings underscore the need for improved healthcare infrastructure, resource availability, and financial support to enhance health security in rural households. The findings are in accordance with the NRHM report (2013) that 66.00 percent of the rural Indians do not have the access to the medicines, 8.00 percent primary health centers do not have doctors, 18.00 percent PHC's do not have pharmacists and 31.00 percent of the population travels more than 30 km to seek health in rural areas. Similar findings were also reported by Kumar et al. (2014) that in rural India the average distance to the nearest PHC, CHC were 9.06 km respectively and the average distance to the nearest private clinic and private hospital were 10.38 and 18.69 km respectively.

Table 8.Distribution of respondents according to their education security

S. No.	Education security	Bikaner n=150		Hanumangarh n=150		Total N=300	
		f	%	F	%	F	%
1.	**Household literacy level**						
	Illiterate	35	23.3	40	26.7	75	25.0
	Literate (can read/write, but no schooling)	12	8.0	10	6.7	22	7.3
	Primary	38	25.3	41	27.3	79	26.3
	Secondary	30	20.0	28	18.7	58	19.3
	Sr. Secondary	20	13.3	18	12.0	38	12.7
	Graduation & above	15	10.0	13	8.7	28	9.3
2.	**Accessibility of school**						
	<1 Km	66	44.0	61	40.7	127	42.3
	1–2 Km	45	30.0	48	32.0	93	31.0
	2.1–4 Km	26	17.3	27	18.0	53	17.7
	4.1–6 Km	9	6.0	10	6.7	19	6.3
	>6 Km	4	2.7	4	2.7	8	2.7
3.	**Accessibility of higher/vocational education**						
	<1 Km	21	14.0	18	12.0	39	13.0
	1–2 Km	36	24.0	30	20.0	66	22.0
	2.1–4 Km	44	29.3	45	30.0	89	29.7

	4.1–6 Km	27	18.0	29	19.3	56	18.7
	>6 Km	22	14.7	28	18.7	50	16.7
4.	**Availability of educational institutes**						
	Primary school	145	96.7	142	94.7	287	95.7
	Middle school	129	86.0	134	89.3	263	87.7
	Sr. Secondary school	102	68.0	98	65.3	200	66.7
	College Education	55	36.7	48	32.0	103	34.3
5.	**Cost of education (Cost includes fee, shoes, books, etc.)**						
	Most expensive (>10 Lakh ha. /Yr.)	6	4.0	5	3.3	11	3.7
	Expensive	32	21.3	29	19.3	61	20.3
	Undecided	22	14.7	20	13.3	42	14.0
	Cheap	57	38.0	61	40.7	118	39.3
	Very Cheap (<1. Lakh ha. /Yr.	33	22.0	35	23.3	68	22.7

The assessment of educational security among respondents in Bikaner and Hanumangarh districts revealed substantial variation across literacy levels, accessibility, affordability, and institutional availability. Household literacy showed that 23.3% of respondents in Bikaner and 26.7% in Hanumangarh were illiterate, with a combined average of 25.0%. Primary education was the most common attainment, reported by 25.3% in Bikaner and 27.3% in Hanumangarh, totaling 26.3%. Secondary education accounted for 20.0% in Bikaner and 18.7% in Hanumangarh, while senior secondary completion was lower at 13.3% and 12.0%, respectively. Graduation and above were achieved by only about one-tenth of households (10.0% in Bikaner, 8.7% in Hanumangarh). Regarding school accessibility, nearly half of respondents had educational institutions within 1 km (44.0% in Bikaner, 40.7% in Hanumangarh), with 31.0% accessing schools within 1–2 km, and 2.7% reporting distances beyond 6 km. Higher and vocational education institutions were mostly located at moderate distances: 29.3% in Bikaner and 30.0% in Hanumangarh within 2.1–4 km, 18–19% within 4.1–6 km, and 16.7% beyond 6 km. Availability of primary schools was high (96.7% in Bikaner, 94.7% in Hanumangarh), and middle schools accessible to over 87%, but senior secondary schools reached only two-thirds of households, and colleges were accessible to just 34.3%. Affordability perceptions varied, with around 38–41% categorizing education as cheap, 22% as very cheap, 20.3% as expensive, and 3.7% as most expensive. The data indicate that educational security in rural Rajasthan faces dual challenges: structural access barriers and household-level literacy limitations. Persistently high illiteracy (around one-fourth of households) points to intergenerational educational disadvantage, consistent with rural literacy surveys in South Asia (UNESCO, 2022; NFHS-5, 2021). Despite near-universal access to primary schooling, the steep decline in availability of senior secondary schools and colleges constrains educational mobility and skill acquisition, reflecting patterns of rural educational infrastructure gaps reported in prior studies (Mehrotra, 2019). While primary schools are relatively accessible with over 70% within 2 km the situation deteriorates for higher and vocational education, where approximately 35.4% of respondents face distances over 4 km, disproportionately affecting female students and first-generation learners, as observed in Rajasthan and Haryana field studies.

It can be concluded that, while basic education has become widely accessible, significant barriers remain in achieving continuity to higher and vocational education. Household-level literacy limitations, distance to institutions, and cost perceptions constrain educational attainment and opportunities for skill development. The findings underscore the need for targeted interventions to bridge gaps in higher education access, reduce financial barriers, and improve educational equity, particularly for marginalized and first-generation learners.

These results are supported by prior research, including NFHS-5 (2021) and UNESCO (2022), which highlight persistent illiteracy and limited access to higher education in rural areas. Studies on rural educational infrastructure in Rajasthan also emphasize the challenges of institutional gaps, distance barriers, and affordability issues, confirming the patterns observed in the current study.

Table 9. Distribution of respondents according to their overall comparative analysis of livelihood security

S. No.	Comparative Analysis	Bikaner n=150	Hanumangarh n=150	Total N=300	Rank
		WMS			
1	Food security	12.60	13.40	13.00	I
2	Nutrition security	11.90	12.80	12.35	III
3	Economic security	12.10	13.00	12.55	II
4	Health security	11.70	12.50	12.10	V
5	Education security	11.90	12.60	12.25	IV
Overall comparative analysis of livelihood security		12.04	12.86	12.45	

Table 9 presents a comparative analysis of the livelihood security index in Bikaner and Hanumangarh districts across five key dimensions: food, nutrition, economic, health, and education security. Weighted Mean Scores (WMS) indicate that food security ranks first, with Hanumangarh slightly higher (13.40) than Bikaner (12.60), yielding an overall mean of 13.00. Economic security follows in second place, with WMS values of 13.00 for Hanumangarh and 12.10 for Bikaner, resulting in a combined score of 12.55. Nutrition security is ranked third, with a mean of 12.35 (11.90 in Bikaner, 12.80 in Hanumangarh), while education security occupies the fourth rank overall, with WMS of 12.25 (11.90 in Bikaner, 12.60 in Hanumangarh). Health security ranks lowest among the five dimensions, with an overall WMS of 12.10, comprising 11.70 in Bikaner and 12.50 in Hanumangarh. The analysis shows that while basic livelihood foundations such as food and economic security are relatively strong, human development dimensions like education and health lag behind in both districts. The data suggest that livelihood security in the region is anchored primarily in food and economic well-being, whereas human capital dimensions require greater attention. The top rank of food security reflects the effectiveness of agricultural productivity and public distribution systems, consistent with NSSO and FAO (2020) findings that food sufficiency has improved in semi-arid regions through crop diversification and targeted welfare programs. Economic security as the second-ranked dimension highlights diversification into non-farm income sources and social safety nets, supporting observations by Dreze and Khera (2017) on the stabilizing impact of MGNREGA and microcredit. Nutrition security, despite adequate food availability, remains constrained by limited dietary diversity and micronutrient intake, echoing NFHS-5 (2021) reports of persistent anemia and undernutrition in Rajasthan.

Education and health security, ranked fourth and fifth respectively, remain weaker components of livelihood security. Limited access to higher education and affordability issues, as discussed in Table 4.33, constrain education security, while gaps in rural health infrastructure and low health awareness contribute to lower health security scores. Hanumangarh consistently demonstrates higher WMS values across all dimensions compared to Bikaner, likely due to better institutional outreach and higher agricultural productivity in canal-irrigated areas.

DISCUSSION

It can be concluded that, the comparative analysis highlights a recurring rural paradox: food and economic sufficiency are relatively assured, but human development outcomes, particularly education and health, remain inadequately addressed. The findings underscore the need for targeted policy interventions to strengthen nutrition, health services, and educational infrastructure to achieve comprehensive livelihood security in rural Rajasthan.These results are supported by earlier research, including NSSO and FAO (2020), Dreze and Khera (2017), and NFHS-5 (2021), which similarly report strong food and economic security but persistent deficits in human development indicators in semi-arid regions of India.

CONCLUSION

The study concludes that farm families in Bikaner Division of Rajasthan generally exhibited moderate levels of livelihood security. Food security was relatively strong, with households consuming regular meals and adequate quantities of cereals and vegetables; however, low fruit intake and limited dietary quality indicate gaps in nutritional diversity. Nutritional security showed moderate to high household diet diversity, but undernutrition among children, particularly in Bikaner district, remains a concern, emphasizing the need for nutrition-focused interventions. Economic security of farm families was assessed as moderate, characterized by annual incomes ranging between ₹1–3 lakh, moderate asset ownership, and manageable debt levels, suggesting scope for income diversification and financial strengthening. Health and educational security emerged as weaker dimensions, with limited access to healthcare facilities, affordability constraints, and restricted opportunities for higher and vocational education. Overall, comparative analysis revealed that food and economic security were relatively better, while health and education lagged behind, highlighting the need for integrated and balanced development strategies focusing on nutrition-sensitive programs, improved rural healthcare infrastructure, and expanded educational opportunities to enhance the overall livelihood security of farm families.

Funding: There was no funding support for conducting this research.

Declaration of competing interest: The authors have no known competing interests.

Data availability: Data would be made available on request

Acknowledgment: The authors are deeply indebted to the respondents who co-operated during the research. We acknowledge the support rendered directly or indirectly by others during data collection.

Appendix supplementary data: The supplementary data, table for online visibility to the readers are attached in sequence in research paper.

Author's contribution: Both the authors collected and analyzed the data and interpreted the data, participated in contributing to the text and the content of the manuscript, including revisions and edits. All authors approve the content of the manuscript and agree to be held accountable for the work.

REFERENCES

[1] Beevi, A. and Rohit, J. (2018) Constraint analysis of livelihood systems in coral J. *Ext. Educ.* 3(2): 6056-6059.

[2] BHAVYA, A. P., (2019) Exploration of present farming systems for enhancing farm income:An economic analysis of constraints, challenges and potentials in southern and eastern dry zones of Karnataka. Ph.D.Thesis (Unpub), University of Agricultural Sciences, Bengaluru, Karnataka.

[3] Drèze, J., & Khera, R. (2017)Recent social security initiatives in India. World Development, 98, 555–572. https://doi.org/10.1016/j.worlddev.2017.05.035

[4] Dung, P.A. et al. (2024) "Current Changes in the Role of Agriculture and Agri-Farming Structures in Thailand and Vietnam with SLM practices," International Journal of Rural Development, Environment and Health Research, 8(1), pp. 8–14. Available at: https://doi.org/10.22161/ijreh.8.1.3.

[5] FAO. (2000) working with local institutions to support sustainable livelihoods: A conceptual framework. Food and Agriculture Organization of the United Nations https://www.fao.org/4/y5083e/y5083e00.htm

[6] Getnet, M., Melkam, M. and Dejene, M. (2024) "Adaptation of Napier grass varieties in the highlands of East Gojjam," International Journal of Forest, Animal And Fisheries Research, 8(4), pp. 01–06. Available at: https://doi.org/10.22161/ijfaf.8.4.1.

[7] Harishkumar, H. V., (2012) Livelihood security of farm households under different farmingsystems in Kolar district of Karnataka An economic analysis.(Unpublished Ph.D. Thesis), University of Agricultural Sciences, Bengaluru, Karnataka.

[8] Huang, J., Wang, R.-Y. and Chen, L. (2023) "Analysis of Bird Habitat Suitability in Chongming Island Based on GIS and Fragstats," International Journal of Forest, Animal And Fisheries Research, 7(4), pp. 01–23. Available at: https://doi.org/10.22161/ijfaf.7.4.1.

[9] Jellifee D.B. (1966) Nutritional anthropometry, The Assessment of the nutritional status of the community, world Health Organization(WHO) press, Geneva: Pp.55-78.

[10] Kayes, A. et al. (2024) "Effects of biochar and chitosan on morpho-physiological, biochemical and yield traits of water-stressed tomato plants," International Journal of Horticulture, Agriculture and Food science, 8(2), pp. 01–09. Available at: https://doi.org/10.22161/ijhaf.8.2.1.

[11] Kumar, P., Lakra, K., Bairwal, S.L., Kushwaha, S. (2014) Sustainable agriculture and rural livelihood security in India, *J. of Science Agriculture* ISSN 2277 – 3290,Vol 4.

[12] Mehrotra, S. (2019) Realising the demographic dividend: The role of education and skills in rural India. Margin: The *J.* of Applied Economic Research, 13(1), 1–24. https://doi.org/10.1177/0973801018817165

[13] National Sample Survey Office (NSSO) (2019) Household Social Consumption: Education in India (NSS 75th Round, July 2017–June 2018) Ministry of Statistics and Programme Implementation, Government of India. Retrieved from https://mospi.gov.in/

[14] Shakti, Dubey, R. P. and Sheikhy, S. (2013) Assessment of food consumption pattern and nutritional status of school going children of Faizabad district.*Trends in Biosci.*6(6): 755-757.

[15] UNESCO.(2022) *Education for Sustainable Development: Progress and Challenges. United* Nations Educational, Scientific and Cultural Organization, Paris. Retrieved from https://unesdoc.unesco.

International Journal of Environment, Agriculture and Biotechnology
Vol-11, Issue-2; Mar-Apr, 2026
Peer-Reviewed International Journal
Journal Home Page Available: https://ijeab.com/
Journal DOI: 10.22161/ijeab

The growth and yield characteristics of guava (*Psidium guajava* L.) cv. Gwalior 27 are affected by the addition of borax and zinc sulphate

Komal Yadav[1], Pinky Yadav[2,*], Manju Verma[3], Priyadarshani Arun Khambalkar[4], Shashi S. Yadav[4]

[1]Department of Horticulture, College of Agriculture, Rajmata Vijayaraje Scindia Krishi Vishwa Vidyalaya Gwalior, M.P.- 474002, India
[2]Department of Education in Science and Mathematics, Regional Institute of Education, Mysore, NCERT, Karnataka -570006, India
[3]Department of horticulture, College of Agriculture, Nagaur, Rajasthan-34100, India [4]Department of soil science, College of Agriculture, Rajmata Vijayaraje Scindia Krishi Vishwa Vidyalaya Gwalior, M.P.-474002, India
*Correspondence Author

Received: 23 Jan 2026; Received in revised form: 25 Feb 2026; Accepted: 06 Mar 202; Available online: 14 Mar 2026

***Abstract*— *In 2016–2017, a field study named "Effect of foliar application of borax and zinc sulphate on growth, yield, and quality of guava (Psidium guajava L.) cv. Gwalior-27" was conducted at Agrotechnology Park, Krishi Vigyan Kendra, College of Agriculture, Gwalior (M.P.). There were nine treatments in the trial, each with two amounts of zinc sulfate (0.4 and 0.6%) and borax (0.2 and 0.4%). Three replications and factorial randomized block design were used to set up the experiment. In terms of guava growth and yield characteristics, treatment B_2Z_2 (Borax at 0.4% & Zinc sulfate at 0.6%) was found to be considerably better than the control across various foliar spray nutrient dosages.*

***Keywords*— Intraction, borax, zinc sulphate, guava, Psidium guajava**

I. INTRODUCTION

One of the most common fruit plants grown in tropical, subtropical, and some dry regions of India is the guava (*Psidium guajava* L.), also known as the apple of the tropics. The fruit is a member of the Myrtaceae family. After banana, mango, citrus, and papaya, it is the fifth most significant fruit in terms of area. It is also the fifth most important fruit in terms of production. This fruit appears to have grown from Mexico to Peru after originating in tropical America.

It produces roughly 25 t/ha and is appropriate for table use. Uttar Pradesh, Maharashtra, Madhya Pradesh, Bihar, West Bengal, Punjab, and Gujarat are India's top guava-producing states. India, Hawaii, Mexico, Cuba, Sri Lanka, Venezuela, Brazil, Thailand, New Zealand, Philippines, Indonesia, Malaysia, Australia, Israel, Pakistan, Bangladesh, and other tropical and subtropical regions are already growing it. According to *Bhatia et al.* (2001), India is the world's top producer of guava. Berries are a good source of pectin (0.5-1.8%) and vitamin C (210-305 mg/100 g), although they are low in calories (66 Cal/100 g). In addition to having a high tannin content (9–12%), guava leaves also contain 0.3% essential oil (including eugenol) and triterpenoids, which may contribute to their overall therapeutic effect (*Chapman,1964*). The physical characteristics of guava fruit may have been enhanced by borax, which also plays a significant role in the metabolism of sugar and acts as a catalyst in the oxidation and reduction processes. This could have increased the yield per tree as suggested by our findings. The high level of auxin in the different regions of the fruit plant maintained by borax may be the reason for heavier fruits with more fruit weight after borax treatment. According to *Abd-Allah* (2006), borax enhances pollen grain germination, pollen tube elongation, fruit set percentage, and ultimately yield.

For plants, zinc (Zn) is a necessary micronutrient. Numerous enzymatic processes involve it. Zinc is essential for plant growth and development. Additionally, it controls how proteins and carbohydrates are metabolized (*Trivedi, N.,* 2012). High pH soils restrict its availability to plants. It is well recognized that zinc plays a significant part in many different types of enzymes, either as a metal component or as a structural, functional, or regulatory element. One heavy non-metal micronutrient is boron. Plants absorb it as boric acid (H_3BO_3). Boron is required for the transfer of sugar, plant reproduction, and pollen grain germination. Its function in active salt absorption and hormone transport has been noted. It plays a significant part in fruit quality as well. In addition to having a significant impact on root growth and cell elongation (pollen tube), boron also affects the construction of cell walls (*Meena, 2008 and Rajput, 1986*).

II. METHOD MATERIALS

The current study, "Effect of foliar application of borax and zinc sulphate on growth, yield, and quality of guava (*Psidium guajava* L.) cv. Gwalior-27," was conducted in 2016–2017 at Agrotechnology Park, Krishi Vigyan Kendra, College of Agriculture, Gwalior (M.P.). Seven-year-old guava plants spaced six by six meters apart in a square planting method were used for the experiment. During the experimentation period, all of the plants were subjected to consistent cultural methods in order to evaluate the impacts of different treatments. Three replications of each treatment, each consisting of a single plant, were used in the randomized block design experiment.

Treatments	Details of the treatment
Control	Control (Water spray)
B_1	Borax (0.2%)
B_2	Borax (0.4%)
Z_1	ZnSO4 (0.4%)
Z_2	ZnSO4 (0.6%)
B_1Z_1	Borax (0.2%) + ZnSO4 (0.4%)
B_1Z_2	Borax (0.2%) + ZnSO4 (0.6%))
B_2Z_1	Borax (0.4%) + $ZnSO_4$ (0.4%)
B_2Z_2	Borax (0.4%) + Znso4 (0.6%))

Solution preparation: The necessary amounts of zinc sulfate and boric acid were dissolved in the necessary amount of water to create the stock solution of various concentrations of zinc sulphate (neutralized with hydrated lime) and borax.

Observations Recorded: In accordance with normal methods, observations on a variety of plant characteristics, such as growth and yield attributes of fruits of various treatments used, were calculated. As recommended by *Panse and Sukhatme* (1985), a factorial randomized block design was used to statistically examine the data gathered on various crop characteristics.

III. RESULTS

The interaction effect of borax and $ZnSO_4$ significantly improved the vegetative parameters of the guava plant. The maximum tertiary shoot length (8.08 cm), were recorded under B_2Z_2 (Borax @ 0.4% & ZnSo4 @ 0.6%), followed by B_1Z_2 (Borax @ 0.2% & ZnSo4 @ 0.6%), whereas the minimum tertiary shoot length (3.70 cm) was recorded under control B_0Z_0. The maximum shoot diameter (0.38 cm) was recorded under B_2Z_2 (Borax at 0.4% & $ZnSO_4$ at 0.6%), while the minimum shoot diameter (0.31 cm) was recorded under B_2Z_0 (Borax at 0.4% & no $ZnSO_4$). The mean maximum number of leaves per shoot (26.30) was recorded under B_2Z_2 (Borax @ 0.4% & $ZnSO_4$ @ 0.6%), followed by B_2Z_1 (Borax @ 0.4% & $ZnSO_4$ @ 0.4%), while the minimum number of leaves per shoot (15.65) was under the control (B_0Z_0). These findings are in line with earlier reports of *Lal and Sen* (2000) and *Kumawat et al.* (2012), who have shown that application of micronutrients alone or in combinations had a significant effect on plant height, plant spread, shoot length, and leaf area in guava plants. The foliar sprays of chemicals, viz., B and Zn, might have induced the synthesis of chlorophyll.

The combined sprays of borax and Zinc sulphate showed great improvement in yield-attributing characters of guava. The maximum number of fruit (322.5) was obtained under B_2Z_2 (Borax at 0.4% & $ZnSO_4$ at 0.6%), while the minimum yield was obtained with control. similar result also found by Meena et al. (2005) and Shukla et al. (2011) The higher fruit weight (147.83 g), fruit yield per tree (48.71 kg) and fruit yield per hectare (135.29 q), polar diameter (7.33 cm), pulp weight (297.00 g) and minimum seed weight (1.69 g)were noted under B_2Z_2 (Borax @ 0.4% & ZnSo4@ 0.6 %), The maximum radial diameter (6.83 cm) was recorded under the treatment B_1Z_2 (Borax @ 0.2% & ZnSo4@ 0.6%) and the maximum pulp weight (297.00 g) was recorded under the treatment B_2Z_1 (Borax @ 0.4% & ZnSo4@ 0.4%) , Whereas, the minimum number of fruit (289), fruit weight (128.67 g), fruit yield per tree (37.92 kg), fruit yield per hectare (105.31q), maximum seed weight (3.63 g) and minimum pulp weight (150 g) noticed under control. Minimum polar diameter (5.51 cm) was recorded under the treatment B_1Zo (borax at 0.2% & control). The minimum radial diameter (5.8 cm) was recorded under the treatment B_0 Z_1 (control

& $ZnSO_4$ at 0.4%). Trivedi *et al*. (2012) evaluated the effect of zinc (Zn) and boron (B) on the yield and fruit quality of guava.

Table 1: Interaction effect of Boron and Zinc sulphate on tertiary shoot length, shoot diameter, number of leaves, number of fruits per plant, fruit weight of guava.

B X Z	tertiary shoot length (cm)	shoot diameter (cm)	number of leaves	number of fruits per plant	fruit weight(g)
B_1Z_1	5.94	0.34	19.50	66.35	135.17
B_1Z_2	7.01	0.35	22.33	68.16	141.33
B_2Z_1	6.49	0.33	24.50	68.20	143.00
B_2Z_2	8.08	0.38	26.30	70.00	147.83
S.Em.±	0.058	0.009	0.202	1.635	3.255
CD at 5% level	NS	0.028	NS	NS	NS

Table 2: Intraction Effect of foliar spray of Borax and zinc sulphate on fruit yield per tree, yield per hectare, polar diameter, radial diameter, pulp weight and seed weight of guava

B X Z	fruit yield per tree (kg)	yield per hectare (q)	polar diameter (cm)	radial diameter (cm)	pulp weight (g)	seed weight (g)
B_1Z_1	42.03	116.73	6.30	6.12	172.00	2.01
B_1Z_2	45.90	127.43	6.36	6.83	171.00	1.92
B_2Z_1	46.18	128.24	6.43	6.69	297.00	1.75
B_2Z_2	48.71	135.29	7.33	6.27	240.00	1.69
S.Em.±	1.213	3.367	0.204	0.208	0.577	0.104
CD at 5% level	NS	NS	NS	NS	NS	NS

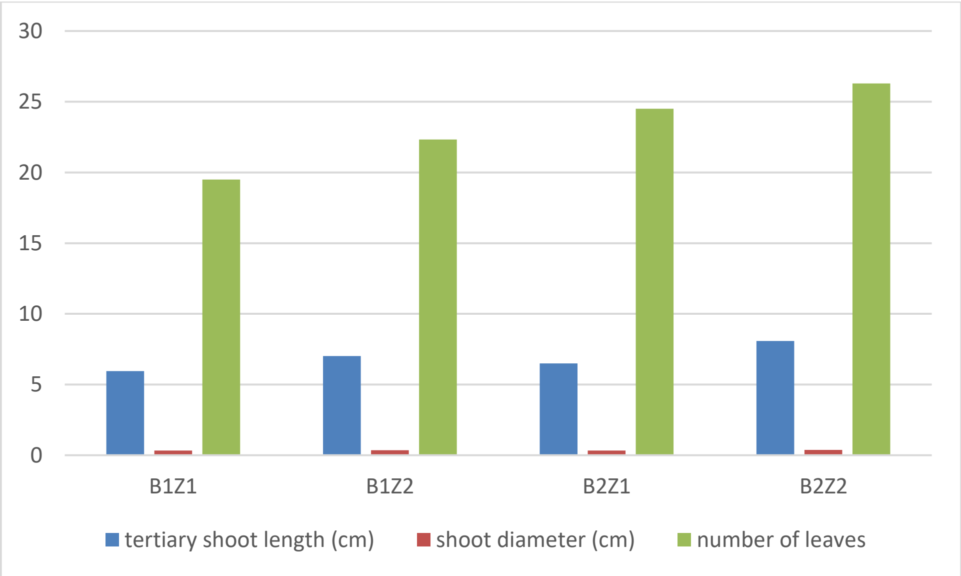

Fig a: Intraction Effect of foliar spray of Borax and zinc sulphate on tertiary shoot length (cm), shoot diameter (cm), and Number of leaves, of Guava.

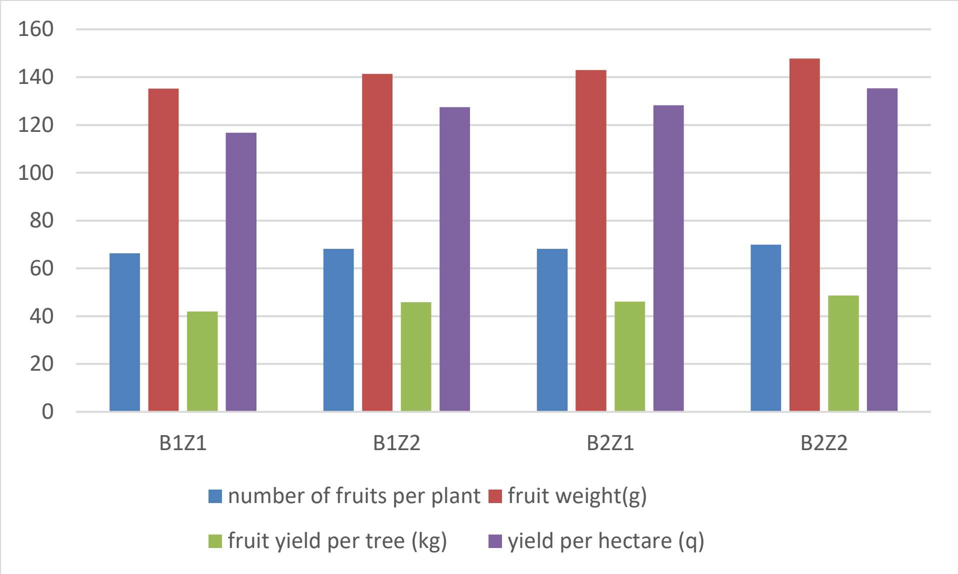

Fig. b: Intraction Effect of foliar spray of Borax and zinc sulphate on Number of fruits per plant, fruit weight (g), fruit yield per tree(kg), fruit yield per tree (kg) and yield per hectare (q) of Guava.

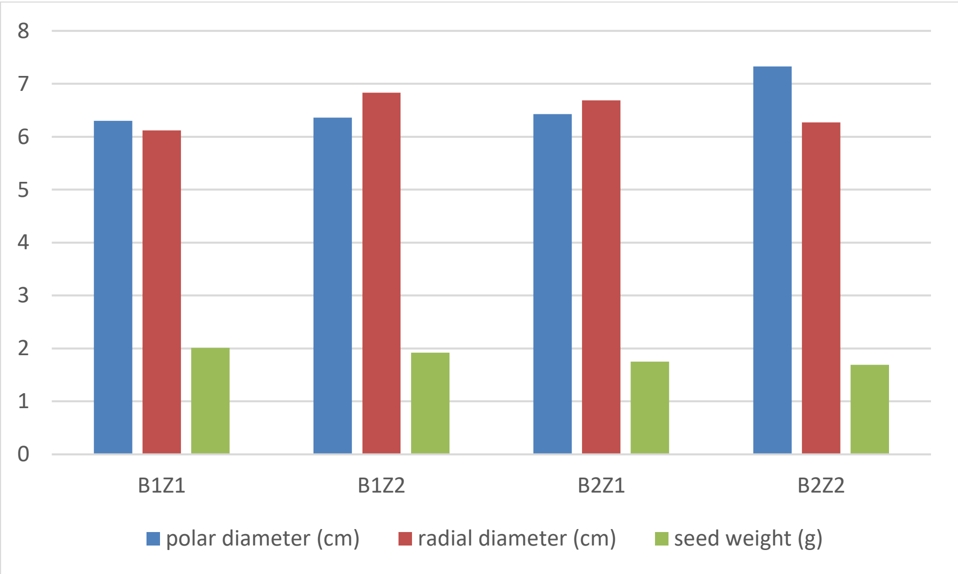

Fig. c: Intraction Effect of foliar spray of Borax and zinc sulphate on polar diameter (cm), radial diameter (cm) and seed weight (g) of Guava.

IV. CONCLUSIONS

According to the findings of the current study, "Effect of foliar application of Borax and Zinc sulphate on growth, yield, and quality of Guava (Psidium guajava L.) cv. Gwalior-27," foliar spraying borax and zinc sulphate together greatly improved fruit growth parameters and yield attributes. The treatment B_2Z_2 (borax at 0.4% & zinc sulphate @ 0.6%) was shown to be the best for nearly all growth metrics and fruit yield features in the interaction impact of borax and zinc sulfate.

REFERENCES

[1] Abd-Allah AS. (2006). Effect of spraying some macro and micro nutrients on fruit set, yield and fruit quality of Washington navel orange trees. *J Appl. Sci. Res.* **2**:1059-1063.

[2] Bhatia SK, Yadav S, Ahlawat VP, Dahiya SS. (2001). Effect of foliar application of nutrients on the yield and fruit quality of winter season guava cv. L-49. *Haryana Journal of Horticultural Sciences*.,**30**:6-7.

[3] Chapman HD (1964). Suggested foliar sampling and handling techniques for determining the nutrient status of some field, horticultural and plantation crops. *Indian Journal of Horticulture*.;**21**:97-119.

[4] Huang, J., Wang, R.-Y. and Chen, L. (2023) "Analysis of Bird Habitat Suitability in Chongming Island Based on GIS and Fragstats," International Journal of Forest, Animal And Fisheries Research, 7(4), pp. 01–23. Available at: https://doi.org/10.22161/ijfaf.7.4.1.

[5] Kaushik DK, Gupta M, Kumawat KL, Basu A. (2012). NLRP3 in flamma some: key mediator of neuro inflammation in murine Japanese encephalitis. *PLoS One*. **7**(2)e32270.

[6] Kayes, A. et al. (2024) "Effects of biochar and chitosan on morpho-physiological, biochemical and yield traits of water-stressed tomato plants," International Journal of Horticulture, Agriculture and Food science, 8(2), pp. 01–09. Available at: https://doi.org/10.22161/ijhaf.8.2.1.

[7] Lal G, Sen NL, Jat RG. (2000). Yield and leaf nutrient composition of guava as influenced by nutrients. *Indian Journal of Horticulture*. **57(**2):130-132.

[8] Manikandhan, C., Daniel, V. and Daniel, K. (2023) "Transmission Electron Microscopic (TEM) analysis of STZ-diabetes induced Cardiac Structural changes in Rats.," International Journal of Rural Development, Environment and Health Research, 7(5), pp. 27–36. Available at: https://doi.org/10.22161/ijreh.7.5.3.

[9] Meena RP, Mohammed S, Lakhawat SS. (2005). Effect of foliar application of urea and zinc sulphate on fruit quality and yield of pruned guava trees *(Psidium guajava* L.) cv. Sardar under high density planting system. *Journal of Horticulture Science*., **11**:290-93.

[10] Meena, V. S., Yadav, P. K. and Meena, P. M. (2008). Yields attributes of ber (Ziziphus mauritiana) cv. Gola as influenced by foliar application of ferrous sulphate and borax. *Agriculture Science Digest*, **28**(3): 219-221.

[11] Panse, V.G., and Sukhatme, P.V. (1985). Statistical Methods for Agriculture Workers. *ICAR, New Delhi.*

[12] Rajput, C. B. S. and Chand, S. (1986). Effect of boron and zinc on the physico-chemical composition of guava fruits (*Psidium guajava L.*). *J. Nat. Agric. Sci. Ceylon*. **13**: 49-54.

[13] Shukla AK. (2011). Effect of foliar application of calcium and boron on growth, productivity and quality of Indian gooseberry (*Emblica officinalis*). *Indian Journal of Agriculturre Science* **81**(7):628-632.

[14] Trivedi, N., Singh, D., Bahadur, V., Prasad, V.M. and Collis, J. P. (2012). Effect of foliar application of zinc and boron on yield and fruit quality of guava (*Psidium guajava L.*). *Hort. Flora Research Spectrum,* **1(**3): 281- 283.

International Journal of Environment, Agriculture and Biotechnology
Vol-11, Issue-2; Mar-Apr, 2026
Peer-Reviewed International Journal
Journal Home Page Available: https://ijeab.com/
Journal DOI: 10.22161/ijeab

Development and Evaluation of Tensile Strength, Water Resistance, and Biodegradability of Bioplastic using Mermaid's Fan (*Padina pavonica)* Seaweed and Extracted Cellulose from Coconut (*Cocos nucifera)* Lumber Sawdusts

Lara Melisa O. Bauyot*, Guerrero T. Nucos, Wendyl M. Aligato, Eunice Glenn G. Bangcaya, Hanifa B. Benito, Jhun Evans L. Sedoripa, Reggie M. Macumbes, Princess Dianne D. Guias, Ron Angelo A. Rodriguez, Alexis John A. Orejas

*Immaculate Heart of Mary Academy, Manuel L. Quezon St., Central, City of Mati, 8200 Davao Oriental, Philippines.
Email: bauyotlara@gmail.com

Received: 25 Jan 2026; Received in revised form: 27 Feb 2026; Accepted: 08 Mar 202; Available online: 16 Mar 2026

***Abstract*— Plastic pollution has increased demand for bioplastic alternatives. This study developed bioplastic from Mermaid's fan seaweed alginate and cellulose extracted from coconut lumber sawdust. Bioplastics were produced through alginate extraction, cellulose isolation, and material testing, with data analyzed using one-way ANOVA at 0%, 35%, and 70% cellulose concentrations. Results showed no statistically significant differences in tensile strength and water resistance among treatments ($p > 0.05$). However, water degradation differed significantly ($p < 0.05$), with the 35% cellulose formulation exhibiting the highest mass loss and fastest degradation. These findings indicate cellulose mainly affects degradation behavior. Therefore, Mermaid's fan-based bioplastic shows eco-friendly potential as an alternative to conventional plastics.*

Keywords*— Bioplastic, Cellulose, Padina pavonica, Tensile strength, Water Degradation, Water resistance

I. INTRODUCTION

[1] Plastic pollution has become a serious environmental problem due to the continuous production and improper disposal of petroleum-based plastics. Millions in tons of plastic waste enter marine environments annually, threatening biodiversity, ecosystems, and human health. [2-3] In the Philippines, microplastic contamination has been reported in Laguna de Bay, while coastal ecosystems such as Pujada Bay in Davao Oriental continue to experience increasing plastic accumulation. These environmental concerns highlight the urgent need for biodegradable and sustainable alternatives to conventional plastics.

[4] Previous studies have shown that seaweeds are promising raw materials for bioplastic production because of their polysaccharide content, particularly alginate, which has film-forming and biodegradable properties. The brown seaweed *Padina pavonica* has been identified as a potential source of alginate for sustainable applications. [5] Meanwhile, cellulose derived from plant materials has been recognized for enhancing the mechanical properties of bioplastics, including tensile strength and structural stability. In particular, cellulose extracted from *Cocos nucifera* lumber contains high cellulose content and is suitable as a reinforcing material. However, limited research has examined the combined use of Mermaid's

Fan seaweed and coconut lumber-derived cellulose in developing bioplastics and evaluating on how varying cellulose concentrations influence tensile strength, water resistance, and degradation.

This study aimed to develop a biodegradable bioplastic using alginate extracted from *Padina pavonica* and cellulose extracted from *Cocos nucifera* lumber sawdust. Specifically, the objectives of the study were to: (1) determine whether varying cellulose concentrations (0%, 35%, and 70%) significantly affect tensile strength; (2) evaluate the effect of cellulose concentration on water resistance through mass gain testing; and (3) assess the effect of cellulose concentration on degradation rate through mass loss analysis.

The contribution of this paper lies in providing experimental evidence on the reinforcing effect of coconut lumber cellulose in seaweed-based bioplastic and identifying which material properties are significantly influenced by cellulose concentration. The findings contribute to the development of locally sourced, environmentally sustainable bioplastic alternatives.

1.1 Characteristics of Mermaid's Fan (*Padina pavonica*)

[6] *Padina pavonica*, also referred to as Mermaid's Fan, is a type of brown seaweed characterized by its calcified fronds in the shape of a fan with concentric bands and a lightly mineralized surface texture from calcium carbonate deposits. These characteristics result in the rigidity of the seaweed. Mermaid's Fan is usually found in shallow waters and on coral reefs in tropical and temperate ocean environments, providing food sources and breeding places for different marine life. [7] However, the occurrence of massive quantities of the seaweed on coastlines has resulted in environmental concerns because the decomposing seaweed releases toxic gases such as hydrogen sulfide and ammonia. [8] Massive quantities of the seaweed have also been observed in the Caribbean region, Central America, North America, and Africa. As a result, the governments in these regions are working hard to manage the seaweed.

1.2 Characteristics of cellulose from coconut *(Cocos nucifera)* lumber

[22] Coconut fiber is composed of approximately 67% holocellulose and 25% lignin, values comparable to those of hardwoods, making it a promising source of cellulose for industrial applications. [22] Its most common derivative, cellulose acetate, exhibits excellent transparency, tensile strength, and thermal stability, which supports its widespread use in food packaging, textiles, cigarette filters, and fashion accessories. [23] Furthermore, a study demonstrated that increasing hydrogen peroxide concentration and extending bleaching time significantly improved cellulose quality, with the optimal treatment being 40% hydrogen peroxide for 120 minutes, resulting in high-purity, highly white cellulose with low hemicellulose and lignin content, suitable for bioplastic production, including blends with Sargassum spp. to enhance durability and flexibility.

1.3 Characteristics of cellulose derived from sawdust in bioplastics

[9] Sawdust is a wood-processing byproduct rich in cellulose, hemicellulose, and lignin, with cellulose valued for its strength, renewability, and wide applications. [10] As a sustainable and accessible material, sawdust provides an eco-friendly alternative to synthetic polymers through cellulose extraction. [11] Additionally, cellulose fibers enhance the tensile strength, rigidity, impact resistance, and durability of bioplastics, making them suitable for packaging and structural applications.

1.4 Sargassum -based bioplastic specifically Mermaid's Fan (*Padina pavonica*)

[12] Bioplastics from Mermaid's Fan contain alginate and other polysaccharides used in the production of biodegradable polymers. [13] These are more environmentally friendly than petroleum-based polymers. Research also proves the addition of biodegradable additives improves the mechanical properties and durability of the seaweed-based bioplastics. [14] Mermaid's Fan also shows promising results in the yield of alginate and its positive mechanical properties, achieving a tensile strength of 2.34 MPa and 24.02% elongation. These characteristics are promising for the production of an eco-friendly biodegradable plastic.

1.5 Mechanical and biodegradation properties of seaweed-based bioplastic

[15] Seaweed-based bioplastics exhibit enhanced tensile strength, flexibility, and barrier properties against water vapor and oxygen, making them ideal for packaging, while also demonstrating rapid composting biodegradability as a sustainable option. [16] Their mechanical performance, thermal stability, water resistance, and biodegradability can be further improved using additives such as glycerol, starch, cellulose, and carrageenan, allowing tailored properties for eco-friendly packaging applications. [17] Additionally, alginate-based seaweed bioplastic materials incorporating invert sugar and glycerol display better flexibility and strength, allowing for full biodegradation within days and reducing environmental harm compared with conventional disposing methods.

II. MATERIALS AND METHODS

This study used a quantitative experimental research design to identify the precise effect on key characteristics of bioplastics. Before application, seaweed was harvested, dried, cleaned, and processed uniformly according to standard practices, ensuring reliable and reproducible results There were two sites that the researchers visited. The first research site was Dahican–Bobon Road shoreline, City of Mati, Davao Oriental, where Mermaid's Fan seaweed was collected as the primary raw material. The second site was the Science Laboratory of Immaculate Heart of Mary Academy (IHMA), City of Mati, Davao Oriental, where the collected seaweed was processed and developed into bioplastic. The same laboratory also served as the testing ground for evaluating the produced bioplastic in terms of biodegradability, water resistance, and tensile strength. Lastly, the manuscript were also finished in the same instituition.

2.1 Collection and cleaning of *Padina pavonica* Seaweed

Fig.1. Mermaid's Fan (Padina pavonica)

Fresh Mermaid's Fan seaweed was collected from Bangunay Beach. It is collected fresh and it was thoroughly washed with tap water to remove dirt, sand, salt, and other impurities. After soaking, the seaweed was drained and dried either through air drying, under sunlight, or using an oven at 50°C until fully dehydrated, once dried the seaweed was cut into small pieces.

2.2 Extraction of sodium alginate from *Padina pavonica*

To extract sodium alginate, the dried seaweed was mixed with a 2–3% sodium carbonate solution using a typical weight-to-volume ratio of 1:2. This mixture was heated between 60°C and 80°C for 10 minutes while being continuously stirred to dissolve the alginate. After extraction, the mixture was filtered using filter paper to remove the solid residue, leaving behind a brownish liquid rich in sodium alginate.

2.3 Extraction of cellulose from coconut lumber sawdust

The dried sawdust from Coconut Lumber was first boiled in a sodium hydroxide (NaOH) solution to remove lignin and hemicellulose. This process helped isolate the cellulose content. After boiling, it was then filtered to collect the solid residue and washed to remove remaining chemicals

2.4 Combination of coconut lumber sawdust-derived cellulose and *Padina pavonica* seaweed

The dried powder, which was the alginate extracted from Mermaid's Fan seaweed, was mixed in 100 mL of distilled water. The cellulose from Coconut Lumber sawdust was also added. While stirring, glycerol (30% of the total polymer weight) was added to improve flexibility. The mixture was stirred continuously until everything was smooth and well combined, forming a ready-to-cast bioplastic solution.

2.5 Molding and drying

Once the bioplastic mixture was prepared, it was carefully poured into a clean, flat mold or tray to form a thin film, similar to conventional packaging plastic, with dimensions of 6 cm × 5 cm. The surface was then leveled to ensure uniform thickness, typically maintained within the range of 0.1–0.25 mm.

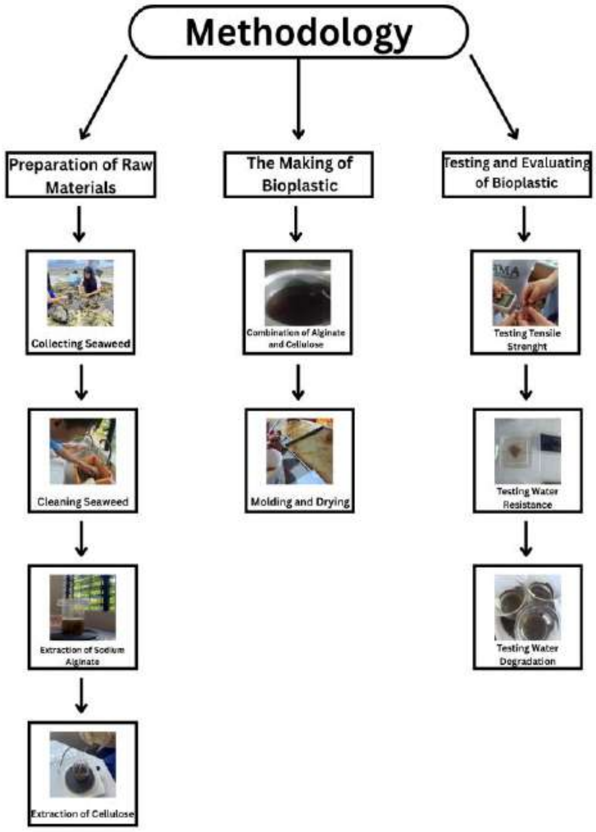

Fig.2. Summary of Methods

2.6 Testing for tensile strength

In order to determine the tensile strength of the developed bioplastic, a force gauge was used. The cut bioplastic was prepared and tested using a force gauge. Each specimen was securely clamped onto the force gauge, and a steadily increasing tensile force was applied until the material fractured, the maximum force at break was recorded for each sample.

2.7 Testing of bioplastic's water resistance

Water resistance was evaluated following the ASTM D570 method. The bioplastic samples were dried and weighed prior to testing, then fully immersed in separate containers containing 200 mL of distilled water at room temperature with a time interval of 2, 4, 6, 8 minutes. Each bioplastic sample was 2 grams.

2.8 Testing of bioplastic's degradation

For biodegradability testing, a seawater immersion test was conducted. The bioplastic samples were dried, and their initial weight (W_0) was recorded prior to testing. Each sample was immersed in a beaker containing 100 mL of seawater at room temperature for 15 minutes, and every sample weighed 1 gram.

III. RESULTS

3.1 The bioplastic performance profile

The samples were analyzed based on tensile strength, water resistance, and biodegradability using experimental testing procedures. Tables 1, 2, and 3 present the summarized results.

Table 1. Tensile Strength of Bioplastic Samples

Cellulose Concentration	***Number of Trials***	***Mean Tensile Strength (MPa)***
0% Cellulose	3	4.97
35% Cellulose	3	8.87
70% Cellulose	3	6.50
Total	***9***	-

Most of the samples showed improved tensile strength with the addition of cellulose. The 35% cellulose concentration recorded the highest mean tensile strength. However, statistical testing indicated no significant difference ($p > 0.05$).

Table 2. Water Resistance Test Results

Cellulose Concentration	***Mean Mass Gain (g)***	***Interpretation***
0% Cellulose	2.87	Moderate Absorption
35% Cellulose	3.10	High Absorption
70% Cellulose	2.73	Low Absorption

The 70% cellulose sample demonstrated better water resistance based on lower mass gain values. No significant difference was observed among treatments ($p > 0.05$).

Table 3. Degradation Test Results

Cellulose Concentration	***Mean Mass Loss (g)***	***Interpretation***
0% Cellulose	0.17	Moderate Degradation
35% Cellulose	0.33	Fast Degradation
70% Cellulose	0.07	Slow Degradation

The 35% cellulose formulation degraded the fastest among treatments. Statistical analysis confirmed a significant difference in degradation ($p < 0.05$).

Most of the bioplastic samples demonstrated improved performance with the incorporation of cellulose. The 35% cellulose concentration recorded the highest mean tensile strength (8.87 MPa), while the 0% cellulose obtained the lowest value (4.97 MPa), indicating that moderate cellulose addition enhances mechanical properties. In terms of water resistance, the 70% cellulose sample showed the lowest mean mass gain (2.73 g), suggesting better resistance to moisture absorption compared to the other treatments. For biodegradability, the 35% cellulose formulation exhibited the highest mean mass loss (0.33 g), reflecting faster degradation, whereas the 70% cellulose degraded the slowest. Statistical analysis revealed no significant difference in tensile strength and water resistance ($p > 0.05$), but a significant difference was observed in degradation ($p < 0.05$), implying that cellulose concentration significantly affects the biodegradation behavior of the developed bioplastic

3.2 Analysis of variance (ANOVA)

Table 4. One-Way ANOVA for Tensile Strength

Source of Variation	***SS***	***df***	***MS***	***F***	***p-value***
Between Groups	*23.17*	*2*	*11.585*	*3.33*	*> 0.05*
Within Groups	*20.87*	*6*	*3.478*		
Total	***44.04***	***8***			

The mechanical testing aimed to determine if adding cellulose increased the structural integrity of the bioplastic. While the 35% concentration reached a peak mean tensile strength, the statistical analysis suggests this increase was not definitive.

As shown in Table 1, the One-Way ANOVA for tensile strength resulted in an *F*-value of (3.33) and a p-value of (0.11). Since the *p*-value is greater than the significance level of (> 0.05), the researchers fail to reject the null hypothesis. This indicates that there is no statistically significant difference in tensile strength between the three groups, implying that under the current formulation, the amount of cellulose did not significantly change the material's resistance to breaking.

Table 5. One-Way ANOVA for Water Resistance

Source of Variation	*SS*	*df*	*MS*	*F*	*p-value*
Between Groups	*0.21*	*2*	*0.1*	*1.21*	*> 0.05*
Within Groups	*0.51*	*6*	*0.09*		
Total	***0.72***	***8***			

The results for water resistance showed that the F-value is 1.21 and the p-value is greater than 0.05. Since the *p*-value is greater than the significance level of (> 0.05), the researchers fail to reject the null hypothesis. The researchers did see some differences in how much mass was gained by each treatment but these differences in water resistance are not really significant, for the cellulose treatments. The water resistance of the cellulose treatments does not have any differences.

Table 6. One-Way ANOVA for Degradation

Source of Variation	*SS*	*df*	*MS*	*F*	*p-value*
Between Groups	*0.11*	*2*	*0.055*	*13.75*	*< 0.05*
Within Groups	*0.02*	*6*	*0.004*		
Total	***0.13***	***8***			

The results of the One-Way ANOVA showed a *F*-value of 13.75 with a p-value less than 0.05. Since the *p*-value is lower than the 0.05 level of significance, the null hypothesis is rejected. This indicates that there is a statistically significant difference in degradation among the cellulose concentrations. Therefore, cellulose content significantly influences the biodegradation behavior of the developed bioplastic.

IV. DISCUSSION

In this study, the effects of varying cellulose concentrations on the tensile strength, water resistance, and water degradation of alginate-based bioplastic films were evaluated. Statistical analysis was conducted to determine whether differences among treatments were significant at the 0.05 level of significance, and the findings were interpreted in relation to existing literature.

The results showed that varying cellulose concentrations did not produce a statistically significant difference in tensile strength, as indicated by a p-value greater than 0.05. Although the 35% cellulose formulation exhibited the highest mean tensile strength, the differences among treatments were not statistically significant, suggesting that cellulose content did not substantially enhance the mechanical strength of the bioplastic films. [18] Similar findings have been reported in previous studies where natural fiber incorporation into alginate matrices did not always result in significant tensile improvement due to limitations in fiber–matrix interaction.

The reinforcing efficiency of cellulose depends largely on strong interfacial adhesion and effective stress transfer between the fiber and polymer matrix. [25] Research has shown that insufficient bonding between reinforcing fibers and the surrounding polymer can significantly reduce mechanical enhancement even when fibers are uniformly dispersed. In the present study, weak interfacial compatibility between cellulose and alginate may have limited effective load transfer, thereby minimizing the expected strengthening effect. These findings suggest that cellulose incorporation alone may not significantly improve tensile properties without additional surface treatment or processing modification.

Similarly, varying cellulose concentrations did not produce a statistically significant difference in water resistance (mass gain), as indicated by the computed *F*-value of 1.21 and *p*-value of 0.36, which is greater than the 0.05 level of significance. Although the 35% cellulose formulation exhibited the highest mean mass gain and the 70% formulation showed the lowest, these differences were not statistically significant, indicating that cellulose content did not substantially influence the material's resistance to water absorption. [19] Comparable results have been observed in cellulose–glycerol bioplastics, where changes in cellulose concentration did not significantly alter moisture-related properties such as water uptake and barrier performance. [20] Furthermore, studies explain that cellulose incorporation alone does not necessarily enhance water resistance in bioplastic films because both cellulose and seaweed-based polymers contain hydroxyl groups that attract water molecules. Due to this hydrophilic nature, improvements in moisture resistance often require hydrophobic modification or crosslinking strategies rather than simply increasing cellulose content. Thus, both the present findings and supporting literature indicate that cellulose addition alone may not significantly change the water resistance of alginate-based bioplastics.

In contrast, cellulose concentration influenced the water degradation behavior of the bioplastic films. The treatment containing 35% cellulose demonstrated the highest mean mass loss (0.33 g), indicating a faster degradation rate, while the 70% formulation showed lower mass loss, suggesting slower degradation. These results indicate that cellulose concentration plays a role in controlling the degradation performance of the material.

Previous research has demonstrated that cellulose can affect degradation behavior due to its hydrophilic characteristics, which promote water penetration into the polymer matrix and accelerate hydrolytic breakdown. Moderate cellulose concentrations may increase matrix porosity and enhance water interaction, thereby accelerating degradation. [21] Similar findings were also reported in the studies conducted to explore the aqueous biodegradation of polysaccharide-based composites, where films containing alginate and cellulose nanocrystals showed considerable mass loss and degradation when exposed to water, suggesting that the nature of the component, being hydrophilic, plays an important role in the degradation process. [19] However, higher cellulose content may contribute to a denser internal structure that restricts water diffusion, resulting in slower degradation. Overall, the findings suggest that while cellulose incorporation may not significantly enhance tensile strength and water resistance, it can influence degradation rate, highlighting the importance of formulation balance and material compatibility in optimizing bioplastic performance.

V. CONCLUSION

1. Varying cellulose concentrations (0%, 35%, and 70%) did not significantly affect the tensile strength of the developed bioplastic ($p > 0.05$), indicating that mechanical strength is largely independent of cellulose content.
2. Water resistance of the bioplastic was not significantly influenced by cellulose concentration, suggesting that cellulose does not enhance this property.
3. Water Degradation was significantly affected by cellulose concentration ($p < 0.05$), as shown by differences in water degradation among samples.
4. The formulation containing 35% cellulose exhibited the highest mass loss and fastest degradation rate, indicating that this concentration optimizes biodegradability.
5. Overall, cellulose acts as a key determinant of bioplastic biodegradability while having minimal impact on mechanical strength and water resistance.

RECOMMENDATIONS

Following recommendations should be suggested:

1. The study recommends testing a wider range of cellulose concentrations to determine the optimal balance between tensile strength, water resistance, and water degradation.

2. The use of other additives, reinforcing materials, or alternative processing methods should be explored to further improve the quality and performance of the bioplastic.

3. The cellulose extraction process should be improved to ensure more consistent and higher-quality cellulose, which may enhance the properties of the bioplastic.

4. The number of trials and samples should be increased to obtain more reliable, accurate, and statistically valid results.

5. The bioplastic should be evaluated under real-life conditions, such as packaging applications, to gain better insights into its durability, usability, and practical performance.

REFERENCES

[1] Ritchie, H., Samborska, V., & Roser, M. (2023). Plastic pollution. Our World in Data. https://ourworldindata.org/plastic-pollution

[2] Arcadio, C. G. L. A., Navarro, C. K. P., Similatan, K. M., Inocente, S. A. T., Ancla, S. M. B., Banda, M. H. T., Capangpangan, R. Y., Torres, A. G., & Bacosa, H. P. (2023). Microplastics in surface water of Laguna de Bay: first documented evidence on the largest lake in the Philippines. Environmental Science and Pollution Research, 30(11), 29824–29833. https://doi.org/10.1007/s11356-022-24261-5

[3] Abreo, N. A. S., Siblos, S. K. V., & Macusi, E. D. (2021). Anthropogenic Marine Debris (AMD) in Mangrove Forests of Pujada Bay, Davao Oriental, Philippines. Journal of Marine and Island Cultures, 9(1), 38–53. https://doi.org/10.21463/jmic.2020.09.1.03

[4] Rajendran, N., Puppala, S., Raj, M. S., Angeeleena, B. R., & Rajam, C. (2020). Seaweed : A Potential Source for Bioplastics. Journal of Pharmacy Research, 5(3), 1476–1479. https://www.researchgate.net/publication/346941540_Seaweed_A_Potential_Source_for_Bioplastics

[5] Adegoke, K. A., Adesina, O. O., Okon-Akan, O. A., Adegoke, O. R., Olabintan, A. B., Ajala, O. A., Olagoke, H., Maxakato,

N. W., & Bello, O. S. (2022). Sawdust-biomass based materials for sequestration of organic and inorganic pollutants and potential for engineering applications. Current Research in Green and Sustainable Chemistry, 5(January), 100274. https://doi.org/10.1016/j.crgsc.2022.100274

[6] Helm, R. R. (2021). The mysterious ecosystem at the ocean's surface. *PLoS Biology*, *19*(4), 1–15. https://doi.org/10.1371/journal.pbio.3001046

[7] Resiere, D., Valentino, R., Nevière, R., Banydeen, R., Gueye, P., Florentin, J., Cabié, A., Lebrun, T., Mégarbane, B., Guerrier, G., & Mehdaoui, H. (2018). *Sargassum* seaweed on Caribbean islands: an international public health concern. *The Lancet*, *392*(10165), 2691. https://doi.org/10.1016/S0140-6736(18)32777-6

[8] Resiere, D., Kallel, H., Florentin, J., Banydeen, R., Compton, K., Gueye, P., Mehdaoui, H., & Neviere, R. (2023). *Sargassum seaweed in the Caribbean: A major public health problem still unsolved*. Journal of Global Health, 13, 03017. https://doi.org/10.7189/jogh.13.03017

[9] Adegoke, K. A., Adesina, O. O., Okon-Akan, O. A., Adegoke, O. R., Olabintan, A. B., Ajala, O. A., Olagoke, H., Maxakato, N. W., & Bello, O. S. (2022). Sawdust-biomass based materials for sequestration of organic and inorganic pollutants and potential for engineering applications. *Current Research in Green and Sustainable Chemistry*, *5*(January), 100274. https://doi.org/10.1016/j.crgsc.2022.100274

[10] Meas, A., Wi, E., Chang, M., & Hwang, H. S. (2024). Carboxylmethyl cellulose produced from wood sawdust for improving properties of sodium alginate hydrogel in dye adsorption. *Separation and Purification Technology*, *341*(August), 1–10. https://doi.org/10.1016/j.seppur.2024.126906

[11] Hendrawati, Liandi, A. R., Ahyar, H., Maladi, I., Azhari, A., & Cornelia, M. (2023). The influence of the filler addition of rice husk cellulose, polyvinyl alcohol, and zinc oxide on the characteristics of environmentally friendly cassava biodegradable plastic. *Case Studies in Chemical and Environmental Engineering*, *8*(December), 1–27. https://doi.org/10.1016/j.cscee.2023.100520

[12] Santana, I., Felix, M., & Bengoechea, C. (2024). Seaweed as basis of eco-sustainable plastic materials: Focus on alginate. *Polymers,* *16*(12), 1662. https://doi.org/10.3390/polym16121662

[13] Kanagesan, K., Abdulla, R., Derman, E., Sabullah, M. K., Govindan, N., & Gansau, J. A. (2022). A sustainable approach to green algal bioplastics production from brown seaweeds of Sabah, Malaysia. *Journal of King Saud University - Science*, *34*(7), 102268. https://doi.org/10.1016/j.jksus.2022.102268

[14] Dalal, S. R., El-Naggar, N. E.-A., & El Naeem, G. A. (2023). Biosynthesis of sustainable biodegradable bioplastics using alginate extracted from *Padina pavonica*: Optimization and characterization. *Algal Research*. https://doi.org/10.1016/j.algal.2023.103325

[15] Kumar, M., Rathour, R., Gupta, P., Chaurasia, P., Shukla, P., & Thakur, I. S. (2024). Production and evaluation of a seaweed-based bioplastic sheet for food packaging. Uttar Pradesh Journal of Zoology, 45(13), 60-69. https://doi.org/10.47278/journal.upjoz/2024.13/artl15

[16] Siracusa, V., & La Rosa, A. D. (2024). Seaweed-based polysaccharides – Review of extraction, characterization, and bioplastic application. Green Chemistry. Advance online publication. https://doi.org/10.1039/D3GC04009G

[17] Kanagesan, K., Abdulla, R., Derman, E., Sabullah, M. K., Govindan, N., & Gansau, J. A. (2022). A sustainable approach to green algal bioplastics production from brown seaweeds of Sabah, Malaysia. *Journal of King Saud University - Science*, *34*(7), 102268. https://doi.org/10.1016/j.jksus.2022.102268

[18] Putri, F. A., Rianjanu, A., & Sipahutar, W. S. (2024). *Cellulose impact on bioplastic performance: A study on mechanical strength, physical properties, and degradation of water hyacinth and kepok banana peel-derived materials*. Jurnal Teori Dan Aplikasi Fisika, 12(02). https://doi.org/10.23960/jtaf.v12i02.407

[19] Biodegradation of polysaccharide-based biocomposites with acetylated cellulose nanocrystals, alginate and chitosan in aqueous environment. *International Journal of Biological Macromolecules*, 252, 126433.https://doi.org/10.1016/j.ijbiomac.2023.126433

[20] V. Siracusa and M. D. La Rosa, "Biopolymer films from seaweed and cellulose: Structure, water interaction, and barrier properties," *Carbohydrate Polymers*, vol. 315, pp. 120–132, 2024.

[21] Benitez, J. J., Florido-Moreno, P., Porras-Vázquez, J. M., Tedeschi, G., Athanassiou, A., Heredia-Guerrero, J. A., & Guzman-Puyol, S. (2024). *Transparent, plasticized cellulose-glycerol bioplastics for food packaging applications*. International Journal of Biological Macromolecules, 273, 132956. https://doi.org/10.1016/j.ijbiomac.2024.132956

[22] Bonifacio, A., Bonetti, L., Piantanida, E., & De Nardo, L. (2023). Plasticizer Design Strategies Enabling Advanced Applications of Cellulose Acetate. *European Polymer Journal*, *197*(August), 112360. https://doi.org/10.1016/j.eurpolymj.2023.112360

[23] Lee, C. H. Y., Tang, A. M. C., Lai, D. Y. F., Tai, A. P. K., Leung, A. S. L., Tao, D. K. C., Leung, F., Leung, S. S. M., Wu, C., Tong, S. C. S., & Ng, K. T. K. (2021). Problems and management of Acacia-dominated urban forests on man-made slopes in a subtropical, high-density city. *Forests*, *12*(3), 1–12. https://doi.org/10.3390/f12030323

[24] Andari, I. G. a. a. U., Arnata, I. W., & Anggreni, A. a. M. D. (2022). PENGARUH KONSENTRASI HIDROGEN PEROKSIDA DAN WAKTU PROSES BLEACHING TERHADAP KARAKTERISTIK SELULOSA SERAT SABUT KELAPA (*Cocos nucifera* L.). JURNAL REKAYASA DAN MANAJEMEN AGROINDUSTRI, 10(3), 237. https://doi.org/10.24843/jrma.2022.v10.i03.p01

[25] Abdullah, C. K., Khalil, H. P. S. A., Baharudin, M. S., Fazita, M. R. N., Ahmad, A., Norizan, M. N., & Bairwan, R. D. (2025). Enhancement of seaweed-based biofilms with cellulose nanofiber: A comparative study on raw seaweed and semi-refined carrageenan for sustainable packaging applications. *Polymer Engineering and Science*, *65*(5), 2177–2191. https://doi.org/10.1002/pen.27112

International Journal of Environment, Agriculture and Biotechnology
Vol-11, Issue-2; Mar-Apr, 2026
Peer-Reviewed International Journal
Journal Home Page Available: https://ijeab.com/
Journal DOI: 10.22161/ijeab

Efficacy of New-Era Combined Herbicides on Weed Dynamics, Productivity and Economics of Summer Green Gram (*Vigna radiata* L.)

Rima H. Patel[1], Rahul R. Pisal[2], P. Sowjanya Deepthi[3], Payal A. Patel[4]* and Nayan M. Thesiya[5]

[1]M.Sc Student, Department of Agronomy, N.M. College of Agriculture, Navsari Agricultural University, Navsari – 396 450, Gujarat, India.
[1,5]Assistant professor, Department of Agronomy, N.M. College of Agriculture, Navsari Agricultural University, Navsari – 396 450, Gujarat, India.
[3,4]Ph.D. Scholar, Department of Agronomy, N.M. College of Agriculture, Navsari Agricultural University, Navsari – 396 450, Gujarat, India.
*Corresponding Author

Received: 03 Feb 2026; Received in revised form: 04 Mar 2026; Accepted: 09 Mar 2026; Available online: 18 Mar 2026

Abstract*— A field experiment titled "Efficacy of new-era combined herbicides on weed dynamics, productivity and economics of summer green gram (Vigna radiata L.)" was carried out during the summer season of 2018 at the Instructional Farm, N. M. College of Agriculture, Navsari Agricultural University, Navsari, Gujarat. The study comprised ten weed management treatments, evaluated in a RBD (Randomized block design) with three replications. The treatments included: (T_1): pendimethalin at 900 g ha^{-1} as pre-emergence followed by one hand weeding at 30 DAS, (T_2): sodium acifluorfen + clodinafop-propargyl (ready-mix) at 250 g ha^{-1} as post-emergence applied at 20 DAS, (T_3): imazethapyr + pendimethalin (ready-mix) at 750 g ha^{-1} as pre-emergence, (T_4): imazethapyr + imazamox (ready-mix) at 70 g ha^{-1} as pre-emergence, (T_5): imazethapyr + propaquizafop (ready-mix) at 125 g ha^{-1} as post-emergence at 20 DAS (T_6): quizalofop-p-ethyl at 100 g ha^{-1} as post-emergence at 20 DAS, (T_7): fenoxaprop-p-ethyl at 100 g ha^{-1} as post-emergence at 20 DAS, (T_8): two hand weedings at 20 and 40 DAS, (T_9): unweeded control and (T_{10}): weed-free check. From the results of experiment observed that significantly highest value of growth parameters yield attributes and yield of green gram seed yield, straw yield and harvest index were observed under weed free (T_{10}) treatment, which was statistically at par with the treatment pendimethalin 900 g /haas pre-emergence + 1 HW at 30 DAS (T_1) and followed by sodium acifluorfen + clodinafop-propargyl $_{(RM)}$ 250 g /haas post-emergence at 20 DAS and 2 HW at 20 and 40 DAS (T_2).

***Keywords*— Weed, Green gram, Herbicides, Yield attributes and Yield.**

I. INTRODUCTION

Green gram (*Vigna radiata* L.), commonly known as mung bean, is a short-duration, protein-rich pulse crop of significant agronomic and nutritional importance in India. As a legume, it contributes to soil fertility through biological nitrogen fixation, making it integral to sustainable farming systems and crop rotations with cereals such as rice and wheat (Agricultural Market Intelligence Centre, PJTAU, 2025). India accounts for more than 70 per cent of the world's green gram production, positioning itself as the largest global producer and consumer of this pulse crop (Agricultural Market Intelligence Centre, PJTAU, 2025).

At the national level, green gram area and production have shown an upward trend in recent seasons. According to the third advance estimates of the Ministry of

Agriculture and Farmers Welfare, the total area under green gram in India during the 2024–25 crop year was approximately 35.27 lakh hectares, with production estimated at 3.82 million tonnes (Agricultural Market Intelligence Centre, PJTAU, 2025). The expansion in cultivated area and output reflects both increased farmer interest and supportive policy measures aimed at enhancing pulse production under India's broader agricultural development agenda. In the western Indian state of Gujarat, green gram (locally referred to as moong) constitutes an emerging but comparatively smaller component of the overall pulse production. Recent state data indicates that during the 2024–25 season, the area under moong cultivation in Gujarat reached about 1.38 lakh hectares with a production of approximately 1.26 lakh tonnes, indicating both area expansion and yield stabilization among growers (Gujarat Agriculture Department, as reported in *Pulses Production Doubles in Gujarat in Six Years*, 2026). These green gram figures are part of a broader pattern of growth in the state's pulse sector, where total pulse cultivation area expanded from 9 lakh hectares in 2019–20 to 14.39 lakh hectares in 2024–25, with total pulse output doubling over the same period (Times of India, 2026).

The sustained improvements in area, production and yield at both national and state levels underline the dynamic nature of green gram cultivation in India. Detailed analysis of spatial and temporal trends in green gram production is essential for identifying agronomic constraints and opportunities, guiding policy interventions and fostering enhanced productivity within diversified cropping systems. Weed competition is recognized as one of the major constraints in mung bean (*Vigna radiata* L.) production, particularly during the early stages of crop growth. Yield losses due to weed infestation in mung bean have been reported to range from 65.4 to 79.0 per cent, indicating the severity of this constraint under uncontrolled conditions (Dungarwal *et al*., 2003). The extent of yield reduction largely depends on the composition of the weed flora, duration of crop–weed competition and the intensity of weed infestation. Effective weed management plays a crucial role in enhancing green gram productivity, as weeds compete aggressively with crop plants for essential growth resources such as nutrients, moisture, light and space, especially during the critical early growth period of the crop. Failure to control weeds during this phase often results in irreversible yield losses. Herbicide combinations or mixtures, consisting of two or more herbicides, are increasingly used for effective and economical weed control. No single herbicide can provide complete control of diverse weed species without posing a risk of crop injury, as higher doses are often required to broaden the spectrum of weed control. In contrast, herbicide mixtures help broaden the spectrum of herbicidal activity, enabling effective control of both grassy and broad-leaved weeds while reducing the likelihood of phytotoxicity. Therefore, minimizing weed growth during the critical period of crop–weed competition is essential, as it can result in crop yields comparable to those obtained under weed-free conditions.

II. MATERIALS AND METHODS

A field experiment was carried out during the summer season of the year 2018 at College Farm, N. M. College of Agriculture, Navsari Agricultural University, Navsari (Gujarat). The experimental field was clayey in texture and showed low, medium and high rating for available N, P_2O_5 and K_2O, respectively. The soil was found slightly alkaline (P^H 8.1) with normal electrical conductivity. Green gram (*Vigna radiata* L.) variety Meha was used for the experiment. Prior to sowing, the seeds were treated with ceresan at 3.0 g kg^{-1}seed to protect against seed-borne fungal diseases. Subsequently, the seeds were inoculated with rhizobium culture to enhance biological nitrogen fixation. After treatment, the seeds were shade-dried before sowing. Sowing was carried out on 5th February 2018 using the line sowing method, maintaining a spacing of 30 cm × 10 cm between rows and plants, respectively. A seed rate of 20 kg ha^{-1} was used to ensure optimum plant population. A basal dose of fertilizers, comprising 20 kg N ha^{-1} and 40 kg P_2O_5 ha^{-1}, was applied just before sowing in the form of urea and single superphosphate (SSP), respectively. No potassium fertilizer was applied.

Herbicides evaluated in the study included pendimethalin, imazethapyr + pendimethalin (RM), imazethapyr + imazamox (RM), sodium acifluorfen + clodinafop-propargyl (RM), imazethapyr + propaquizafop (RM), quizalofop-p-ethyl, and fenoxaprop-p-ethyl. The required quantities of each herbicide were measured using a graduated measuring cylinder at the time of application, as per the respective treatment requirements. Herbicide spraying was carried out using a knapsack sprayer fitted with a flat-fan nozzle, applying 500 L of water ha^{-1} to ensure uniform coverage. Pendimethalin, imazethapyr + pendimethalin (RM), and imazethapyr + imazamox (RM) were applied as pre-emergence (PE) herbicides, whereas sodium acifluorfen + clodinafop-propargyl (RM), imazethapyr + propaquizafop (RM), quizalofop-p-ethyl, and fenoxaprop-p-ethyl were applied as post-emergence (PoE) herbicides.

Pre-emergence herbicide application was carried out on the second day after sowing, one day after irrigation. The quantity of commercial formulation required for each treatment was calculated based on the active ingredient content using the following formula:

$$Rh = \frac{Ai \times At}{Ci} \times 100$$

where,

Rh=Required quantity of trade formulation of herbicide (ha^{-1}),

Ai=Quantity of active ingredient to be applied (kg),

At=Area to be treated (ha), and

Ci = concentration of active ingredient (%) in the commercial formulation.

III. RESULTS AND DISCUSSION

Growth Attributes

Plant height recorded at 30 and 60 DAS as well as at harvest was significantly influenced by different weed management treatments. Significantly higher plant height at 30 DAS (22.43 cm), 60 DAS (41.70 cm) and at harvest (52.40 cm), along with a higher number of branches per plant (22.67), was observed under the weed-free treatment (T_{10}). This treatment remained statistically at par with T_1 (pendimethalin 900 g ha^{-1} as pre-emergence + one hand weeding at 30 DAS), T_2 (sodium acifluorfen + clodinafop-propargyl [RM] 250 g ha^{-1} as post-emergence at 20 DAS) and T_8 (two hand weddings at 20 and 40 DAS).

The significant improvement in plant height and branching under these treatments may be attributed to effective weed control during the critical period of crop–weed competition, which minimized competition for nutrients, moisture, light and space. Consequently, enhanced availability of growth resources promoted better vegetative growth and development of summer green gram. Plant height at 60 DAS was particularly sensitive to weed management practices, indicating the importance of maintaining a weed-free environment during the mid-growth stage of the crop. Similar findings was observed by Bareek *et al.* (2024) and Shilurenla *et al*. (2025).

Table 1: Plant height (cm) and branches per plant of green gram as influenced by various weed management treatments

Treatments	Plant height (cm)			Branches/plant
	30 DAS	60 DAS	At Harvest	
T_1 = Pendimethalin 900 g /ha as pre emergence + 1 HW at 30 DAS	19.27	36.87	48.87	18.87
T_2 = Sodium acifluorfen +clodinafop-propargyl $_{(RM)}$ 250 g /ha as post emergence at 20 DAS	20.13	37.80	50.40	21.67
T_3 = Imazathapyr + pendimethalin $_{(RM)}$ 750 g /ha as pre emergence	18.60	34.20	45.67	18.53
T_4 = Imazathapyr + imazamox $_{(RM)}$ 70 g /ha as pre emergence	18.67	34.77	45.90	17.67
T_5 = Imazethapyr + propaquizafop$_{(RM)}$ 125 g /ha as post emergence at 20 DAS	16.93	33.70	45.47	18.07
T_6 = Quizalofop-p-ethyl 100 g /ha post emergence at 20 DAS	19.03	35.53	48.20	19.40
T_7 = Fenoxaprop-p-ethyl 100 g /ha post emergence at 20 DAS	19.00	34.87	47.80	18.60
T_8 = 2 HW at 20 and 40 DAS	19.33	37.27	50.60	19.87
T_9 = Unweeded control	14.93	28.73	40.73	14.80
T_{10} = Weed free	22.43	41.70	52.40	22.67
S.Em. ±	1.13	1.74	1.76	1.33
C.D at 5 %	3.34	5.16	5.22	3.96
C.V. %	10.35	8.46	6.39	12.13

Yield Attributes and Yield

Yield attributes of summer green gram were significantly influenced by different weed management treatments. The weed-free treatment (T_{10}) produced the highest number of pods per plant (34.63), seeds per pod (10.20) and pod length (7.54 cm) were highest under T_{10}, remaining comparable to several other effective weed control treatments, while the unweeded control (T_9) consistently recorded the lowest values for these parameters. The improved vegetative and reproductive growth under weed-free and effectively managed treatments may be attributed to reduced competition with weeds for nutrients, moisture, light and space, which allowed better resource allocation to both vegetative development and pod formation. However, 1000-seed weight was not significantly affected by weed management, suggesting that seed size in summer green gram is largely determined by genetic potential rather than external competition. The mean data on seed and straw yield of summer green gram, recorded at harvest indicated that weed management treatments significantly influenced both parameters. The weed-free treatment (T_{10}) resulted in the highest seed yield (1319 kg ha^{-1}) and straw yield (1632 kg ha^{-1}), which were statistically comparable to T, T_2, and T_8. In contrast, the lowest seed (687 kg ha^{-1}) and straw yields (932 kg ha^{-1}) were recorded under the unweeded control (T_9), reflecting a 92% increase in seed yield under the weed-free treatment over the unweeded control. The superior yields under weed-free and effectively managed treatments can be attributed to reduced competition from weeds for essential resources such as nutrients, moisture, light and space, which enhances crop growth, dry matter accumulation and reproductive success. (Parihar *et al.*, 2024; green gram yield losses due to weed competition range from 30–40% when not controlled. Similar findings were reported by Yadav *et al.* (2019), who observed significant increases in seed and straw yield with effective weed control in green gram, while harvest index remained unaffected by weed management or planting methods.

Table 2: Yield attributes and yield of green gram as influenced by various weed management treatments

Treatments	Pods/plant	Seeds/pod	Pod length (cm)	Yield (kg/ha)		Harvest index (HI)
				Seed	Stover	
T_1 = Pendimethalin 900 g /ha as pre emergence + 1 HW at 30 DAS	29.33	9.30	7.05	1121	1367	44.05
T_2 = Sodium acifluorfen +clodinafop-propargyl $_{(RM)}$ 250 g /ha as post emergence at 20 DAS	32.87	10.07	6.85	1099	1376	44.36
T_3 = Imazathapyr + pendimethalin $_{(RM)}$ 750 g /ha as pre emergence	26.20	9.47	6.53	1030	1314	43.86
T_4 = Imazathapyr + imazamox $_{(RM)}$ 70 g /ha as pre emergence	25.17	8.67	6.41	976	1198	44.93
T_5 = Imazethapyr + propaquizafop$_{(RM)}$ 125 g /ha as post emergence at 20 DAS	24.83	8.40	6.38	932	1144	44.82
T_6 = Quizalofop-p-ethyl 100 g /ha post emergence at 20 DAS	29.53	8.97	7.48	995	1256	44.27
T_7 = Fenoxaprop-p-ethyl 100 g /ha post emergence at 20 DAS	26.77	9.67	7.05	882	1113	44.21
T_8 = 2 HW at 20 and 40 DAS	32.67	9.83	7.34	1184	1453	44.94
T_9 = Unweeded control	17.83	7.20	5.93	687	932	42.09
T_{10} = Weed free	34.63	10.20	7.54	1319	1632	44.72
S.Em. ±	1.74	0.44	0.25	77.24	90.26	0.89
C.D at 5 %	5.17	1.32	0.75	229.48	268.18	NS
C.V. %	10.76	8.37	6.35	13.08	12.23	3.49

Weed Studies

The predominant weed flora observed in the experimental field is presented in Table 3. The major monocot weeds were samo, bermuda grass and crab grass, while pig weed, amaranthus and field bindweed were the dominant dicot weeds. Nut sedge was the only sedge weed recorded during the experiment.

Weed population: Presented data revealed that weed population of monocot, dicot and sedge weeds at 30, 60 DAS and at harvest was significantly influenced by different weed management treatments. Treatment T_{10} (weed-free) recorded almost nil weed population throughout the crop growth period. Among the remaining treatments, T_8 (two hand weedings at 20 and 40 DAS) registered the lowest population of monocot, dicot and sedge weeds at 30, 60 DAS and at harvest, which was statistically at par with T_1 and T_2, while T_6 was at par in case of monocot weeds.

Table 3: Weeds population at harvest as influenced by various weed management treatments

Treatments	Weed population at 30 DAS (No. m^{-2})			Weed population at 60 DAS (No. m^{-2})			Weed population at harvest (No. m^{-2})		
	Monocot	**Dicot**	**Sedge**	**Monocot**	**Dicot**	**Sedge**	**Monocot**	**Dicot**	**Sedge**
T_1 = Pendimethalin 900 g ha^{-1} as pre emergence + 1 HW at 30 DAS	3.18 (9.67)	3.33 (10.67)	2.46 (5.67)	3.72 (13.33)	4.02 (15.67)	3.07 (9.00)	4.05 (16.00)	4.37 (18.67)	3.34 (10.67)
T_2 = Sodium acifluorfen + clodinafop-propargyl (RM) 250 g ha^{-1} as post emergence at 20 DAS	3.32 (10.67)	3.53 (12.00)	2.60 (6.33)	3.80 (14.00)	3.89 (14.67)	3.23 (10.00)	4.13 (16.67)	4.33 (18.33)	3.44 (11.33)
T_3 = Imazathapyr + pendimethalin (RM) 750 g ha^{-1} as pre emergence	3.89 (14.67)	4.09 (16.33)	2.67 (6.67)	4.60 (20.67)	4.64 (21.00)	4.29 (10.33)	4.70 (21.67)	4.84 (23.00)	3.53 (12.00)
T_4 = Imazathapyr + imazamox (RM) 70 g ha^{-1} as pre emergence	3.92 (15.00)	4.14 (17.00)	2.85 (7.67)	4.56 (20.33)	4.86 (23.33)	3.49 (11.67)	4.81 (22.67)	5.14 (26.00)	3.76 (13.67)
T_5 = Imazethapyr + propaquizafop(RM) 125 g ha^{-1} as post emergence at 20 DAS	3.47 (11.67)	4.01 (15.67)	2.72 (7.00)	4.23 (17.67)	4.66 (21.33)	3.48 (11.67)	4.40 (19.00)	5.01 (24.67)	3.80 (14.00)
T_6 = Quizalofop-p-ethyl 100 g ha^{-1} post emergence at 20 DAS	3.12 (9.33)	4.45 (19.33)	2.75 (7.33)	4.04 (16.00)	4.58 (20.67)	3.38 (11.00)	4.24 (17.67)	5.11 (25.67)	3.63 (12.67)
T_7 = Fenoxaprop-p-ethyl 100 g ha^{-1} post emergence at 20 DAS	3.43 (11.33)	4.49 (19.67)	2.90 (8.00)	4.22 (17.33)	4.70 (21.67)	3.53 (12.00)	4.44 (19.33)	5.24 (27.00)	3.89 (14.67)
T_8 = 2 HW at 20 and 40 DAS	2.79 (7.33)	3.02 (8.67)	2.11 (4.00)	3.34 (10.67)	3.48 (11.67)	2.86 (7.67)	3.66 (13.00)	3.96 (15.33)	3.13 (9.33)
T_9 = Unweeded control	6.33 (39.67)	7.34 (53.33)	2.96 (8.33)	7.25 (52.00)	8.11 (65.33)	3.62 (12.67)	7.49 (55.67)	8.19 (66.67)	3.93 (15.00)
T_{10} = Weed free	0.70 (0.0)	0.70 (0.0)	0.70 (0.0)	0.70 (0.0)	0.70 (0.0)	0.70 (0.0)	0.70 (0.0)	0.70 (0.0)	0.70 (0.0)
S.Em. ±	0.19	0.18	0.20	0.18	0.20	0.13	0.17	0.16	0.11
C.D at 5 %	0.56	0.54	0.60	0.53	0.58	0.37	0.52	0.48	0.33
C.V. %	9.55	8.00	14.13	7.58	7.76	7.11	7.09	5.94	5.88

*Data in parenthesis indicate square root transformation $\sqrt{(X+0.5)}$ value and out side parenthesis indicate actual value.

The unweeded control (T_9) recorded the highest population of monocot, dicot, and sedge weeds. The superior performance of T_8 may be attributed to timely removal of weeds during the critical crop–weed competition period, which prevented weed establishment, reduced regrowth, and minimized soil seed bank replenishment. Repeated hand weeding also disrupted weed root systems, resulting in lower weed emergence at later growth stages. Similar findings related to Chaudhary *et al*. (2011) and Singh and Yadav (2014).

Dry weed weight (kg ha^{-1}): Data presented in Table 4 indicated that dry weed weight at harvest was significantly influenced by weed management treatments. The unweeded control (T_9) recorded the highest dry weed biomass (2062 kg ha^{-1}). Among the weed management practices, T_8 (two hand weedings at 20 and 40 DAS) resulted in the lowest dry weed weight (315 kg ha^{-1}), which was statistically at par with T_1 (437 kg ha^{-1}). The reduced weed biomass under T_8 may be attributed to effective and timely removal of weeds during the critical competition period, leading to reduced weed growth, suppression of regrowth, and depletion of assimilate accumulation in weeds.

Table 4: Dry weed weight, weed control efficiency and weed index as influenced by various weed management treatments

Treatments	Dry weed weight (kg ha^{-1})	WCE (%)	WI (%)
T_1 = Pendimethalin 900 g ha^{-1} as pre emergence + 1 HW at 30 DAS	437	78.83	15.22
T_2 = Sodium acifluorfen + clodinafop-propargyl $_{(RM)}$ 250 g ha^{-1} as post emergence at 20 DAS	493	76.07	16.14
T_3 = Imazathapyr + pendimethalin $_{(RM)}$ 750 g ha^{-1} as pre emergence	501	75.72	22.09
T_4 = Imazathapyr + imazamox $_{(RM)}$ 70 g ha^{-1} as pre emergence	556	73.03	26.10
T_5 = Imazethapyr + propaquizafop$_{(RM)}$ 125 g ha^{-1} as post emergence at 20 DAS	569	72.41	29.48
T_6 = Quizalofop-p-ethyl 100 g ha^{-1} post emergence at 20 DAS	539	73.76	24.28
T_7 = Fenoxaprop-p-ethyl 100 g ha^{-1} post emergence at 20 DAS	603	70.81	33.21
T_8 = 2 HW at 20 and 40 DAS	315	84.69	10.07
T_9 = Unweeded control	2062	0.00	48.28
T_{10} = Weed free	-	100	0.00
S.Em. ±	51.68	-	-
C.D at 5 %	153.54	-	-
C.V. %	14.72	-	-

Weed control efficiency (%): Weed control efficiency (WCE) at harvest varied significantly among treatments. The weed-free treatment (T_{10}) recorded the highest WCE (100%), followed by T_8 (82.87%). The overall trend of WCE was:

$T_{10} > T_8 > T_1 > T_2 > T_3 > T_6 > T_4 > T_5 > T_7 > T_9$. Higher WCE under T_{10} and T_8 was due to complete or repeated elimination of weeds, which restricted weed establishment and growth throughout the crop period.

Weed index (%): Weed index (WI), which indicates yield reduction due to weed competition, was lowest under T_{10}, followed by T_8 (10.07%). The trend of WI among treatments was: $T_{10} < T_8 < T_1 < T_2 < T_3 < T_6 < T_4 < T_5 < T_7 < T_9$. Lower WI under T_8 can be attributed to effective weed suppression during early and mid-crop growth stages, resulting in reduced crop–weed competition and better utilization of nutrients, moisture and light by the crop.

Table 5: Economics as influenced by different weed management treatments in green gram

Treatments	Yield (kg ha^{-1})		Income (₹ ha^{-1})		Gross return (₹ ha^{-1})	Total cost of Cultivation (₹ ha^{-1})	Net return (₹ ha^{-1})	B: C Ratio
	Seeds	Straw	Seeds	Straw				
T_1	1083	1367	64982	4786	69768	23756	46012	1.94
T_2	1099	1376	65922	4815	70737	19190	51547	2.69
T_3	1031	1314	61856	4600	66456	18912	47544	2.51
T_4	977	1199	58608	4195	62803	18773	44030	2.35
T_5	932	1144	55946	4005	59951	18679	41272	2.21
T_6	996	1256	59740	4396	64136	20546	43590	2.12
T_7	883	1114	52964	3899	56863	19595	37268	1.90

T_8	1184	1453	71062	5085	76147	26406	49741	1.88
T_9	687	932	41248	3261	44509	17506	27003	1.54
T10	1319	1632	79166	5712	84878	33348	51530	1.55

Selling price of green gram Seed = ₹ 60 kg^{-1}

Straw = ₹ 3.5 kg^{-1}

Economics: Among different treatment of weed management, the highest net return ₹ 51,547 was obtained with treatment T_2 (Sodium acifluorfen + clodinafop-propargyl $_{(RM)}$ 250 g ha^{-1} as post em. at 20 DAS) followed by treatment T_{10}, T_8, T_3 and T_1 where as in case of benefit cost ratio the highest BCR value of 2.69 recorded with treatment T_2, while it was followed by T_3, T_4, T_5, T_6, T_1 and T_7. Similar, results were also reported by Khot *et al.* (2012) and Patel and Thanki (2004).

IV. CONCLUSION

Based on the results of the present field investigation, it can be concluded that sodium acifluorfen + clodinafop-propargyl (RM) @ 250 g ha^{-1} applied as post-emergence at 20 DAS proved most effective in achieving efficient weed control, higher productivity and improved economic returns in summer green gram compared to other individual and combined herbicidal treatments. The superior performance of this treatment may be attributed to its broad-spectrum control of monocot, dicot and sedge weeds during the critical crop–weed competition period, resulting in reduced weed biomass, higher weed control efficiency and lower weed index. However, under conditions of adequate labour availability, manual weeding at critical stages was found to be an equally effective alternative for maintaining weed-free conditions and ensuring potential and profitable green gram production.

REFERENCES

[1] Agricultural Market Intelligence Centre, PJTAU. (2025). *Green gram Outlook – October 2025* (3rd advance estimates). Punjab Agricultural University. https://www.pjtau.edu.in/files/AgriMkt/2025/October/Green gram-October-2025.pdf

[2] Barik, C., Sar, K., Padhi, I., Barsha, N., and Pradhan, A. (2024). Weed growth and productivity of green gram (*Vigna radiata* L.) under different weed control practices. *International Journal of Plant and Soil Science*, 36 (9): 683–689.

[3] Chaudhary, S. U., Hussain, M., and Ali, M. A. (2011). Effect of weed management practices on growth and yield of mungbean (*Vigna radiata* L.). *Journal of Animal and Plant Sciences*, 21 (4): 847–850.

[4] Dungarwal, H. S., Chaplot, P. C., and Nagda, B. L. (2003). Effect of weed management practices on weed dynamics and yield of mung bean (*Vigna radiata* L.). *Indian Journal of Weed Science,* 35 (3–4): 283–285.

[5] Khot, D. B., Munde, S. D., Khanpara, V. D. and Pagar, R. D. 2012. Evaluation of new herbicides for weed management in summer black gram (*Vigna mungo* L.). *Crop Research,* 44 (3): 326-330.

[6] Parihar, C., Kushwah, S. S., Parmar, B., Verma, B., and Chauhan, A. P. S. (2024). Effect of planting methods and weed control treatments on weed dynamics, yield and economics of green gram *(Vigna radiata* L.*). Journal of Experimental Agriculture International,* 46 (7): 325–335.

[7] Patel, V. M. and Thanki, J. D. 2004. Effect of irrigation level and weed management practices on growth, yield and quality of summer urd bean. *Indian Journal of Pulses Research,* 17 (1): 93-94.

[8] Production of pulses in Gujarat doubles in six years: Govt. (2026, January). *The Times of India*. https://timesofindia.indiatimes.com/city/ahmedabad/production-of-pulses-in-gujarat-doubles-in-six-years-govt/articleshow/126359650.cms

[9] Pulses production doubles in Gujarat in six years. (2026, January 7). *iGrain*. https://igrain.in/posts/pulses-production-doubles-in-gujarat-in-six-years

[10] Shilurenla, D. Nongmaithem, N. A. Baite, L. Tzudir, A. P. Singh, and R. Yadav. (2025). Response of green gram [*Vigna radiata* (L.) Wilczek] to different weed management practices. *Indian Journal of Agricultural Research*, 59 (6): 940–947.

[11] Singh, G., and Yadav, A. (2014). Effect of integrated weed management on weed dynamics and productivity of green gram (*Vigna radiata* L.). *Indian Journal of Weed Science*, 46(2): 165–168.

[12] Yadav, R., Satish, K., Dhaka, A. K., and Kumar, N. (2019). Effect of planting methods and weed management practices on yield of green gram *(Vigna radiata* L.*). Indian Journal of Agricultural Research*, 53 (2): 158–164.

International Journal of Environment, Agriculture and Biotechnology
Vol-11, Issue-2; Mar-Apr, 2026
Peer-Reviewed International Journal
Journal Home Page Available: https://ijeab.com/
Journal DOI: 10.22161/ijeab

Milk Cooling Prototype and its Economics

Gaurav Sharma[1], Dr. Amandeep Sharma[2] and Dr. Inderpreet Kaur[3]

[1]Dairy Engineering Division, ICAR- National Dairy Research Institute, Karnal, Haryana
[2]Department of Dairy Engineering, College of Dairy Science and Technology, Guru Angad Dev Veterinary and Animal Sciences University, Ludhiana, Punjab, India
[3]Department of Agriculture Economics, College of Dairy Science and Technology, Guru Angad Dev Veterinary and Animal Sciences University, Ludhiana, Punjab, India

Received: 01 Feb 2026; Received in revised form: 03 Mar 2026; Accepted: 13 Mar 2026; Available online: 21 Mar 2026

***Abstract*— *Milk is nearly complete food but as well as it is very perishable in nature, rapid preservation techniques are required to preserve its quality and to increase its spoilage time. Although, milk is nearly sterile when it comes out from the udder of a milch animal but when microbes get entry they deteriorate its quality. With the 23% contribution or 1st in milk production, India is not even in the top 10 in the export list of milk and milk product due to quality issues; so, there is need to preserve the quality of milk right from farm. In India 57% out of total milk production is produced by small farmers who have average herd size less than 3 milch animals so, there is need of small scale cooling system. The present study is focused for the small scale milk cooling system to maintain the cooling chain from farm to consumer.A vacuum chamber along with vacuum pump was used to for the cooling of milk. Milk cooled down from 36.3°C to 21.5°C just by using water as refrigerant, which may prevent milk spoilage up to 8 hours. The cooling cost is Rs 3.12 per litre of product.*

***Keywords*— Dairy, Milk production, Vacuum chamber, Vacuum pump, Milk spoilage**

I. INTRODUCTION

In recent month "International Dairy Federation World Dairy Summit 2022" was organised in India the last such summit was held in India nearly 50 years ago in 1974, when India's milk production was 23 million tonnes which has now reached nearly 220 million tonnes, nearly 10 times increment. In these years India moved from milk deficient country to largest milk producing country and now India is contributing nearly 23% to world milk production and still the growth rate of India's milk production is about 6% against 2% growth of world milk production.

Milk is almost sterile when it comes out from udder of milch animal (Uddin et al., 2011) but when microbes get entry into it, they lead to its deterioration because nearly neutral pH, high nutrient content, the ambient environment temperature and high water activity all are favourable condition for the rapid replication of microbes (Srairi et al., 2013). To supress the growth of microbes, the favourable condition are required to change; milk cooling is best for preservation.

Although some other systems are there, by taking the advantage of the antimicrobial compound, Lacto peroxidase system milk can be preserved for several hours, only lacto peroxides have no antibacterial effect but when it combined with hydrogen peroxide and oxidize thiocyanate the resulting compound have antibacterial effect. Lacto peroxides is present in milk and is sufficient for antibacterial action. Thiocyanate is also present in milk in 4-5 ppm which is not sufficient so, to adjust 15 ppm concentration, for required hydrogen peroxide granulated sodium carbonate peroxide is added to milk which produce 8-9 ppm hydrogen peroxide. If milk kept in dark ventilated place at 30 degree Celsius temperature lactoperoxidase (LP) system's preservative effect lasts for 7-8 hour (Seifu, E. et al., 2005).

Milk may get spoiled due to the growth of fermentative bacteria during the storage at ambient temperature. The spoilage causing microbes for milk are gram – positive spore forming bacteria (*Clostridium spp.*), gram – negative bacteria (*pseudomonas spp. Coliforms*) Lactic acid bacteria (*streptococcus*) (TeGiffel& Wells-Bennik, 2010). According to the climatic condition of India which provide favourable temperature for the growth of microbes, rapid cooling system is required for milk cooling to prevent milk spoilage.

Table 1 shows some refrigerants with their ozone depletion and global warming potential, so there is need of eco – friendly cooling system to reduce the global warming effect.

Table 1 Various refrigerants with the ozone depletion and global warming potential

S.no	Refrigerant number	Chemical composition	ODP	GWP 100 YEAR
1	R-11	CCl_3F	1	4750
2	R-12	CCl_2F_2	1	10890
3	R-13	$CClF_3$	1	14420
4	R-23	CHF_3	0	14760

ODP- Ozone depletion potential, GWP- Global warming potential (Calm &Hourahan, 2007)

In India 57% out of total milk production is produced by small farmers who have average herd size less than 3 milch animals (Juniwal et al., 2022).In India "production of milk by masses" more than by "mass production" so, there is need of small scale cooling system. On the basis of these problems the present study is framed for small scale milk cooling system.

II. MATERIALS AND METHODS

Materials

A 500 mL stainless steel bottle wrapped with cotton and vacuum machine setup as shown in Fig. 1 was used. Thermometer and weighing balance was used for the measurement of temperature and weight respectively.

Fig. – 1 Cotton wrapped bottle inside vacuum machine

A vacuum chamber made up off stainless steel with accessories opening/closing valve and vacuum gauge and RTD (resistance temperature difference) thermometer for temperature measurement along with vacuum pump to create vacuum inside the chamber as shown in Fig. 2 and table – 2 shows the dimensions of the vacuum chamber and table – 3 shows the specifications of vacuum pump.

Fig. 2: - A - Vacuum chamber, B - Vacuum gauge, C - Valve, D - Display, E - Temperature sensor, F - Vacuum pump

Table – 2 Dimensions of vacuum chamber

	Diameter (mm)	Height (mm)
Cavity	420	520

Table – 3 Specifications of vacuum pump

Sr. No.	**Specification**	**Vacuum pump (flow tech)**
1	Motor speed (rpm)	1440
2	Motor power (W)	1HP
3	Frequency (Hz)	50
4	Oil capacity (ml)	750

III. METHODOLOGY

Pre – trials for cooling under vacuum were taken by using cotton wrapped bottle and vacuum machine setup. 500 ml water filled in bottle (temperature measured using thermometer) and cotton was wrapped over the bottle. Water was sprayed over the cotton wrapped bottle and weighed before and after spraying water to measure the quantity of sprayed water, this was kept under vacuum using vacuum machine and again weighed to measure the quantity of water and final temperature of water was recorded to check the cooling effect.

Fig. 3 shows the arrangement of Can inside the vacuum chamber, the Can was filled with product and the space between the Can and vacuum chamber was filled with water as refrigerant. The RTD (temperature sensor) was dipped inside the Can to measure the temperature of inner cavity product and the vacuum chamber closed, and vacuum was created inside the vacuum chamber which help to reduce the boiling point of water. When water evaporate by taking the latent heat of evaporation and convert from liquid form to vapour and give cooling effect.

Fig. 3 The Can inside vacuum chamber

IV. RESULTS AND DISCUSSION

Pre – trial on cotton covered bottle in vacuum packaging machine

The results of this experiment are shown in table- 4; the cumulative temperature drop and quantity of water evaporated was14°C and 27.16 g respectively in 1680 sec.

Table 4: Temperature profile and water evaporation of cotton covered bottle

Duration (second)	**Water in inner cavity(mL)**	**Water on outersurface (absorbed in cotton) evaporation**	**Cumulative water evaporation (g)**	**Temperature (mean value) of water in inner cavity (°C)± SE**	**Cumulative decrease in temperature in inner Cavity (°C)**
0	500	50 ± 0.00	0	39 ± 0.577	0
240	500	37.22 ± 0.295	12.78	34 ± 0.00	5
480	500	34.13 ± 0.066	15.87	32 ± 0.33	7
720	500	31.22 ± 0.070	18.78	30 ± 0.33	9
960	500	28.34 ± 0.036	21.66	28 ± 0.577	11
1200	500	25.94 ± 0.176	24.06	27 ± 0.577	12
1440	500	23.92 ± 0.179	26.08	26 ± 0.577	13
1680	500	22.84 ± 0.242	27.16	25 ± 0.577	14

N=3, Valuesareaverage± SE(standard error)

Fig. 4 shows the temperature profile of water in inner cavity of SS bottle covered with cotton and Fig. 5 shows the evaporation of quantity of water from outer surface of bottle. As shown in Fig. 4 and 5 initially the cooling effect was high as the quantity of water evaporated was also high.

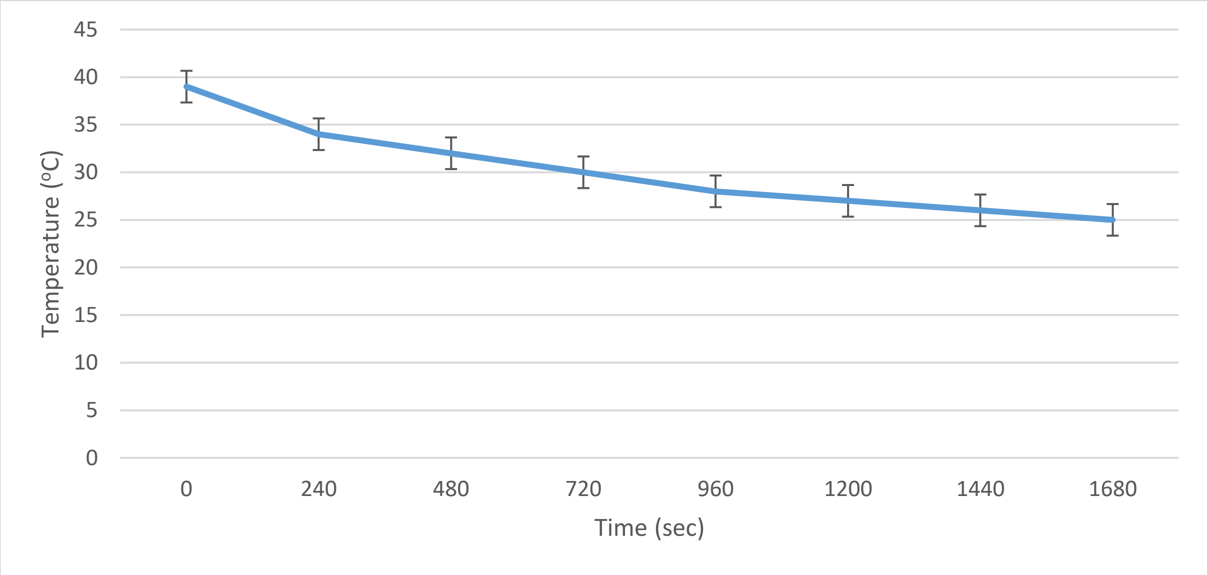

Fig. 4: Temperature profile of water in inner cavity cotton covered bottle

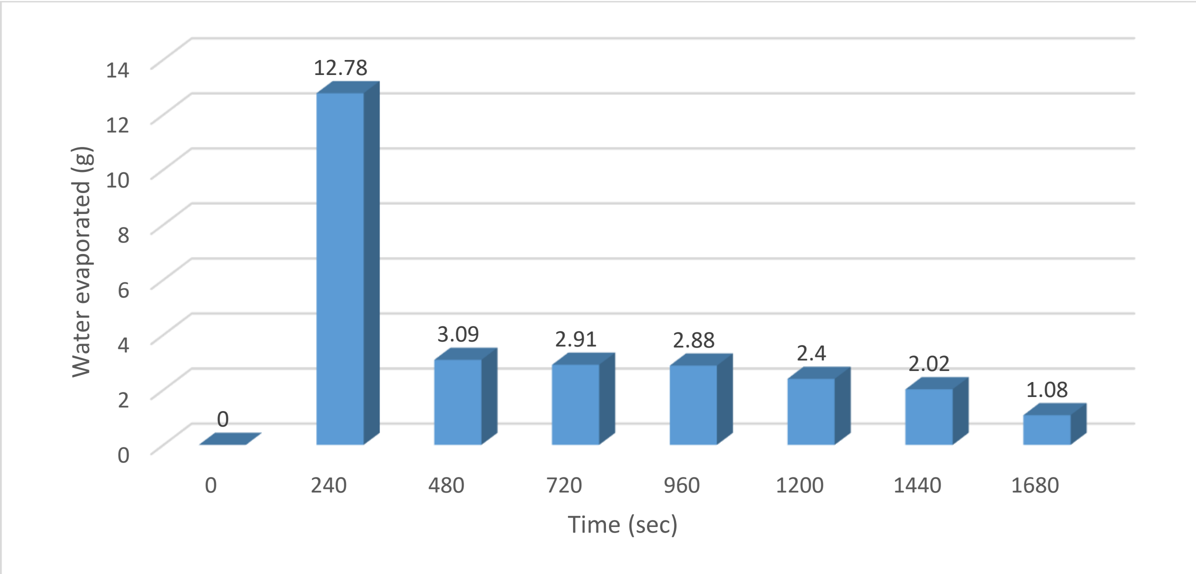

Fig. 5: Quantity of water evaporated from outer surface of cotton covered bottle

It may be concluded that there is a direct relation between the rate of evaporation of water and cooling effect in the inner cavity of the bottle

Cooling effect in inner cavity Can in vacuum chamber

Methodology provided above, 5000 mL water was filled in vacuum chamber and 10000 mL product filled in 40 litre (capacity) Can. The filled Can was directly kept inside the vacuum chamber. Table 5 and table 6 shows the temperature profile of inner cavity Can in vacuum chamber at 710 and 730 mmHg vacuum respectively. The cumulative temperature drop in inner cavity product at 710 mmHg was 7.4ºC, at 730 mmHg 9.6ºC after 5400 and 9000 sec respectively.

Table 5: Temperature profile of inner cavity water (Can) in vacuum chamber at 710 mmHg vacuum

Duration (sec)	Vacuum in outer cavity (mmHg)	Temperature in inner cavity (ºC) (5000 mL and 10000 mL water in vacuum chamber and inner cavity (can) respectively) ± SE	Cumulative decrease in temperature in inner cavity(ºC)
0	710	36.3 ± 0.212	0
900	710	33.6±0.212	2.7
1800	710	32.5±0.212	3.8
2700	710	31.6 ± 0.212	4.7
3600	710	30.6±0.212	5.7
4500	710	29.6 ± 0.212	6.7
5400	710	28.9 ± 0.212	7.4

N=3, Values are average ± SE(standard error)

Fig. 6 shows the cooling effect in inner cavity water of Can placed in the vacuum chamber at the vacuum of 710 mmHg and Fig. 7 shows the temperature profile of water at 730 mmHg vacuum.

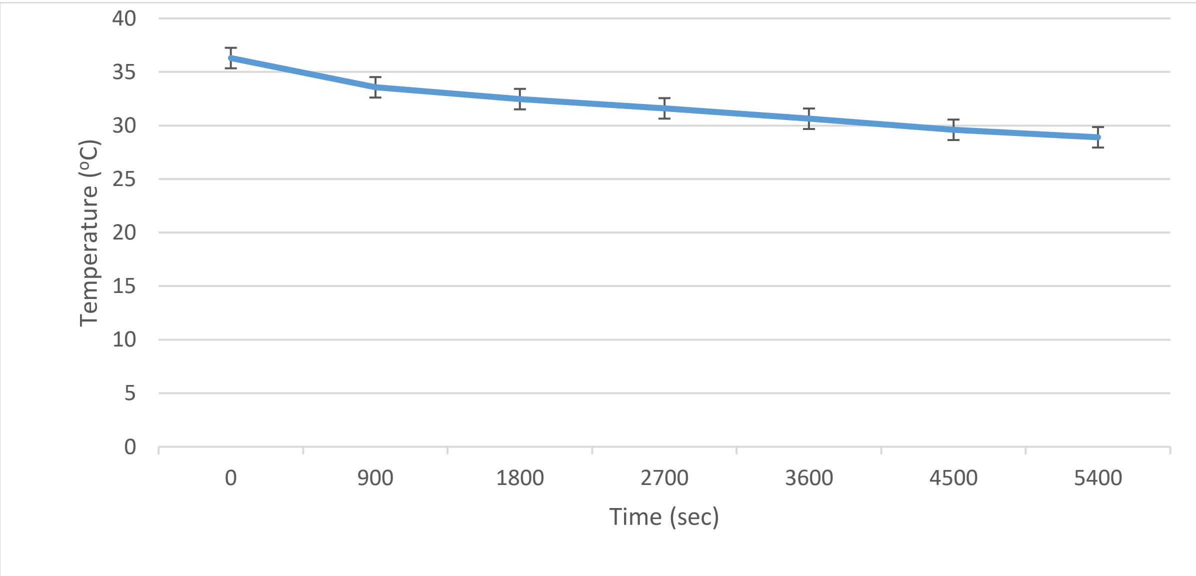

Fig. 6: Temperature profile of inner cavity water (Can) in vacuum chamber at vacuum 710 mmHg

Table 6: Temperature profile of water in Can placed in vacuum chamber at 730 mmHg vacuum

Duration(sec)	Vacuum in outer cavity (mmHg)	Temperature in inner cavity (ºC) (5000mLand10000 mL water in vacuum chamber and inner cavity (can) respectively) ± SE	Cumulative decrease in temperature in inner cavity(ºC)
0	730	31.1 ± 0.293	0
900	730	28.6±0.293	2.5
1800	730	27.1±0.293	4.0

2700	730	26.1 ± 0.293	5.0
3600	730	25.1±0.293	6
4500	730	24.3 ± 0.293	6.8
5400	730	23.6 ± 0.293	7.5
6300	730	23.1 ± 0.293	8
7200	730	22.6 ±0.293	8.5
8100	730	22.1 ± 0.293	9.0
9000	730	21.5 ± 0.293	9.6

N=3, Valuesareaverage± SE(standard error)

Fig.7 shows the cooling effect in water in Can placed in the vacuum chamber at the vacuum of 730 mmHg.

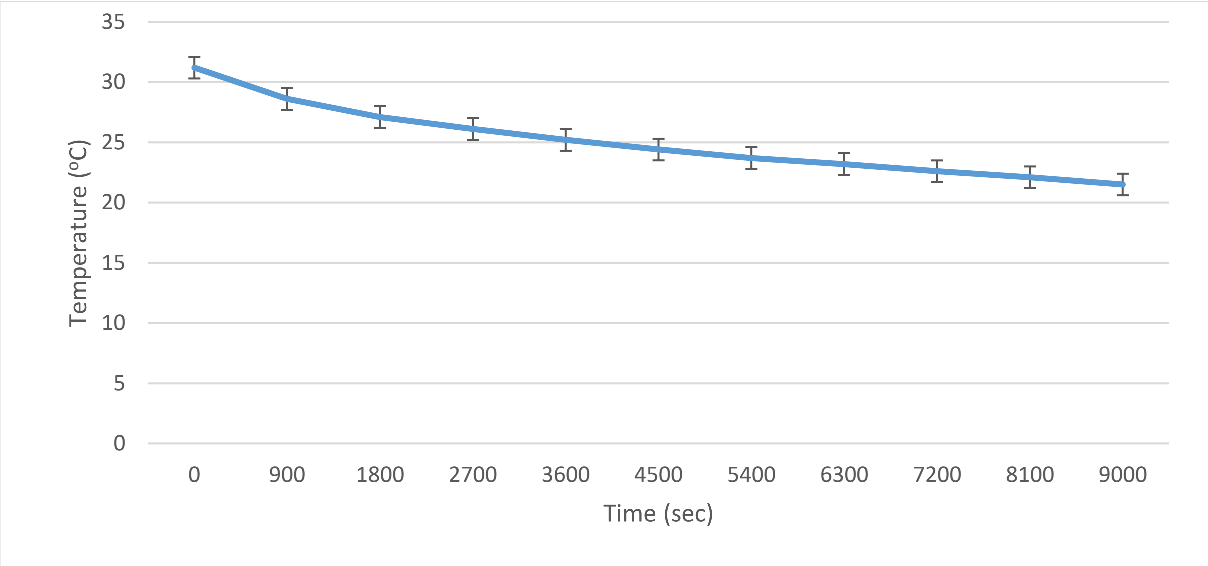

Fig. 7: Temperature profile of water in Can placed in vacuum chamber at vacuum 730 mmHg

The temperature drop in inner cavity water was very low. Fig. 8 shows the water vapour condensed on the surface of lid. The vapour generation in vacuum chamber was more as compare to vapour removal from the chamber, and vapour started to exert vapour pressure on evaporation and reduce the vapour formation so the cooling rate was less even at higher vacuum level.

Fig. 8: Condensed vapour inside the chamber

The mass flow rate of vapour through the vacuum pump depends on the density of vapour and speed of vacuum pump (Wang and Sun, 2001).

$Mv=Sp\times\rho v$

Where

Mv=Massflowthroughvacuumchamber Sp= Speed of vacuum pump (rpm)

ρv = Density of vapour

One kg water vapour require 2000 m^3 volume (Barger, 1961) so, at that much volume vapour do not exert any vapour pressure and not affect water evaporation rate from the free surface of water.

ECONOMICS OF DEVELOPED PROTOTYPE

Cost analysis of milk cooling system for future scale up of the prototype (expected)

The milk cooling cost of the developed prototype,10 litre milk cool down from 36.3°C to 21.5°C by running vacuum pump for 4h (14400 sec). For milk cooling purpose energy (electricity) input only to run the vacuum pump, so cost of electricity consumed by vacuum pump. Table 7 shows the energy consumption by vacuum pump.

1unit electricity =1KWh =1000×3600 joule

Electricity consumption by vacuum pump= 2225280 joule (from table 7)

Electric unit consumption by vacuum pump = 2225280/3600000 = 0.61813 unit (in50min.) Electricity consumption in 240 min. = (0.61813 ÷ 50) × 240 = 2.96 unit

Table 7: Energy consumption by vacuum pump

I(Current)	V (voltage)	Cosϕ(power factor)= real power/apparent power	ACsupply Power = V×I×Cosϕ Watt	Power= watt= Joule /sec	Total energy consumption = W×Time(sec) joule
3A	248V	248×3/746 = 0.997	3×248×0.997= 741.76	741.76 J/sec	741.76×3000= 2225280joule

Table 8 and 9 shows the fixed and variable cost for milk cooling respectively.

Table 8: Fixed cost for 10 litre set up (assumption)

s.no.	Item	Cost	Per hour working cost	Total time per batch	Total cost Rs
1	Equipment cost	20,000			
2	Depreciation on equipment @10% /annum	2000	Depreciation on equipment@10% /hour= 0.2283	Total working hour per batch = 4h	0.9132
3	Interest on capital investment @12% /annum	2400	Interest on capital investment@12% /Hour =0.2739	Total working hour per batch = 4h	1.0956
4	Cost of vacuum pump	40,000			
5	Depreciation on equipment @10% /annum	4000	Depreciation on equipment@10% /hour=0.4566	Total working hour per batch = 4h	1.8264
6	Interest on capital investment @12% /annum	4800	Interest on capital investment@12% /Hour= 0.5479	Total working hour per batch = 4h	2.1916
	Total fixed cost				6.02

Table 9: Variable cost for 20 litre milk cooling

s.no	Item	Cost	Per unit charge	Total cost (Rs)
1	Electricity cost	Total consumed =2.96unit	Per unit price = 5.76	17.049
2	Cleaning cost @1% of Production cost			0.38
3	Maintenance cost @2% of equipment cost	43000 @ 2%/annum	Maintenance Cost per hour= 0.1369	0.55
4	Labour cost	10 min.	Rs –350 Unskilled labour per day 8h	7.29
	TotalVariablecost	-	-	25.269

Total cost = fixed cost + variable cost = 6.02 +25.269 = 31.289

Per litre milk cooling cost(10 litre product from 36.3°C to 21.5°C) = 31.289/10= Rs3.12

V. CONCLUSION

The temperature of product is reduced from 36.3 °C to 21.5 °C in 14400 sec. In this cooling system water was used as refrigerant so, this cooling system will help to control the effect of global warming and ozone depletion. The cooling of milk right from farm will help to preserve the quality of milk by inhibiting the growth of microbes.

REFERENCES

[1] Barger, W. R. (1961). *Factors affecting temperature reduction and weight-loss in vacuum-cooled lettuce* (No. 469). US Department of Agriculture, Marketing Quality Research Division, Agricultural Marketing Service.

[2] Calm, J. M., &Hourahan, G. C. (2007). Refrigerant data update. *Hpac Engineering*, *79*(1), 50-64.

[3] Juniwal, C., Khan, A. R., Ganesh, A., Carvalho, R. M., &Karunamay, S. (2022). Constraints in milk production of dairy cattle. *The Pharma Innovation Journal*, SP-11(7): 3991-3994

[4] Seifu, E., Buys, E. M., & Donkin, E. F. (2005). Significance of the lactoperoxidase system in the dairy industry and its potential applications: a review. *Trends in Food Science & Technology*, *16*(4), 137-154.

[5] Sraïri, M. T., Benyoucef, M. T., & Kraiem, K. (2013). The dairy chains in North Africa (Algeria, Morocco and Tunisia): from self sufficiency options to food dependency?. *SpringerPlus*, *2*(1), 1-13.https://doi.org/10.1186/2193-1801-2-162

[6] TeGiffel, M. C., & Wells-Bennik, M. H. J. (2010). Good hygienic practice in milk production and processing. In *Improving the Safety and Quality of Milk* (pp. 179-193). Woodhead Publishing.https://doi.org/10.1533/9781845699420.2.179

[7] Uddin, M. A., Motazzim-ul-Haque, H. M., & Noor, R. (2011). Isolation and identification of pathogenic Escherichia coli, Klebsiella spp. and Staphylococcus spp. in raw milk samples collected from different areas of Dhaka City, Bangladesh. *Stamford Journal of Microbiology*, *1*(1), 19-23.

[8] Wang, L., & Sun, D. W. (2001). Rapid cooling of porous and moisture foods by using vacuum cooling technology. *Trends in food science & technology*, *12*(5-6), 174-184.https://doi.org/10.1016/S0924-2244(01)00077-2

International Journal of Environment, Agriculture and Biotechnology
Vol-11, Issue-2; Mar-Apr, 2026
Peer-Reviewed International Journal
Journal Home Page Available: https://ijeab.com/
Journal DOI: 10.22161/ijeab

Kinnow Plants (*Citrus nobilis* x *Citrus deliciosa*) Disease-Induced Alterations in Biochemical Composition: A comparison of Healthy and Gummosis-Infected Plants

Priya Kumari[1], Smita Jain[2]

[1]Ph.D Scholar, Department of Botany, Govt. Dungar College, Bikaner, Rajasthan, India
[2]Professor, Department of Botany, Govt. Dungar College, Bikaner, Rajasthan, India

Received: 13 Feb 2026; Received in revised form: 16 Mar 2026; Accepted: 22 Mar 2026; Available online: 30 Mar 2026

***Abstract*— *A economically significant citrus cultivar, the Kinnow mandarin (Citrus nobilis x Citrus deliciosa) is grown extensively throughout the Indian subcontinent, especially in northern india. In Rajasthan state, Kinnow is mainly produced in Sri ganganagar and Hanumangarh district. Kinnow plants affected by some diseases like; Citrus canker, Phytophthora, Greening (Huanglongbing), Gummosis, Citrus scab, Black fly infestation, Dieback, Anthracnose and sooty mold. Disease management is more important for decrease losses of fruit yield. A comparative analysis of the chosen biochemical parameters between healthy and diseased plants was attempted in the current study. Gummosis-infected Kinnow plants (Citrus nobilis x Citrus deliciosa) show notable biochemical alterations, according to the study, including higher concentrations of Alkaloids compounds, Phenolic, Terpenoids, Proline, MDA (Malondialdehyde) and ROS (Reactive oxygen species) and lower Chlorophyll content. According to these alterations, the disease caused a complex response in the plants that impact both primary and secondary metabolism.*

***Keywords*— Kinnow mandarin, Gummosis, Plant metabolites.**

I. INTRODUCTION

The Kinnow, a high-yielding mandarin hybrid, is widely grown throughout the Punjab region of Pakistan and India. It is a cross between the citrus cultivars king (*Citrus nobilis*) and willow leaf (*Citrus deliciosa).* Howerd B. Frost first developed it at the Citrus Research Center (University of Callifornia) Riverside in the United state. In 1915 after a long evaluation period of 20 years, it was introduced as a new variety for commercial production (Frost and Soost, 1968). Kinnow mandarin become one of the most important citrus crops in the country due to its adaptability, high productivity, and superior fruit quality (Mahajan *et al.,* 2015).

Kinnow fruits are medium to large-sized with a rich orange colour and a smooth, thin peel. The Kinnow mandarin is rich in various biochemical compounds that contribute to its nutritional value and health benefits. The fruit contains high levels of vitamin C, β- carotene, vitamin B, calcium and phosphorous (Mahawar *et al.,* 2019). They are known for their juicy segments and sweet-tart- flavor, making them popular for fresh consumption and juice production. The trees are vigorous and bear fruit early, with a tendency towards heavy and alternate bearing patterns (Singh *et al.,* 2010). The fruit's rich, sweet-tart taste with a balanced sugar-acid ratio makes it highly palatable and preferred for both fresh consumption and juice production (Ludaniya, 2008).

The kinnow mandarin possesses several unique qualities that distinguish it from other citrus fruit: high yield potential, adaptability, flavor profile, extended harvest season, post-harvest longevity. Kinnow trees are known for their prolific bearing capacity, often producing higher yields than other mandarin varieties under similar cultivation condition (Sharma and Singh, 2013). This makes them economically advantageous for farmers. The Kinnow mandarin is well-suited to a range of climatic conditions, including subtropical regions with hot summers and cool winters its adaptability extends to various soil types, contributing to its widespread cultivation. Kinnow mandarins have a relatively long harvest period, often from December to March in the Northern Hemisphere, providing an extended market window compared to other citrus fruits With proper handling, Kinnow fruits exhibit good shelf life and can withstand transportation over long distances, which is beneficial for commercial distribution (Mahajan *et al*., 2015).

However, the high seed content can be considered a drawback in markets where consumers prefer seedless varieties. Efforts are being made through breeding programmes to develop low-seed or seedless Kinnow variants to meet consumer demands (Singh *et al*., 2017).

Plant diseases pose significant economic challenges to Kinnow cultivation in india, affecting both income of the farmers and the broader agricultural economy. Citrus disease cause substantial economic losses worldwide through reduced yields, increased production costs, and diminished fruit quality. Managing these diseases often requires significant investment in control measures, which increases the cost of production (Gottwald *et al*., 2007).

Kinnow plants affected by some diseases like; Citrus canker, Phytophthora, Greening (Huanglongbing), Gummosis, Citrus scab, Black fly infestation, Dieback, Anthracnose and sooty mold. Gummosis is the one of Devastating disease affecting kinnow fruit yield. Gummosis, a disease affecting Kinnow or citrus trees, is primarly caused by Phytophthora fungi and characterized by the oozing of gum from the trunk and branches, effective management involves a combination of cultural practice, biological control, and chemical treatment (Erwin and Ribeiro, 1996).

Kinnow plants, like other citrus varieties, exhibit various physiological and biochemical changes when affected by diseases. The plants are continuous exposure to microoraganism in the environment, as a result, have developed complex defense mechanism to recognize and protect themselves against potential pathogens. Photosynthesis and other basic metabolism related processes that are vital to plant growth are downregulated as a result of these reactions (Rojas *et al*., 2014). According to Piasecka et al. (2015) and Sudha & Ravishankar (2002), secondary metabolites in plants are essential for their defense against a variety of biotic and abiotic stresses. Plants innate immunity response to pathogen infections frequently involves an increase in the synthesis of protective secondary metabolites. These substances may have a role in regulating immunological responses such callose deposition and programmed cell death.

The goal of the current study to conduct a comparative biochemical analysis of Gummosis-infected and healthy Kinnow plants. It involve quantify and compare the amounts of primary and secondary metabolites in infected and healthy Kinnow plants. According to the research work, the primary and secondary metabolite profile of Kinnow plants will change significantly as a result of Gummosis infection. This work attempts to advance our knowledge of the Kinnow plants response to Gummosis disease by clarifying these disease-induced alteration.

II. MATERIAL AND METHODS

2.1 Study area

Six marked Kinnow orchards (sample sites) were used for the study, which was carried out in Sri Ganganagar, Rajasthan, India. The Kinnow mandarin (*Citrus nobilis* x *Citrus deliciosa*) plants that were both healthy and diseases with gummosis were selected from these orchards. Visually inspection of characteristic oozing of the gum from the trunk or branches were used to confirm the condition prior to sampling (Adesemoye *et al.* (2014).

2.2 Sample Collection

At each sampling location, leaf samples were taken from both healthy and diseased plants (10 leaves) to ensure that the plant ages and leaf positions were similar. additionally, samples were marked and transferred to an ice box in the field. Until further investigation, the leaves were kept in the labs refrigerated facility at -12ºC to prevent water loss and biochemical alteration. Glass homogenizer was used to homogenize samples before each biochemical test.

2.3 Biochemical Analysis in Kinnow plant (Citrus nobilis x Citrus deliciosa)

2.3.1 Total Chlorophyll Content

The method described by Lichtenthaler and Buschmann (2001) was used to determine the total chlorophyll content. In this process, 0.1 g of fresh leaf tissue was blended with 10ml of 80% acetone. The homogenate was centrifuged at 3,000 rpm for 5 minutes, and the absorbance of the supernatant was recorded at 663nm and 645 nm with a UV-visible spectrophotometer.

2.3.2 Total Phenolic Content

The Folin-Ciocalteu method was used to measure total phenolic content (Singleton *et al*., 1999). Fresh leaf samples (0.5g) were extracted with 80% methanol, and the extract was reacted with Folin-Ciocalteu reagent. Absorbance was measured at 765nm, and outcomes were expressed as µg of gallic acid equivalent per gram of fresh weight.

2.3.3 Protein Content

The Bradford method (Bradford, 1976) was utilized to measure protein content. Fresh leaf tissue (0.5 g) was homogenized in phosphate buffer (pH 7.0), and the solution was treated with Bradford reagent. Absorbance was measured at 595nm, using bovine serum albumin as a standard.

2.3.4 Total Alkaloid Content

The total alkaloid content was determined using the technique described by Sreevidya and Mehrotra (2003). Ethanol was used to exract fresh leaf samples, and the resulting exract was treated with Bromocresol Green solution. Absorbance was measured at 470nm.

2.3.5 Terpenoid Content

The terpenoid content was determined using the method Ghorai *et al*. (2012).fresh leaf samples were extract was combined with Vanillin-sulfuric acid reagent. Absorbance was recorded at 608nm.

2.3.6 Proline Content

The Ninhydrin method (Bates *et al.,* 1973) was used to assess proline content. Fresh leaf samples (0.5 g) were blended in Sulfosalicylic acid and treated with acid ninhydrin. The absorbance was measured at 520nm.

2.3.7 Malondialdehyde (MDA) Content

Lipid peroxidation was evaluated by determing MDA levels via the Thiobarbituric acid (TBA) technique (Heath and Packer, 1968). Fresh leaf tissue (0.5 g) was homogenised in trichloroacetic acid and then centrifuged. The supernatant was mixed with TBA and heated. Absorbance was recorded at 532 nm and 600nm.

2.3.8 Reactive Oxygen Species (ROS)

Reactive Oxygen Species (ROS) were considered in terms of the level of H_2O_2 present. The H_2O_2 levels, which indicate ROS were determined using the method of Valikova *et al.* (2000). Fresh leaf samples (0.5 g) were homogenised in trichloroacetic acid and spun in a centrifuge. The supernatant was mixed with Potassium phosphate buffer and Potassiun iodide. Absorbance was measured at 390nm.

III. OBSERVATION

The following finding was obtained by comparing the biochemical parameters of Gummosis-infected and healthy Kinnow plants (Table-1). The eight biochemical parameters were recorded at six distinct sampling locations (Daulatpura, 7 F, Koni, Mirzawala, Madera, Fatuhi) using both Gummosis-infected and healthy plants.

Table -1 Biochemical Parameters in healthy Kinnow plants and Gummosis diseased Plants at different sampling sites.

S.N.	Biochemical Parameter	Study Site ►	Daulat-pura	7F	Koni	Mirzawala	Maderan	Fatuhi
1.	Total Chlorophyll Content (µg/g)	Healthy plant	675	715	742	752	702	682
		Diseased plant	452	512	556	426	516	612
2.	Total Phenolic Content (µg GAE/g)	Healthy plant	34.16	42.26	45.6	38.26	32.65	42.5
		Diseased plant	45.65	58.56	52.56	39.65	38.65	43.55
3.	Protein Content (µg/g)	Healthy plant	1.2	1.1	1.56	2.1	1.5	1.6
		Diseased plant	1.65	1.2	1.59	1.85	1.68	1.89
4.	Total Alkaloid Content (µg/g)	Healthy plant	2.3	2.4	2.5	2.2	2.8	3.1
		Diseased plant	3	3.5	3.1	3.2	3.5	3.5
5.	Terpenoid Content (µg/g)	Healthy plant	845	756	856	721	722	765
		Diseased plant	892	865	859	813	810	812
6.	Proline Content	Healthy plant	3.85	4.56	3.65	4.65	4.98	3.59

	(µg/g)	Diseased plant	5.65	6.6	5.6	8.56	5.65	4.65
7.	Malondialdehyde (MDA) Content (µg/g)	Healthy plant	0.01	0.02	0.02	0.01	0.02	0.03
		Diseased plant	0.02	0.03	0.03	0.02	0.02	0.04
8.	Reactive oxygen species (ROS) (µmol/g)	Healthy plant	1.6	2.15	1.82	2.59	1.85	1.66
		Diseased plant	2.65	3.56	3.12	3.65	3.58	3.5

IV. RESULT AND DISCUSSION

The research investigated the biochemical changes in Kinnow plants induces by Gummosis disease, comparing important biochemical parameters between healthy and diseased plants. (Table-1) the data show notable changes in various biochemical compounds suggesting a strong influence of the disease on the metabolic functions of plants (Figure-1, 2,3,4) additionally, these increased parameters were analyzed for statistical significance using a t-test (Table-2).

Table -2 Average value of Biochemical Parameters and their statistical significance test

S.N.	**Biochemical Parameter**	**Plants (Healthy/diseased)**	**Average value**	**Conclusion**
1.	Total Chlorophyll Content (µg/g)	Healthy plant	711.3 ± 12.75	Highly significant difference ($p \leq 0.001$)
		Diseased plant	512.3 ± 27.66	
2.	Total Phenolic Content (µg GAE/g)	Healthy plant	39.24 ± 2.085	Non-significant difference
		Diseased plant	46.44 ± 3.163	
3.	Protein Content (µg/g)	Healthy plant	1.510 ± 0.1441	Non-significant difference
		Diseased plant	1.643 ± 0.1007	
4.	Total Alkaloid Content (µg/g)	Healthy plant	2.550 ± 0.1384	significant difference ($p \leq 0.01$)
		Diseased plant	3.300 ± 0.0930	
5.	Terpenoid Content (µg/g)	Healthy plant	777.5 ± 24.23	significant difference ($p \leq 0.05$)
		Diseased plant	841.8 ± 14.24	
6.	Proline Content (µg/g)	Healthy plant	4.213 ± 0.2406	significant difference ($p \leq 0.01$)
		Diseased plant	6.118 ± 0.5495	
7.	Malondialdehyde (MDA) Content (µg/g)	Healthy plant	0.01833±0.003073	Non-significant difference
		Diseased plant	0.02667±0.003333	
8.	Reactive oxygen species (ROS) (µmol/g)	Healthy plant	1.945 ± 0.1509	Highly significant difference ($p \leq 0.001$)
		Diseased plant	3.343 0.158	

4.1 Chlorophyll content

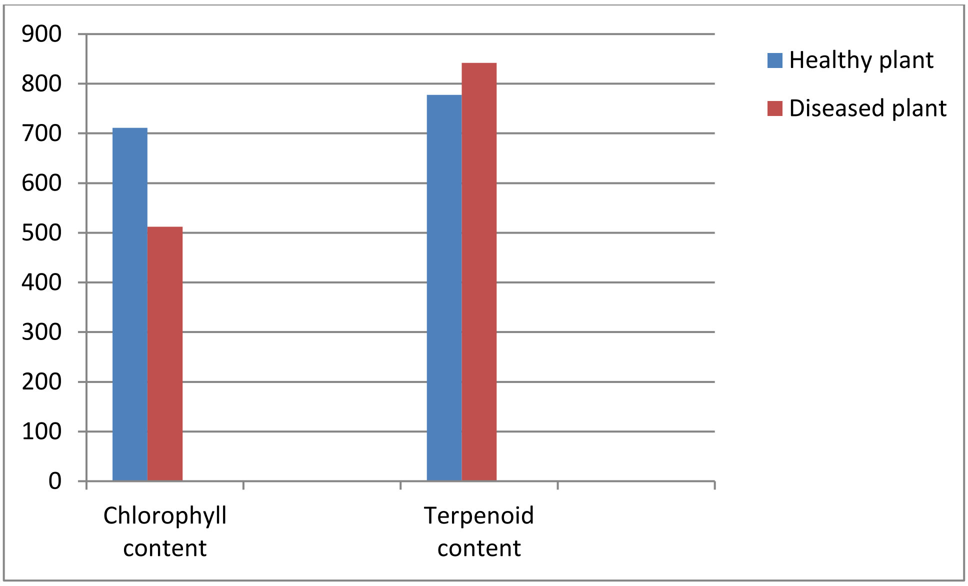

Fig.1: Alteration in Biochemical Parameter (Chlorophyll and Terpenoid content) of healthy and diseased plants

Diseased plants had a much lower total Chlorophyll content (512.3 µg/g) than healthy plants (711.3 µg/g), according to the study the significant drop in chlorophyll content marked to a sharp decline in photosynthetic efficiency, which is a typical sign of stress in plants attacked by diseases. Gummosis infection- induced oxidative stress and cellular damage may be the cause of the drop in chlorophyll content.

4.2 Protein, Alkaloid, Proline, and ROS

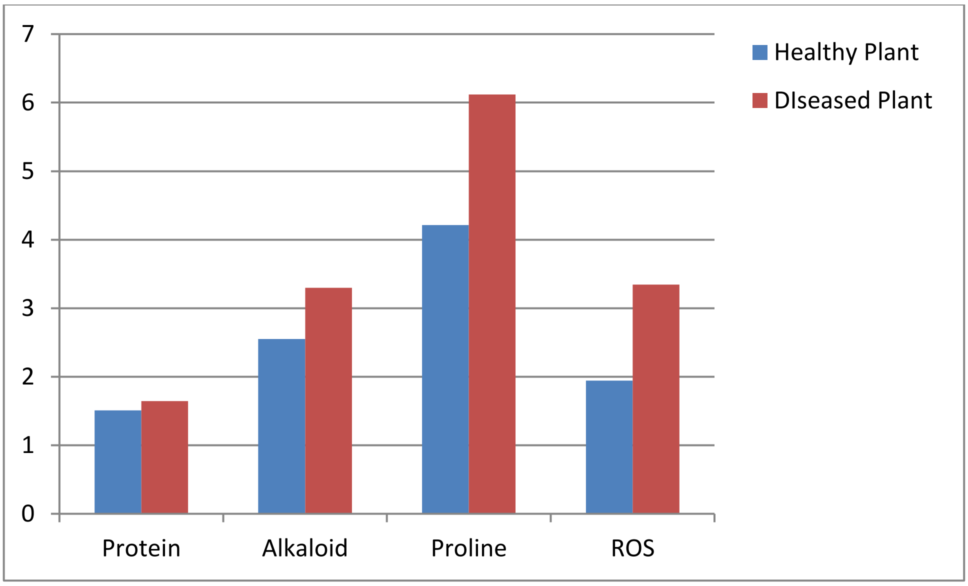

Fig.2: Alteration in Biochemical Parameter (Protein, Alkaloid, Proline, and ROS) of healthy and diseased plants

There were very slight variation in the Protein concentration between the diseased plants (1.643 µg/g) and the healthy plants (1.510 µg/g). The slight alteration seen in the investigation signifies that the Gummosis disease had minimal change on the overall synthesis or degradation of proteins, suggesting that fundamental metabolic processes remained largely unaffected by the diseases.

An increase in Alkaloids, which are secondary metabolites frequently linked to plant defense, indicate an active biochemical reaction to pathogen invasion. The study found that diseased plants had a significantly higher total alkaloid content (3.300 µg/g) than healthy plants (2.550 µg/g). The higher Alkaloid content in diseased Kinnow plants points to an activated defence system mechanism that might help the plant resist the infection or slow its spread.

Similarly, the Proline content was significantly higher in diseased Kinnow plants (6.118 µg/g) than in healthy plants (4.213 µg/g). Adverse environmental condition and pathogen attack tend to raise Proline levels. Diseased plants increased Proline levels suggested stress responses, which might have helped the plant handle the oxidative damage brought on by the infection.

According to the study, diseased plants had considerably higher levels of Reactive oxygen species (3.343 µmol/g) than healthy plants (1.945 µmol/g). Reactive oxygen species (ROS) are frequently generated in reaction to pathogen infection and can cause damage. Reactive oxygen species are also trigger signalling pathways for defense mechanism. The higher reactive oxygen species levels in diseased plants show reactive oxygen species function as both harmful and signalling agents in the plants response to Gummosis infection.

4.3 Malondialdehyde (MDA)

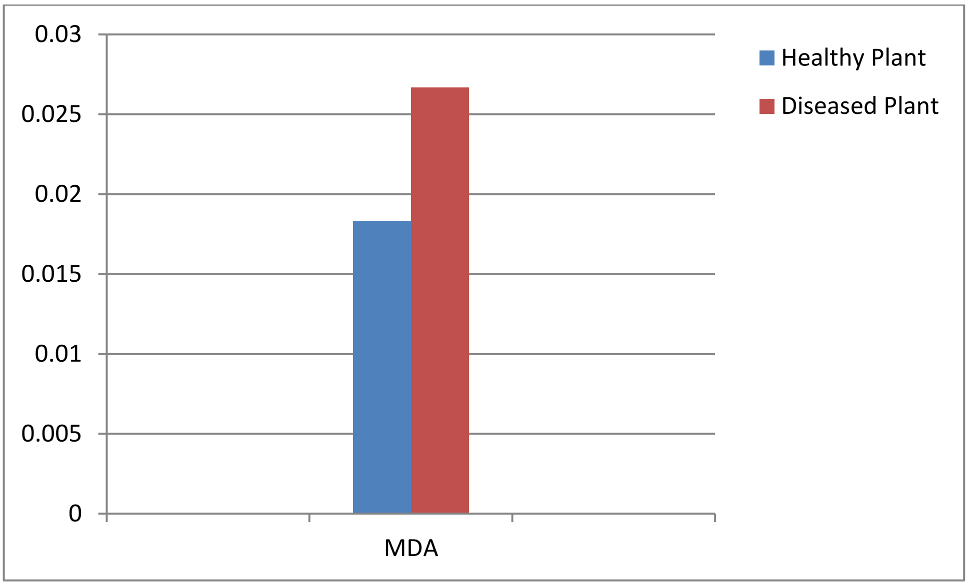

Fig.3: Alteration in Biochemical Parameter (MDA-Malondialdehyde) of healthy and diseased plants

Diseased plants had a slightly higher Malondialdehyde content (0.02667 µg/g) and healthy Kinnow plants (0.01833 µg/g). The non-significant difference in this study, implies that lipid peroxidation may not be the predominat response in plants to Gummosis infection.

4.4 Phenolic content

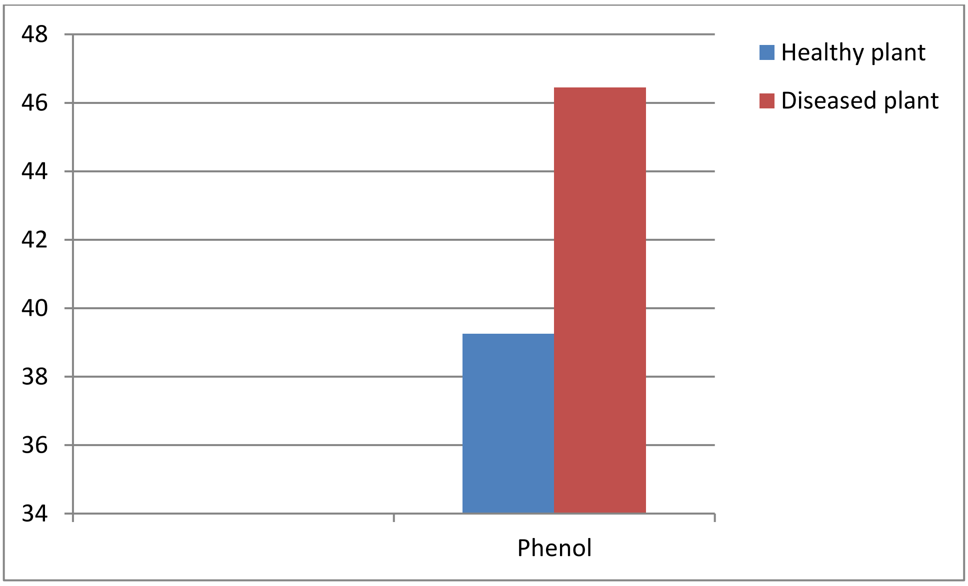

Fig.4: Alteration in Biochemical Parameter (Phenol content) of healthy and diseased plants

The total phenolic content was found to be higher in diseased plants (46.44 µgGAE/g) than in healthy plants (39.24 µgGAE/g). Phenolics are defence compounds that help to strengthen cell walls and prevent the infection of pathogen. An active defence response may be indicated by the elevated phenolic content in diseased plants, which could strengthen resistance to the gummosis infection.

V. CONCLUSION

The comparison of biochemical compounds between Gummosis diseased and healthy Kinnow plants illustrate the diseases widespread effect on plant metabolism. The considerable decrease in chlorophyll content suggest that photosynthesis activity decreases. Increased concentration of secondary metabolites (Alkaloids, Phenolics, Terpenoids) that emphasize an improved defense response. Reactive oxygen species (ROS) and Proline concentration higher in diseased Kinnow plants. They are responsible for trigger signalling pathways and defense mechanism in plants biochemical alteration induced by Gummosis disease in Kinnow plants, providing information that may guide future disease management.

REFERENCES

[1] Adesemoye, A. O., Mayorquin, J. S., Wang, D. H., Twizeyimana, M., Lynch, S. C., & Eskalen, A. (2014). Identification of species of Botryosphaeriaceae causing bot gummosis in citrus in California. Plant disease, 98(1), 55-61.

[2] Bates, L. S., Waldren, R. P., & Teare, I. D. (1973). Rapid determination of free proline for water-stress studies. Plant and Soil, 39(1), 205-207.

[3] Bradford, M. M. (1976). A rapid and sensitive method for the quantitation of microgram quantities of protein utilizing the principle of protein-dye binding. Analytical Biochemistry, 72(1-2), 248-254.

[4] Erwin, D. C., & Ribeiro, O. K. (1996). *Phytophthora diseases worldwide* (pp. xii+-562).

[5] Frost, H. B., & Soost, R. K. (1968). Seed reproduction: Development of gametes and embryos. In W. Reuther, L. D. Batchelor, & H. J. Webber (Eds.), The Citrus Industry (Vol. 2, pp. 290-324). University of California.

[6] Ghorai, N., Chakraborty, S., Gucchait, S., Saha, S. K., & Biswas, S. (2012). Estimation of total Terpenoids concentration in plant tissues using a monoterpene, Linalool as standard reagent. Protocol Exchange, 5, 1-6.

[7] Gottwald, T. R., Graça, J. V. D., & Bassanezi, R. B. (2007). Citrus huanglongbing: the pathogen and its impact. *Plant Health Progress*, *8*(1), 31.

[8] Heath, R. L., & Packer, L. (1968). Photoperoxidation in isolated chloroplasts: I. Kinetics and stoichiometry of fatty acid peroxidation. Archives of Biochemistry and Biophysics, 125(1), 189-198.

[9] Ladaniya, M. S. (2008). Citrus Fruit: Biology, Technology and Evaluation. Academic Press.

[10] Lichtenthaler, H. K., & Buschmann, C. (2001). Chlorophylls and carotenoids: Measurement and characterization by UV-VIS spectroscopy. Current Protocols in Food Analytical Chemistry, 1(1), F4-3.

[11] Mahajan, B. V. C., Dhatt, A. S., & Sandhu, K. S. (2015). Postharvest handling and storage of Kinnow mandarin. Indian Journal of Horticulture, 72(1), 1-9.

[12] Mahawar, M. K., Bibwe, B., Jalgaonkar, K., & Ghodki, B. M. (2019). Mass modeling of kinnow mandarin based on some physical attributes. *Journal of Food Process Engineering*, *42*(5), e13079.

[13] Piasecka, A., Jedrzejczak-Rey, N., & Bednarek, P. (2015). Secondary metabolites in plant innate immunity: conserved function of divergent chemicals. *New Phytologist*, *206*(3), 948-964.

[14] Rojas, C. M., Senthil-Kumar, M., Tzin, V., & Mysore, K. S. (2014). Regulation of primary plant metabolism during plant-pathogen interactions and its contribution to plant defense. *Frontiers in plant science*, *5*, 17.

[15] Sharma, N., & Singh, J. (2013). Constraints of Kinnow cultivation in arid zone of Rajasthan. Agricultural Science Digest, 33(2), 139-142.

[16] Singh, S., Sharma, R. R., & Tyagi, S. K. (2010). Pre-harvest foliar application of calcium and boron influences physiological disorders, fruit yield and quality of Kinnow mandarin. Scientia Horticulturae, 127(3), 234-238.

[17] Singleton, V. L., Orthofer, R., &Lamuela-Raventós, R. M. (1999). Analysis of total phenols and other oxidation substrates and antioxidants by means of Folin-Ciocalteu reagent. Methods in Enzymology, 299, 152-178.

[18] Sreevidya, N., & Mehrotra, S. (2003). Spectrophotometric method for estimation of alkaloids precipitable with Dragendorff's reagent in plant materials. Journal of AOAC International, 86(6), 1124-1127.

[19] Sudha, G., & Ravishankar, G. A. (2003). Elicitation of anthocyanin production in callus cultures of Daucus carota and involvement of calcium channel modulators. *Current Science*, 775-779.

[20] Velikova, V., Yordanov, I., &Edreva, A. (2000). Oxidative stress and some antioxidant systems in acid rain-treated bean plants: Protective role of exogenous polyamines. Plant Science, 151(1), 59-66.

International Journal of Environment, Agriculture and Biotechnology
Vol-11, Issue-2; Mar-Apr, 2026
Peer-Reviewed International Journal
Journal Home Page Available: https://ijeab.com/
Journal DOI: 10.22161/ijeab

Evaluating Climate-Smart Agricultural Systems: A Comparative Analysis of Policy, Practices, and Impacts in India and New Zealand

Disha Chahal

Discipline of Geography, School of Sciences, Indira Gandhi National Open University (HQ), New Delhi-110068, India
disha1chahal@gmail.com

Received: 15 Feb 2026; Received in revised form: 20 Mar 2026; Accepted: 27 Mar 2026; Available online: 06 Apr 2026

***Abstract*— Climate-smart agriculture (CSA) has emerged as a critical framework for addressing food security challenges under climate change. This study presents a comparative analysis of CSA systems in India and New Zealand, focusing on policy frameworks, agricultural practices, and socio-economic and environmental impacts. A systematic review of recent literature (2020–2025) was conducted to evaluate implementation outcomes. Results indicate that India prioritizes adaptation strategies and livelihood resilience among smallholder farmers, whereas New Zealand emphasizes greenhouse gas mitigation and precision agriculture. While India faces constraints such as fragmented landholdings and limited access to technology, New Zealand demonstrates strong institutional capacity and innovation-driven systems. The study highlights the need for integrated approaches combining resilience and mitigation strategies for sustainable agricultural development.*

***Keywords*— Climate-smart agriculture, sustainability, adaptation, mitigation, comparative analysis, food security**

I. INTRODUCTION

Agriculture is one of the most climate-sensitive sectors, directly affected by rising temperatures, altered precipitation patterns, and increasing frequency of extreme weather events (Kumar et al., 2024; Smith et al., 2020; Thornton and Herrero, 2021). These changes threaten global food security, rural livelihoods, and ecosystem stability, particularly in developing countries where agriculture remains a primary source of income (Maya et al., 2025).

Climate-smart agriculture (CSA) has emerged as a transformative framework to address these challenges by simultaneously enhancing productivity, strengthening resilience, and reducing greenhouse gas (GHG) emissions (Bompotas et al., 2025; Haq et al., 2026; Lipper et al., 2020; Rosenstock et al., 2021; Sharma and Singh, 2025)

CSA is not a single technology but an integrated approach encompassing sustainable land management, efficient resource use, and climate-resilient innovations. Its implementation varies significantly across regions depending on agroecological conditions, socio-economic factors, and institutional capacity (Kumar et al., 2024; Haq et al., 2026; Pretty and Bharucha, 2021; Sharma and Singh, 2025). While the concept is globally endorsed, its practical application often reflects national priorities and developmental contexts.

India represents a highly vulnerable agrarian economy characterized by smallholder-dominated farming systems, high dependence on monsoon rainfall, and limited access to advanced agricultural technologies (Birthal et al., 2021). Climate variability in India has led to increased incidences of droughts, floods, and yield instability, necessitating the adoption of adaptation-focused CSA strategies (Sharma and Singh, 2025; Shirsath et al., 2020). Government initiatives such as the National Mission for Sustainable Agriculture (NMSA) and the National Innovations in Climate Resilient Agriculture (NICRA) have sought to enhance resilience through water-use efficiency, soil health management, and climate-resilient crop varieties (Maya et al., 2025).

In contrast, New Zealand presents a technologically advanced agricultural system with strong institutional frameworks and significant global market integration. Agriculture in New Zealand is a major contributor to national greenhouse gas emissions, particularly from livestock production, prompting a strong policy emphasis on mitigation and sustainability (Bompotas et al., 2025; Kumar et al., 2024; Reisinger et al., 2021; Ledgard et al., 2020). The country has adopted innovative approaches such as precision agriculture, low-emission livestock systems, and advanced nutrient management to reduce environmental impacts while maintaining high productivity.

Despite the growing body of literature on CSA, comparative studies examining diverse agroecosystems across developed and developing economies remain limited. Understanding the differences in policy design, technology adoption, and impact outcomes is critical for identifying scalable and context-specific solutions. A comparative analysis between India and New Zealand provides valuable insights into how CSA strategies can be tailored to different socio-economic and environmental conditions.

The specific objectives of this study are:

1. To evaluate CSA-related policy frameworks in India and New Zealand
2. To analyze key climate-smart agricultural practices and their adoption
3. To assess environmental, economic, and social impacts of CSA
4. To identify challenges and opportunities for improving CSA implementation

This study contributes to the existing literature by offering a cross-country comparative perspective, highlighting the interplay between policy, technology, and institutional capacity in shaping CSA outcomes. The findings aim to inform policymakers, researchers, and practitioners in designing more effective and inclusive climate-smart agricultural systems.

II. MATERIALS AND METHODS

2.1 Research Design

This study employs a comparative qualitative research design to evaluate climate-smart agriculture (CSA) systems in India and New Zealand. A comparative approach is particularly suitable for examining differences in policy frameworks, technological adoption, and impact outcomes across diverse agroecological and socio-economic contexts. The study integrates systematic literature review and thematic analysis, enabling a comprehensive synthesis of existing knowledge on CSA practices and their effectiveness.

2.2 Data Sources

Data were collected from multiple secondary sources (Peer-reviewed journal articles; Scopus-indexed; International reports from organizations such as FAO and World Resources Institute; Government policy documents from India and New Zealand and Research papers on CSA adoption, impacts, and sustainability) to ensure robustness and reliability:

Key databases consulted include Scopus, Web of Science and ScienceDirect. The selection of recent literature ensures that the analysis reflects current trends, technological advancements, and policy developments in CSA.

2.3 Inclusion and Exclusion Criteria

To maintain the quality and relevance of the analysis, the following criteria were applied: The Inclusion Criteria embrace studies published between 2020 and 2025, Peer-reviewed and Scopus-indexed articles, Studies focusing on CSA practices, policies, or impacts and Research specific to India, New Zealand, or comparable agroecosystems. The Exclusion Criteria excludes non-peer-reviewed articles and opinion pieces, Studies lacking empirical or analytical evidence and the Publications prior to 2020 (unless highly relevant foundational works)

2.4 Analytical Framework

The analysis is structured around the three core pillars of CSA:

1. Productivity – improvement in agricultural output
2. Adaptation – resilience to climate variability
3. Mitigation – reduction of greenhouse gas emissions

Each country's agricultural system was evaluated using the following dimensions:

- Policy frameworks
- Agricultural practices
- Environmental impacts
- Economic outcomes
- Social implications

This multidimensional framework allows for a holistic comparison of CSA systems.

2.5 Data Analysis

A thematic synthesis approach was used to analyze qualitative data. Key themes were identified, coded, and compared across the two countries. The analysis focused on:

- Patterns of CSA adoption
- Effectiveness of policy interventions
- Socio-economic and environmental outcomes

Comparative insights were derived by identifying similarities and differences in CSA implementation and outcomes.

2.6 Limitations of the Study

Despite its comprehensive approach, the study has certain limitations such as reliance on secondary data may introduce bias from original sources; Differences in data availability between India and New Zealand and Limited quantitative comparison due to variability in reported indicators. However, the use of multiple high-quality sources and recent literature enhances the reliability and validity of the findings.

III. RESULTS AND DISCUSSION

3.1 Policy Frameworks and Institutional Approaches

Climate-smart agriculture (CSA) policies in India and New Zealand reflect fundamentally different developmental priorities and institutional capacities. In India, CSA is embedded within broader rural development and food security programs such as the National Mission for Sustainable Agriculture (NMSA) and the National Innovations in Climate Resilient Agriculture (NICRA). These initiatives emphasize adaptation, risk reduction, and livelihood security, particularly for smallholder farmers (Birthal et al., 2021; Haq et al., 2026; Shirsath et al., 2020). The policy focus is largely reactive, addressing climate vulnerabilities such as droughts, floods, and soil degradation (Kalisetti et al., 2025; Kumar et al., 2024; Sharma and Singh, 2025).

In contrast, New Zealand adopts a proactive and mitigation-oriented policy framework, integrating agricultural emissions reduction targets into national climate commitments. Policies are strongly supported by scientific research and institutional coordination, enabling precise monitoring and reporting of agricultural greenhouse gas emissions (Ledgard et al., 2020; Reisinger et al., 2021). The presence of well-developed extension systems and data-driven governance enhances the effectiveness of CSA implementation (Maya et al., 2025).

Comparatively, while India demonstrates strong policy intent, challenges remain in implementation due to fragmented governance and limited access to resources (Aryal et al., 2021; Kumar et al., 2024; Sharma and Singh, 2025). New Zealand's success highlights the importance of institutional coherence, policy integration, and technological infrastructure in achieving CSA objectives.

3.2 Adoption of Climate-Smart Agricultural Practices

The adoption of CSA practices varies significantly between the two countries due to differences in socio-economic conditions, farm size, and technological access.

3.2.1 India

CSA practices in India are primarily **adaptation-driven** and include conservation agriculture, agroforestry, crop diversification, and water-efficient irrigation systems (Jat et al., 2020; Haq et al., 2026; Shirsath et al., 2020). Conservation agriculture, characterized by minimal soil disturbance and residue retention, has been shown to improve soil organic carbon and reduce input costs (Jat et al., 2020). Similarly, agroforestry systems enhance carbon sequestration while providing additional income streams (Kalisetti et al., 2025; Maya et al., 2025; Pretty and Bharucha, 2021).

However, adoption rates remain uneven across regions. Socio-economic barriers such as limited access to credit, lack of technical knowledge, and small landholdings significantly constrain widespread implementation (Aryal et al., 2021; Ma and Rahut, 2024). Studies indicate that farmer awareness and institutional support are critical determinants of CSA adoption in developing countries (Roy et al., 2025; Rosenstock et al., 2021; Sharma and Singh, 2025).

3.2.2 New Zealand

In New Zealand, CSA practices are **technology-intensive and mitigation-focused**, including precision agriculture, digital farming, and low-emission livestock management systems (Ledgard et al., 2020; Reisinger et al., 2021). Precision agriculture enables optimized use of inputs such as fertilizers and water, reducing environmental impacts while maintaining high productivity.

Livestock systems, which contribute significantly to national emissions, are being transformed through improved feed efficiency, methane inhibitors, and advanced breeding techniques (Ledgard et al., 2020). Additionally, climate forecasting and decision-support tools allow farmers to proactively manage climate risks.

Overall, New Zealand exhibits higher adoption rates due to better access to capital, advanced research infrastructure, and strong policy support (Figure 1).

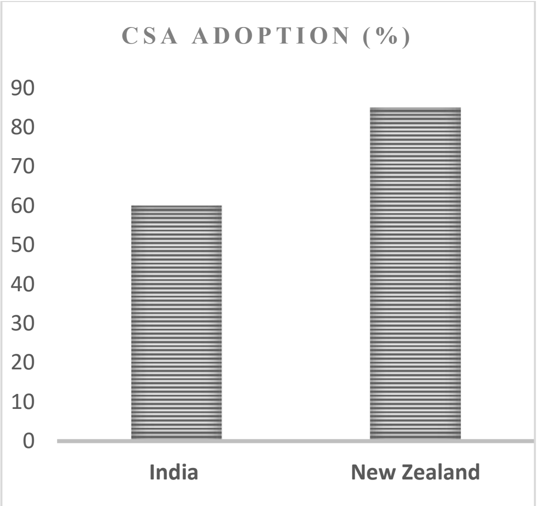

Fig 1: Comparative adoption levels of climate-smart agriculture practices in India and New Zealand, indicating higher technological uptake in New Zealand.

3.3 Environmental Impacts

CSA practices contribute significantly to environmental sustainability in both countries, although the nature and scale of impacts differ.

In India, CSA interventions have been shown to: Enhance soil fertility and organic carbon content; Improve water-use efficiency and Reduce land degradation (Jat et al., 2020; Shirsath et al., 2020; Roy et al., 2025; Zhao et al., 2023)

However, mitigation outcomes remain limited due to the dominance of small-scale farming and low mechanization levels (Sharma and Singh, 2025; Smith et al., 2020). The primary environmental benefit lies in adaptation and resilience building rather than emission reduction.

In contrast, New Zealand demonstrates strong performance in GHG mitigation, particularly in reducing methane and nitrous oxide emissions from livestock systems (Reisinger et al., 2021). Advanced nutrient management systems also minimize nitrogen leaching and water pollution (Ledgard et al., 2020; Haq et al., 2026).

Despite these achievements, challenges persist in balancing productivity with environmental sustainability, particularly in intensive dairy farming systems.

3.4 Economic Impacts

CSA adoption has significant economic implications for farmers in both countries. In India, CSA practices contribute to increased crop yields, reduced input costs and improved income stability (Aryal et al., 2021; Ma and Rahut, 2024; Zhao et al., 2023). However, initial investment costs and risk aversion among farmers can limit adoption. Economic benefits are often realized in the long term, making policy support and financial incentives crucial.

In New Zealand, economic impacts are more pronounced due to high productivity levels, efficient resource utilization and strong market integration. CSA practices enhance export competitiveness while ensuring compliance with environmental regulations. The integration of technology reduces operational costs and increases profitability.

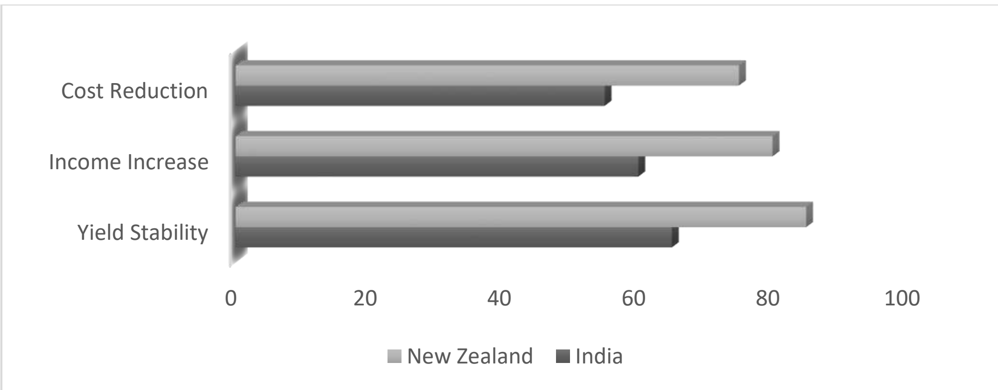

Fig 2: Comparative economic benefits of climate-smart agriculture practices, showing higher performance indicators in New Zealand relative to India.

3.5 Social Impacts and Livelihood Resilience

CSA plays a critical role in enhancing social resilience and food security. In India, CSA contributes to improved livelihood security for smallholder farmers, reduced vulnerability to climate shocks and enhanced food security (FAO et al., 2023; Roy et al., 2025). However, social inequalities, including gender disparities and unequal access to resources, remain significant challenges.

In New Zealand, social impacts are linked to improved farmer awareness and education, strong institutional support systems and community-based sustainability initiatives. The emphasis is less on survival and more on sustainable intensification and environmental stewardship.

3.6 Integrated Comparative Insights

The comparative evaluation reveals three key insights:

1. *Adaptation vs Mitigation Divide*
   India prioritizes adaptation due to high climate vulnerability, while New Zealand emphasizes mitigation aligned with global climate commitments (Lipper et al., 2020; Smith et al., 2020; Roy et al., 2025).
2. *Role of Technology and Institutions*
   Technological advancement and institutional capacity are critical drivers of CSA success. New Zealand's integrated systems outperform India's fragmented implementation (Reisinger et al., 2021).
3. *Scalability and Inclusivity Challenges*
   India's challenge lies in scaling CSA across millions of smallholders, whereas New Zealand must address emissions from intensive livestock systems.

3.7 Synthesis

The findings suggest that an integrated CSA framework combining India's resilience-focused strategies with New Zealand's mitigation-driven innovations can significantly enhance global agricultural sustainability. Strengthening policy coherence, improving access to technology, and promoting farmer participation are essential for scaling CSA effectively (Pretty and Bharucha, 2021; Rosenstock et al., 2021; Roy et al., 2025; Sharma and Singh, 2025).

Fig 3: Comparative framework of climate-smart agriculture (CSA) systems in India and New Zealand, illustrating the integration of adaptation-focused smallholder resilience in India and mitigation-driven technological innovations in New Zealand within the three core CSA pillars—productivity, adaptation, and mitigation.

IV. CHALLENGES

The implementation of climate-smart agriculture (CSA) in India and New Zealand is constrained by a range of socio-economic, technological, and institutional challenges, reflecting their distinct agricultural contexts.

4.1 Challenges in India

4.1.1 Structural and Socio-economic Constraints

Agriculture in India is dominated by small and marginal farmers, often operating on fragmented landholdings. This limits economies of scale and restricts the adoption of advanced CSA technologies (Birthal et al., 2021). Financial constraints, including limited access to credit and insurance, further hinder investment in climate-resilient practices (Aryal et al., 2021).

4.1.2 Knowledge and Institutional Gaps

A major barrier to CSA adoption is the lack of awareness and technical knowledge among farmers. Extension services remain underdeveloped, leading to inadequate dissemination of CSA practices (Rosenstock et al., 2021).

Additionally, policy implementation is often fragmented across multiple institutions, reducing overall effectiveness.

4.1.3 Technological Limitations

Access to modern technologies such as precision agriculture, climate forecasting tools, and digital advisory systems remains limited, particularly in rural areas. This digital divide restricts the scalability of CSA interventions (Ma and Rahut, 2024; Roy et al., 2025; Sharma and Singh, 2025).

4.1.4 Climate Vulnerability

India's high exposure to climate risks, including droughts, floods, and heatwaves, exacerbates agricultural uncertainty. These conditions necessitate continuous adaptation, making long-term planning challenging (Shirsath et al., 2020; Sharma and Singh, 2025).

4.2 Challenges in New Zealand

4.2.1 Livestock-Related Emissions

Agriculture in New Zealand is a significant source of greenhouse gas emissions, particularly methane from ruminant livestock. Reducing these emissions without compromising productivity remains a key challenge (Reisinger et al., 2021; Ledgard et al., 2020).

4.2.2 Trade-offs Between Productivity and Sustainability

Efforts to reduce environmental impacts may conflict with the goal of maintaining high agricultural output and export competitiveness. Balancing these competing objectives requires innovative solutions and policy support.

4.2.3 Policy and Market Pressures

Stringent environmental regulations and international market expectations place additional pressure on farmers to adopt sustainable practices. Compliance costs may be high, particularly for smaller farming enterprises.

4.2.4 Technological and Behavioral Barriers

While technological solutions are available, their adoption depends on farmer willingness, awareness, and cost considerations. Behavioral resistance to change can slow down the transition to low-emission farming systems (Tsoumas et al., 2022).

4.3 Cross-Cutting Challenges

Both India and New Zealand face common challenges, including:

- Uncertainty in climate projections
- Need for improved data and monitoring systems
- Integration of policies across sectors
- Ensuring equitable access to CSA technologies

Addressing these challenges requires coordinated policy efforts, technological innovation, and stakeholder engagement (Pretty and Bharucha, 2021; Roy et al., 2025).

V. FUTURE PROSPECTS

The future of climate-smart agriculture lies in integrating technological innovation, policy coherence, and inclusive development strategies. Both countries present unique opportunities for advancing CSA at national and global levels.

5.1 Technological Innovations

Emerging technologies such as artificial intelligence, remote sensing, and precision agriculture have the potential to revolutionize CSA. In New Zealand, these technologies are already being integrated into farming systems, enhancing efficiency and reducing environmental impacts (Ledgard et al., 2020).

In India, expanding access to digital agriculture platforms, mobile-based advisory services, and climate forecasting tools can significantly improve CSA adoption and effectiveness (Ma and Rahut, 2024; Roy et al., 2025).

5.2 Policy Integration and Institutional Strengthening

Future CSA strategies must focus on policy coherence and institutional coordination. Aligning agricultural, environmental, and climate policies can enhance implementation efficiency. Strengthening extension services and farmer training programs is particularly critical in India.

New Zealand can further refine its policies by integrating economic incentives with environmental goals, promoting sustainable intensification.

5.3 Climate Finance and Investment

Access to climate finance is essential for scaling CSA. In India, targeted subsidies, credit schemes, and insurance programs can support smallholder farmers in adopting climate-resilient practices (Aryal et al., 2021; Godwin, and Mwebaze.,2025).

International funding mechanisms and public-private partnerships can play a key role in promoting CSA globally.

5.4 Knowledge Sharing and International Collaboration

Collaboration between developed and developing countries can facilitate the exchange of knowledge, technologies, and best practices. Lessons from New Zealand's mitigation strategies can inform India's policies, while India's large-scale adaptation approaches can provide insights for other vulnerable regions. (Tsoumas et al., 2022).

5.5 Sustainable Intensification and Food Systems Transformation

CSA must evolve towards sustainable intensification, ensuring increased productivity without environmental degradation (Pretty and Bharucha, 2021; Roy et al., 2025; Zhao et al., 2023). This includes efficient resource use, reduced emissions and enhanced ecosystem services. Transforming food systems to be more resilient, inclusive, and sustainable is essential for achieving global climate and development goals (Godwin, and Mwebaze.,2025; Tsoumas et al., 2022).

VI. CONCLUSION

Climate-smart agriculture represents a comprehensive and adaptive framework for addressing the complex challenges posed by climate change to agricultural systems. This study provides a comparative analysis of CSA in India and New Zealand, highlighting significant differences in policy priorities, technological adoption, and impact outcomes.

The findings reveal that India's CSA approach is largely adaptation-oriented, focusing on enhancing resilience among smallholder farmers and ensuring food security under climate stress. In contrast, New Zealand emphasizes mitigation and technological innovation, driven by strong institutional frameworks and advanced research systems.

Despite these differences, both countries demonstrate the potential of CSA to improve agricultural sustainability, reduce environmental impacts, and enhance economic outcomes. However, challenges such as resource constraints, technological gaps, and policy fragmentation in India, and emission reduction pressures in New Zealand, highlight the need for targeted interventions.

A key contribution of this study is the identification of a hybrid CSA model, integrating:

- India's strengths in resilience and adaptation
- New Zealand's advancements in mitigation and technology

Such an integrated approach can significantly enhance global agricultural sustainability and climate resilience. Future efforts should focus on strengthening policy coherence, promoting technological innovation, and ensuring inclusive participation of farmers.

Ultimately, achieving the goals of climate-smart agriculture requires a multi-dimensional and collaborative approach, involving governments, researchers, private sector stakeholders, and farming communities. The insights from this comparative analysis provide a foundation for designing more effective CSA strategies that can contribute to sustainable food systems and climate change mitigation at a global scale.

VII. HIGHLIGHTS

- Comparative evaluation of climate-smart agriculture (CSA) systems in India and New Zealand
- India emphasizes adaptation and smallholder resilience
- New Zealand focuses on mitigation and technological innovation
- Institutional capacity and policy frameworks drive CSA adoption
- Cross-learning enhances global sustainability outcomes

DECLARATION REGARDING CONFLICT OF INTEREST

The author declares no conflict of interest. Disha Chahal conceptualized, analyzed the literature, and wrote the manuscript. The ethics approval is not applicable.

REFERENCES

[1] Aryal, J.P., Rahut, D.B., Maharjan, S., Erenstein, O. (2021). Adoption of climate-smart agricultural practices and their impacts on farm income: Evidence from South Asia. *Agricultural Economics* **52**: 651–665. https://doi.org/10.1111/agec.12645

[2] Birthal, P.S., Hazrana, J., Negi, D.S. (2021). Impacts of climate change on Indian agriculture: Evidence from panel data analysis. *Ecological Economics* **190**, 107187. https://doi.org/10.1016/j.ecolecon.2021.107187

[3] Bompotas, A., Koutras, K., Kalogeropoulos, N.R., Kechagias, P., Gariza, D, Kalogeras, A.P., and Alexakos, C. (2025). Smart farming integration platform for sustainable agriculture automation. *Agricultural Systems*. https://doi.org/10.1016/j.agsy.2025.103700

[4] Food and Agriculture Organization (FAO). (2021). *Climate-smart agriculture sourcebook*. FAO, Rome.

[5] Food and Agriculture Organization (FAO). (2023). International Fund for Agricultural Development (IFAD), UNICEF, World Food Programme (WFP), World Health Organization (WHO), 2023. *The State of Food Security and Nutrition in the World* **2023**. FAO, Rome. https://doi.org/10.4060/cc3017en

[6] Godwin, N., Mwebaze, J.(2025). IoT framework for climate-resilient and sustainable maize farming systems. *Computers and Electronics in Agriculture*. https://doi.org/10.1016/j.compag.2025.108500

[7] Haq, I., Rahman, M., Datta, T. (2026). Determinants of adoption of climate-smart agriculture practices in mushroom farming. *Scientific Reports*. https://doi.org/10.1038/s41598-026-39761-4

[8] Jat, M.L., Chakraborty, D., Ladha, J.K., Rana, D.S., Gathala, M.K., McDonald, A.J., Gerard, B. (2020). Conservation

agriculture for sustainable intensification in South Asia. *Field Crops Research* 248, 107658. https://doi.org/10.1016/j.fcr.2020.107658

[9] Kalisetti, V.S., Sudharshanam, U., Venkata, N.K.M. (2025). Smart agriculture: A climate-driven approach to modelling and forecasting crop pests using machine learning. *Frontiers in Plant Science*. https://doi.org/10.3389/fpls.2025.1636412

[10] Kumar, R., Singh, R., Sharma, P. (2024). Climate-smart agriculture: Insights, frameworks, and challenges for sustainable development. *Climate Smart Agriculture Journal* **1**, 100003. https://doi.org/10.1016/j.csag.2024.100003

[11] Ledgard, S.F., Lieffering, M., McDevitt, J., Boyes, M., Kemp, R. (2020). Mitigating greenhouse gas emissions from livestock systems in New Zealand. *Agriculture, Ecosystems & Environment* **292**, 106807. https://doi.org/10.1016/j.agee.2020.106807

[12] Lipper, L., McCarthy, N., Zilberman, D., Asfaw, S., Branca, G. (2020). Climate-smart agriculture: Building resilience to climate change. *Nature Climate Change* **10**, 1068–1072. https://doi.org/10.1038/s41558-020-00927-0

[13] Ma, W., Rahut, D.B. (2024). Climate-smart agriculture adoption and its impact on farm performance. *Mitigation and Adaptation Strategies for Global Change* **29**, 44. https://doi.org/10.1007/s11027-024-10139-z

[14] Maya, K., Raj, S., Kumar, A. (2025). Performance and conceptual structure of climate-smart agriculture research: A bibliometric analysis (2010–2023). *Frontiers in Sustainable Food Systems*. https://doi.org/10.3389/fsufs.2025.1499982

[15] Pretty, J., Bharucha, Z.P. (2021). Sustainable intensification in agricultural systems. *Annals of Botany* **128**, 157–168. https://doi.org/10.1093/aob/mcab091

[16] Reisinger, A., Clark, H., Cowie, A.L., Emmett-Booth, J., Gonzalez Fischer, C., Herrero, M., Howden, M., Leahy, S., Newton, P., Schulte, R.P.O. (2021). How necessary and feasible are reductions of methane emissions from livestock to support stringent temperature goals? *Environmental Research Letters* **16**, 024038. https://doi.org/10.1088/1748-9326/abd123

[17] Rosenstock, T.S., Lamanna, C., Chesterman, S., Hammond, J., Kadiyala, S., Lipper, L., Mann, W., McCarthy, N., Rufino, M.C., Richards, M.(2021). The scientific basis of climate-smart agriculture: A systematic review. *Agricultural Systems* **190**, 103098. https://doi.org/10.1016/j.agsy.2021.103098

[18] Roy, S., Hoque, A., Saikia, P., Padhiary, M. (2025). Climate-smart agriculture: AI-based solutions for enhancing crop resilience and reducing environmental impact. *Asian Research Journal of Agriculture* **18**: 291–310. https://doi.org/10.9734/arja/2025/v18i1665

[19] Sharma, A., Singh, V. (2025). Revitalizing agriculture through climate change mitigation: A systematic review of smart technologies and sustainable practices. *International Journal of Climate Change Strategies and Management* **17**, 483–501. https://doi.org/10.1108/IJCCSM-05-2024-0071

[20] Shirsath, P.B., Aggarwal, P.K., Thornton, P.K., Dunnett, A. (2020). Prioritizing climate-smart agricultural land use options at regional scale. *Climate Risk Management* **29**, 100239. https://doi.org/10.1016/j.crm.2020.100239

[21] Smith, P., Soussana, J.F., Angers, D., Schipper, L., Chenu, C., Rasse, D.P., Batjes, N.H., van Egmond, F., McNeill, S., Kuhnert, M. (2020). How to measure, report and verify soil carbon change to realize the potential of soil carbon sequestration. *Global Change Biology* **26**, 219–241. https://doi.org/10.1111/gcb.14815

[22] Thornton, P.K., Herrero, M. (2021). Climate change impacts on livestock systems and adaptation strategies. *Annual Review of Environment and Resources* **46**, 1–28. https://doi.org/10.1146/annurev-environ-012220-010314

[23] Tsoumas, I., Giannarakis, G., Sitokonstantinou, V. (2022). Evaluating digital tools for sustainable agriculture using causal inference. *Computers and Electronics in Agriculture*. https://doi.org/10.1016/j.compag.2022.107010

[24] Zhao, J., Liu, D., Huang, R. (2023). A review of climate-smart agriculture: Recent advancements, challenges, and future directions. *Sustainability* **15**, 3404. https://doi.org/10.3390/su15043404

International Journal of Environment, Agriculture and Biotechnology
Vol-11, Issue-2; Mar-Apr, 2026
Peer-Reviewed International Journal
Journal Home Page Available: https://ijeab.com/
Journal DOI: 10.22161/ijeab

Evaluation of nitrate-based chitosan nanofertilizer on the morpho-physiological responses of maize under semi-field condition

Ranjana Bai Yadav[1]*, Kinjal Mondal[1], Vinod Saharan[1], Devendra Jain[1], Priya Meena[1], Abhay Dashora[2], Subash Chandar Meena[3]

[1]Department of Molecular Biology and Biotechnology, MPUAT, Udaipur-313001 (Raj.), India
[2]Department of Genetics and Plant Breeding, MPUAT, Udaipur-313001 (Raj.), India
[3]Department of Soil science, MPUAT, Udaipur-313001 (Raj.), India
*Corresponding author: yadavranjana9057@gmail.com

Received: 25 Feb 2026; Received in revised form: 30 Mar 2026; Accepted: 03 Apr 2026; Available online: 11 Apr 2026

***Abstract*— *Global agriculture is frantically seeking for ways to mitigate the detrimental environmental effect of standard chemical fertilizers. Next-generation fertilizers made from biodegradable, eco-friendly, renewable energy sources may be the answer, allowing for greater nutrient efficiency and a lower environmental footprint. Chitosan nanoparticles (NPs) have recently been characterized as a viable way to improve plant immune systems through slow, controlled, and targeted nutrient delivery. Chitosan is a linear amino polysaccharide having a rigid structure, hydrophilic properties, and crystal structures. Chitosan, due to its amino group content, can combine with other chemicals, penetrate the plant's vascular system, and activate plant metabolic-physiological pathways. Surface-functionalization of chitosan with additional active compounds improves the bio-functionalities of the structure. In the current study, a nitrate-based chitosan nanofertilizer was formulated by ionic gelation, and its foliar efficacy on maize was comprehensively examined in a semi-field condition. The manufactured nanofertilizer, at 2% (w/v), had a substantial influence on root dynamics as compared to control groups. The current study strongly anticipates the potential of novel nitrate-based chitosan nanofertilizer to be a very valuable and novel bio-stimulant, as well as a good supply of macronutrients for agricultural plants. It may also be thoroughly researched for other crops in order to further develop the technique.*

***Keywords*— Chitosan, Surface-functionalization, ionic-gelation, bio-stimulant**

I. INTRODUCTION

Maize (Zea mays L.) is the third most important cereal for global food security after wheat and rice. Maize belongs to the family Poaceae and is believed to be originated from Mexico and Central America (**Nawaz *et al.*, 2020**). The word "maize" is thought to be derived from the ancient word "mahiz" and it was brought to India in 17th century (**Messias *et al.*, 2015**; **Tanumihardjo *et al.*, 2020**). Maize is monoecious plant with tassel, pistillate flowers on axillary shoots; ear shoot consists of a shank or cob, florets with long filamentous stigmas, silk. The total global production of maize in the year 2022 was 1163.9 million metric tonnes (MMT). For optimum maize production, loam, clay loam, sandy clay and pH 5.6 are considered as the best combination (**Pilevar *et al.*, 2020**; **Muhammad *et al.*, 2022**). To achieve higher production nutrient management is crucial at every developmental stage. An inadequate and imbalanced supply of nutrients to the crop results in yield diminution. In addition, the continuous practice of cultivating maize-wheat cropping sequence deterioration soil exhaustively; thus, it is difficult to sustain both grain quality and crop productivity. Therefore, it is necessary to provide balanced nutrition to the crop which may sustain soil fertility and lead to higher productivity. Eventually, in order to higher productivity, farmers are compelled to use an excess quantity of inefficient traditional fertilizers, which may lead to soil corrosion, deprivation of agroecosystems, deposition of excess chemicals, heavy metal accumulation, eutrophication, nitrate accumulation, global warming and increased resistivity in pathogens towards chemicals (**Subramanian *et al*., 2015**; **Singh *et al*., 2017**; **Sharma and Bhende, 2024**). Apart from them, only half of the applied supplements are taken up by plants; the rest is discharged into the environment as noxious vapor or harmful leachates, causing environmental nuisance (**Chouhan and Mandal, 2021**). The structure and functionality of conventional fertilizers and their applications are therefore needed to be redefined in order to maintain sustainable agricultural output without endangering the ecosystem. In this alarming scenario, nano-enabled next-generation fertilizers are anticipated as substitutes to, or even full alternatives for, traditional chemical fertilizers. Moreover, a smart delivery system of potential agrochemicals should be developed to allow immobilization, protection, and controlled release of active compounds (**Kumaraswamy *et al*., 2021**). In this scenario, nanobiotechnology can be a promising way for achieving a revolution in agriculture by providing agrochemicals according to crop demand. Nanotechnology has many applications in all stages of production, processing, storing, packaging and transport of agricultural products and other marketing facilities (**Kumaraswamy *et al*., 2019**). Despite of having various benefits, accumulation of metal-based NMs in plants and subsequent possible deposition in food and soil can pose a great threat to human health. The possible interaction of metallic NMs with soil irreversibly impact on chemical-biological and physical structure of soil (**Simonin and Richaume, 2015**). In the current scenario, biopolymer-based nanofertilizers have currently been reported as promising alternatives of commercially available chemical fertilizers due to its biodegradable nature and potential to maintain food security throughout the globe. Biogenic materials can be explored as matrices for nutrient supply to plants with inbuilt character of slow/control release (**Prajapati *et al*., 2022**). Keeping all this in mind there are several delivery systems were developed by scientist such as flexible biopolymer capable of forming films, hydrogels, scaffolds, fibers, microspheres, and nanoparticles; used as a good delivery system for the controlled release of active compounds (**Rani *et al*., 2024**). The first report on chitin traces back to 1811 by French Professor of natural history Henri Braconnot. He found out the alkaline-insoluble fraction from mushrooms and named it "fungine" (**Haghighi *et al*., 2020**).

Chitosan, a seaweed product, is biodegradable, biocompatible, and ecologically benign, making it a viable alternative to standard chemical fertilizers (**Prajapati *et al*., 2022**). It has several biological activities, including antifungal, antibacterial, antiviral, and plant growth regulator (**Saharan and Pal, 2016**). Furthermore, chitosan is known to enhance plant defence responses (**Kumaraswamy *et al*., 2018**). Although chitosan is a biopolymer with high added value, and its properties are related to its molecular weight. Thus, high molecular weight values provide low solubility of chitosan, presenting limitation in its use. Based on this, several studies have developed for different hydrolysis methods to reduce the molecular weight of chitosan and also to enhance its activity. There is a great deal of potential to increase agricultural productivity. When chitosan is factionalized with additional compounds having potential relevance in agriculture.

Maize production is critical for global food and nutritional security, with its versatile uses making it a vital component of the agri-food system. Maize production heavily relies on adequate nutrient management, with nitrogen, phosphorus, and potassium being the most critical nutrients. Among the essential nutrients, nitrogen (N) is the most vital nutrient element, performing as a component of many organic compounds viz., proteins, amino acids, nucleic acids and nucleotides, enzymes, vitamins, hormones, alkaloids etc. Empirically, a ton of grain maize requires almost 9-11 kg of N (**Kumar *et al*., 2021**). Potassium (K) fertilization on the other hand plays a significant role in enhancing the yield, water use efficiency and nutrient utilization proficiency in maize. K has vital role in photosynthesis, water storage control and stomata opening in leaves (**Kandil *et al*., 2020**). Application of KNO_3, have differential response in terms of growth and development of a crop. The cob girth increased progressively with the foliar applications of either water or KNO_3, during drought, stressed plants uptake more K to regulate the internal mechanisms and ameliorate water deficiency. The use of K as a compatible solute can osmo-regulate the cellular environments in water stress conditions. The effects of K deficiency stress on root morphology and function are not significant, but nevertheless observable (**Lacerda *et al*., 2018**).

II. MATERIALS & METHODS

2.1 Synthesis and characterization

In the current study, we used the ionic-gelation approach to develop the nitrate-based chitosan nanofertilizer and evaluated its foliar efficacy on the morpho-physiological responses of maize. Initially, 1% (w/v) chitosan was dissolved in 0.5% (v/v) acetic acid *via* electrospinning at 320 rpm until clear, homogenous solutions were obtained, followed by cross-linking with

0.5% TPP (Sodium tripolyphosphate) solution (w/v). Following that, surface functionalization of chitosan was achieved by manually introducing a potassium-nitrate (0.2g/100 ml) to the chitosan-TPP complex. At the end of the process, 5% surfactant (NP 40) was added drop-by-drop to obtain a stable formulation that was suitable for characterization.

The structural characteristics and stability parameters of the newly synthesized nanostructure were studied and confirmed using dynamic light scattering (DLS), viscosity, and TEM (Transmission Electron Microscopy) analysis. The Z-average size (hydrodynamic size) of the component particles, poly dispersive index (PDI), and zeta potential were determined using a Zetasizer (ZS90, Malvern) at a constant temperature of 30°C and a scattering angle of 90° during the DLS investigation. Viscosity of the formulation was tested at 30°C in a rotating viscometer (ViscoQC 100, Anton Paar) using an L1 spindle at 100 rpm. TEM was performed in accordance with the standard protocol (Ottaviani *et al.*, 2000) to better understand the structural features and morphology of the components in the sample under consideration.

2.2 Experimental design and treatment details

The current study was carried out under the supervision of Department of Molecular Biology and Biotechnology, Rajasthan College of Agriculture (RCA), Maharana Pratap University of Agriculture and Technology (MPUAT), Udaipur. The seeds of maize cultivar PHM-3 were procured from the Department of Soil Science and Agriculture Chemistry, RCA, MPUAT, Udaipur. A pot experiment was carried out in a cage-house, where pots were arranged in CRD (Completely Randomized Design) way with three replications. Each pot contained the same amount of soil and recommended dose of fertilizer for maize growth. A total of 6 treatments were considered under the study (**Table 1**) and in each pot, 5 healthy seeds were sown and watered regularly.

Table 1 Experimental outline

Treatments, replication	6, 3
Experimental design	CRD
T1	Control (water)
T2	KNO_3 (2%)
T3	Nitrate-CS NF* (2%)
T4	Nitrate-CS NF (1%)
T5	Nitrate-CS NF (2%)
T6	Nitrate-CS NF (3%)
Mode of experiment	In pots
Pot size, number of seed per plot	25cm x 25cm, 05
Plant protection	As per recommendation
Stage of application	1st foliar at 25 DAS, 2nd foliar at 55 DAS

*Surfactant free

2.3 Foliar application

The maize cultivar PHM-3 seeds underwent the treatment outlined in **Table 1** and were subsequently planted in plastic pots, with five seeds per pot, filled with soil collected from a maize field. Foliar application of nanofertilizer was performed with three different concentrations (1, 2 and 3% v/v) along with 2% KNO_3 and water as control. One treatment of 2% nanofertilizer was also performed without surfactant. 1st foliar was performed at 25 DAS and 2nd at 55 DAS. Growth parameters including shoot length (cm), root length (cm), pre-embryonic root number, lateral root number, stem diameter (cm), leaf area (cm^2) was recorded at the stage of physiological maturity.

2.4 Statistical analysis

Statistical analysis was conducted utilizing JMP software, specifically version 12, to rigorously analyse the data. A significance level of $P=0.05$ was employed to ascertain significant differences among the various treatment groups. It is important to note that all experiments were carried out with a minimum of three replicates, and each experiment was conducted three times for robustness and reliability. This approach ensured the consistency and credibility of the experimental results.

III. RESULTS AND DISCUSSION

This study was undertaken to synthesize, characterize and investigate the impact of foliar nitrate-based chitosan nanofertilizer on morpho-physiological characteristics of maize (*Zea mays* L.) under the semi-field condition (in pots). First of all, nitrate-based chitosan nanofertilizer was prepared with the concept of ionic-gelation (**Choudhary *et al.*, 2019**). Initially, a constructive chemical interaction among the positively charged amino groups ($-NH_2$) of chitosan and negatively charged sodium tripolyphosphate (TPP) yielded a nano-matrix (milky white in colour), in which potassium nitrate solution (0.2g in 100ml) was plunged to obtain a stable nano-formulation. Next, 5% surfactant (NP 40) was mixed to the solution very carefully to make it stable. Afterwards, the newly synthesized nano-formulation was characterized and employed for subsequent applications in maize, aligning with the research objectives and experimental design.

DLS analysis of the synthesized nitrate-based chitosan nanofertilizer revealed an average hydrodynamic diameter (Z-average) of 303.5 nm with a polydispersity index (PDI) of 0.248 (**Figure 1a**) and zeta potential of +22.3 mV (**Figure 1b**). The obtained particle size confirms the formation of nanoparticles within the acceptable nano-range for chitosan-based delivery systems. The relatively low PDI value (<0.3) indicates narrow and uniform particle size distribution, suggesting controlled nanoparticle formation through ionic gelation. The positive zeta potential is attributed to the protonated amino groups ($-NH_3^+$) of chitosan, which contribute to moderate colloidal stability of the formulation. Furthermore, the number distribution data indicated that the majority of nanoparticles were present in the size range of 50–70 nm, with the highest population observed at 58.77 nm (25.8%) (**Figure 1c**). Structural morphology of nitrate-based chitosan nanofertilizer was studied by Transmission Electron Microscopy (TEM), which revealed the synthesized formulation under investigation containing discrete spherical aggregates, typically falling within the size range of 40 to 80 nm (**Figure 2**). The presence of uniformly distributed nanoparticles with positive surface charge suggests improved interaction with plant surfaces and enhanced nitrate delivery efficiency in maize. Viscosity analysis indicated that the encapsulation of potassium nitrate with in chitosan matrix influenced flow properties of the synthesized nitrate-based chitosan nanofertilizer. The formulation exhibited a low viscosity value of 7.4 cP, which is suitable for agricultural spray applications and may facilitate better interaction with plant surfaces. The particles appeared as dark, discrete nanostructures forming moderate aggregates of 40-80 nm. Such aggregation may result from intermolecular hydrogen bonding and electrostatic interactions during sample preparation. The nanoscale morphology supports successful formation of nitrate-based chitosan nanofertilizer through ionic gelation.

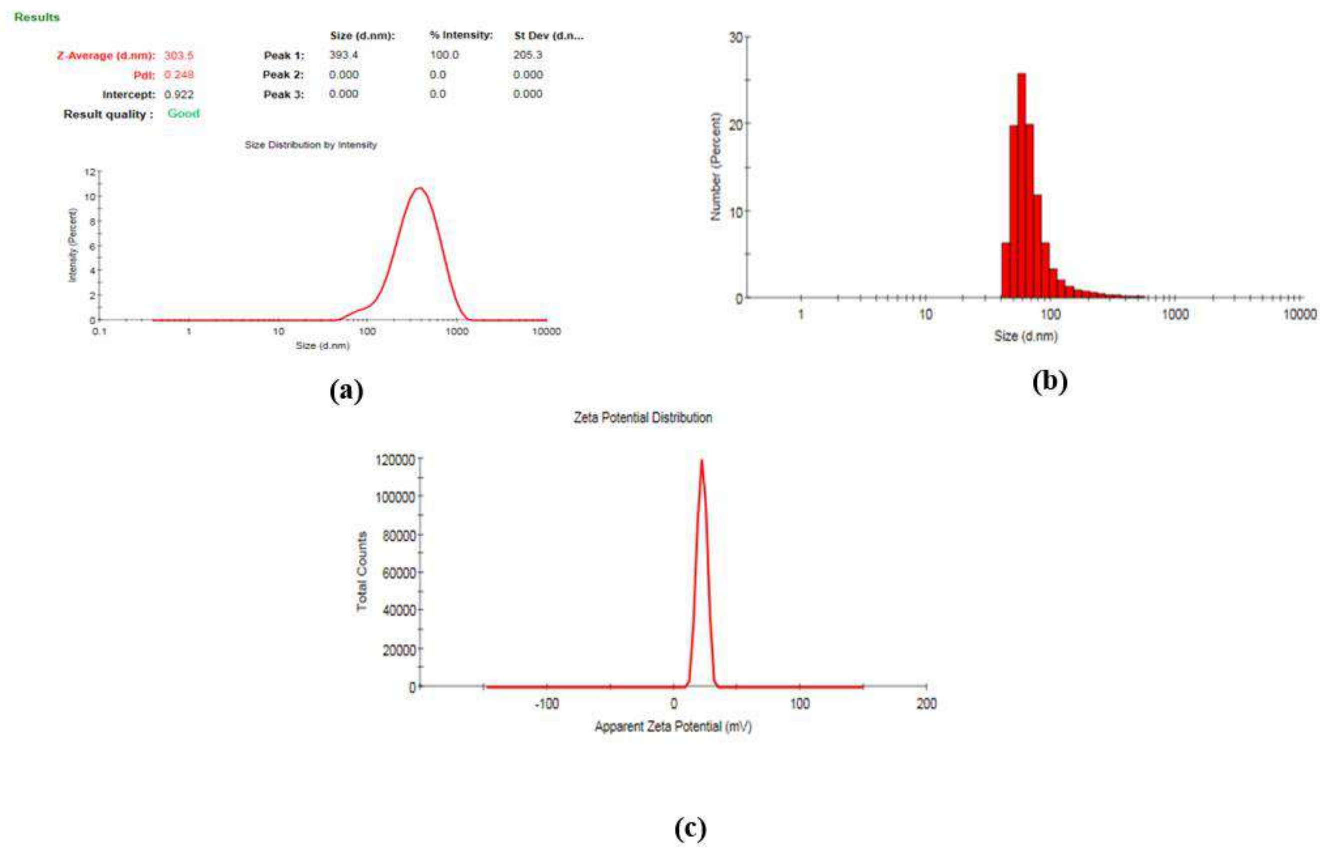

Fig.1 DLS analysis of nitrate-based chitosan nanofertilizer (a) Z-average and size distribution by intensity (b) number distribution by per cent (c) Zeta potential

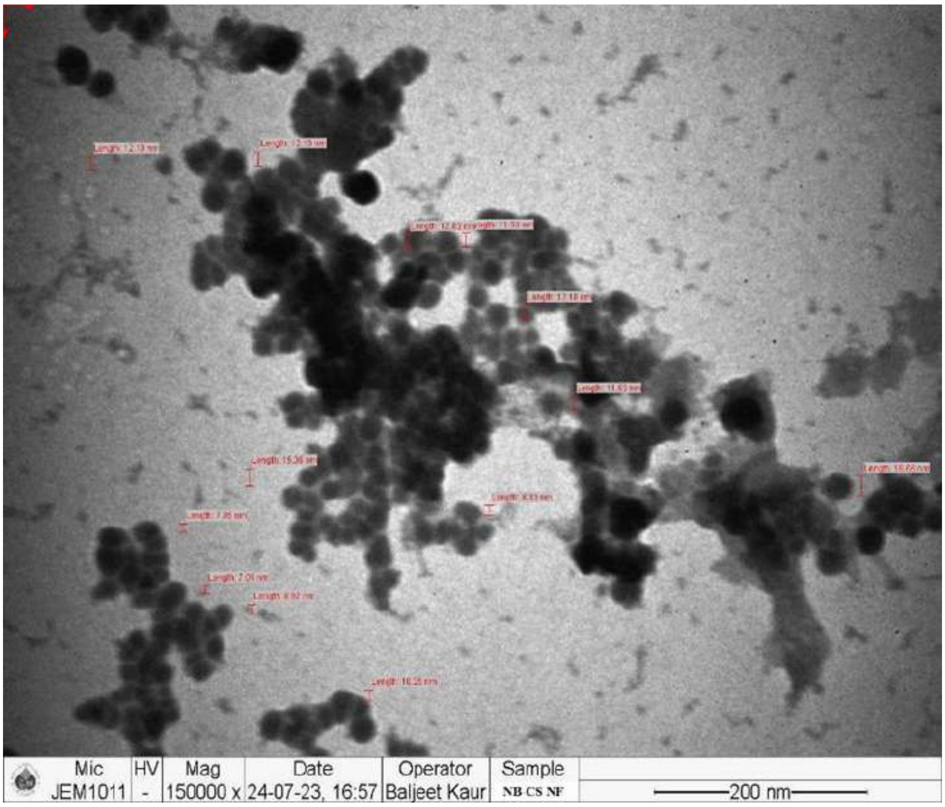

Fig.2 TEM micrograph of nitrate-based chitosan nanofertilizer at 150Kx magnification

Table 2 Morphological responses of maize towards nitrate-based chitosan nanofertilizer

Treatments	Shoot length (cm)	Root length (cm)	Pre-embryonic root number	Lateral root number	Stem diameter (cm)	Leaf area (cm^2)
Control (Water)	75.00 ± 1.73^{c}	16.00 ± 1.53^{b}	19.00 ± 1.53^{a}	222.67 ± 4.85^{d}	2.610 ± 0.14^{a}	85.06 ± 2.61^{b}
KNO_3 (2%)	78.67 ± 2.96^{bc}	19.67 ± 0.88^{a}	19.00 ± 0.58^{a}	327.33 ± 7.42^{ab}	2.92 ± 0.32^{a}	104.52 ± 1.10^{a}
Nitrate-based chitosan nanofertilizer						
2%*	87.67 ± 2.60^{ab}	20.33 ± 1.20^{ab}	20.67 ± 1.76^{a}	322.33 ± 4.81^{b}	2.70 ± 0.13^{a}	97.82 ± 4.11^{ab}
1%	87.33 ± 1.45^{ab}	16.67 ± 0.88^{ab}	18.33 ± 0.67^{a}	311.67 ± 3.76^{b}	2.60 ± 0.13^{a}	95.58 ± 3.53^{ab}
2%	89.67 ± 1.20^{a}	23.33 ± 1.20^{a}	22.00 ± 2.31^{a}	361.00 ± 10.97^{a}	3.29 ± 0.17^{a}	106.49 ± 1.94^{a}
3%	83.33 ± 2.33^{abc}	20.00 ± 1.54^{ab}	20.00 ± 2.64^{a}	261.00 ± 9.54^{c}	2.72 ± 0.11^{a}	93.38 ± 3.05^{ab}

*Surfactant-free

Various growth parameters were recorded at physiological maturity of the plants. Each value is the mean of triplicate with 5 plants in each replication. Mean ± SE values not connected by same letter are significantly different at *p=0.05* as determined by Turkey-Karmer HSD.

The combined characterization results collectively validate the successful synthesis of a stable, nitrate-based chitosan nanofertilizer system with desirable physicochemical properties. In the current study, impact of nitrate-based chitosan nanofertilizer has been comprehensively explored in terms of growth and root dynamics in maize at a semi-field condition. Foliar application of nitrate-based chitosan nanofertilizer at a lower dose (2%) significantly increased root length, pre-embryonic root number and lateral root number as compared to KNO_3 (2%) and control (water). But in contrary, shoot length, stem diameter and leaf area have not been significantly influenced. Higher dose (3%) of crafted material negatively impacted the root system (root length, pre-embryonic root number and lateral root number), indicating the plant's sensibility of critical limit to respond towards the foliar feeding of nitrate-based chitosan nanofertilizer (**Table 2**).

These findings collectively suggest that the foliar application of nitrate-based chitosan nanofertilizer (2%) attributed an impactful nutrition to the plant, resulting in better maize growth and development. Moreover, chitosan as nanocarrier is thought to play significant role in delivering the active ingredients into the plant cells as the promising affinity of natural chitin and/or chitosan receptors on the plant surfaces towards chitosan nanomaterials persuades (Parodi *et al*., 2015). Altogether, the fine-tuned physicochemical properties and availability of nitrogen and intrinsic bioactivity of chitosan in nitrate-based chitosan nanofertilizer, have contributed to enhance biochemical and physiological responses of maize plant. We recommend the formulation to evaluate its potential in other crops in field condition.

IV. CONCLUSION

Together, these thorough results highlight the many facets of the research, from material characterisation to real-world uses in enhancing plant health and development. With foliar application of nitrate-based chitosan nanofertilizer, maize crop growth and yield are increased, which is explained by its special physiochemical properties: larger surface area, higher number of nanoparticles, and lower PDI value with low viscosity. Compared to potassium nitrate (2% w/v) and water, foliar application of nitrate-based chitosan nanofertilizer at an optimal dose (2% w/v) significantly increased shoot length, root length, pre-embryonic root number, lateral root number, and leaf area. According to the study, laboratory-synthesized nitrate-based chitosan nanofertilizer can be a highly beneficial and innovative bio-stimulant, as well as a good source of macronutrients for agricultural plants, and should be investigated on a large scale for various crops to further mature the technology.

REFERENCES

[1] Choudhary, R. C., Kumari, S., Kumaraswamy, R. V., Sharma, G., Kumar, A., Budhwar, S., & Saharan, V. (2019). Chitosan nanomaterials for smart delivery of bioactive compounds in agriculture. *In Nanoscale Engineering in Agricultural Management* (pp. 124-139). CRC Press.

[2] Chouhan, D. and Mandal, P. (2021). Applications of chitosan and chitosan based metallic nanoparticles in agrosciences-A review. *International Journal of Biological Macromolecules*, 166:1554-1569

[3] Haghighi, H., Licciardello, F., Fava, P., Siesler, H. W. and Pulvirenti, A. 2020. Recent advances on chitosan-based films for sustainable food packaging applications. *Food Packaging and Shelf Life*, 26: 100551

[4] Kandil, E. E., Abdelsalam, N. R., Mansour, M. A., Ali, H. M and Siddiqui, M. H. 2020 Potentials of organic manure and potassium forms on maize (*Zea mays* L.) growth and production. *Scientific Reports*, 10(1): 8752

[5] Kumar, A. K., Kumar, Y., Savitha, A. S., kumar, M. Y. A., Narayanaswamy, C., Raliya, R., Krupashankar, M. R. and Bhat, S. N. 2021. Effect of IFFCO nanofertilizer on growth, grain yield and managing turcicum leaf blight disease in maize. *International Journal of Plant and Soil Science*, 33(16): 19-20

[6] Kumaraswamy, R. V., Kumari, S., Choudhary, R. C., Pal, A., Raliya, R., Biswas, P. and Saharan, V. 2018. Engineered chitosan-based nanomaterials: Bioactivities, mechanisms and perspectives in plant protection and growth. *International Journal of Biological Macromolecules*, 113: 494-506

[7] Kumaraswamy, R. V., Kumari, S., Choudhary, R. C., Sharma, S. S., Pal, A., Raliya, R. and Saharan, V. 2019. Salicylic acid functionalized chitosan nanoparticle: a sustainable biostimulant for plant. *International Journal of Biological Macromolecules*, 123: 59 69

[8] Kumaraswamy, R. V., Saharan, V., Kumari, S., Choudhary, R. C., Pal, A., Sharma, S. S. and Biswas, P. 2021. Chitosan-silicon nanofertilizer to enhance plant growth and yield in maize (Zea mays L.). *Plant Physiology and Biochemistry*, 159: 53-66

[9] Lacerda, C.F.D., Ferreira, J.F.D.S., Suarez, D.L., Freitas, E.D., Liu, X. and Ribeiro, A.D.A., 2018. Evidence of nitrogen and potassium losses in soil columns cultivated with maize under salt stress. *Revista Brasileira de Engenharia Agrícola e Ambiental*, 22 pp.553 557

[10] Messias, R. D. S., Galli, V., Silva, S. D. D. A. E., Schirmer, M. A. and Rombaldi, C. V. 2015. Micronutrient and functional compounds biofortification of maize grains. *Critical Reviews in Food Science and Nutrition*, 55(1): 123-139

[11] Muhammad, I., Lv, J. Z., Yang, L., Ahmad, S., Farooq, S., Zeeshan, M. and Zhou, X. B. 2022. Low irrigation water minimizes the nitrate nitrogen losses without compromising the soil fertility, enzymatic activities and maize growth. *BioMed Central (BMC) Plant Biology*, 22(1): 159

[12] Nawaz, H., Hussain, N., Jamil, M., Yasmeen, A., Bukhari, A., Auringzaib, M., & Usman, M. (2020). Seed biopriming mitigates terminal drought stress at reproductive stage of maize by enhancing gas exchange attributes and nutrient uptake. *Turkish Journal of Agriculture and Forestry*, 44(3), 250-261.

[13] Ottaviani, M.F., Favuzza, P., Bigazzi, M., Turro, N.J., Jockusch, S. and Tomalia, D.A. 2000. A TEM and EPR investigation of the competitive binding of uranyl ions to starburst dendrimers and liposomes: Potential use of dendrimers as uranyl ion sponges. *Langmuir*, 16(19): 7368-7372

[14] Parodi, A., Corbo, C., Cevenini, A., Molinaro, R., Palomba, R., Pandolfi, L., Agostini, M., Salvatore, F. and Tasciotti, E. 2015. Enabling cytoplasmic delivery and organelle targeting by surface modification of nanocarriers. *Nanomedicine*, 10(12): 1923-1940

[15] Pilevar, A. R., Matinfar, H. R., Sohrabi, A. and Sarmadian, F. 2020. Integrated fuzzy, AHP and GIS techniques for land suitability assessment in semi-arid regions for wheat and maize farming. *Ecological Indicators*, 110: 105887

[16] Prajapati, D., Pal, A., Dimkpa, C., Singh, U., Devi, K.A., Choudhary, J.L. and Saharan, V., 2022. Chitosan nanomaterials: A prelim of next-generation fertilizers; existing and future prospects. *Carbohydrate Polymers*, 288: p.119356.

[17] Rani, S., Dahiya, R., Kumar, V., Berwal, P., Sihag, S., & Jatrana, A. (2024). Development of Novel Zeolite-Based Controlled-Release Zinc Fertilizers: Synthesis, Characterization, and Release Kinetics. *ACS Agricultural Science & Technology*, 4(6), 664-672.

[18] Saharan, V. and Pal, A., 2016. Chitosan based nanomaterials in plant growth and protection pp (33-41). New Delhi, India: Springer

[19] Sharma, S., & Bhende, M. (2024). An overview: non-toxic and eco-friendly polysaccharides—its classification, properties, and diverse applications. *Polymer Bulletin*, 81(14), 12383-12429.

[20] Simonin, M. and Richaume, A. 2015. Impact of engineered nanoparticles on the activity, abundance, and diversity of soil microbial communities: a review. *Environmental Science and Pollution Research*, 22: 13710-13723

[21] Singh, H., Singh, M. and Kang, J. S. 2017. Effect of potassium nitrate on yield and yield attributes of spring maize (Zea mays L.) under different dates of planting. *International Journal Current Microbiology Applied Science*, 6: 1581-1590

[22] Subramanian, K.S., Manikandan, A., Thirunavukkarasu, M. and Rahale, C.S. (2015). Nano-fertilizer for balanced crop nutrition. *Nanotechnologies in Food and Agriculture*,69-80

[23] Tanumihardjo, S. A., McCulley, L., Roh, R., Lopez-Ridaura, S., Palacios-Rojas, N. and Gunaratna, N. S. 2020. Maize agro-food systems to ensure food and nutrition security in reference to the Sustainable Development Goals. *Global Food Security*, 25: 100327

International Journal of Environment, Agriculture and Biotechnology
Vol-11, Issue-2; Mar-Apr, 2026
Peer-Reviewed International Journal
Journal Home Page Available: https://ijeab.com/
Journal DOI: 10.22161/ijeab

Analysis of Medicinal Compounds in Rice at Mekong Detal Vietnam

Nguyen Thi Lang, Le Nguyen Thanh Ngoc, Nguyen Trong Phuoc, Bui Chi Buu

High Agricultural Technology Research Institute (HATRI), Vietnam
Web: hatri.org

Received: 12 Mar 2026; Received in revised form: 10 Apr 2026; Accepted: 15 Apr 2026; Available online: 25 Apr 2026

Abstract*— This study aimed to quantify flavonoids and polyphenols among 10 different rice varieties, from white to brown rice, and to describe the gene expression profiles related to biosynthesis.The study analyzed the phenolic content (TPC), flavonoid content (TFC), and total anthocyanin content (TAC) of 10 rice varieties in HATRI . Results showed:The TPC of brown rice and white rice of different varieties differed significantly ($p < 0.05$). The measured TPC in brown rice was significantly higher (118.98-206.06%) than in white rice. The highest TPC (Total Flavouring Content) of brown rice was found in Black Rice (771,15 mg/100 g).The TFC of brown rice and white rice from different varieties differed significantly. The TFC of brown rice ranged from 178.74–526.65mg/100 g, while white rice ranged from 85.41–432.15 mg/100 g: brown rice had a 10%–20% higher total flavonoid content than white rice. Among these, the difference between brown rice and white rice from the OM5451 and HATRI 722 varieties was smaller. The content of free and binding anthocyanins in the rice fraction of ten different genotypes of rice with brown rice and white rice ranged from 15.32 to 183.05 and 6.18 to24.16 mg of Cy3-GE/100 g DM, respectively. The highest anthocyanin concentrations were found in free form. Black rice (HATRI 40) showed the highest anthocyanin content (234.62 mg Cy3-GE/100 g DM), followed by HATRI 11 variety (73.88 mg Cy3-GE/100 g DM) and white rice (50.42 mg Cy3-GE/100 g DM). Our studies have enriched the active compounds of rice and laid a solid foundation for improving the active compounds for functional food rice in Vietnam.

***Keywords*— phenolic compounds (TPC), flavonoid content (TFC) and anthocyanin content (TAC), rice**

I. INTRODUCTION

Rice is a staple food for more than half of the global population. The majority of rice consumers are observed to suffer from problems such as malnutrition, Fe and Zn deficiency, and health problems related to oxidative stress such as stroke, psoriasis, type II diabetes, heart disease, obesity, cancer, dermatitis, and rheumatoid arthritis (Shridhar, and et al.,2015). Antioxidants protect cells against free radicals, which can cause disease in humans. Since much of the global population depends on rice, grain enrichment with Fe, Zn, and antioxidant compounds are priority areas of rice research (Kuma et al.,2020; Zhu et al.,2018). Consuming antioxidant-rich rice is a better and cheaper option to combat stress-related disorders and gain other health benefits (Zhu et al.,2018). Enhancing the nutritional value of the antioxidant compounds in rice, is the best and cheapest way to achieve health.

There is growing interest in identifying new natural sources of potential compounds in food and medicinal chemistry. Rice contains special bioactive compounds, such as ferulic acid and hydroxycinnamic acid, which have attracted increasing attention from scientists and consumers alike (Alvese et al.,2016). These phenolic compounds have antioxidant and anti-inflammatory properties. They are correlated with a reduced risk of various chronic diseases, including heart disease, and a reduction in type 2 diabetes symptoms (Liu et al.,2015). These highly bioactive compounds are distributed mainly in the bran layer (Verardo et al.,2016). Therefore, the uneven distribution of bioactive compounds can affect functional characteristics in rice (Shen et al.,2009).

Polyphenols are are good in phytochemicals , which have wide uses. Phenolic compounds are common secondary metabolites in rice plant growth, and they are useful in pollination, seed diffusion, and disease and pest prevention (Cheynier, 2012). Plant phenols include monophenols, diphenyl phenols and polyphenols. Plant polyphenols are beneficial to human health, accounting for a relatively high percentage in phenolic substances. Plant polyphenols are phenylpropanoid derivatives, including flavonoids, phenolic acids, stilbenes and curcumin (Quideau et al., 2011). These compounds display many biological activities such as antioxidant, antibacterial, anti-inflammatory, anti-tumor and antiviral effects (Maleki et al., 2019), possessing great application potential in the medicine, foods, cosmetics and chemicals (Yahfoufi et al., 2018; Fraga et al., 2019).

Binding phenolic compounds, such as ferulic, coumaric and caffeic acids, can be hydrolyzed in the large intestine by intestinal enzymes, freeing them from binding macromolecules (Pang et al .,2018; Ge et al.,2021). Phenolic compounds are synthesized in plant cells, and are often referred to as functional components as hydrogen atoms on aromatic rings with hydroxyl (Alu'datt et al., 2017). Their antioxidant capacity is important in minimizing the negative effects of oxidative stress, which has been linked to the pathogenesis of many diseases (Ma et al., 2019). These substances can generally be divided into two main groups, flavonoids (flavanols, flavonols, anthocyanins) and non-flavonoids (phenolic acids, stilbenes, tannins and their derivatives) (Zhang and Tsao, 2016; Alu'datt et al., 2017). On this point, the nutritional and bioactive values of phenolic compounds have been confirmed from several crops, medicinal plants and rice plants (Neri-Numa et al., 2020; de Araújo et al, 2021).

Antioxidants are present in plants both in the form of enzymes and non-enzymes. Enzymatic antioxidants are catalase, peroxidase, superoxide dismutase, glutathione and other proteins and non-enzymatic antioxidants including phenolic protective compounds (vitamin E, flavonoids, phenolic acids and others); Nitrogenous compounds (alkaloids, amino acids and amines), carotenoids and chlorophyll derivatives (Govindaraj et al.,2017). Enzymatic antioxidants protect plant cells from damage caused by reactive oxygen species and act as a defense system to maintain cellular structural and functional integrity by inhibiting oxidative degradation to macromolecules such as lipids, proteins and nucleic acids (Rossatto et al.,2017). Therefore, improving these characteristics in rice will lead to the development of better quality rice. Non-enzymatic antioxidants such as phenolic acids, flavonoids, anthocyanins and proanthocyanidins, tocopherols and tocotrienols (vitamin E), andγ-oryzanol have been reported...

The antioxidant activity of rice plants is promoted by various phytochemicals in experiments (Gong,et al.,2017). Polyphenols are the main antioxidants in rice, while other bioactive compounds, such as phytosterols, also have antioxidant properties (Ragaee et al.,2013). These bioactive antioxidants act as a preventive and protective mechanism against chronic diseases caused by oxidative damage caused by excessive free radical production in living organisms (Podio et al.,2017). There are many methods for measuring the antioxidant activity of these substances in vitro, such as DPPH, ABTS, PSC, and ORAC, based on different antioxidant mechanisms (Desta et al.,2022).

Understanding the genetic basis of these complex antioxidant traits and identifying key QTLs is essential to improving these phytochemicals through molecular breeding to improve the growing nutritional issues of rice-fed populations and seed quality. The identification of QTLs/genes for higher carotenoid content and the development of functional markers is slow in rice because reports of carotenoids are not available in rice (Zhai et al.,2016). Widespread genetic variation for carotenoid content exists in rice. White rice accumulates very small amounts of carotenoids (Ashraf et al.,2017).

The pigments that provide color, anthocyanidins and proanthocyanidins, are present in the pericardium and aleurone of rice grains. Eleven QTLs such as qTAC1.1 and qTAC5.1 controlling anthocyanin content, qSOD1.1, qSOD5.1 and qSOD10.1 for superoxide dismutase (SOD), qTFC6.1, qTFC11.1 and qTFC12.1 for total flavonoid content (TFC), qOZ8.1 and qOZ11.1 for γ-oryzanol (OZ) and qAC11.1 for ABTS activity were discovered as novel locus. The chromosome position on 11 at 45.3 cM modulates GO, TFC, and anthocyanin content (TAC), and on chromosome 12 at 101.8 cM controls TAC and ABTS activity, respectively, were found to be antioxidant hotspots. (Bastia et al.,2022)

This study to quantify flavonoids and polyphenols between 10 different rice varieties from white and brown rice, describes gene expression profiles associated with biosynthesis. Polyphenols and flavonoids and the mechanism of rice growth and development from the limited description of previous works. Our studies have enriched the active compounds of rice and laid a solid foundation to improve the active compounds for the type of rice served as functional foods for Vietnam.

II. METHODS AND MATERIALS

Ten rice varieties grown at HATRI (High Agricultural Technology Research Institute) (table 1). After harvesting, seeds are dried to 13 ± 1% moisture at temperatures below 40°C. All rice samples are peeled and polished by rice peeling machine and rice milling machine, set to 8% milling level, to obtain ground rice bran. To separate the grains from the rice bran, they are sieved through a sieve of 180 µm (80 mesh).

Table 1 . 10 lines varieties at High Agricultural Technology Research Institute for Mekong delta(HATRI)

Lines	Crossing	Traits	Bwown rice	White rice
HATRI11	jinmibyeo/Dular//5*jinmi byeo	Red color , Tolerance for drought	84.71	6.28
HATRI 144	OM 1490/ *Pi 40*	Tolerance for salt	82.45	76.57
HATRI 200	Kuming/SP6	Aroma , Japonica , salinity tolerance	85.42	76.98
HATRI 20	OM4900/Pokkali	Aroma , salt tolerance	83.63	75.47
OM5451		Popular at MEKong	81.15	74.62
HATRI722	Jasmine 85/ PCR 4	Aroma	84.42	73.65
OM4900	C53/Jasmine 85	Submergence, salinity and drought	86.42	74.68
HUYẾT RỒNG	landrace	Can Tho Landace	88.96	7.52
HATRI 40	Thai lan/ Dular	Black color	88.56	0
IR64	IRRI	Good genes	82.42	76.25

Extraction of free phenolics and favonoids

Extraction of free phenolics and favonoids 10 rice (0.5 g) were treated with 50 mL of acidifed methanol solution (95% methanol: 1 M HCl 85:15, v/v). The mixture was homogenised using homogenizer for 5 min in an ice bath. Solutions were centrifuged at 2500g for 10 min and supernatants were removed. Te fltered supernatants were concentrated by evaporation at 45 °C using hot plate. The concentrated fltrate was then diluted with 10 mL of acidifed methanol and stored until analysis. Extraction of bound phenolics and favonoids The residue obtained from the free phenolics extraction was hydrolyzed with NaOH (40 mL, 2 M) at room temperature for 1 h with continuous shaking. Hexanes (10 mL) were used to extract lipids. The hydrolysate was then neutralised with 10 mL of 2 M HCL. Solution was transferred to separation funnel and was then extracted fve times with ethyl acetate. Ethyl acetate layer (supernatants) were pooled and evaporated using hot plate (at 45 °C). Residue was dissolved in distilled water (10 mL) and then stored until analysis.

Extraction of bound phenolics and favonoids

The residue obtained from the free phenolics extraction was hydrolyzed with NaOH (40 mL, 2 M) at room temperature for 1 h with continuous shaking. Hexanes (10 mL) were used to extract lipids. The hydrolysate was then neutralised with 10 mL of 2 M HCL. Solution was transferred to separation funnel and was then extracted fve times with ethyl acetate. The ethyl acetate layer (supernatants) were pooled and evaporated using hot plate (at 45 °C). Residue was dissolved in distilled water (10 mL) and then stored until analysis.

Determination of Total Phenolic

Total favonoid content Extracts (1 mL) were mixed with NaNO2 solution (4 mL, 1:5, w/v) and incubated at room temperature for 6 min. 0.3 mL of AlCl3 solution (1:10, w/v) was added, the reagents were mixed well, and the reaction was allowed to stand for another 6 min. Immediately after that, 1M NaOH solution (2.0 mL) was added to each extract and incubated for 10 min at room temperature. Te absorbance of the solutions was read at 510 nm using a spectrophotometer (UV2550, Shimadzu, Japan). Diferent concentrations of quercetin standard were used to prepare a calibration curve. Results were expressed as milligram quercetin equivalents (QE)/100 gDM . (Ghasemzadeh et al.,2015).

Determination of Flavonoid Content

Currently, the determination of TFC was depended on the aluminium chloride colorimetric method described by(Qiu, et al., 2010). Briefly, a 50 µL supernatant was mixed with 100 µL distilled water. Then, 5% $NaNO_2$ was added into the mixture and incubated for 5 min. Subsequently, 10% $AlCl_3$ $6H_2O$ solution was drawn and added to the mixture for incubation for 3 min. Finally, 60 µL 4%NaOH was added to the termination reaction. The samples were read at 510 nm. Absolute methanol was used as the control, while a standard rutin curve was used to calculate the content of TFC. Results were recorded as mg of RE/100 g DW.

***Determination of DPPH* (1,1-Diphenyl-2-picrylhydrazyl) assay** Radical Scavenging Activity

The method by (Ghasemzadeh et al.,2015), was used with slight modifications to assess DPPH. The mixtures were shaken vigorously, and the sample was taken then incubated for 30 min in the dark. Mixture was measured at 517 nm.

DPPH radical scavenging effect (%)=1−Asample−AbackgroundAcontrol×100%DPPH radical scavenging effect (%)=1−Asample−AbackgroundAcontrol×100%

(3)

where A_{sample}, $A_{control}$, and $A_{background}$ refer to sample (sample and DPPH), control (without sample), and background (without sample), respectively.

Statistical Analyses

All measurements in this study were presented as means ± standard deviations. Each antioxidant activity assay was carried out three times from the same extracts in order to determine their reproducibility. Statistical differences and principal component analysis were analyzed with SPSS 25 (SPSS Inc., Chicago, IL, USA) (Li et al .2021). Canonical correspondence analysis and networks were conducted with Origin software.

III. RESULT AND DISCUSSION

3.1. The phenolic content (TPC) of 10 rice varieties in the Mekong Delta :TPC of brown rice and white rice of different rice varieties differed significantly ($p < 0.05$). The TPC measured in brown rice was significantly higher (118.98-206.06%) than in white rice. Brown rice TPC levels were highest in HATRI 40 (771.12 mg/100 g), while the lowest levels were found in OM5451 (100.12GAE mg/100 g). The highest and lowest levels of GAE were found in HATRI 11 (215.06 mg/100 g) and OM5451 (133.08 mg/100 g). The difference in the total phenolic content between varieties can be attributed to differences in genotype. It is noteworthy that HATRI 11's TPC is the highest among white rice, but it is only 119.47% higher than the lowest white rice varieties.

This may indicate that milling during rice processing has different effects on the active compounds of different varieties. Meanwhile, the difference between the ratio of brown rice and white rice in different varieties can be attributed to inconsistent trends. The content of free phenolics and favonoids, binding and total phenolic acid content in brown and white rice portions of sixteen different genotypes of pigmented rice is shown in Table 1. The free phenolic content in brown rice portion varies from 153.30 to 771.15 mg GAE / 100 g DM. The binding phenolic content ranges from 102.05 to 443.55 mg GAE / 100 g. Total phenolic (4) Viability (%) = 100 – optical density of sample / optical density of control × 100 (5) Optical density of sample = absorption of cells treated with extraction – absorption of cells treated with an average DMSO content of 0.1% ranged from 269.85 to 1214.7 mg GAE/100 g DM. As shown in the Table 1

Brown rice contains the highest content of free phenolics, binding and total phenolics (771.15; 374.15 and 1,145.3 mg GAE/100 g DM), followed by white rice (521.36; 386.22 and 907.58 mg GAE/100 g DM, respectively) In one study by (Shen et al. 2009) the total free favonoid content of white, red and black rice was compared and it was found that the average favonoid content in white rice was lower than in red and black rice. The current results suggest that phenolic and favonoid compounds in rice bran are mostly present in free form, and this is an important issue for future research. Forms of phenolics and favonoid bonds are covalently conjugated to the structure of cell walls via ester bonds (Ali et al.,2018).

They are broken down by microfora and can release phenolics that are bound to carry out beneficial biological activities (Choi et al.,2010). The current results are consistent with previous reports, in which phenolics and favonoids in rice are mainly distributed in free form (Zhang et al.,2010, Ti et al.,2014).

3.2. The flavonoid content (TFC) of 10 TFC rice varieties of brown rice and white rice of different rice varieties differed significantly (table 1; statistically significant < 0.05). The TFC of brown rice is in the range of 142.26–919.1RE mg/100 g, while white rice is in the range of 68.72–645.29RE mg/100 g: brown rice has a total flavonoid content 10%-20% higher than white rice. Among them, the difference between brown rice and white rice from HATRI 722 and OM5451 varieties is smaller. Different trends in TFC and TPC are variation in the ten varieties, possibly because the distribution positions of total phenols and flavonoids in rice are influenced by genotype. In 10 rice varieties, the free flavonoid content of brown rice and white rice differed significantly ($p < 0.05$). In brown rice, it is in the range of 146.98 – 193.65 RE mg/100 g, with OM5451 and HATRI 40 having higher contents, and the content of free flavonoids in white rice is between 55.47 – 432.15 RE mg/100 g respectively.

There were significant differences in binding flavonoid content in brown and white rice of 10 statistically significant rice varieties ($p < 0.05$). The flavonoid content of the free, binding HATRI 11 variety in brown rice and white rice is in the range of 491.56b –367.8RE mg/100 g and260.48 –156.14 RE mg/100 g, respectively. The binding flavonoid content in brown rice varies 0.59 – 1.50 times that of white rice for the same variety, while OM4900, IR64, HATRI722 and OM5451 all have lower binding flavonoid content in brown rice than in white rice. The binding content in brown rice is 0.48 - 1.28 times higher than in white rice. Notably, the binding flavonoid content in brown rice of OM 5451 is lower than the content in white rice.

Table 2. Identifed free, bound and total individual phenolics, favonoidsfrom 10 varieties rice

line	Brown rice		Wilte rice		TPC	Brown rice		White rice		TFC
	TPC free (GAE mg/ 100g)	TPC bound (GAE mg/ 100g)	TPC free (GAE mg/ 100g)	TPC bound (GAE mg/ 100g)	Total brown rice (GAE mg/ 100g)	TFC free (mg QE/ 100g DM)	TFC bound (mgQE/100gDM)	TFC free (mg QE/ 100g DM)	TFC bound (mgQE/100 gDM)	Total TFC white rice(mg QE/ 100g DM)
HATRI 11	268.74d	216.25c	125.17e	108.75c	485d	245.35d	166.15c	216.15b	107.14d	411.5d
HATRI 144	285.16d	124.27d	220.25d	112.42c	409.43d	245.85d	156.24c	201.44b	123.10c	402.0d9
HATRI 200	175.50e	132.23d	107.14e	85.52d	307.73e	188.16e	110.25c	98.57c	65.12	298.4e1
HATRI 20	100.12f	85.74e	95.45f	56.15d	185.86g	106.74e	35.52d	155.47c	13.25f	142.2f6
OM 5451	144.20e	118.25d	98.38f	55.47d	262.45f	135.15e	105.25c	85.41c	52.14e	204.4e
HATRI 722	145.60e	132.23d	107.14e	85.52d	277.83f	133.25e	114.52	90.45c	59.78e	247.7e7
OM 4900	489.56c	274.33c	344.28c	256.14b	763.83c	342.51c	207.15b	215.12b	142.41b	549.6c6
HUYẾT RỒNG	771.15a	374.15a	521.36a	386.22a	1.145.3a	526.65a	392.45a	432.15a	213.14a	919.1a
HATRI 40	162.30e	122.45d	100.37e	92.56d	284.75f	128.17e	109.33c	90.53c	74.15e	237.5e
IR 64	162,30e	122,45d	100,37e	92,56d	284,75f	128,17e	109,33c	90,53c	74,15e	237,5e

3.3. Anthocyanin content in 10 rice varieties :The content of free and associated anthocyanins in ten varieties with different genotypes of pigmented rice is presented in Table 2. The total anthocyanin content in free form and the bonds vary between different genotypes of pigmented rice bran. The content of free and binding anthocyanins in the rice fraction of ten different genotypes of rice with brown rice and white rice ranged from 15.32 to 183.05 and 6.18 to24.16 mg of Cy3-GE/100 g DM, respectively. The highest concentration of anthocyanins was detected in free HATRI 40 . HATRI 40 showed the highest anthocyanin content (234.62 mg Cy3-GE/100 g DM), followed by HATRI 11 (73.88 mg Cy3-GE/100 g DM) and white rice (50.42 mg Cy3-GE/100 g DM).

Table 3. Identifed free, bound and total individual anthocyanin from 10 varities rice

lines	Brown rice		TAC Total brown rice(GAE mg /100 g)	White rice		TAC (White rice) Total g (GAE mg /100 g)
	TAC free(GAE mg /100g	TAC bound (GAE mg /100 g)		TAC free (GAE mg /100g)	TAC bound (GAE mg /100g)	
HATRI 11	68.33b	15.55b	73.88b	42.27b	8.15c	50.42b
HATRI 144	38.77c	6.27e	45.04c	8.75h	3.14d	11.89d
HATRI 200	15.32e	6.18e	21.50d	10.48g	3.45d	13.93d
HATRI 20	15.8e	7.25d	23.05d	10.42g	0.55g	10.97d
OM5451	16.57	9.25c	25.82d	11.45g	0.25g	11.70d
HATRI722	20.15d	9.56c	29.71d	17.14e	2.85e	19.99d

OM4900	24.56d	10.12b	34.68c	18.25d	1.65f	19.90d
HUYẾT RỒNG	63.20b	16.47b	79.67b	20.34c	14.78b	36.12c
HATRI 40	183.05a	24.16a	234.62a	58.56a	15.35a	73.34a
IR 64	20.69d	9.45c	30.14c	15.71f	0.8g	16.51d

3.4. The composition and content of phenolic acids vary significantly between varieties While the phenolic acid content in each brown rice is significantly higher than that of white rice ($p < 0.05$) (table 3). Glutinous brown rice contains relatively high levels of caffeic acid, sinapic acid (a hydroxycinnamic acid), ferulic acid and p-hydroxybenzoic acid, while the overall content of six phenolic acids of OM5451, HATRI20, IR64 is lower than that of other brown rice varieties. Meanwhile, HATRI 200 white rice has a relatively higher overall content of phenolic acids. The p-hydroxybenzoic acid content of brown rice in HATRI 200 is more than twice that of white rice. Phenolics and favonoid composition: Five phenolic compounds (protocatechuic acid, syringic acid, ferulic acid, cinnamic acid and p-coumaric acid) have been detected in white and brown rice of different varieties (Table 4). Protocatechuic acid, with content from 0.99 to 4.55 mg/100g DM on brown rice and highest content (in Glutinous Coal)

Table 4: Content of phenolic acids 10 varieties

lines	Brown rice	White rice	Brown rice	White rice	Brown rice	White rice	Brown rice	White rice	Brown rice	White rice
	protocatechuic acid (mg/ 100g DM	protocatechuic acid (mg/ 100g DM	axit syringic (mg/ 100g DM	axit syringic (mg/ 100g DM	axit ferulic (mg/ 100g DM	axit ferulic kết (mg/ 100g DM	cinnamic acid (mg/ 100g DM	cinnamic acid (mg/ 100g DM	p-coumaric acid (mg/100g DM)	p-coumaric acid (mg/ 100g DM)
HATRI 11	2.56c	1.95c	15.25a	6.45a	5.25c	3.85c	15.44b	0	24.15a	20.55a
HATRI 144	1.25d	0.88f	10.25b	3.15c	4.22d	2.56d	14.55b	12.33b	15.47c	14.25c
HATRI 200	2.15c	1.12d	10.56b	3.22c	3.25e	1.03f	11.25c	10.99c	14.23c	13.48d
HATRI 20	1.08d	0.56g	9.35c	2.14d	3.10e	0.95g	10.58c	9.50d	13.25d	10.66e
OM5451	0.99e	0.23g	6.45e	1.25e	2.90f	0.35h	9.25d	5.11d	10.47e	8.62g
HATRI 722	1.44d	0.45g	7.56d	1.54e	2.65f	1.48f	9.50d	8.25d	11.52e	9.55f
OM4900	1.55d	0.62f	6.78e	1.89e	3.16e	1.75e	9.98d	8.75d	11.54e	8.73g
HUYẾT RỒNG	3.25b	2.66b	11.25b	4.15b	6.15b	5.99b	14.55b	12.78b	15.77c	13.28d
HATRI 40	4.55a	3.15a	15.21a	6.24a	9.25a	8.10a	19.25a	14.15a	18.74b	17.25b
IR64	1.62d	0.55g	8.25c	1.99e	3.56e	1.02f	10.28c	8.28d	10.99f	8.27g

Ferulic acid is an important phenolic acid component in rice; The content of varied varieties was 18.85-29.71 mg/kg in brown rice and 9.54-18.66 mg/kg in white rice. The white rice content of these two acids is 2.0-2.4% and 1.4-2.2% lower than brown rice, respectively. Both syringic acid and p-coumaric acid show similar trends in different varieties, with little variation in p-coumaric acid content in different varieties. The cinnamic acid content in brown rice is in the range of 9.25-19.25 mg/kg, which is 1.25-2.0 times higher than the content of white rice. P-coumaric acid is lowest in brown rice with 10.47 mg/kg in OM5451 and with white rice as low as 8.27 mg/kg in IR64. Among the favonoid compounds identified in various rice varieties.

Favonoid compounds (quercetin, apigenin, catechins, luteolin and myrecitin) The content of quercetin in free and bound form ranged from 2.71 to 11.89 mg/100 g DM and from 0.16 to 3.66 mg/100 g DM, respectively. Apigenin in concentrations between 5.75 and 10.55 and 4.52 and 9.55 mg/100g DM, for brown rice and white rice respectively. Catechins also exist in brown rice and white rice with concentrations ranging from 10.11 to 20.14 and 7.25 and 18.23 mg/100 g DM, respectively (Table 5).

*Table **5:** Favonoid compounds (quercetin, apigenin, catechins, luteolin and myrecitin)in 10 varieties*

LINES	**Brown rice**	**White rice**	**Brown rice**	**White rice**	**Brown rice**	**White rice**	**Brown rice**	**White rice**
	quercetin (mg/100g DM)	quercetin (mg/100 gDM)	apigenin (mg/100 gDM)	apigenin (mg/100g DM)	catechin (mg/100 gDM)	catechin (mg/100 gDM)	luteolin (mg/100g DM)	luteolin (mg/100 gDM)
HATRI 11	6.18c	5.55c	8.14c	6.25c	15.66b	13.23b	7.72b	5.25c
HATRI 144	4.15d	3.25d	7.88d	5.22d	10.12d	8.55d	6.14c	4.66d
HATRI 200	4.55d	3.47d	7.99d	6.10c	12.11c	10.22c	6.55c	4.29d
HATRI 20	3.66e	2.15e	6.22e	5.22d	11.25d	8.54d	5.57d	3.22e
OM5451	3.58e	1.22	5.75f	4.52e	10.11d	7.25e	5.01d	2.95f
HATRI 722	3.78e	2.55f	6.25e	4.58e	10.56d	8.54d	5.78d	4.15d
OM4900	3.47e	2.45f	6.78e	4.55e	10.98d	7.58e	5.67d	4.47d
HUYẾT RỒNG	10.52b	7.25b	9.25b	8.10b	15.90b	13.25b	7.98b	6.18b
HATRI 40	12.55a	10.25a	10.55a	9.25a	20.14a	18.23a	9.21a	8.71a
IR64	3.45e	2.68f	6.45e	4.25e	10.99d	8.29d	5.66d	4.57d

Luteolin in brown rice, with concentrations ranging from 5.01 to 9.21 mg/100 g DM and 2.95 to 8.71 mg/100 g DM, respectively. Furthermore, catechins and myrecitin are the most abundant favonoid compounds in brown and red rice bran, while apigenin and quercetin are the most abundant favonoid compounds in black rice bran (Zhou et al.,2004) showing that brown rice contains high levels of ferulic acid and p-coumaric acid and gallic acid content, Low vanillic, caffeinic and syringic, consistent with current studies.

5/DPPH activity Free radicals are an intermediate metabolite of various biochemical reactions in human life activities. It has high chemical activity and is an effective defense system of the human body. However, the excessive accumulation of free radicals that cannot be scavenged in time will attack life macromolecules and various organelles, and cause interhuman damage at the molecular, cellular and tissue level, which can further accelerate the human aging process and cause various chronic diseases (Akbari et al, 2022).

Various mechanisms, such as free radical scavenging, capacity reduction, metal ions, and lipid peroxidation inhibition, have been studied to explain how rice bran extract can be used as an antioxidant (Ghasemzadeh et al.,2015). DPPH radical scavenging tests are based on the transfer of electrons from the molecule of the donor radical to the corresponding radical. The DPPH method is the simplest method for measuring the ability of antioxidants to block free radicals. DPPH thoroughly scavenged the effects of all extracts in white rice and brown rice (free and bonded) increased with increasing concentration (Figure 1a,b).

DPPH operations have been markedly affected. The rate of DPPH root scavenging varied significantly in brown rice (64.72–70.92%, $p < 0.05$). Brown rice of OM5451 has the lowest antioxidant capacity for removing DPPH radicals and is significantly different from other varieties ($p < 0.05$). The coefficient of variation between different breeds is 3.1%. Meanwhile, the scavenging rate of DPPH free radicals in white rice was on average 24.5% lower than brown rice at 37.8% (OM5451). Spirit and Dragon Blood had the highest scavenging rates (61.8,-68.9%), while HATRI 722 and OM 5451 had the lowest scavenging rates (36.7-37.8%). The DPPH antioxidant activities of different white rice varieties are significantly different ($p < 0.05$).

The 10-variety extract demonstrated the highest DPPH activity, followed by rice extraction. DPPH activity of different varieties ranges from 24.5 to 60.4%, for white rice

ISSN: 2456-1878 (Int. J. Environ. Agric. Biotech.)
https://dx.doi.org/10.22161/ijeab.112.12

and DPPH activity in free fractions and bonds respectively ranges from within brown rice 36.7 to 68.9% (figure 1a,b)

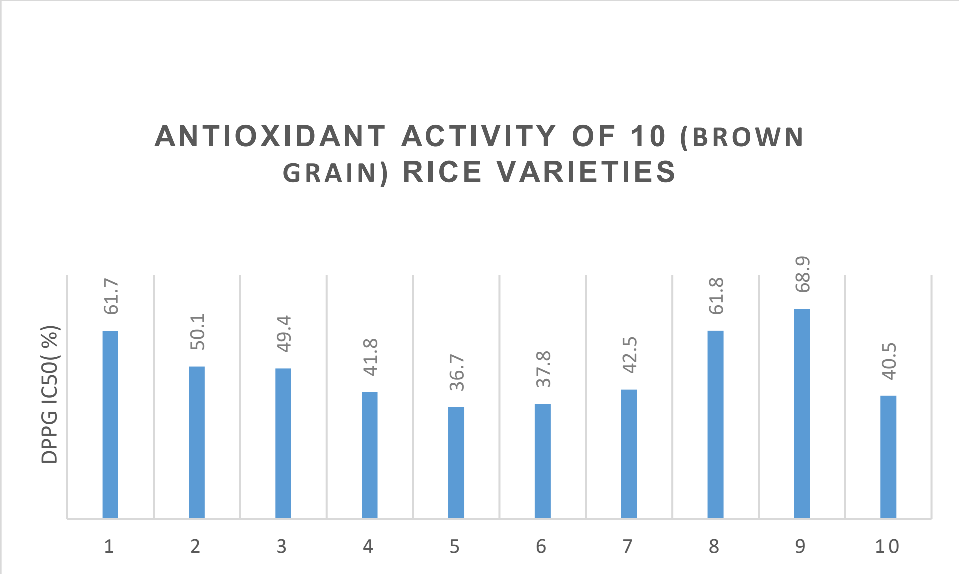

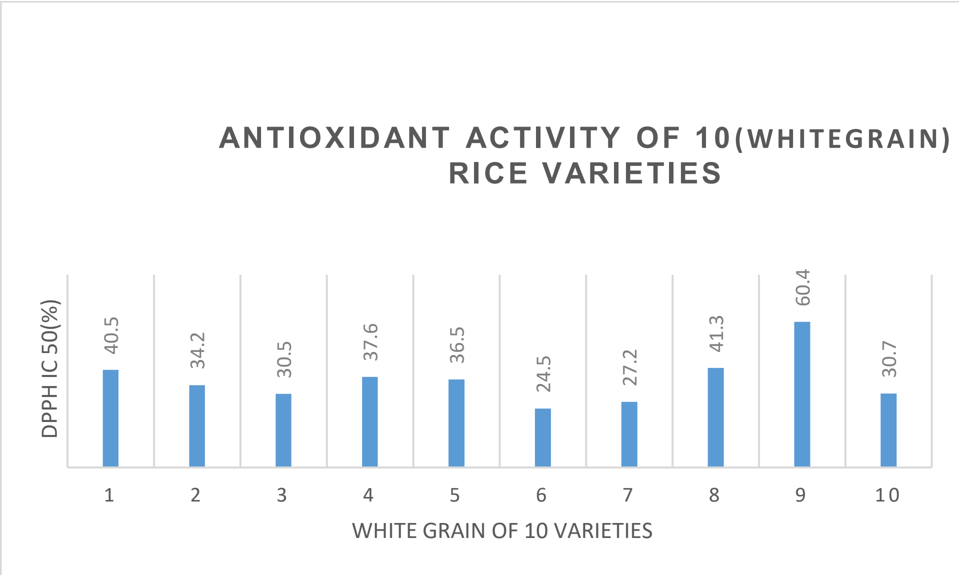

Fig.1: Antioxidant activity value of ten rice varieties (Figure 1A: Antioxidant activity of brown rice of 10 rice varieties. Figure 1B: Antioxidant activity of White rice of 10 rice varieties

IV. CONCLUSIONS

Looking at a series of analytical results, the determination of polyphenols in rice extract aims to determine the quantitative profile of the quality of rice grains. Significant strides have been made in elucidating the chemical structure of these bioactive compounds but while mass spectrometry based techniques certainly represent a powerful tool for defining brown rice phenolic profiles, white rice. We strongly believe that the research efforts undertaken to date constitute an excellent starting point towards the development of analytical tools aimed at investigating the phenolic fraction of rice for demand in medicinal chemistry.

FUTURE PROSPECTS

1) Consequently, the flavonoid and phenolic compounds which are abundant found in a large number of rice and other plants may possible be an interesting choice of molecules for drug and medical product development.
2) In the same species of medicinal rice , the different cultivars may provide different amount of flavonoid and phenolic compounds as well as the biological activities. Thus, the cultivars of medicinal plant should be taken into account for the future medical and pharmaceutical research studies.

3) The geographic areas of raw rice material should also be analyzed and compared in the future research. Since the environmental factors e.g., nutrients and mineral in soil are also effect on the quality and quantity of phytochemical compounds in some species of medicinal rice.
4) The molecular mechanism and signaling pathway of many known flavonoid and phenolic compounds are need to be done in the future, so as to apply this knowledge to the drug development processes.
5) The need of purified compounds to confirm data obtained with the rice extracts.

ACKNOWLEDGEMENT

The authors are extremely grateful to Vinfuture for providing funding to implement this project. Thanks are due to HATRI and our colleagues in the Genetics and Plant Breeding Division for their support and valuable suggestions.

REFERENCES

[1] Akbari, B., Baghaei-Yazdi, N., Bahmaie, M., Abhari, F. M. (2022). The role of plant-derived natural antioxidants in reduction of oxidative stress. *Biofactors* 48, 611–633.

[2] Ali Ghasemzadeh, Mohamad Taghi Karbalaii, Hawa Z. E. Jaafar & Asmah Rahmat 2018. Phytochemical constituents, antioxidant activity, and antiproliferative properties of black, red, and brown rice bran. *Chemistry Central Journal* volume 12, Article number: 17 (2018)

[3] Alu'datt, M. H., Rababah, T., Alhamad, M. N., Al-Mahasneh, M. A., Almajwal, A., Gammoh, S., et al. (2017). A review of phenolic compounds in oil-bearing plants: Distribution, identification and occurrence of phenolic compounds. *Food Chem.* 218, 99–106.

[4] Alves, G.H.; Ferreira, C.D.; Vivian, P.G.; Fernandes Monks, J.L.; Elias, M.C.; Vanier, N.L.; De Oliveira, M. The revisited levels of free and bound phenolics in rice: Effects of the extraction procedure. *Food Chem.* 2016, *208*, 116–123.

[5] Ashraf, H.; Murtaza, I.; Nazir, N.; Wani, A.B.; Naqash, S.; Husaini, A.M. Nutritional profiling of pigmented and scented rice genotypes of Kashmir Himalayas. J. Pharmacogn. Phytochem. 2017, 6, 910–916.

[6] Bastia, R.; Pandit, E.; Sanghamitra, P.; Barik, S.R.; Nayak, D.K.; Sahoo, A.; Moharana, A.; Meher, J.; Dash, P.K.; Raj, R.; et al. Association Mapping for Quantitative Trait Loci Controlling Superoxide Dismutase, Flavonoids, Anthocyanins, Carotenoids, γ-Oryzanol and Antioxidant Activity in Rice. Agronomy 2022, 12, 3036. https://doi.org/10.3390/ agronomy12123036

[7] Cheynier, V. (2012). Phenolic compounds: From plants to foods. *Phytochem. Rev.* 11, 153–177.

[8] Choi SP, Kim SP, Kang MY, Nam SH, Friedman M (2010) Protective effects of black rice bran against chemically-induced inflammation of mouse skin. J Agric Food Chem 58(18):10007–10015

[9] de Araújo, F. F., de Paulo Farias, D., Neri-Numa, I. A., Pastore, G. M. (2021). Polyphenols and their applications: An approach in food chemistry and innovation potential. *Food Chem.* 338, 127535.

[10] Desta, K.T.; Hur, O.S.; Lee, S.; Yoon, H.; Shin, M.J.; Yi, J.; Choi, Y.M. Origin and seed coat color differently affect the concentrations of metabolites and antioxidant activities in soybean (*Glycine max* (L.) Merrill) seeds. *Food Chem.* 2022, *381*, 132249.

[11] Fraga, C. G., Croft, K. D., Kennedy, D. O., Tomás-Barberán, F. A. (2019). The effects of polyphenols and other bioactives on human health. *Food Funct.* 10, 514–528.

[12] Ge, X.; Jing, L.; Zhao, K.; Su, C.; Zhang, B.; Zhang, Q.; Han, L.; Yu, X.; Li, W. The phenolic compounds profile, quantitative analysis and antioxidant activity of four naked barley grains with different color. *Food Chem.* 2021, *335*, 127655.

[13] Ghasemzadeh A, Jaafar HZ, Juraimi AS, Tayebi-Meigooni A (2015) Comparative evaluation of diferent extraction techniques and solvents for the assay of phytochemicals and antioxidant activity of Hashemi rice bran. Molecules 20(6):10822–10838

[14] Ghasemzadeh A, Jaafar HZ, Rahmat A (2015) Phytochemical constituents and biological activities of diferent extracts of Strobilanthes crispus (L.) Bremek leaves grown in diferent locations of Malaysia. BMC complement Altern Med 15(1):422

[15] Gong, E.S.; Luo, S.J.; Li, T.; Liu, C.M.; Zhang, G.W.; Chen, J.; Liu, R.H. Phytochemical profiles and antioxidant activity of brown rice varieties. *Food Chem.* 2017, *227*, 432–443.

[16] Govindaraj, M.; Masilamani, P.V.; Albert, A.; Bhaskaran, M. Role of antioxidant in seed quality—A review. Agric. Rev. 2017, 38, 180–190.

[17] Kumar, A.K.; Govindaraj, M.; Karthikeyan, A.; Shobhana, V.G.; Warkentin, T.D. Genomics-Integrated Breeding for Carotenoids and Folates in Staple Cereal Grains to Reduce Malnutrition. Front. Genet. 2020, 11, 414.

[18] Liu, L.; Guo, J.; Zhang, R.; Wei, Z.; Deng, Y.; Guo, J.; Zhang, M. Effect of degree of milling on phenolic profiles and cellular antioxidant activity of whole brown rice. *Food Chem.* 2015, *185*, 318–325.

[19] Li, W.; Wen, L.; Chen, Z.; Zhang, Z.; Pang, X.; Deng, Z.; Guo, Y. Study on metabolic variation in whole grains of four proso millet varieties reveals metabolites important for antioxidant properties and quality traits. *Food Chem.* **2021**, *357*, 129791. Ma, L. K., Tang, L. L., Yi, Q. (2019). Salvianolic acids: potential source of natural drugs for the treatment of fibrosis disease and cancer. *Front. Pharmacol.* 10.

[20] Neri-Numa, I. A., Arruda, H. S., Geraldi, M. V., Júnior, M. R. M., Pastore, G. M. (2020). Natural prebiotic carbohydrates, carotenoids and flavonoids as ingredients in food systems. *Curr. Opin. Food Sci.* 33, 98–107. doi: 10.1016/j.cofs.2020.03.004.

[21] Pang, Y.; Ahmed, S.; Xu, Y.; Beta, T.; Zhu, Z.; Shao, Y.; Bao, J. Bound phenolic compounds and antioxidant properties of

whole grain and bran of white, red and black rice. *Food Chem.* 2018, *240*, 212–221.
[22] Podio, N.S.; Baroni, M.V.; Wunderlin, D.A. Relation between polyphenol profile and antioxidant capacity of different Argentinean wheat varieties. A Boosted Regression Trees study. Food Chem. 2017, 232, 79–88.
[23] Quideau, S., Deffieux, D., Douat-Casassus, C. (2011). Plant polyphenols: chemical properties, biological activities and synthesis. *Angew. Chem. Int. Ed.* 50, 586–621.
[24] Ragaee, S.; Seetharaman, K.; Abdel-Aal, E.S. The impact of milling and thermal processing on phenolic compounds in cereal grains. *Crit. Rev. Food Sci. Nutr.* 2014, *54*, 837–849.
[25] Rossatto, T.; de-Amaral, M.N.; Benitez, L.C.; Vighi, I.L.; Braga, E.; de Magalhães, J.; Maia, A.M.M.; da Silva, P.L. Gene expression and activity of antioxidant enzymes in rice plants, cv. BRS AG, under saline stress. Physiol. Mol. Biol. Plants 2017, 23, 865–875.
[26] Shen, Y.; Jin, L.; Xiao, P.; Lu, Y.; Bao, J. Total phenolics, flavonoids, antioxidant capacity in rice grain and their relations to grain color, size and weight. J. Cereal Sci. 2009, 49, 106–111.
[27] Shridhar, G.; Rajendra, N.; Murigendra, H.; Shridevi, P.; Prasad, M.; Mujeeb, M.A.; Arun, S.; Neeraj, D.; Vikas, S.; Suneel, D.; et al. Modern Diet and its Impact on Human Health. J. Nutr. Food Sci. 2015, 5, 6.
[28] Qiu, Y.; Liu, Q.; Beta, T. Antioxidant properties of commercial wild rice and analysis of soluble and insoluble phenolic acids. *Food Chem.* **2010**, *121*, 140–147. [**Google Scholar**] [**CrossRef**]
[29] Ti H, Li Q, Zhang R, Zhang M, Deng Y, Wei Z, Chi J, Zhang Y (2014) Free and bound phenolic profiles and antioxidant activity of milled fractions of different indica rice varieties cultivated in southern China. Food Chem 159:166–174
[30] Verardo, V.; Gmez-Caravaca, A.; Marconi, E.; Segura-Carretero, A.; Garrido-Frenich, A.; Fernmndez-Gutirrez, A. Determination of lipophilic and hydrophilic bioactive compounds in raw and parboiled rice bran. RSC Adv. 2016, 6, 50786–50796.
[31] Yahfoufi, N., Alsadi, N., Jambi, M., Matar, C. (2018). The immunomodulatory and anti-inflammatory role of polyphenols. *Nutrients* 10, 1618–1640. doi: 10.3390/nu10111618.
[32] Zhai, S.N.; Xia, X.C.; He, Z.H. Carotenoids in Staple Cereals: Metabolism, Regulation, and Genetic Manipulation. Front. Plant Sci. 2016, 7, 1197
[33] Zhang MW, Zhang RF, Zhang FX, Liu RH (2010) Phenolic profiles and antioxidant activity of black rice bran of different commercially available varieties. J Agric Food Chem 58(13):7580–7587
[34] Zhang, H., Tsao, R. (2016). Dietary polyphenols, oxidative stress and antioxidant and anti-inflammatory effects. *Curr. Opin. Food Sci.* 8, 33–42.
[35] Zhu, C.; Kobayashi, K.; Loladze, I.; Zhu, J.; Jiang, Q.; Xu, X.; Liu, G.; Seneweera, S.; Ebi, K.L.; Drewnowski, A.; et al. Carbon dioxide (CO2) levels this century will alter the protein, micronutrients, and vitamin content of rice grains with potential health consequences for the poorest rice-dependent countries. Sci. Adv. 2018, 4, eaaq1012.
[36] Zhou Z, Robards K, Helliwell S, Blanchard C (2004) The distribution of phenolic acids in rice. Food Chem 87(3):401–406

International Journal of Environment, Agriculture and Biotechnology
Vol-11, Issue-2; Mar-Apr, 2026
Peer-Reviewed International Journal
Journal Home Page Available: https://ijeab.com/
Journal DOI: 10.22161/ijeab

Strategic Framework for Winter Air Pollution Control in Haryana: Challenges and Opportunities

Anuradha Panwar* and Rahul

Assistant Professor Department of Civil Engineering, Dev Bhoomi Uttarakhand University, Dehradun, Uttarakhand, India-248007
*Corresponding Author

Received: 15 Mar 2026; Received in revised form: 13 Apr 2026; Accepted: 17 Apr 2026; Available online: 25 Apr 2026

***Abstract*— Air pollution in Haryana is a major environmental and health concern, especially during the winter season. The adverse meteorological conditions during the winter enhance the level of air pollution. The present study proposes a strategic framework for the control of air pollution during the winter. The present research focuses on the analysis of the spatio-temporal trends of air quality over several areas in Haryana, covering the period from 2020 to 2024. The results showed that there was an improvement in air quality during the early part of 2023. However, the improvement was not long-lasting, and the areas showed a constant level of pollution during 2024. The areas such as Gurugram, Faridabad, Manesar, etc., showed high levels of pollution, while areas like Panchkula and Karnal showed good trends of air quality. The emphasis is on the need for a multi-sectoral strategy to be implemented through emission control, sustainable transport systems, agricultural management practices, and effective enforcement of regulations. The proposed Winter Action Plan is in line with the national environment policy and is designed to improve the effectiveness of monitoring, enforcement, and public involvement. It is a practical and policy-driven approach to addressing air quality and health risks and is beneficial for sustainable environment management in Haryana.*

***Keywords*— Air Pollution, Winter Action Plan, Haryana, Air Quality Management, Sustainable Environmental Policy**

I. INTRODUCTION

The escalating trend of ambient air pollution has emerged as a critical environmental and public health concern in recent years, with peak severity observed during the winter season due to unfavorable dispersion conditions (WHO, 2021; HEI, 2020). The adverse health impacts of air pollution are well documented in scientific literature. A 2019 assessment estimated that prolonged exposure to elevated pollution levels has reduced the average life expectancy of the Indian population by approximately 6–9 years and contributed to nearly 1.7 million premature deaths nationwide. Open burning of solid waste constitutes a major source of atmospheric pollution, particularly in association with unmanaged open dumping practices. Additionally, seasonal combustion of agricultural residues in post-harvest fields represents a substantial contributor to air pollutant emissions, as documented by UNEP (2021). Exposure to ambient air pollution, both short- and long-term, leads to reduced lung function, respiratory infections, and aggravated asthma. It is also associated with adverse reproductive outcomes and emerging risks such as type 2 diabetes, obesity, systemic inflammation, and neurodegenerative diseases (WHO, 2005; 2013a; EEA, 2020). Empirical studies further indicate that air pollution significantly exacerbates morbidity and mortality risks among individuals suffering from chronic respiratory and cardiovascular disorders, including chronic obstructive pulmonary disease (COPD), lung cancer, ischemic heart disease, stroke, and pneumonia (Kumar et al., 2020; WHO, 2018). Assessment of health impacts from ambient air pollution is complicated by indoor exposure variability, long-term effects of episodic events such as wildfire smoke, and uncertainties related to emerging particulate matter, including brake and tire wear and microplastics (HEI, 2023). Vulnerable population groups, particularly children and the elderly, are disproportionately affected due to their heightened physiological sensitivity and weaker adaptive capacity (WHO, 2021). Consequently, air pollution must be addressed not only as an environmental degradation issue but also as a pressing public health emergency requiring integrated, multi-sectoral policy interventions. According to global air quality assessments based on World Health Organization (WHO) standards, India ranks third globally in terms of population exposure to $PM_{2.5}$ concentrations exceeding recommended limits, underscoring the urgency of strengthened mitigation and regulatory strategies (IQAir, 2024; WHO, 2021). The mean winter concentration of PM_{10} is approximately 600 µg/m³, significantly exceeding the permissible limit of 100 µg/m³, while $PM_{2.5}$ levels average around 375 µg/m³ compared to the acceptable standard of 60 µg/m³ (Sharma et al., 2016). Haryana represents a predominantly agrarian economy complemented by a rapidly expanding industrial sector (HSPCB, 2023). Despite its economic growth, the state continues to face substantial environmental pressures, particularly elevated concentrations of particulate matter ($PM_{2.5}$ and PM_{10}), with acute severity during the winter season due to adverse meteorological conditions and transboundary influences (Jain & Sharma, 2021; Singh et al., 2019). Thermal power plants, vehicular emissions, industrial activities, agricultural practices, and solid waste disposal constitute the primary sources of air pollutant emissions in Indian megacities (Gurjar et al., 2016). The proposed action framework is formulated by critically examining the state's geographical characteristics, emission sources, and socio-economic structure to design sector-specific, technically feasible, and outcome-oriented interventions. The strategy builds upon the prevailing regulatory architecture and is harmonized with national and state environmental policies (MoEFCC, 2019; CPCB, 2023). It integrates directives and standards prescribed by the Central Pollution Control Board (CPCB) and operationalizes state-specific regulatory mechanisms to strengthen enforcement, monitoring, and compliance. This integrated approach ensures systematic and effective implementation of air quality management measures across multiple sectors. The objective of the study is to analyze the spatio-temporal variation of ambient air quality over different districts of Haryana from 2020 to 2024, with specific reference to winter pollution patterns, regional variations, and concentrations of particulate matter (PM2.5, PM10), to formulate a strategic multi-sectoral Winter Action Plan that would cover issues related to emissions, sustainable transport, agriculture, and enforcement.

Table 1: Comparative Assessment of Population-Weighted Annual Mean $PM_{2.5}$ Concentrations in India and Neighbouring Countries Relative to the WHO Annual Guideline (2024)

Country	Population-Weighted Annual Mean $PM_{2.5}$ (µg/m³)	WHO Annual Guideline (5 µg/m³)	Exceedance Ratio
Bangladesh	78.0	5	15.6×
Pakistan	73.7	5	14.7×
India	50.6	5	10.1×
Nepal	42.8	5	8.6×

Table 2: Compliance Status of Annual Average $PM_{2.5}$ Concentrations in India and Selected Neighbouring Countries with WHO Guidelines, WHO Interim Target-1, and India's NAAQS {WHO (2021); CPCB (2023)}

Country	Annual Avg. $PM_{2.5}$ (µg/m³)	Meets WHO 5 µg/m³?	Meets WHO IT-1 (35)	Meets India NAAQS (40)
Bangladesh	78.0	×	×	×
Pakistan	73.7	×	×	×
India	50.6	×	×	×
Nepal	42.8	×	×	×

II. STUDY AREA

Haryana sub-region of the National Capital Region (NCR), a vital economic and administrative zone surrounding New Delhi. Geographically, this territory is situated roughly between 27.65 ° to 29.80 ° latitude and 76.10 ° to 77.55 ° longitude. The visualization highlights a collection of districts that serve as the industrial and urban backbone of Northern India. At the heart of this region is Gurugram, a global corporate hub for IT and finance, alongside Faridabad, one of the state's oldest and largest industrial centers. Moving toward the north and west, the map identifies Sonepat and Panipat, which are critical for their educational institutions, textile industries, and historical significance. The central and southern portions of the map showcase districts like Rohtak, Jhajjar, Rewari, and Palwal. These areas act as strategic transit points, connected by a massive network of highways and the KMP (Kundli-Manesar-Palwal) Expressway, which facilitates seamless logistics bypass around the national capital. To the far north of the NCR boundary lies Karnal, known as the "Rice Bowl of India," representing the region's strong agricultural foundation. Collectively, this map depicts an integrated urban ecosystem designed to decentralize Delhi's population by providing world-class infrastructure, manufacturing zones, and residential hubs within the state of Haryana (HSPCB, 2023; MoEFCC, 2020).

Fig.1: NCR region of Haryana

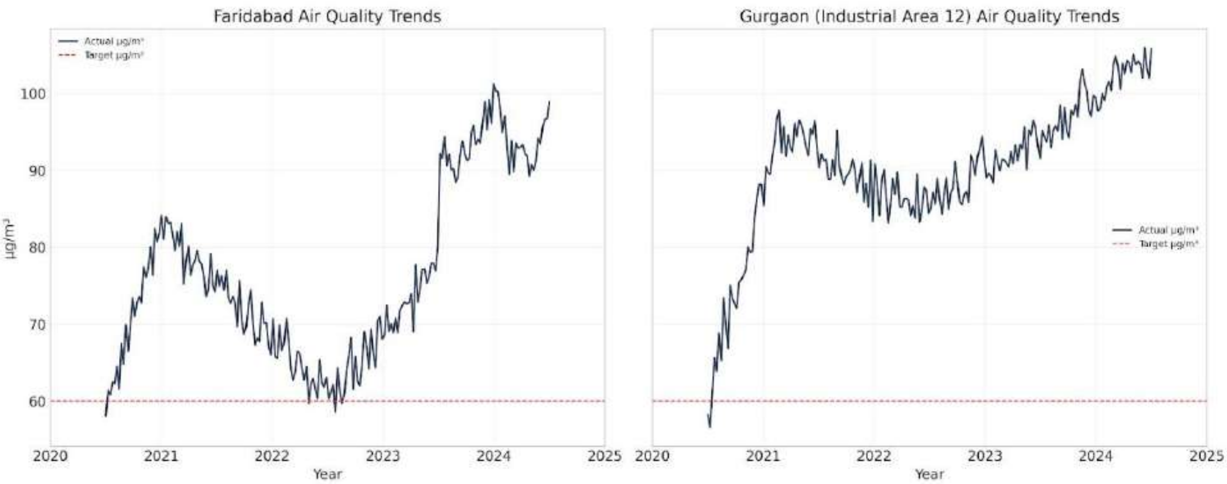

Fig.2. Comparative Air Quality Trends in Faridabad and Gurgaon (2020–2025)

In Figure 2, the Faridabad Air Quality Trends chart on the left shows a fluctuating trend in particulate matter concentration from 2020 to 2024. After a sharp increase in early 2021, the city saw a significant improvement throughout 2022, where levels briefly approached the 60 ug/m^3 target line. However, this progress reversed in early 2023, as concentrations rose steadily to nearly 100 µg/m^3 by mid-2024. The Gurgaon (Industrial Area 12) Air Quality Trends chart on the right indicates a more severe, ongoing pollution issue. After a rapid rise in late 2020, Gurgaon's air quality stayed consistently poor and never returned to the target level. While there was a slight decrease in 2022, the trend since 2023 has shown a sharp increase, with levels peaking above 105 ug/m^3 by mid-2024.

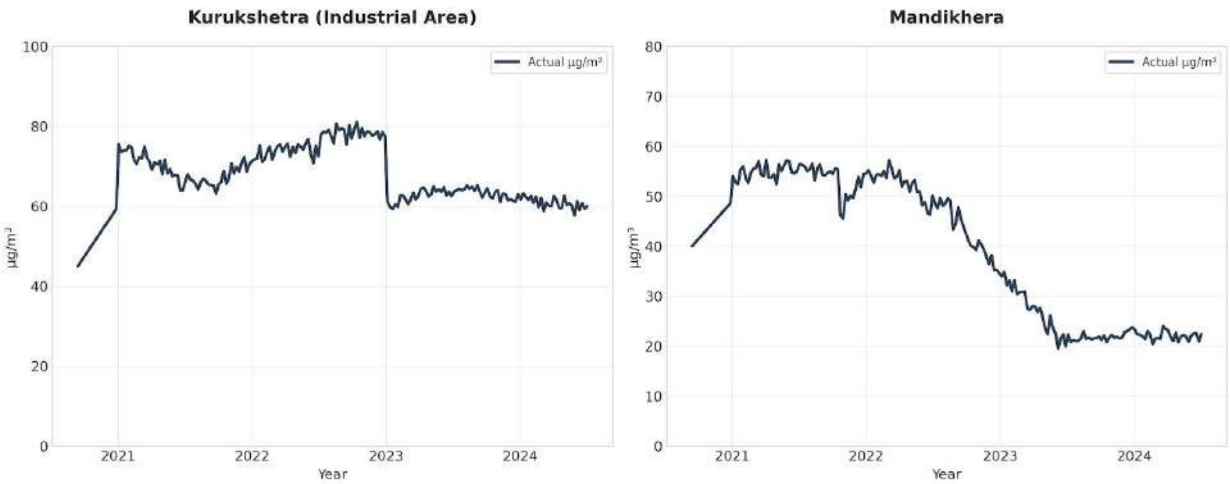

Fig.3. Air Quality Trends in Kurukshetra (Industrial Area) and Mandikhera (2020–2025)

The Kurukshetra (Industrial Area) chart shows a period of high particulate matter starting in 2020. Levels rose from 45 μg/m^3 to a peak between 70 and 80 μg/m^3 during 2021 and 2022. A sharp drop happened at the beginning of 2023, lowering the concentration to a more stable range of around 60 μg/m^3 until mid-2024. The Mandikhera chart reveals a very positive trend, showing the most significant air quality improvement among the areas studied. After peaking near 60 μg/m^3 in early 2022, the concentration steadily declined for the rest of the year. By mid-2023, levels dropped to about 20 μg/m^3 and have stayed low through 2024, indicating a successful shift to much cleaner air.

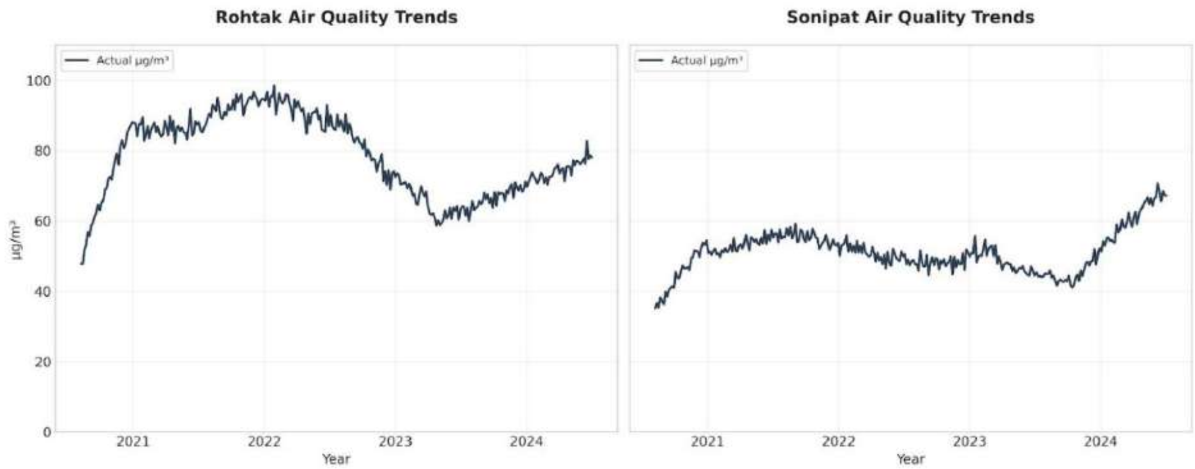

Fig.4. Assessment of PM Concentration Trends in Rohtak and Sonipat

The Rohtak Air Quality Trends chart on the left shows a clear wave-like pattern in particulate matter levels over the four years. After a sharp rise from 50 μg/m^3 to nearly 100 μg/m^3 by early 2022, Rohtak saw a notable improvement throughout 2023, with levels dropping back down toward 60 μg/m^3. However, since the start of 2024, air quality has begun to decline again, steadily rising toward 80 μg/m^3 by mid-year. The Sonipat Air Quality Trends chart on the right reflects a generally lower but increasingly unstable pollution profile. For much of 2021 through 2023, Sonipat maintained stable levels, fluctuating between 40 and 60 μg/m^3, which was better than many neighboring regions. This stability ended in early 2024, as the chart shows a sharp and consistent upward trend, with concentrations hitting a four-year high of about 70 μg/m^3 by mid-2024.

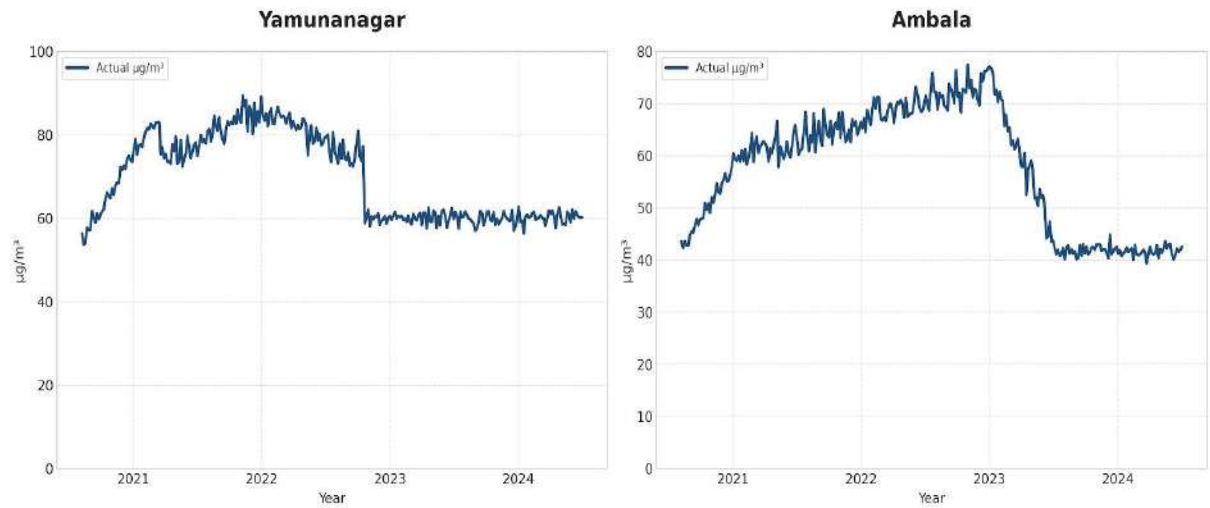

Fig.5. Air Quality Trend Analysis in Yamunanagar and Ambala (2020–2025)

The above figure presents two line graphs representing the recorded air pollutant concentration in ug/m^3 for the cities of Yamunanagar and Ambala from the end of 2020 to the middle of 2024. The cities have a similar long-term pattern, showing a rise in air pollutant concentration from 2021 and 2022, reaching a peak of 80-90 ug/m^3 for Yamunanagar and 75 ug/m^3 for Ambala. It is observed that from early 2023, a considerable and steep fall in air pollutant concentration was observed for both cities. Subsequently, from 2024, a significant stabilization in air pollutant concentration was observed, reaching a baseline of 60 ug/m^3 for Yamunanagar and 40 ug/m^3 for Ambala, which might be a result of a change in environmental policy for these cities.

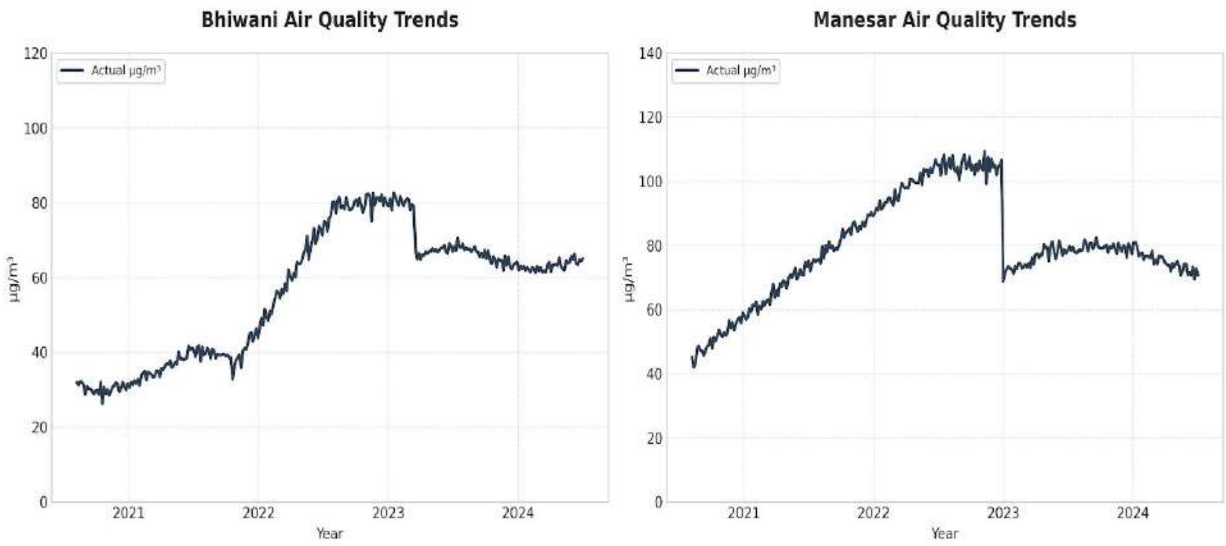

Fig.6. Comparative Assessment of Ambient Air Quality in Bhiwani and Manesar

The figure provided above represents air quality trends for both Bhiwani and Manesar from the end of 2020 until mid-2024, represented in units of ug/m^3. From the figure, it is evident that both cities have shown a steady rise in air quality from the end of 2020 until the end of 2022, at which time both cities reached their peak, with Bhiwani reaching a peak of around 80 ug/m^3, and Manesar reaching a peak of around 105 ug/m^3. Similar to the previous air quality trends for Yamunanagar and Ambala, both cities showed a sharp, vertical drop in pollutant concentration at the start of 2023. Following this drop, both cities showed air quality levels of around 60-70 ug/m^3 in Bhiwani and around 70-80 ug/m3 in Manesar until the end of 2024. Both cities are showing higher levels of air quality compared to their starting points at the end of 2020.

ISSN: 2456-1878 (Int. J. Environ. Agric. Biotech.)
https://dx.doi.org/10.22161/ijeab.112.13

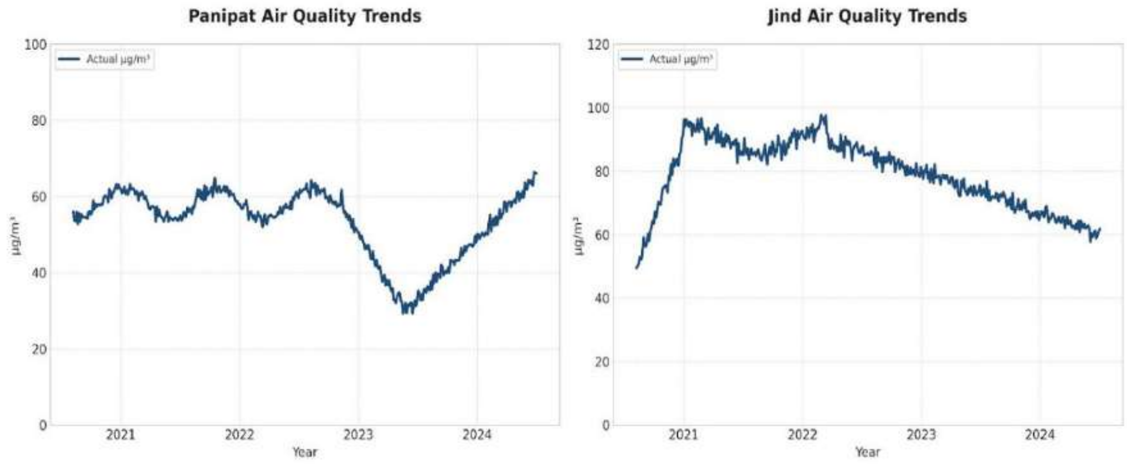

Fig.7. Air Quality Trend Analysis in Panipat and Jind (2020–2025)

The figure provided above represents the air quality trend for Panipat and Jind from the end of 2020 to mid-2024. Unlike the other cities, these cities have shown a gradual and distinct trend. The air quality in Panipat has shown a cyclical trend with peaks around 60-65 ug/m^3 every year. However, there was a sharp decline in early 2023 to a minimum of 30 ug/m^3, and then air quality gradually increased back to 65 ug/m^3 by 2024. Unlike Panipat, the air quality in Jind increased sharply to reach a peak of almost 100 ug/m^3 by early 2021. However, after reaching this peak, there has been a constant decline in air quality. By mid-2024, the air quality in Jind has decreased to almost 60 ug/m^3.

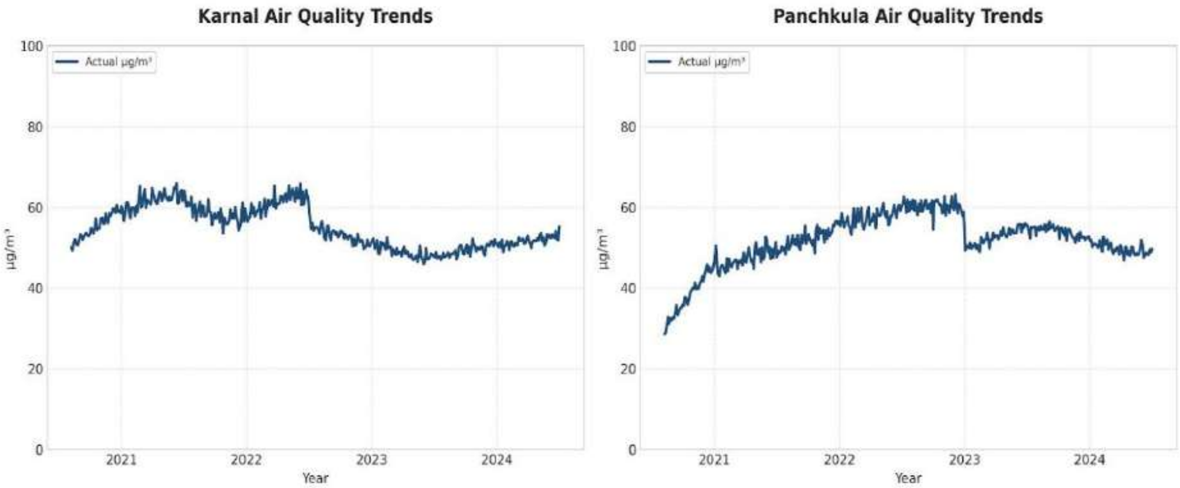

Fig.8. Air Quality Trend Analysis in Karnal and Panchkula (2020–2025)

The figure provided below presents the air quality trends for both cities from late 2020 to mid-2024. As presented in the figure, both cities demonstrate relatively lower overall pollutant concentration compared to previous datasets. The peak concentration for both cities remains below 70 ug/m^3. The air quality trend for Karnal demonstrates a plateau from 2021 to 2022, with concentrations ranging between 55 and 65 ug/m^3. It then reduces moderately by the start of 2023 and increases slightly and steadily to reach 55 ug/m^3 by 2024. The air quality trend for Panchkula demonstrates a sharp increase from a minimum of 30 ug/m^3 in 2020 to a peak of 60 ug/m^3 by the end of 2022. Similar to several cities in this dataset, Panchkula also demonstrates a sharp drop in concentration by the start of 2023. However, by then, Panchkula demonstrates a very stable concentration, with a minor variation around 50 ug/m^3 by mid-2024.

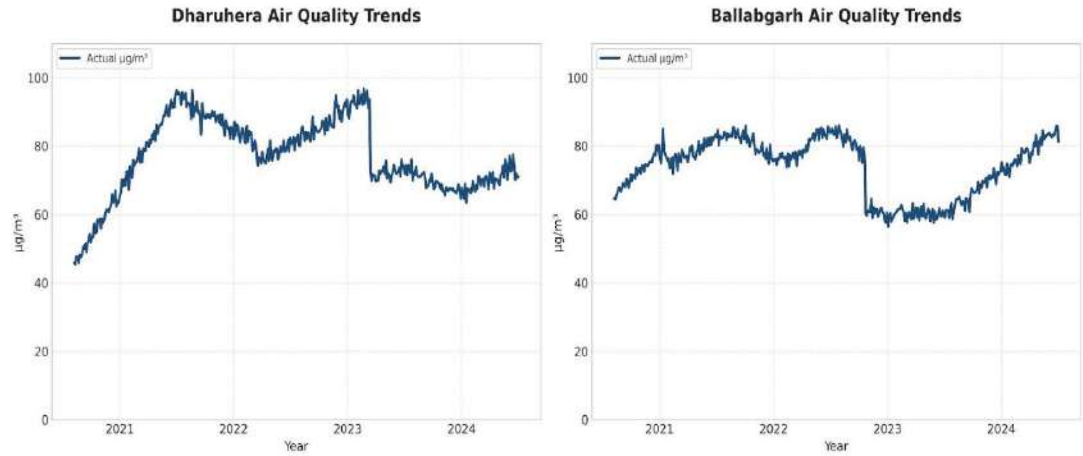

Fig.9. Air Quality Trend Analysis in Dharuhera and Ballabgarh

The figure provided indicates air quality over time for Dharuhera and Ballabgarh from late 2020 to mid-2024. It is represented in units of ug/m$^{3.}$ As shown in the figure, Dharuhera has a double peak in late 2021 and then again in late 2022, both times reaching almost 100 ug/m3. It then significantly drops to around 70 ug/m^3 at the start of 2023. It then plateaus before rising moderately in early 2024. Ballabgarh follows a similar trend with multiple peaks between 80 and 85 ug/m^3 between 2021 and 2022. Similar to several other cities in this dataset, Ballabgarh has a significant vertical drop to a baseline of around 60 ug/m^3 at the start of 2023. However, over 2024, there has been a steady and consistent increase. By mid-2024, Ballabgarh has risen back to almost 85 ug/m$^{3.}$

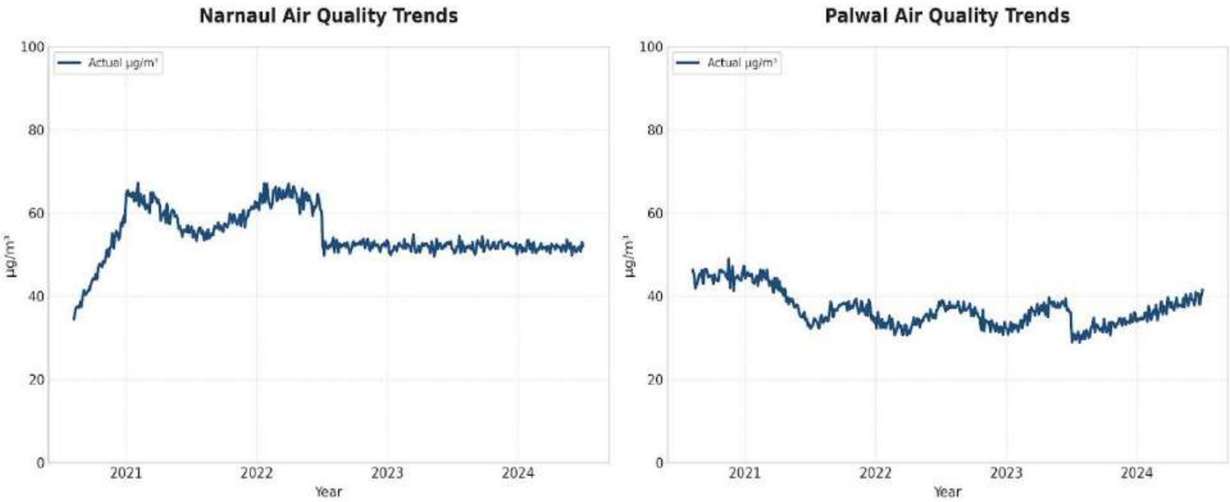

Fig.10. Comparative Analysis of Air Quality Variability in Narnaul and Palwal Regions

The figure provided illustrates the air quality trends for Narnaul and Palwal from late 2020 through mid-2024. Of all the cities considered, these two have the lowest overall pollutant concentrations, with neither city exceeding 70 ug/m^3. The city of Narnaul has had two spikes, both of which were about 65 ug/m^3, once in early 2021 and once in early 2022, followed by a sharp drop in early 2023. Since then, this city has maintained a remarkably steady state of about 52 ug/m^3 through 2024. The city of Palwal has a fluctuating, cyclical pattern, but with a much lower intensity overall. It started in late 2020, dipping in 2022, and hit a low point of about 30 ug/m^3 in early 2023. Unlike all the other cities, which have maintained a horizontal line since the drop in early 2023, the city of Palwal has a steady rise starting in late 2023, reaching back up towards 40 ug/m^3 by mid-2024.

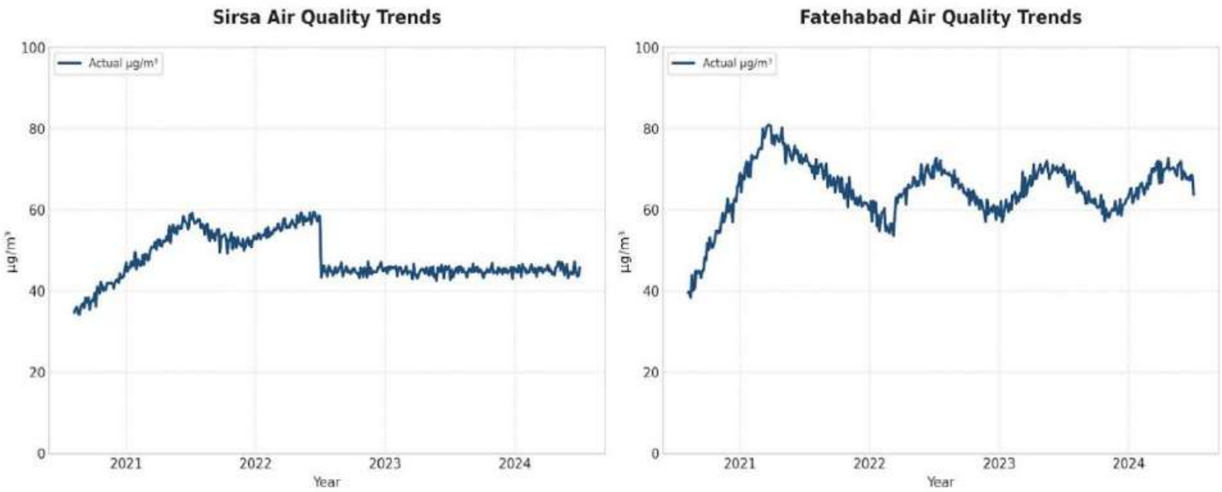

Fig.11. Analysis of Air Quality Variability in Sirsa and Fatehabad Regions

The figure provided plots the trends in air quality for Sirsa and Fatehabad from late 2020 to mid-2024 in terms of ug/m^3. From the figure, it is evident that for Sirsa, the concentration of pollutants increased steadily throughout 2020, starting at a concentration of around 35 ug/m^3 before peaking at a concentration of around 60 ug/m^3 in late 2022. Following this peak, there is a vertical drop in concentration in early 2023 before settling at a remarkably consistent concentration of around 45 ug/m^3 throughout 2024. For Fatehabad, however, the plot shows a more cyclical pattern for the concentration of pollutants throughout the period. Following a peak concentration in early 2021 of approximately 80 ug/m^3, the plot shows annual fluctuations between a concentration of 60 ug/m^3 and a concentration of 75 ug/m^3. Unlike the remarkably consistent pattern observed for Sirsa, Fatehabad maintains this cyclical pattern throughout the period

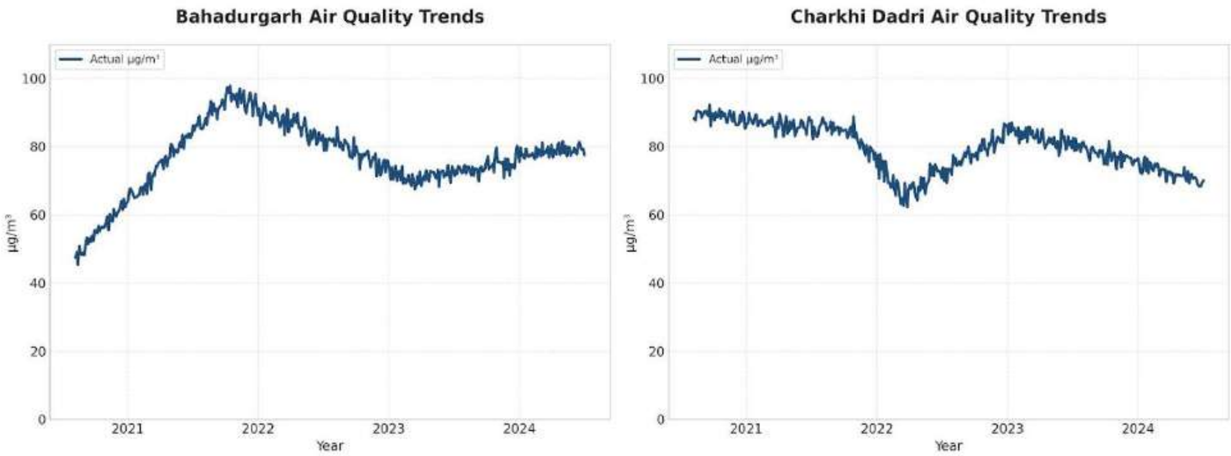

Fig.12. Analysis of Air Quality Variability in Bahadurgarh and Charkhi Dadri Regions

The figure provided indicates the air quality trends for Bahadurgarh and Charkhi Dadri from late 2020 to mid-2024. The air quality is represented in terms of ug/m^3. Bahadurgarh initially recorded a sharp increase in air quality. It began around 50 ug/m^3 and peaked around 100 ug/m^3 by the end of 2021. It then gradually decreased to a minimum of 70 ug/m^3 in 2022 before rising to around 80 ug/m^3 in 2024.

In Charkhi Dadri, air quality began at a high point of around 90 ug/m^3 in 2020 and continued with a slight decline. It then sharply dropped to around 65 ug/m^3 in early 2022. It then rose to a peak of around 85 ug/m^3 in early 2023 before maintaining a steady decline to around 70 ug/m^3 by mid-2024. Unlike other cities, both cities recorded a gradual and fluctuating change in air quality.

III. CONCLUSION

The air pollution level in Haryana during winters is one of the critical environmental issues, which is affected by the meteorological factors and various emission sources. The analysis reveals the variation in the air pollution level in the districts, which is due to the variation in the level of industrialization, urbanization, and agricultural activities. Although it was observed that significant improvements occurred in the air pollution level during the early part of 2023, it was not sustained over the period, and the trends showed stabilization or increasing trends in 2024. The major cities, such as Gurugram, Faridabad, Manesar, etc., are affected due to higher air pollution levels.

The cities such as Panchkula and Karnal show relatively better air quality trends, which reveal the success of the measures implemented in these regions. The analysis reveals the importance of the long-term measures for the improvement of air quality, along with the immediate measures. The Winter Action Plan focuses on the combination of immediate measures along with the long-term measures for the improvement of air quality.

REFERENCES

[1] Central Pollution Control Board (CPCB). (2023). *National Air Quality Monitoring Programme (NAMP) Report*. Ministry of Environment, Forest and Climate Change, Government of India, New Delhi, India.

[2] Central Pollution Control Board (CPCB). (2022). *Guidelines for Air Quality Management in India*. CPCB, New Delhi, India.

[3] Government of India. (2019). *National Clean Air Programme (NCAP)*. Ministry of Environment, Forest and Climate Change (MoEFCC), New Delhi, India.

[4] World Health Organization (WHO). (2021). *WHO global air quality guidelines: Particulate matter ($PM_{2.5}$ and PM_{10}), ozone, nitrogen dioxide, sulfur dioxide and carbon monoxide*. WHO, Geneva, Switzerland.

[5] World Health Organization (WHO). (2018). *Ambient air pollution: A global assessment of exposure and burden of disease*. WHO, Geneva, Switzerland.H

[6] Health Effects Institute (HEI). (2020). *State of global air 2020*. Special Report, HEI, Boston, MA.

[7] Health Effects Institute (HEI). (2023). *State of global air 2023 report*. HEI, Boston, MA.

[8] Ministry of Environment, Forest and Climate Change (MoEFCC). (2020). *India state-level climate change trends and air quality status report*. Government of India, New Delhi, India.

[9] Haryana State Pollution Control Board (HSPCB). (2023). *Annual air quality status report of Haryana*. HSPCB, Panchkula, India.

[10] IQAir. (2024). *World air quality report 2024*. ⟨https://www.iqair.com⟩ (accessed Month Day, Year).

[11] Gurjar, B. R., Ravindra, K., and Nagpure, A. S. (2016). "Air pollution trends over Indian megacities and their local-to-global implications." *Atmospheric Environment*, 142, 475–495.

[12] Sharma, M., and Dikshit, O. (2016). *Comprehensive study on air pollution and greenhouse gases (GHGs) in Delhi*. Indian Institute of Technology Kanpur, Kanpur, India.

[13] Kumar, P., et al. (2020). "The nexus between air pollution, climate change and human health in India." *Atmospheric Chemistry and Physics*, 20, 1–21.

[14] Jain, S., and Sharma, S. K. (2021). "Wintertime air quality deterioration in North India: Role of meteorology and emissions." *Environmental Pollution*, 268, 115–128.

[15] Singh, V., et al. (2019). "Impact of crop residue burning on air quality in northern India." *Aerosol and Air Quality Research*, 19(5), 1234–1245.

[16] European Environment Agency (EEA). (2020). *Air quality in Europe – 2020 report*. EEA, Luxembourg.

[17] United Nations Environment Programme (UNEP). (2021). *Actions on air quality*. UNEP, Nairobi, Kenya.

International Journal of Environment, Agriculture and Biotechnology
Vol-11, Issue-2; Mar-Apr, 2026
Peer-Reviewed International Journal
Journal Home Page Available: https://ijeab.com/
Journal DOI: 10.22161/ijeab

Community Perceptions and Spatial Patterns of the Effectiveness of Human-elephant conflict Mitigation strategies Around Mikumi National Park, Tanzania

Deusdedith Bwenge Fidelis[1,2*], Reuben Mpuya Joseph Kadigi[1], Vedasto Gabriel Ndibalema[1], Robert Modest Byamungu[1]

[1]Department of Wildlife Management, SUA, P.O. Box 3073, CHUO KIKUU, Morogoro.
[2]Tanzania Wildlife Research Institute, P.O. Box 661, Njiro, Arusha.
* Corresponding Author email: deusdedith.fidelis@tawiri.or.tz

Received: 13 Mar 2026; Received in revised form: 11 Apr 2026; Accepted: 16 Apr 2026; Available online: 25 Apr 2026

Abstract— *Human–elephant conflict is a critical challenge in elephant-dominated landscapes, significantly affecting community livelihoods. Various mitigation measures have been implemented to reduce conflicts and promote coexistence, yet evidence of their effectiveness in deterring elephant incursions remains limited. In villages adjacent to Mikumi National Park (MNP), similar strategies as used in other elephant-dominated areas have been applied, but their efficacy has largely been undocumented. This study evaluated the perceived effectiveness of these measures using household questionnaires with a five-point Likert scale (1 = extremely less effective; 5 = extremely effective). Descriptive analyses estimated mean scores, while Kendall's coefficient of concordance (W) and Fleiss' Kappa assessed the level of agreement among respondents. Spatial patterns were analyzed in QGIS by overlaying village boundary shapefiles with perception scores to generate heatmaps of mitigation effectiveness. Results show that the perceived effectiveness of mitigation measures ranged from low to moderate, with considerable variation across mitigation strategies. Kendall's W was weak but statistically significant agreement among respondents, reflecting respondents' rankings were not random. This supported the null hypothesis that communities generally share similar perceptions of mitigation effectiveness. Nevertheless, the weak agreement among respondents reflects diverse experiences and local contexts. Spatially, the effectiveness of mitigation strategies was unevenly distributed across villages, underscoring the need for locally tailored interventions and context-specific approaches. Based on these findings, this study advocates combined mitigation methods to achieve utmost efficacy and recommends further complement to existing strategies by use of biological control methods particularly use of lions' and army ants' scents to scare elephants.*

Keywords*— *Biological control methods, Elephant conflicts, Elephant Conflict mitigations, Mitigation effectiveness, Mitigation effectiveness patterns

I. INTRODUCTION

Human–elephant conflict is a critical issue in Africa and Asia, posing threats to both human livelihoods and elephant conservation (Raycraft *et al*., 2024; Zang *et al*., 2024). Various mitigation measures have been implemented to reduce conflicts, promote coexistence, and support long-term ecosystem sustainability (Shaffer *et al*., 2019; Montgomery *et al*., 2021). Common strategies include chili-based deterrents, flashlights, shouting and banging objects, digging trenches, beehive fences, live fences, electric fences, and watchtowers (Gunaryadi & Hedges, 2017; Montgomery *et al.,* 2021). The effectiveness of these measures, however, varies across locations and is intended to increase local tolerance of elephants and willingness to coexist (Kissui *et al*., 2019; Terada *et al*., 2021).

Despite widespread implementation, the actual efficacy of conflict mitigation measures is rarely evaluated systematically, limiting the ability of communities to make informed decisions (Kapos *et al*., 2009; Artelle *et al*., 2018). This knowledge gap is particularly problematic in areas with high wildlife populations, where ineffective mitigation can exacerbate human–elephant conflicts (Gunaryadi & Hedges, 2017; Montgomery *et al*., 2021). Consequently, there is a pressing need for community-based evaluations to assess the cost-effectiveness and practical outcomes of mitigation strategies, thereby supporting sustainable human–elephant coexistence.

Human–elephant conflict mitigation strategies effectiveness has been studied extensively across elephant-dominated landscapes, providing insights into mitigation effectiveness under varying ecological and socio-economic contexts. In West Bengal, India, Chakraborty & Nabanita, (2021) evaluated community-based interventions in areas affected by crop-raiding Asian elephants and found only partial effectiveness of commonly applied measures. In southern India, Prasad *et al*., (2025) examined mitigation decisions across elephant conflict zones and highlighted the role of environmental and socio-economic factors in shaping community responses. In Indonesia, near Way Kambas National Park, Gunaryadi & Hedges, (2017) documented high success of chilli-based deterrents in reducing elephant incursions at the farm scale. In western Thailand, Van de Water & Matteson, (2018) assessed mitigation outcomes across villages and reported that firecrackers were more effective than non-electrical fences or watchtowers. Across Africa, Montgomery *et al*., (2021) conducted multi-country evaluations of interventions to protect crops from African elephants, emphasizing context-specific effectiveness. Despite this growing body of research, systematic assessments of mitigation effectiveness remain limited in Tanzania, particularly in villages surrounding Mikumi National Park (MNP), highlighting a critical knowledge gap that this study aims to address.

In villages surrounding MNP, mitigation measures have been widely employed to reduce crops and property damage and associated economic losses (Chang'a *et al*., 2017). However, there is limited information on how local communities perceive the effectiveness of these interventions, which constrains evidence-based decisions regarding their use. This study therefore aims to assess the effectiveness of existing mitigation measures in villages adjacent to MNP by examining community perceptions.

Specifically, the study assessed: (1) the perceived extent of effectiveness of the available mitigation measures, and (2) the spatial patterns of mitigation effectiveness across communities. It was hypothesized that communities would have similar perceptions on mitigation measures effectiveness in minimizing effects of human-elephant interactions within the surveyed villages. Furthermore, it was predicted that the effectiveness of mitigation measures would be consistent across the surveyed communities.

II. CONCEPTUAL FRAMEWORK FOR HUMAN-ELEPHANT INTERACTIONS

To guide this study, a conceptual framework integrating Human–Wildlife Conflict (HWC) theory and Social–Ecological Systems (SES) theory is adopted to examine how socio-ecological factors shape human–elephant interactions (HEI) and influence the effectiveness of conflict mitigation strategies (Fig. 1). The framework links ecological processes, human wellbeing, institutional governance, community resilience, and adaptive capacity to both direct and indirect effects of HEI, highlighting feedback loops through which repeated interactions shape community attitudes, governance responses, and long-term conservation outcomes (Barua et al., 2013; Shaffer et al., 2019; Zang et al., 2024). Indirect effects—such as psychosocial stress, disrupted routines, reduced safety, and food insecurity—accumulate over time, affecting household and community wellbeing and shaping perceptions of mitigation effectiveness (Mayberry et al., 2017; Jadhav & Barua, 2012).

Central to the framework are ecological and landscape drivers, including elephant and human population densities, shared access to water and forage, and human land-use patterns around protected areas. Habitat fragmentation, agricultural expansion, and settlement growth along park boundaries increase spatial overlap between farms and elephant movement routes, triggering crop raiding, property damage, night-time farm guarding, and household tensions (Barua et al., 2013; Shaffer et al., 2019; Zang et al., 2024). Empirical studies in Tanzanian landscapes, including Mikumi, indicate that these drivers strongly influence the timing and spatial distribution of elephant foraging in human-dominated areas (Sampson et al., 2021; Tripathy et al., 2022).

HEI generates direct effects—crop loss, property and livestock damage, and occasional human injury—that subsequently trigger indirect effects, including psychosocial stress, disrupted routines, reduced productivity, food insecurity, and economic vulnerability (Sitati et al., 2003; Sampson et al., 2021; Nyumba et al., 2020). Psychosocial impacts, such as fear, sleep disruption, and anxiety, reduce mental wellbeing and alter household dynamics, influencing how communities perceive mitigation strategies (Barua et al., 2013; Mayberry et al., 2017).

Institutional interventions, including compensation schemes, fencing, chili-based deterrents, and community engagement, moderate HEI outcomes. However, perceived inefficiencies, delays, or inequities can erode trust in governance, reduce tolerance for elephants, and weaken support for conservation policies (Naughton-Treves et al., 1998; Ogra & Badola, 2008; Zang et al., 2024). Household and community factors—wealth, livelihood diversity, social networks, farm location, and governance effectiveness—further shape vulnerability, either buffering or exacerbating indirect effects and influencing community perceptions and spatial patterns of mitigation effectiveness (Nyumba et al., 2020; Barua et al., 2013).

Overall, this conceptual framework links ecological drivers, socio-economic vulnerabilities, and governance responses to both direct and indirect impacts of HEI. It emphasizes feedback loops whereby community experiences and perceptions of mitigation strategies influence future exposure, risk, and conservation outcomes, providing a foundation for evidence-based interventions and spatially targeted management in Mikumi and similar human–elephant landscapes.

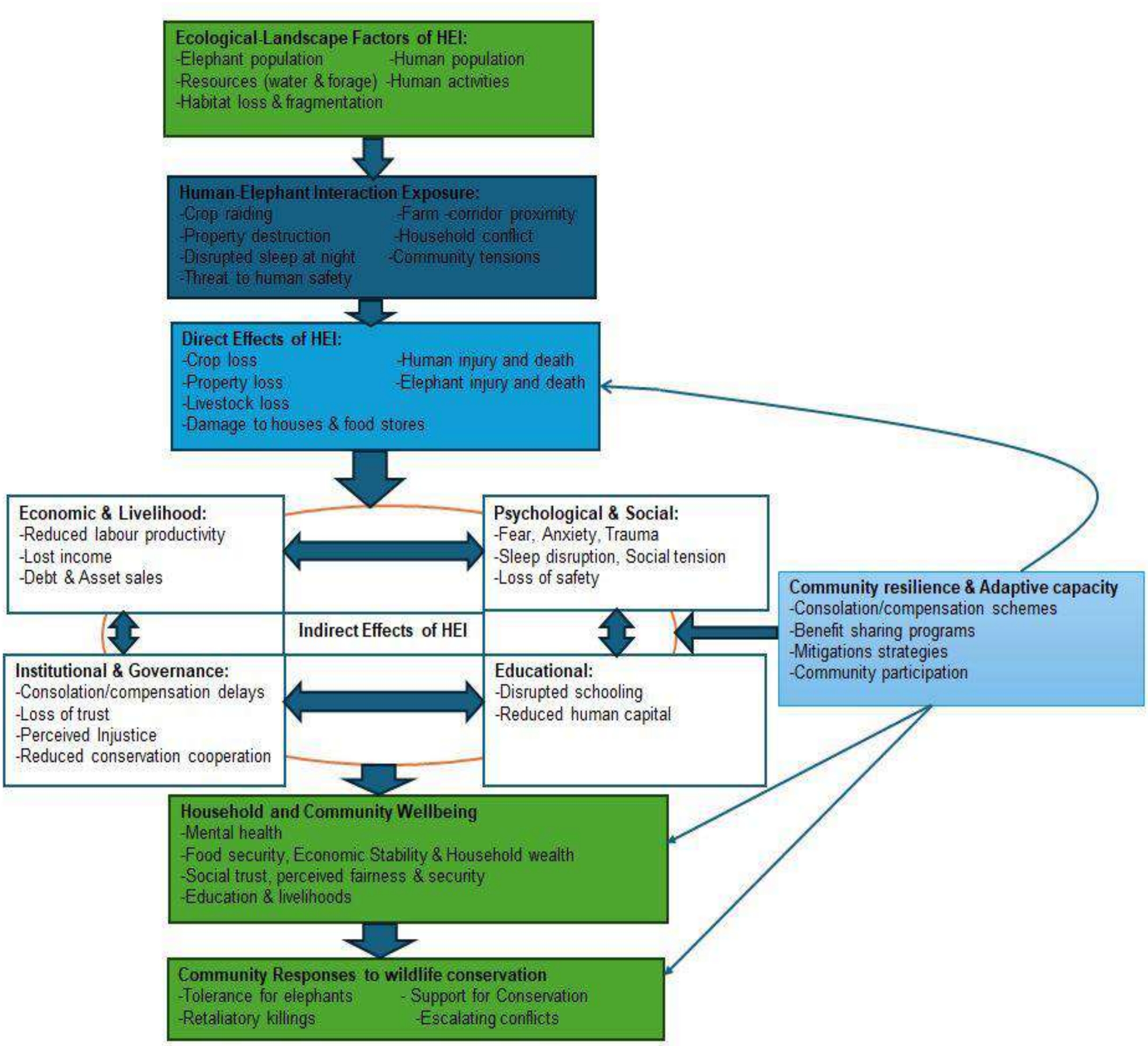

Fig.1 Conceptual framework model for human-elephant interactions illustrating how socio-ecological factors interact to produce direct and indirect effects (Adopted from Human–Wildlife Conflict theory & Social–Ecological System theory)

Guided by the conceptual framework of human–elephant interactions, this paper evaluates elephant mitigation effectiveness as an intervention point within the causal pathway linking direct elephant incursions to the indirect socio-economic and psychosocial effects on communities. Within the framework, mitigation measures are expected to disrupt or weaken the transmission of direct effects, such as crop damage and incursions into broader livelihood and wellbeing consequences. Assessing community-perceived effectiveness therefore provides a critical test of whether existing mitigation strategies meaningfully reduce exposure, vulnerability, and severity of human–elephant interaction outcomes.

III. METHODOLOGY

3.1 Study area

The study was conducted in ten villages bordering Mikumi National Park (MNP) in south-eastern Tanzania: Mikumi, Ihombwe, Kitunduweta, Mhenda, Mbamba, Kiduhi, Kilangali, Mkata, Doma, and Maharaka (Gunn *et al*., 2013; Fig. 2). These villages are part of the broader Nyerere–Mikumi–Selous landscape, which supports one of Tanzania's largest elephant populations, estimated at approximately 15,217 individuals (Lohay *et al*., 2020). Human–elephant interactions in these communities have historically led to intense conflicts, including crop raiding, human injuries and fatalities, and retaliatory killings of elephants (Gunn *et al*., 2013; Mayengo *et al*., 2017). To reduce these conflicts, a range of mitigation strategies have been implemented across the villages, including chili-based deterrents, beehive fences, trenches, and community guarding systems (Chang'a *et al*., 2016). The varied socio-ecological and livelihood contexts of the villages, combined with these interventions, provide the framework for assessing the effectiveness of mitigation measures in reducing the impacts of human–elephant interactions.

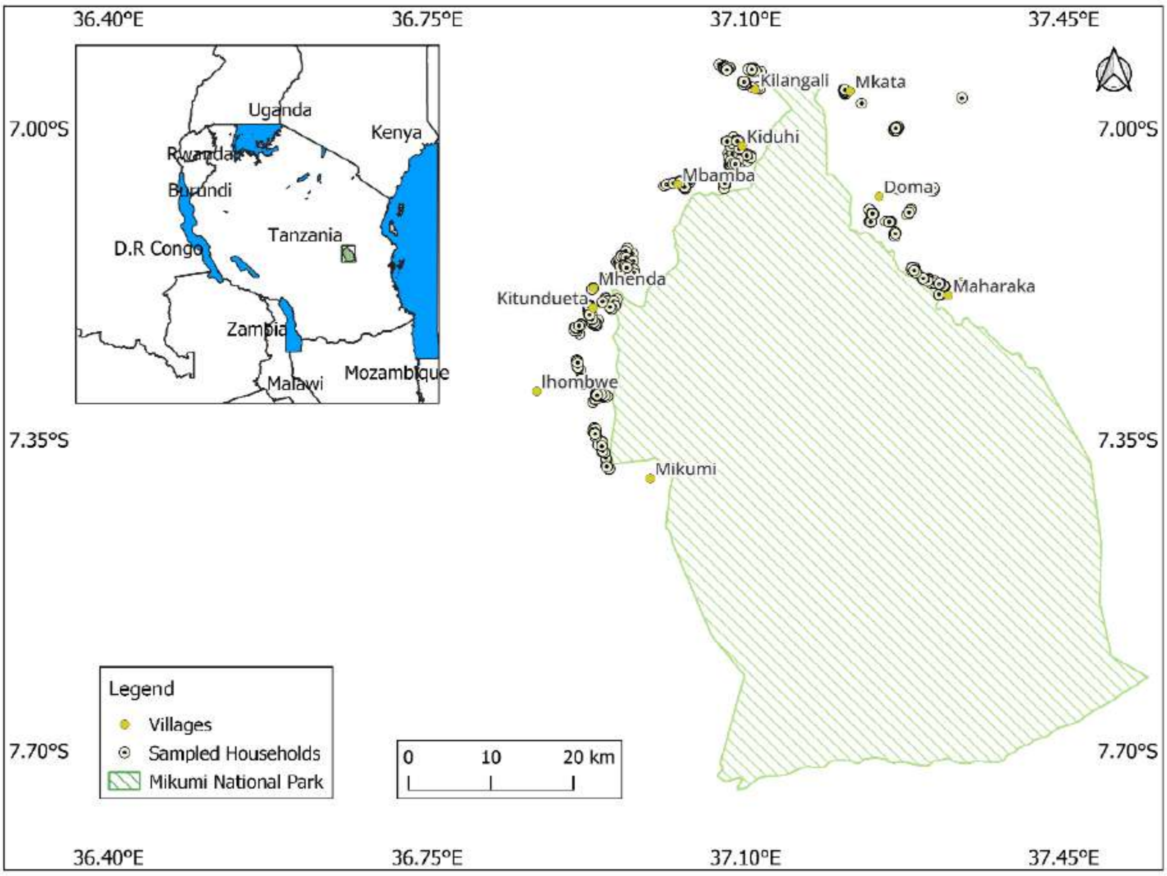

Fig.2 Locations of sampled households in villages adjacent to MNP (January-December 2023)

3.2 Study design and sampling strategy

The study employed a repeated cross-sectional observational design, using both closed- and open-ended questionnaires administered during the wet and dry seasons of 2023. The wet season, spanning January to June, coincides with peak crop cultivation and adequate rainfall for agricultural activities, while the dry season, from July to December, is characterized by reduced rainfall and drought conditions. Household surveys were conducted among 405 households across ten villages directly bordering Mikumi National Park (MNP). Villages were purposively selected based on a documented history of human–elephant conflict, accessibility, and direct adjacency to the park. The sample size was determined using Cochran's formula 1977 shown in equation (1) to ensure statistical representativeness (Uarkarn *et al.,* 2021).

$$n_0 = \frac{Z^2 \cdot P \cdot Q}{e^2} \dots\dots\dots (1)$$

Where $n_0$is the required sample size, $Z = 1.96$ corresponds to the 95% confidence level, $P = 0.5$is the estimated population proportion to maximize sample size, $Q = 1 - P$, and $e = 0.05$ represents the 5% margin of error.

Household selection followed a systematic sampling approach. The first household was selected from the one nearest the village office, and subsequent households were chosen using a sampling interval calculated by dividing the total number of households in each village by 40. Only 1 respondent from each household was interviewed from either of the household heads, spouses, or any other adult aged 18 years older who had resided in the household for at least 12 months. Questionnaires were translated into Kiswahili and pretested on 20 households in Sewe and Mangae villages neighboring villages. These pretested villages did not participate in the survey.

Furthermore, prior to data collection, ethical clearance and research permits were obtained from relevant national institutions and local government authorities. Study objectives were clearly explained to respondents, and verbally informed consent was secured, with participation being entirely voluntary and without financial incentives. Strict confidentiality and anonymity were maintained throughout the research. Also, interviews with households affected by severe elephant-related losses, including injury or death of family members, were conducted sensitively to minimize emotional distress.

3.3 Data collection methods

Respondents were asked to evaluate the perceived effectiveness of existing mitigation measures used to prevent or deter elephant incursions into homesteads and/or agricultural fields, thereby reducing crop damage, property destruction, injuries and other elephant-related losses, following the approach of Shrestha *et al*. (2025). Prior to the main survey, a reconnaissance survey was conducted within the study area to identify mitigation strategies currently implemented by local communities. Based on this assessment, a standardized list of mitigation measures was developed and presented to respondents. Participants were then asked to rate the perceived effectiveness of each measure in deterring elephants using a five-point Likert scale ranging from 1 (extremely ineffective) to 5 (extremely effective). In addition, GPS coordinates were recorded for each interviewed household to enable spatial mapping of mitigation effectiveness patterns across the study area as in Mamboleo *et al.* (2021).

3.4 Data analysis

Descriptive statistical analyses were conducted using RStudio version 4.3.1 based on R (programming language) (R Core Team, 2020) to estimate mean perception scores for each mitigation method. Data was reshaped using the *pivot_longer* function to generate summary tables for comparative analysis. The internal consistency and reliability of Likert-scale items used to measure community perceptions of mitigation effectiveness were evaluated using Cronbach's Alpha, with values of 0.70 or higher considered acceptable. Respondents' consensus on the perceived effectiveness of mitigation measures was assessed using Kendall's coefficient of concordance followed by Fleiss' Kappa test on reliability of agreement among respondents. Spatial patterns in perceived mitigation effectiveness were analyzed using QGIS by overlaying village boundary shapefiles with respondents' perception scores to generate heatmaps highlighting spatial hotspots of mitigation effectiveness across surveyed villages.

IV. RESULTS

4.1 Effectiveness of mitigation measures

The mean scores for effectiveness of elephant conflicts mitigations for communities adjacent to MNP are shown in Table 1. Overall, the respondents' rating shows that most of conflict mitigation effectiveness was between moderate to low. Digging trenches around farms and homestead, Flashlights, and Making noise /shouting through bang of tins and other noise making objects with mean scores 2.61, 2.38, and 2.18 respectively. Consolation scheme, Disturbance of elephants by shooting, and Use of human urine to scare elephant were ranked between not effective at all and less effective with mean scores 1.32, 1.21 and 1.11 respectively. Kendall's coefficient of concordance test (W = 0.222, df(9) = 809.19, p < 0.001), indicating weak positive agreement among respondents on the perceived levels of effectiveness of the 10 elephant conflict mitigation measures**.**

Although the magnitude of concordance is relatively low, the significant result indicates that respondents' rankings of mitigation strategies are not random and reflect a consistency of agreement between the levels of effectiveness of the mitigations assigned by respondents. This accepts the null hypothesis which stated that; Communities would have similar perceptions on mitigation measures effectiveness towards minimizing effects of Human-elephant interactions within the surveyed villages. However, the weak agreement among respondents reflects the diverse perceptions and experiences among respondents, highlighting the need specific tailored conflict mitigations at specific localities because effectiveness of mitigation measures might vary depending on the context, location, or specific scenario.

Table 1 Communities' perceived effectiveness of elephant conflicts mitigations

Mitigation Method	Mean score effectiveness
Digging trenches around the farms	2.61
Flashlights and fire lights	2.38
Making noise /shouting through bang of tins and other noise making objects	2.18
Chilli fences and Oils	1.95
Building fences around the farms/houses	1.88
Chilli bombs	1.70
Beehives fences	1.62
Consolation/compensation schemes	1.32
Disturbance of elephants by shooting	1.21
Use of human urine to scare elephant	1.11
Kendall's Coefficient of Concordance among respondents (W = 0.222)	
Key:1= Extremely less effective, 2=Less effective,3=Moderate,4=Effective,5= Extremely effective	

4.2 Elephant conflict mitigation effectiveness patterns

The perceptions of local communities on elephant conflict mitigation patterns in villages adjacent to MNP is shown on Fig. 3. Mikumi, Mhenda, and Maharaka villages show dark shading as highly effective mitigations, indicating that respondents believed their conflict mitigations work relatively well to evict elephants and reduce conflicts between humans and elephants.

On the other hand, Kilangali and Mkata villages show lighter shading, indicating that measures are viewed between less effective to extremely less effective. In these locations, communities may still be experiencing significant challenges despite the interventions in place. Other villages like Kiduhi and Doma had perceptions of moderate effectiveness of conflict mitigations. The results highlight that some progress has been made in managing elephant conflicts, and that effectiveness mitigation strategies is not uniform across all villages. Fleiss Kappa test results for consistency of respondents on the effectiveness of mitigation measures (K= -0.011, p = 0.379), indicating very low level of agreement among respondents, slightly worse than what would be expected. The p-value shows that this lack of agreement is not statistically significant, meaning the differences in opinions could easily occur by chance. This rejects the Prediction which stated that effectiveness of mitigation measures would be consistent across the surveyed communities.

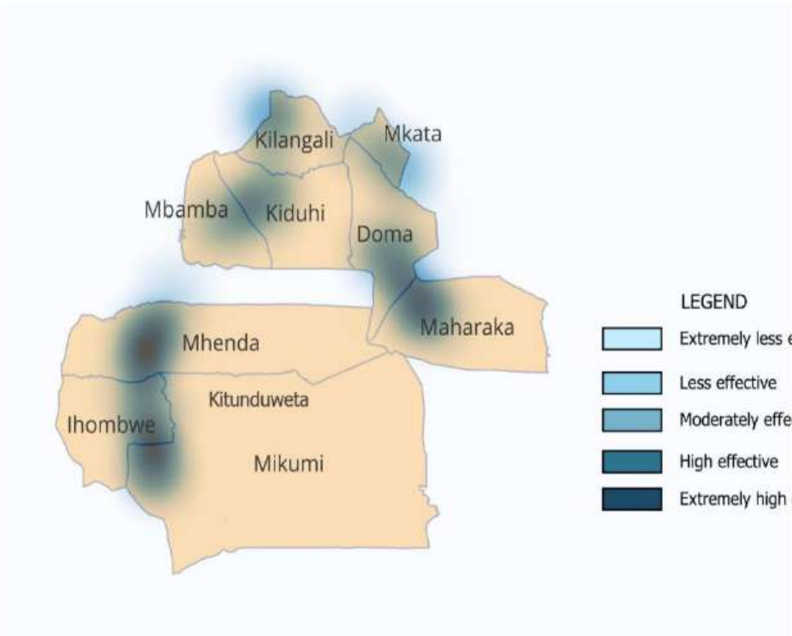

Fig.3 The heatmap of patterns of community perceptions of mitigation effectiveness against human–elephant interaction conflicts across villages

V. DISCUSSION

5.1 Effectiveness of mitigation measures

Perceived effectiveness of elephant conflict mitigation measures was generally low, with digging trenches ranked highest and compensation schemes, shooting, and human urine ranked lowest. This indicated that the problem is only partially managed and elephant conflicts remain a persistent challenge to villagers. Consistent with the conceptual framework of human–elephant interactions used in this study; ineffective or uneven mitigation measures sustain exposure to direct elephant encounters and perpetuate indirect community-level effects. Reasons for limited success of mitigation strategies potentially include elephants' adaptability behavior to learn and adjust in response to deterrents used. Some strategies are Site-specific working better in one area than in other areas. Further, local communities often operate with limited resources leading to low outputs.

Similar mitigation strategies have been reported globally (Enukwa, 2017; Montgomery *et al*., 2021), including the use of spotlights, fire and noise deterrents, fences (beehive, wire, and electric), chilli-based methods, playbacks, trenches, rapid response teams, and compensation schemes. However, the effectiveness of such interventions remains widely debated (Mumby & Plotnik, 2018; Shaffer *et al*., 2019). Many methods require sustained human presence, making them labor-intensive, costly, and difficult to maintain, particularly for resource-limited communities. In addition, several techniques are sensitive to weather conditions, demand technical expertise beyond local capacity, or incur high financial costs (Montgomery *et al*., 2021). Importantly, many deterrents provide only short-term relief by displacing elephants to nearby areas, while over time elephants habituate to these methods, reducing their long-term effectiveness (Nelson *et al*., 2003).

Chakraborty and Nabanita, (2021) documented that elephant conflict mitigation strategies in West Bengal, India including noisemaking, throwing objects, elephant drives, fire lights, crop guarding, and chilli fencing were only partially effective due to elephant habituation. Elephants often became habituated to these methods, sometimes exhibiting increased aggression toward humans, splitting into smaller groups, and causing more widespread crop invasions. Similarly, Chang'a *et al*., (2017) found that chilli-based deterrents were effective only at the small scale of individual farms near MNP, Tanzania. Comparably, in Way Kambas National Park, Indonesia, chilli-based methods were highly effective when applied systematically at farm scale (Gunaryadi & Hedges, 2017), while in western Thailand's Chong Sadao District, communities perceived firecrackers as effective deterrents, while watchtowers and non-electrical fences were considered less effective (Van de Water & Matteson, 2018). These comparisons underscore the importance of implementing integrated, context-sensitive mitigation strategies, as single interventions rarely achieve uniform success across landscapes.

The low to moderate effectiveness of elephant mitigation measures in the area increases community vulnerability to crop losses, human injuries, and fatalities, leading to food insecurity, economic hardship, and emotional distress. Repeated socio-economic and psychological impacts can foster negative perceptions of elephants and conservation efforts, potentially resulting in retaliatory killings and declines in elephant populations, thereby disrupting ecosystem balance. These socio-ecological challenges underscore the urgent need for evidence-based, scientifically informed mitigation strategies to safeguard both human livelihoods and elephant conservation.

5.2 Elephant conflict mitigation patterns

The perceived effectiveness of elephant conflict mitigation measures exhibited strong spatial heterogeneity, with overall patterns of effectiveness of conflict mitigations indicating that community members do not share a common perception about effectiveness of the current mitigation measures. While some people in different villages feel the protection methods are working, in other areas villagers view mitigations are not helping much. This inconsistency could arise from differences in how each village experiences elephant encounters, differences in landscape, elephant population and movement patterns, and type of interventions used to mitigate elephant conflicts. This highlights the need for more community engagement, awareness, and possibly redesigning or localizing mitigation measures so that they are effective and recognized as such by a larger portion of the community.

Studies across Africa and Asia have consistently shown that individual mitigation methods often fail when used in isolation, and no single approach is universally effective (Enukwa, 2017; Montgomery *et al*.,2021). Optimal outcomes are achieved when multiple strategies are implemented together, supported by regular monitoring and maintenance (Enukwa, 2017; Chakraborty & Nabanita, 2021; Prasad *et al*., 2025). Combined mitigation measures have proven effective in preventing elephant incursions into farms and homesteads (Chang'a *et al*., 2016; Van de Water & Matteson, 2018), but their success also depends on households' capacity to procure and maintain the necessary tools and methods (Jasmine *et al*., 2015; Chakrapani *et al*., 2016). Elephants' ability to learn and habituate can undermine poorly maintained setups, reducing long-term effectiveness (Chakraborty & Nabanita, 2021).

In line with these findings, some study villages, such as Ihombwe and Kilangali, practice large-scale sugarcane and paddy farming with intensive irrigation schemes. These practices compel households to invest more in combined mitigation strategies, which appear to reduce elephant incursions compared to other areas. The observed variation in mitigation effectiveness highlights the need for adaptive, context-specific strategies. Approaches that have proven successful in certain areas should be reinforced and potentially replicated, while areas with weaker measures require targeted improvements or alternative methods. Such tailored interventions, informed by local conditions and continuous monitoring, are essential for sustaining long-term elephant deterrence and reducing human–elephant conflict.

VI. CONCLUSION AND RECOMMENDATIONS

This study demonstrates that the perceived effectiveness of elephant conflict mitigation measures among communities surrounding MNP is generally low to moderate, with considerable variation across villages, highlighting spatial heterogeneity of effectiveness among villages. The study further reveals weak consensus among respondents underscoring the context-specific nature of mitigation effectiveness, influenced by factors such as farming practices, resource availability, local landscapes, and elephants' adaptive behaviors.

These findings highlight the importance of integrated, context-specific mitigation strategies over single or generic measures. Communities that implement combined approaches generally experience fewer crop raids, demonstrating the value of locally tailored interventions. Long-term success depends on continuous monitoring, proper maintenance of deterrent tools, and reinforcing methods that are effective, while simultaneously addressing weaknesses in areas where measures underperform.

Based on the results of this study, the following recommendations are proposed:

1. Adopt integrated mitigation strategies: Communities should implement multiple complementary measures simultaneously, combining physical, behavioral, and biological deterrents to maximize effectiveness.
2. Incorporate evidence-based biological controls: Novel deterrents, such as the strategic use of predator scents from lions and army ants, to be deployed along known elephant movement routes and around farms and homesteads to enhance elephant repellence.
3. Tailor strategies for local conditions: Mitigation approaches could be adapted to village-specific contexts, including farm types, resource availability, and landscape features, to ensure practical applicability and community acceptance.
4. Strengthening community capacity and resource allocation: Support for procurement, maintenance, and technical training is essential to sustain mitigation efforts and prevent habituation of elephants to deterrents.
5. Monitor and evaluate effectiveness regularly: Systematic assessment of mitigation outcomes should guide adaptive management, inform policy decisions, and ensure resources are directed toward strategies that demonstrate measurable success.
6. Promote community engagement and awareness: Involving local communities in designing, implementing, and evaluating mitigation measures to enhance adoption, foster positive attitudes toward elephants, and reduce retaliatory actions.

VII. ACKNOWLEDGEMENTS

We wish to extend our heartfelt thanks to Guy W. Norton, the founding Director of the Animal Behavior Research Unit (ABRU) at MNP for financial support. We are also grateful to the ABRU-TAWIRI staff at MNP for field assistance, specifically Abdulaziz Hatibu, Shaban Fadhil, and Rekichius Kadogo.

FUNDING

Animal Behavior Research Unit (ABRU).

CONFLICT OF INTERESTS

None

DATA AVAILABILITY STATEMENT

Available on request

ETHICAL STANDARDS

Permissions to conduct the research was granted by the Tanzania Commission for Science and Technology (COSTEC) through Tanzania Wildlife Research Institute (TAWIRI) (permit No: CST00000440-2024-01120), and Sokoine University of Agriculture.

AUTHORS' CONTRIBUTIONS

DBF: Design, data collection, analysis, result interpretation, and writing draft; **VGN:** Review and supervision; **RMB:** Review and supervision; **RMJK**: Results interpretation, review and Supervision.

REFERENCES

[1] Artelle, K. A., Reynolds, J. D., Treves, A., Walsh, J. C., Paquet, P. C. & Darimont, C. T. (2018). Hallmarks of science missing from North American wildlife management. *Science Advances*, *4*(3), eaao0167

[2] Barua, M., Bhagwat, A.S.& Jadhav, S. (2013). The hidden dimensions of human wildlife conflict: Health impacts, opportunity and transaction costs. *Biological conservation* 157:309-316

[3] Chakraborty, S. & Nabanita, P. A. U. L. (2021). Efficacy of different human-elephant conflict prevention and mitigation techniques practiced in West Bengal, India. *Notulae Scientia Biologicae*, *13*(3), 11017-11017

[4] Chang'a, A., Souza de, N., Muya, J., Keyyu, J., Mwakatobe, A., Malugu, L. & Olson, D. (2016). Scaling-up the use of chili fences for reducing human-elephant conflict across landscapes in Tanzania. *Tropical Conservation Science*, *9*(2), 921-930

[5] Enukwa, E. H. (2017). Human-Elephant conflict mitigation methods: A review of effectiveness and sustainability. *Journal of Wildlife and Biodiversity*, *1*(2), 69 -78

[6] Lohay, G.G., WeatNhers, T.C., Estes, A.B., McGrath, B.C. & Cavener, D.R. (2020). Genetic connectivity and population structure of African savanna elephants (*Loxodonta africana*) in Tanzania. *Ecology and Evolution* 10(2020):11069-11089

[7] Gunn, J., Hawkins, D., Barnes, R.F.W., Mofulu, F., Grant, R.A. & Norton, G.W. 2013. The Influence of lunar cycles on crop raiding elephants; Evidence for risk avoidance. *African Journal of Ecology* 52(2):129-137

[8] Gunaryadi, D. S. & Hedges, S. (2017). Community-based human–elephant conflict mitigation: the value of an evidence-based approach in promoting the uptake of effective methods. *PLoS One*, *12*(5), e0173742

[9] Jadhav, S. & Barua, M. (2012). The Elephant Vanishes: Impact of human–elephant conflict on people's wellbeing. *Health & place*, *18*(6), 1356-1365

[10] Jasmine, B., Ghose, D. & Das, S. K. (2015). An attitude assessment of human-elephant conflict in a critical wildlife corridor within the Terai Arc Landscape, India. *Journal of Threatened Taxa*, *7*(2), 6843-6852

[11] Kapos, V., Balmford, A., Aveling, R., Bubb, P., Carey, P., Entwistle, A. & Manica, A. (2009). Outcomes, not implementation, predict conservation success. *Oryx*, *43*(3), 336-342.

[12] Kissui, B. M., Kiffner, C., König, H. J. & Montgomery, R. A. (2019). Patterns of livestock depredation and cost-effectiveness of fortified livestock enclosures in northern Tanzania. *Ecology and Evolution*, *9*(19), 11420-11433

[13] Mamboleo, A.A., Doscher, C. & Paterson, A. (2021). A computational modelling approach to human-elephant interactions in the Bunda District, Tanzania. *Ecological Modelling* 443(2021) 109449

[14] Mayberry, L.A., Hovorka, J.A. & Evans, E.K. (2017). Well-being impacts of human elephant conflict in Khumaga, Botswana: Exploring visible and hidden dimensions. *Conservation and Society* 15(3): 280-291

[15] Mayengo, G., Bwagalilo, F. & Kalumanga, E., V. (2017). Human Wildlife Conflicts to communities surrounding Mikumi National Park in Tanzania. A case of selected villages. International Journal of Environment, Agriculture and Biotechnology. 2(4):1777-1784

[16] Montgomery, A.R., Raupp, J., Mukhwana, M., Greenleaf, A., Mudumba, T. & Muruth, P. (2021). The efficacy of interventions to protect crops from raiding Elephants. *Ambio,* 51(2022):716–727

[17] Mumby, S.H. & Plotnik, M.J. (2018). Taking the Elephants' Perspective: Remembering Elephant behaviour, cognition and ecology in Human –Elephant Conflict Mitigation. *Frontiers in Ecology and Evolution* 6(122):8

[18] Naughton-Treves, L., Treves, A., Chapman, C. & Wrangham, R. (1998). Temporal patterns of crop-raiding by primates: linking food availability in croplands and adjacent forest. *Journal of Applied ecology*, *35*(4), 596-606

[19] Nelson, A., Bidwell, P. & Sillero-Zubiri, C. (2003). A review of human-elephant conflict management strategies. People & Wildlife, A Wildlife Conservation Research Unit, Born Free Foundation Partnership

[20] Nyumba, T. O., Emenye, O. E. & Leader-Williams, N. (2020). Assessing impacts of Human elephant conflicts on human well being: An empirical analysis of communities living with elephants around Maasai – Mara National Reserve in Kenya. *PLOS ONE* 15(9):14

[21] Ogra, M. V. & Badola, R. (2008). Compensating human–wildlife conflict in protected area communities: Ground-level perspectives from Uttarakhand, India. *Human Ecology, 36*(5), 717–729

[22] Prasad, S., Aditya, V., Solomon, J., & Karanth, K. K. (2025). Community mitigation decisions in elephant conflict zones of southern India depend on environmental and socio-economic drivers. *Scientific Reports*, *15*(1), 34693

[23] Raycraft, J., George, T. & Edwin, O. (2024). Sharing landscapes with megaherbivores: Human-elephant interactions northeast of Tarangire National Park. *Environmental Challenges*. 17(2024):11

[24] R Core Team, (2020). A language and environment for statistical computing. R Foundation for Statistical Computing, Vienna, Austria. [https://www.R-project.org].Accessed 10 February 2025

[25] Sampson, C., Rodriguez, S.L.; Leimgruber, P., Huang, Q. and Tonkyn, D. (2021). A quantitative assessment of the indirect impacts of Human elephant conflict. *PLOS ONE* 16(7):19

[26] Shaffer, J.L., Khadka, K,. Van den Hoek, J. & Naithani, K. J. (2019). Human elephant conflicts: A review of current management strategies and future directions. Frontiers in ecology and evolution 6(235):12

[27] Shrestha, U. B., Shrestha, S., Khanal, S., Baral, N., Dhungel, U., Shrestha, A., Neupane, D., Dahal, R.B. & Thapa, S. K. (2025). People's perceptions on the effectiveness of human-wildlife conflict mitigation measures in Nepal's Tarai Arc Landscape. *Journal of Environmental Management*, *395*, 127944

[28] Sitati, N. W., Walpole, M. J., Smith, R. J. & Leader-Williams, N. (2003). Predicting spatial aspects of human–elephant conflict. *Journal of applied ecology*, *40*(4), 667-677

[29] Terada, S., Yobo, M., Moussavou, G. & Matsuura, N. (2021). Human elephant conflict around Moukalaba–Doudou National Park in Gabon: Socioeconomic changes and effects of conservation projects on local tolerance. *Trends in Ecology and Evolution*. 14 (2021):16

[30] Tripathy, B. R., Liu, X. & Ranga, V. (2022). Demographic circumstances and people's sentiments towards elephants in the Human–Elephant Conflict Hotspot Villages of Keonjhar Forest Division in Eastern India. *Diversity*, *14*(5), 311

[31] Uarkarn, C., Chaokronithong, K. & Sintao, N. (2021). Sample size Estimation using Yamane and Cochran and Krejcie and Morgan and Green formulas and Cohen Statistical power Analysis by G*power and Comparisons. *Apheit International Journal* 10(2):76-87

[32] Van de Water, A. & Matteson, K. (2018). Human-elephant conflict in western Thailand: Socio-economic drivers and potential mitigation strategies. *PloS one*, *13*(6), e0194736.

[33] Zang, H., Guo, S., Ma, L., Su, K., Lobora, A., Hou, Y. and Wen, Y. (2024). Living with elephants: Analyzing commonalities and differences in human-elephant conflicts in China and Tanzania based on residents' perspectives. *Global Ecology and Conservation* 53(2024):14

International Journal of Environment, Agriculture and Biotechnology
Vol-11, Issue-2; Mar-Apr, 2026
Peer-Reviewed International Journal
Journal Home Page Available: https://ijeab.com/
Journal DOI: 10.22161/ijeab

Enhancing Germination and Seedling Quality of Cashew (*Anacardium occidentale* L.): A Review on Propagation Media and Seed Pre-treatments

Kumaresan Marappan[1]*, Shanmugasundaram P[2], Madhumita G[3], Pavithra Ravichandran[1], Megala Anbunathan[1], Akshaya Balasubaramanian[1] and Mathivathani Dakshinamurthy[1]

[1, 4, 5] School of Agriculture, Vels Institute of Science, Technology and Advanced Studies, Pallavaram, Chennai - 600117, Tamil Nadu, India
Email: kummutnau@gmail.com
[2] School of Pharmaceutical Sciences, Vels Institute of Science, Technology and Advanced Studies, Pallavaram, Chennai - 600117, Tamil Nadu, India
[3] School of Management Studies, Vels Institute of Science, Technology and Advanced Studies, Pallavaram, Chennai - 600117, Tamil Nadu, India
*Corresponding author: Kumaresan Marappan, kummutnau@gmail.com

Received: 15 Mar 2026; Received in revised form: 14 Apr 2026; Accepted: 18 Apr 2026; Available online: 26 Apr 2026

***Abstract*— *The production of high-quality seedlings is essential for improving the establishment, growth, and productivity of cashew (Anacardium occidentale L.). Seed germination and early seedling development are strongly influenced by propagation media and seed pre-treatment methods. Pre-treatments such as water soaking, mechanical scarification, and application of gibberellic acid (GA_3 at 50 - 200 ppm) significantly enhance germination rates from 65 - 70% in untreated seeds to 85 - 95%, while reducing mean germination time by 3 - 6 days. Propagation media enriched with organic components further improve seedling vigour; mixtures of soil, sand, and farmyard manure (1:1:1) increase seedling height, root length, and biomass by 20 - 30% compared to soil alone. Cocopeat-based media enhance moisture retention and root development, resulting in up to 25% higher root volume and improved lateral root growth. The integration of optimized media and effective pre-treatments produces synergistic benefits, including seedling survival rates exceeding 90% and more uniform growth in height, stem diameter, and leaf area. These approaches also improve physiological traits such as chlorophyll content and root-to-shoot ratio, which are critical for successful field establishment. Overall, the combined use of appropriate propagation media and seed pre-treatments enhances nursery efficiency, reduces seedling mortality, and supports sustainable cashew cultivation. Future research should focus on nutrient uptake efficiency and long-term field performance under different treatment combinations.*

***Keywords*— Cashew, cocopeat, germination, propagation media, seed pre-treatments**

INTRODUCTION

Cashew (*Anacardium occidentale* L.) is a perennial, tropical tree crop of high economic importance, cultivated primarily for its edible nuts and agro-industrial products. The successful establishment and long-term productivity of cashew orchards depend fundamentally on the production of vigorous, uniform seedlings in nursery systems [1]. Inherent challenges in cashew propagation include variable germination rates, slow emergence, and uneven seedling growth, which can lead to high mortality rates and irregular field establishment. Improving germination performance and early seedling vigour requires an integrated approach combining effective seed pretreatments and optimized propagation media. Seed priming has been widely studied as a strategy to enhance germination dynamics and seedling quality. Hydropriming (water soaking), chemical priming (e.g., urea, thio urea), and Osmo priming (e.g., potassium nitrate KNO_3) have been tested to improve seed performance. For example, priming with thio urea (5000 ppm) extended the storage life of cashew seeds and maintained >70 % germination after 13 months of storage, compared with poorer vigour in untreated seeds [2]. Chemo priming with KNO_3 (3 %) significantly increased seedling vigour index, seedling length, and the number of leaves in nursery raised rootstock seedlings [3]. In addition to chemical priming, hormonal treatments with growth regulators such as gibberellic acid (GA_3) enhance early growth traits (e.g., shoot length, leaf number) in cashew seedlings, though the optimal concentrations and timing require further refinement. Propagation media composition markedly influences water retention, aeration, nutrient availability, and root proliferation factors that are critical for uniform seedling development. Although many studies focus on simple mixtures of topsoil and sand, research indicates that substrates incorporating organic materials and finely balanced proportions of components often yield superior outcomes. In a comparative evaluation of growing media on cashew varieties, organic materials produced higher germination percentages (e.g., 93.2 %) and superior early growth parameters (height, stem diameter, leaf area) than sawdust or sawdust amended substrates, although the interaction between variety and media also significantly affected growth [4]. Studies conducted in the Philippines further reveal that media containing garden soil, compost, and coco coir dust significantly increased seedling height, leaf number, and leaf area compared with other media combinations, highlighting the importance of organic carbon sources and physical texture in nursery substrates [5]. The interaction between optimized seed pretreatments and propagation media has profound effects on key nursery performance metrics. Enhanced germination percentages, accelerated emergence times, and higher vigour indices have been reported when seeds are primed and sown in carefully formulated substrates, often resulting in improved uniformity, root mass, and survival rates critical for field establishment. Although research in cashew lags behind staple crops, analogous studies in other perennial species affirm these benefits and support their application in cashew nursery protocols. Given the economic significance of cashew and the persistent constraints in nursery propagation, there is a compelling need to synthesize existing knowledge on seed enhancement methods and media development. A comprehensive understanding of how seed pretreatments and substrate composition interact to influence germination, early growth, and seedling quality is essential for establishing standardized nursery protocols that enhance propagation success and contribute to sustainable cashew production systems.

(A) Initial stage showing seed with emergence of radicle and cotyledons.

(B) Early seedling stage with elongation of hypocotyl and emergence of plumule.

(C) Development of young leaves in the nursery bag.

(D) Established nursery seedlings showing healthy vegetative growth.

Fig.1. Stages of seed germination and early seedling development in cashew

Role of Physical Properties of Media in Seedling Growth

The physical properties of propagation media particularly porosity, bulk density, and water holding capacity are fundamental determinants of seed germination, root development, and early seedling establishment. These properties control the availability of water, oxygen, and physical space in the rhizosphere, which collectively regulate physiological processes such as root respiration, nutrient uptake, and cell elongation. Porosity and air-filled pore space govern the balance between water retention and gaseous exchange in the rooting zone. Total porosity refers to the proportion of pore volume (air + water) relative to media volume, and ideal propagation substrates often exhibit total porosities exceeding 70 - 90% to support both moisture storage and aeration, far higher than mineral soils (35 % pore space) due to their lighter texture and engineered structure. Aeration porosity the fraction of pore space filled with air after free drainage is critical for oxygen diffusion to roots; values of 20 - 30% or higher are commonly recommended for vigorous seedling growth [6, 7]. A balanced pore distribution ensures that macropores (>75 µm) provide pathways for oxygen and gas exchange, while micropores (<30 µm) retain water accessible for uptake by the root system, thus supporting both respiration and hydration simultaneously. A total porosity within this range helps maintain oxygen concentrations above the critical threshold needed for root metabolic activity and new root formation (Caron & Michel, 2021)

Bulk density the mass of dry media per unit volume affects media compaction, root penetration, and mechanical resistance to growth. Lower bulk density is generally associated with higher total porosity and enhanced aeration, facilitating root elongation and lateral root proliferation. Fine, lightweight media such as peat and cocopeat often exhibit bulk densities between 0.12-0.25 g cm^{-3}, reflecting high pore space that encourages root exploration and water uptake (physical and chemical properties of soilless media). By contrast, more compacted or heavy media restrict root elongation and can reduce nutrient and water uptake efficiency, leading to reductions in germination success and early seedling growth by 15-25% or more compared with optimal media conditions in sensitive species.

Water holding capacity (WHC) is the volume of water retained in the medium after gravitational drainage and is strongly influenced by particle size distribution and organic content. Media containing high proportions of organic matter (e.g., peat moss, coir) exhibit greater WHC, sustaining soil moisture between irrigations without causing prolonged saturation, which can lead to hypoxia [6]. Ideally, WHC should complement porosity so that water remains available in the smaller pore fractions while large pores maintain aeration. Excessively high-water retention in fine textured media without sufficient macro porosity can impede oxygen diffusion and increase the risk of anaerobic stress, negatively affecting root respiration and seedling vigour. The interaction among these physical properties directly influences root zone processes: Oxygen availability: Adequate air-filled porosity (>20%) ensures sufficient oxygen for aerobic respiration, which is vital for ATP generation and root growth; oxygen deficits reduce root elongation and nutrient uptake. Water dynamics: Balanced WHC supplies water for imbibition and metabolic processes without waterlogging, which can cause hypoxia and root decay. Mechanical resistance: Lower bulk density and proper pore architecture reduce mechanical impedance, allowing roots to penetrate and expand effectively, enhancing overall seedling establishment. Raviv et al. [7] emphasized that media with a balanced air-filled porosity (20 - 30%) and adequate water holding fraction optimize root physiological activity and nutrient uptake, as roots require both water and oxygen in close proximity to sustain metabolic activities such as cell division and elongation. Conversely, poorly structured, compact media (high bulk density, low porosity) restricts root penetration, reduces oxygen diffusion, and can decrease germination efficiency by up to 20 - 25% relative to well aerated substrates in comparable plant systems. The physical properties of propagation media particularly porosity, bulk density, and water holding capacity shape the root zone environment and determine the success of seed germination and early seedling development. Optimizing these properties through appropriate component selection (e.g., peat, cocopeat, perlite, vermiculite) and mix formulation is essential for producing vigorous and uniform seedlings in nursery propagation systems.

Sand as an Aeration-Enhancing Component

Sand is primarily incorporated into propagation media to improve drainage and aeration. Its coarse texture reduces compaction and facilitates root penetration. Hartmann et al. [15] emphasized that sand improves oxygen availability in the root zone, which is crucial during germination. Kumar and Singh [8] observed that sand-amended media increased root length by 10 - 15% and improved root architecture. However, due to its low nutrient content and poor water retention, sand alone is insufficient to support seedling growth and must be combined with other components.

Soil as a Conventional Propagation Medium

Soil is one of the most widely used propagation media in nursery systems due to its natural nutrient content, microbial diversity, and ease of availability. It provides essential macro- and micronutrients, cation exchange capacity, and buffering potential, which support seed germination and early seedling growth. However, despite these advantages, sole soil as a propagation medium often exhibits significant physical and biological limitations that can restrict seedling performance. Compaction and low porosity in many mineral soils reduce aeration and impede root penetration, limiting oxygen diffusion to the root zone, which is critical for cellular respiration and elongation. Poor aeration, in combination with inconsistent water-holding capacity, can result in hypoxic stress, reduced root proliferation, and slower nutrient uptake [3]. Pathogen contamination is also more prevalent in unsterilized or reused soils, increasing susceptibility to root rot and damping-off diseases, particularly in high-density nursery systems. Empirical studies have quantified these limitations. Seedlings grown in sole soil media often exhibit lower germination percentages (60 - 70%), reduced uniformity, and diminished vigour relative to organic-enriched or soilless media. Singh et al. [2] reported that cashew seedlings raised in soil-based media showed 18 - 25% lower biomass accumulation and shorter shoot lengths compared to those grown in mixed media containing soil, sand, and organic amendments. Reduced root length and lateral root development in soil-only substrates were attributed to mechanical impedance and suboptimal aeration, which limited water and nutrient absorption. Moreover, nutrient availability in soil can be inconsistent due to heterogeneity in texture, organic matter content, and mineral composition. In comparison, well-formulated mixed media allow controlled nutrient supply and enhanced moisture retention, promoting more uniform germination and seedling growth. These findings indicate that while soil contributes essential nutrients, its physical limitations and variable properties hinder optimal seedling development, highlighting the need for amendments or alternative substrates in modern nursery propagation [4].

Cocopeat as a Soilless Propagation Medium

Cocopeat, derived from the fibrous husk of coconut (Cocos nucifera L.), has emerged as a highly effective soilless propagation medium due to its favourable physical and hydrological properties. Its high water-holding capacity, approximately 8 - 10 times its dry weight, combined with high total porosity (85 - 95%) and low bulk density (0.12 - 0.25 g cm^{-3}), creates an optimal environment for seed imbibition, root aeration, and uniform seedling growth [9]. The superior porosity of cocopeat ensures adequate oxygen diffusion to the root zone while simultaneously retaining sufficient moisture, minimizing the risk of drought stress or hypoxia. Experimental studies in cashew nursery systems have demonstrated significant improvements in germination and seedling development when using cocopeat-based media. Prasad et al. [9] reported that cocopeat-based substrates increased germination percentage to 85 - 90%, compared with 65 - 70% in conventional soil, and enhanced root biomass by 30 - 40%. Reddy et al. [17] further observed that cocopeat facilitated improved root proliferation, lateral root density, and seedling uniformity, leading to more robust seedlings suitable for transplantation. The light texture of cocopeat also reduces mechanical impedance, allowing easier root elongation and exploration, which is critical for early nutrient acquisition and growth. Despite its physical advantages, cocopeat is low in inherent nutrients, including nitrogen, phosphorus, potassium, and essential micronutrients. Therefore, supplementation with balanced nutrient solutions or slow-release fertilizers is necessary to sustain long-term seedling growth and prevent deficiencies during nursery production. Additionally, because cocopeat is prone to compaction under repeated irrigation cycles, periodic loosening or mixing with coarse materials such as perlite or sand is recommended to maintain optimal aeration.

Vermiculite and Perlite in Media Optimization

Vermiculite and perlite are widely employed as amendments in propagation media to improve their physical and hydrological properties, thereby optimizing seedling growth and uniformity. Vermiculite, a hydrated phyllosilicate mineral, has a high cation exchange capacity (CEC) and large surface area, which enhances water retention and nutrient-holding capacity in soilless and mixed media. Perlite, a volcanic glass that expands upon heating, is chemically inert and highly porous, providing excellent aeration and drainage, reducing waterlogging, and preventing anaerobic stress in the root zone. Quantitative studies have demonstrated the benefits of these media components. Vermiculite incorporation can increase water retention of propagation substrates by 20 - 30%, whereas perlite can improve air-filled porosity and overall aeration by 15 - 25%, creating a balanced environment for root respiration and elongation [10]. Kumar et al. [11] reported that combining vermiculite and perlite in cashew nursery substrates increased germination rates by 15 - 20% and improved the seedling vigour index, including enhancements in shoot length, root length, and leaf area, compared to traditional soil or soil-sand media. Beyond physical improvements, the use of vermiculite and perlite also contributes to disease management. Improved drainage and aeration reduce the prevalence of root rot and damping-off pathogens by minimizing water stagnation in the root zone, thereby creating a less favourable environment for pathogen proliferation [12]. Additionally, vermiculite's nutrient retention capacity supports the sustained availability of macro- and micronutrients, which is particularly beneficial in nutrient-poor or soilless media. The synergistic use of vermiculite and perlite allows for the formulation of propagation media with optimal water-holding capacity, aeration, and nutrient balance, which is essential for achieving uniform germination, enhanced seedling vigour, and robust root development. Incorporating these materials is especially important in commercial nursery systems, where consistency and seedling quality are critical for successful field transplantation [10, 11].

Organic Amendments: Farmyard Manure and Vermicompost

Organic amendments are critical in optimizing propagation media by enhancing chemical, physical, and biological properties, which directly influence seedling growth and development. Farmyard manure (FYM) and vermicompost are widely used organic substrates that supply essential macronutrients (N, P, K), micronutrients, and organic matter, while also improving soil structure, water-holding capacity, and cation exchange capacity. In addition, these amendments support beneficial microbial populations, which facilitate nutrient mineralization, disease suppression, and root–microbe interactions, all of which contribute to improved seedling vigour [13, 14]. Vermicompost, produced through the decomposition of organic residues by earthworms, has been shown to significantly enhance seedling growth. Kumaresan et al. [13] reported that application of vermicompost increased total plant biomass by 20 - 35% compared with control media, attributed to enhanced nutrient availability, improved microbial activity, and the presence of growth-promoting substances such as humic acids, auxins, and cytokinins. These bioactive compounds stimulate cell division, root elongation, and overall plant vigour, making vermicompost a highly effective component in nursery substrates. Similarly, FYM incorporation into propagation media improves nutrient supply and soil physical properties. [14] observed that FYM-enriched media increased seedling height and leaf number by 25 - 30% and enhanced root proliferation due to improved substrate porosity and aeration. The gradual nutrient release from FYM ensures sustained availability throughout the early stages of seedling development, supporting uniform growth. In cashew nursery systems, the addition of organic amendments has been shown to improve the root–shoot ratio, enhance chlorophyll content, and increase overall seedling vigour, leading to higher survival rates during transplantation. The combined effects of improved nutrient availability, microbial activity, and optimized media structure facilitate the production of robust seedlings capable of rapid establishment in field conditions.

Composite Media and Synergistic Effects

Composite propagation media, which combine mineral and organic components such as soil, sand, and organic amendments, provide a balanced environment for seedling growth by integrating the advantages of individual components. Such mixtures optimize physical, chemical, and biological properties including aeration, moisture retention, and nutrient availability thereby supporting vigorous root and shoot development [15, 16]. A widely recommended formulation is soil: sand: FYM in a 1:1:1 ratio, which has been shown to produce superior seedlings in various horticultural crops. The inclusion of sand improves drainage and prevents waterlogging, FYM supplies essential nutrients and enhances microbial activity, and soil provides structural support and baseline fertility. Singh et al. [2] observed that cashew seedlings grown in such composite media exhibited germination rates of 85 - 90%, with seedling height increases of 25 - 35% relative to soil-only media. Similarly, Reddy et al. [17] reported that cashew seedlings raised in composite media achieved maximum root lengths of 15 - 20 cm, shoot growth of 30 - 35 cm, and survival rates exceeding 90%, highlighting the synergistic benefits of combining physical, chemical, and biological enhancements in propagation substrates. The synergistic effects of composite media arise from the complementary roles of their components: enhanced aeration and drainage reduce root hypoxia, organic amendments supply nutrients and stimulate beneficial microbial activity, and a mineral base ensures structural stability. Collectively, these factors improve water and nutrient uptake efficiency, promote uniform seedling growth, and reduce susceptibility to abiotic and biotic stress during early development [10, 15].

Comparative Performance of Different Media

Comparative analyses of propagation media clearly demonstrate that individual components exhibit distinct advantages and limitations. Soil provides inherent fertility but often suffers from poor aeration and compaction, limiting root penetration and germination. Sand improves drainage and reduces waterlogging but lacks organic matter and nutrient supply. Cocopeat and other soilless substrates offer excellent physical properties, including high water-holding capacity, low bulk density, and superior porosity, but require external nutrient supplementation for sustained growth [9, 17]. Vermiculite and perlite improve moisture retention and aeration, whereas organic amendments such as FYM and vermicompost enhance nutrient availability and microbial activity [13]. Raviv and Lieth [10] concluded that optimized composite media, which integrate the advantages of multiple components, can improve seedling growth and vigour by 30 - 50% compared to single-component media. Empirical evidence from cashew nurseries confirms this, showing that carefully formulated mixtures achieve higher germination percentages, increased biomass, improved root-to-shoot ratios, and enhanced survival rates [2]. These findings underscore the importance of media integration, as a single component rarely provides the combination of physical, chemical, and biological properties required for optimal seedling development.

Fig.2. Common propagation media used for seedling production

Table 1. Common propagation media used for seedling production

Propagation Medium	Source / Composition	Key Properties	Role in Seedling Production	References
Soil (Topsoil)	Natural field soil	Moderate nutrient content, low porosity, high bulk density	Provides basic nutrients and anchorage	[10]
Sand	Weathered rock particles	High drainage, low WHC, high aeration	Improves aeration and drainage	[8, 15]
Cocopeat (Coir pith)	Coconut husk residue	High WHC (8–10×), high porosity (85–95%), low BD	Promotes root growth and uniform germination	[9]
Farmyard Manure (FYM)	Decomposed animal waste	Rich in organic matter, improves WHC and nutrients	Enhances fertility and microbial activity	[13]
Vermicompost	Earthworm-processed organic matter	High nutrient content, growth hormones, microbes	Improves seedling vigour and biomass	[16, 18]
Perlite	Expanded volcanic mineral	High aeration, low density, inert	Improves drainage and aeration	[10]
Vermiculite	Hydrated mineral	High WHC, moderate aeration, high CEC	Retains moisture and nutrients	[10]
Compost	Decomposed organic residues	Rich in nutrients, microbial activity	Improves fertility and biological properties	[14, 18]
Sawdust	Wood processing by-product	Low density, high aeration, low nutrients	Used as partial medium for aeration	[4]
Coco coir dust	Processed coconut fibre	High WHC, good aeration	Enhances seedling growth and root development	[5]

Seed pre-treatments

Seed pre-treatments are widely employed in cashew nurseries to enhance germination, improve seedling vigour, and ensure uniform plant establishment. Germination variability in cashew is often due to heterogeneity in seed maturity, moisture content, physiological age, and the presence of physical or physiological dormancy [19]. Pre-sowing treatments stimulate metabolic activity, improve water uptake, and activate hydrolytic and antioxidant enzymes, thereby reducing mean germination time (MGT), improving synchrony of emergence, and promoting early seedling growth.

1. Hydropriming (Water Soaking)

Hydropriming is a cost-effective pre-treatment involving soaking seeds in water for 12 - 24 h, enabling controlled imbibition without radicle protrusion. This process initiates early metabolic processes, including activation of α-amylase, proteases, and lipases, which catalyze the hydrolysis of starch, proteins, and lipids into soluble sugars and amino acids that serve as substrates for cellular respiration and biosynthesis [19]. Rapid cellular hydration during hydropriming restores turgor, facilitates cell division and elongation, and activates mitochondrial respiration, leading to enhanced ATP production and increased synthesis of nucleic acids and proteins. Cashew seeds treated with hydropriming show germination improvements from 65 - 70% to 80 - 85%, with reductions in MGT by 2 - 4 days, while also producing more uniform seedlings suitable for transplanting. Hydropriming also improves early root length (10 - 15 cm) and shoot elongation (20 - 25 cm), contributing to a higher seedling vigour index. Similar improvements have been reported in tomato, pepper, and okra, with 10–20% increases in germination and seedling vigour [19]. Optimization requires careful attention to soaking duration, water temperature, and seed physiological age, as excessive soaking may cause nutrient leaching or hypoxic stress.

2. Hormonal Treatments (Gibberellic Acid, GA_3)

Gibberellic acid (GA_3) is a plant growth-promoting phytohormone that accelerates germination and early seedling growth through multiple mechanisms. GA_3 stimulates embryo elongation, cell division, and expansion, activates α-amylase and other hydrolytic enzymes, and enhances protein synthesis, respiration, and metabolic activity in embryonic tissues [20]. In cashew, GA_3 applied at 50 - 150 ppm increases germination to 90 - 95% and reduces MGT by 3 - 6 days [21]. Seedlings treated with GA_3 also exhibit 20 - 30% increases in shoot length, 15 - 25% increases in root length, higher chlorophyll content, larger leaf area, and improved seedling vigour. GA_3-treated seedlings show better water-use efficiency, stress tolerance, and uniform establishment in the field [17]. GA_3 application is often combined with optimized propagation media, such as soil: sand: FYM (1:1:1) or cocopeat-amended substrates, producing synergistic effects on root and shoot growth, seedling biomass, and survival rates exceeding 90% [2].

3. Osmo priming and Nutrient Priming

Osmo priming involves soaking seeds in osmotic solutions (e.g., polyethylene glycol [PEG] 6000, KCl, or NaCl) to regulate water uptake, preventing overhydration while activating metabolic pathways. This treatment enhances germination uniformity, synchronization, and stress tolerance, particularly under drought or salinity conditions, by increasing the activity of antioxidant enzymes (superoxide dismutase, catalase, peroxidase) and reducing reactive oxygen species [22]. Nutrient priming, using solutions of potassium nitrate (KNO_3), calcium, or micronutrients, supplies readily available nutrients during early germination, supporting radicle emergence, early root elongation, and shoot growth. In cashew, KNO_3-primed seeds germinate faster, with root lengths increased by 12–18% and higher vigour indices compared to unprimed seeds [2]. Osmo priming and nutrient priming can also improve seedling antioxidant capacity, photosynthetic efficiency, and resilience during transplantation.

4. Mechanical and Chemical Scarification

Scarification techniques aim to overcome physical dormancy by weakening the seed coat and improving water permeability. While cashew seeds generally exhibit low dormancy, mild mechanical or chemical scarification enhances water imbibition, reduces emergence variability, and accelerates early root and shoot elongation. Hartmann *et al.* [15] reported that scarification increased germination rates and uniformity in woody species. In cashew, seeds with thicker testa or partial coat imperfections respond particularly well, exhibiting 2 - 5% higher germination and improved initial root growth.

5. Organic and Biological Treatments

Organic pre-treatments, such as soaking seeds in cow dung slurry, compost extracts, or plant bio-extracts, supply nutrients, beneficial microorganisms, and bioactive compounds. [14] observed a 10–15% increase in germination and enhanced seedling vigour in cashew seedlings treated with organic slurries. These treatments also promote beneficial rhizosphere colonization, enhance nutrient cycling, and reduce pathogen incidence. Biological pre-treatments with plant growth-promoting rhizobacteria (PGPR) or arbuscular mycorrhizal fungi improve phosphorus and micronutrient uptake, stimulate root proliferation, and increase seedling biomass by 15 - 25%. Additionally, they enhance tolerance to abiotic stress during transplantation (23, 24). Integration of organic and microbial treatments with hydropriming or GA_3 has been shown to produce synergistic effects, yielding uniform, vigorous seedlings with superior field establishment potential.

6. Integrated Effects and Mechanistic Insights

The effectiveness of seed pre-treatments is maximized when combined with optimized propagation media. GA_3-treated seeds sown in composite media (soil: sand: FYM

1:1:1) achieve >90% germination, root lengths of 15 - 20 cm, shoot lengths of 30–35 cm, and survival rates exceeding 90% [2,17]. Hydro primed seeds in cocopeat or vermiculite-amended media show accelerated emergence, higher root proliferation, and increased vigour indices [9, 21]. These improvements result from synergistic interactions between seed metabolic activation and the physical, chemical, and biological properties of the media. Well-aerated, nutrient-rich, and moisture-retentive media enhance water availability, oxygen diffusion, enzyme activity, reserve mobilization, and microbial interactions, allowing pre-treated seeds to germinate faster, develop stronger roots, and produce robust shoots. Collectively, these processes contribute to faster, synchronized germination, higher seedling uniformity, increased biomass, and improved field establishment [19, 21].

Table 2. Common seed pre-treatments and their effects on germination and seedling development

Pre-treatment Method	Treatment Details	Mechanism of Action	Effect on Germination (%)	Impact on Seedling Growth	References
Hydropriming	Water soaking (12 - 24 h)	Activates enzymes, improves water uptake	80 - 85%	Faster emergence, better root and shoot growth	[19]
Hormonal treatment (GA_3)	50 - 150 ppm GA_3	Stimulates enzyme activity, embryo growth	90 - 95%	Increased shoot length, leaf area, vigour	[17, 21]
Nutrient priming	KNO_3 (2 - 3%) solution	Enhances nutrient availability and metabolism	80 - 88%	Improved root length and vigour index	[2]
Osmo priming	PEG / salt solutions	Regulates water uptake, induces stress tolerance	78 - 85%	Uniform germination, improved stress resistance	[22]
Scarification	Mechanical/chemical	Breaks seed coat, improves permeability	70 - 80%	Faster germination, slight growth improvement	[15]
Organic treatments	Cow dung slurry / compost extract	Supplies nutrients and beneficial microbes	75 - 85%	Enhanced vigour and microbial activity	[14]
Bio-inoculation	PGPR / mycorrhiza	Enhances nutrient uptake and root growth	80 - 90%	Increased biomass, stress tolerance	[24]
Thio-urea treatment	5000 ppm	Enhances enzyme activity and seed viability	75 - 85%	Improved germination and storage life	[2]

Integrated Effects of Seed Pre-treatments

The effectiveness of seed pre-treatments in cashew is strongly influenced by propagation media, environmental conditions, and seed physiological status. Research indicates that combining pre-sowing treatments with optimized propagation media produces synergistic effects, significantly enhancing germination, seedling vigour, uniformity, and survival [17]. For instance, cashew seeds treated with gibberellic acid (GA_3, 50 - 150 ppm) and sown in composite media composed of soil, sand, and organic amendments (1:1:1) achieved germination rates exceeding 90%, compared with 65 - 70% in untreated seeds grown in soil alone. These seedlings demonstrated enhanced root length (15 - 20 cm), shoot growth (30 - 35 cm), and biomass accumulation, as well as improved uniformity and survival rates >90% [2]. Similarly, hydro primed seeds sown in cocopeat or vermiculite-enriched media exhibited accelerated emergence, higher root proliferation, and increased vigour indices, underlining the importance of media pre-treatment interactions in nursery management [9, 21]. The synergistic benefits of combining seed pre-treatments with optimized media are attributed to the complementary effects on water availability, nutrient accessibility, oxygen diffusion, and microbial activity. Well-structured, aerated, and nutrient-rich media facilitate efficient enzymatic activity and mobilization of stored reserves, while pre-treated seeds respond more rapidly to favorable conditions. This results in faster germination, robust root systems, improved shoot growth, and uniform seedlings suitable for transplantation under field conditions.

Physiological Mechanisms Underlying Seed Pre-treatments

Seed pre-treatments enhance germination and early seedling growth by modulating several interrelated physiological and biochemical processes. One of the primary mechanisms involves the activation of hydrolytic enzymes, such as α-amylase, proteases, and lipases, which catalyze the breakdown of stored starch, proteins, and lipids in the seed into soluble sugars and amino acids. These hydrolyzed metabolites provide essential energy and building blocks for embryonic cell division and elongation, thereby supporting radicle protrusion and early seedling establishment [19]. Another critical effect of pre-treatments is the improvement of cell membrane permeability and water uptake. Techniques such as hydropriming, Osmo priming, and scarification increase the fluidity of seed cell membranes, allowing faster and more uniform imbibition of water. This rapid hydration restores turgor pressure, reactivates metabolic pathways, and prevents desiccation stress during the initial stages of germination, ensuring that the embryo can resume growth efficiently [22]. Seed pre-treatments also enhance respiration and energy production. Pre-treated seeds demonstrate increased mitochondrial activity, leading to higher rates of ATP synthesis. This elevated energy supply supports the biosynthetic processes required for radicle emergence and subsequent seedling growth, enabling seedlings to establish more rapidly under favorable conditions [20]. Furthermore, pre-treatments stimulate cell division and elongation. Hormonal applications, particularly gibberellic acid (GA_3), promote the elongation of embryonic cells, while growth regulators present in organic or microbial treatments further stimulate meristematic activity. This coordinated stimulation of cell proliferation and expansion contributes to faster root and shoot elongation, resulting in seedlings with improved structural integrity and vigour. Finally, pre-treatments facilitate the mobilization of stored reserves within the endosperm and cotyledons. Enhanced enzymatic activity ensures that nutrients and energy stored in the seed are rapidly converted into forms available for growth, supporting early seedling vigour and robust development. Collectively, these physiological mechanisms enable pre-treated seeds to germinate more rapidly, produce uniform seedlings, and develop stronger root and shoot systems. The effects are particularly pronounced when seeds are sown in well-structured, nutrient-rich, and aerated propagation media, which further optimize water availability, oxygen diffusion, and nutrient uptake. This integration of seed pre-treatment and media optimization results in seedlings with higher biomass, improved uniformity, and enhanced survival, ultimately strengthening field establishment and nursery performance [19].

Table 3. Physiological mechanisms underlying seed pre-treatments and their effects on germination and seedling development

Physiological Process	Mechanism Activated by Pre-treatment	Key Enzymes / Factors Involved	Effect on Germination	References
Enzyme activation	Pre-treatments stimulate hydrolytic enzyme synthesis	α-amylase, protease, lipase	Faster mobilization of stored reserves, early radicle emergence	[19]
Reserve mobilization	Breakdown of starch, proteins, and lipids into usable forms	Sugars, amino acids, fatty acids	Improved germination rate and uniformity	[19]
Water uptake (Imbibition)	Improved membrane permeability and hydration	Cell membrane proteins, aquaporins	Rapid and uniform germination	[22]
Respiration enhancement	Increased mitochondrial activity and ATP production	ATP, respiratory enzymes	Accelerated metabolic processes	[20]
Hormonal regulation	Increased synthesis/activity of growth hormones	Gibberellins (GA_3), auxins, cytokinins	Reduced dormancy, enhanced germination	[17]
Antioxidant activity	Enhanced ROS scavenging under stress	SOD, catalase, peroxidase	Protects cells from oxidative damage	[22]
Cell division & elongation	Activation of meristematic tissues	DNA, RNA, proteins	Faster radicle protrusion	[20]
Membrane repair	Restoration of membrane	Phospholipids,	Reduces leakage, improves	[19]

	integrity during imbibition	proteins	viability	
Nutrient uptake efficiency	Enhanced early nutrient absorption	Ion transporters, enzymes	Improved seedling establishment	[23]
Microbial interaction	Stimulation of beneficial rhizosphere microbes	PGPR, mycorrhiza	Indirect improvement in germination	[14]

CONCLUSION

This review highlights that combining optimized propagation media with seed pre-treatments significantly improves germination, seedling vigour, and survival in cashew (*Anacardium occidentale* L.). Organic-enriched media enhance root growth and nutrient availability, while treatments such as hydropriming and GA_3 promote faster and more uniform germination. The main advantages include improved nursery efficiency and higher-quality seedlings, though variability in seed quality and lack of standardized protocols remain limitations. These approaches have strong applications in nursery management and sustainable cashew cultivation. Further research should focus on standardization and long-term field performance.

REFERENCES

[1] Kumaresan, M., Shanmugasundaram, P., Sridhar, R., Madhumita, G., & Kamalakkannan, S. (2026). Exploring the multifaceted pharmaceutical and medicinal applications of cashew nut shell liquid (CNSL): Antimicrobial, anti-inflammatory and drug delivery potential. *Journal of Applied and Natural Science*, 18(1), 399 - 418.

[2] Singh, R., Kumar, S., & Singh, B. (2018). Integrated effect of media and seed treatments on cashew seedling growth. *Journal of Plantation Crops*, 46(2), 101–106.

[3] Manjusha, K., & Retheesh, P. S. (2024). Effect of nutrient priming on growth and vigour of cashew seedlings. *Journal of Plantation Crops*, 52(1), 45–50.

[4] Fawole, O. A., Aderounmu, A. F., & Adewale, B. D. (2025). Influence of growing media on germination and seedling growth of cashew (*Anacardium occidentale* L.). *Scientia Horticulturae*, 330, 112345.

[5] Ventura, W., Reyes, M., & Santos, J. (2021). Evaluation of coco coir-based substrates for nursery production of tree crops. *Philippine Agricultural Scientist*, 104(3), 345–356.

[6] Landis, T. D., Tinus, R. W., McDonald, S. E., & Barnett, J. P. (1990). *Containers and growing media*. Agriculture Handbook 674. USDA Forest Service, Washington, D.C.

[7] Raviv, M., Wallach, R., Silber, A., & Bar-Tal, A. (2004). Substrates and their analysis. In D. Savvas & H. C. Passam (Eds.), *Hydroponic production of vegetables and ornamentals* (pp. 25–101). Embryo Publications, Athens.

[8] Kumar, R., & Singh, B. (2017). Effect of growing media on seed germination and seedling growth in horticultural crops. *Journal of Applied Horticulture*, 19(2), 123–127.

[9] Prasad, M., Maher, M. J., & Raviv, M. (2012). Physical and chemical properties of cocopeat-based media. *Horticultural Reviews*, 40, 227–305.

[10] Raviv, M., & Lieth, J. H. (2008). *Soilless culture: Theory and practice*. Elsevier, Amsterdam.

[11] Kumar, P., Sharma, V., & Meena, R. S. (2019). Effect of perlite and vermiculite on seed germination and seedling growth. *International Journal of Chemical Studies*, 7(2), 1592–1596.

[12] Handreck, K., & Black, N. (1984). *Growing media for ornamental plants and turf*. University of New South Wales Press, Sydney.

[13] Kumaresan, M., Khanchana, K., Bavya, N., Arthi, R., & Yogambal, C. (2024). Effect of different organic media on growth and quality of radish (*Raphanus sativus* L.). *Ecology, Environment and Conservation*, 30(2), 210–215.

[14] Muchtar, A., Nirwana, N., Wahyullah, W., Mahmud, M., & Kultsum, U. (2024). Analysis of the success and vigour of cashew seedlings through direct seed planting (*Anacardium occidentale* L.) for sustainable land management. *Jurnal Wasian*, 11(2).

[15] Hartmann, H. T., Kester, D. E., Davies, F. T., & Geneve, R. L. (2011). *Plant propagation: Principles and practices* (8th ed.). Prentice Hall, Upper Saddle River, New Jersey, USA.

[16] Kumaresan, M., Khanchana, K., & Anbarasu, M. (2024). A review on organic composting technology using different microorganisms. *Ecology, Environment and Conservation*, 30(1), 45–52.

[17] Reddy, M. L. N., Reddy, Y. N., & Kumar, B. P. (2015). Influence of growing media and growth regulators on cashew seedling growth. *Indian Journal of Horticulture*, 72(2), 256–260.

[18] Kumaresan, M., Nadhiya Devi, K., & Rajaselvam, M. (2023). Effect of organic media on growth and rooting of medicinal plants. *Research Journal of Agricultural Sciences*, 14(6), 1855–1858.

[19] Bewley, J. D., Bradford, K. J., Hilhorst, H. W. M., & Nonogaki, H. (2013). *Seeds: Physiology of development, germination and dormancy* (3rd ed.). Springer, New York.

[20] Taiz, L., & Zeiger, E. (2015). *Plant physiology and development* (6th ed.). Sinauer Associates, Sunderland, Massachusetts, USA.

[21] Kumar, S., Singh, R., & Verma, A. (2017). Effect of gibberellic acid on seed germination and seedling growth of cashew. *Indian Journal of Agricultural Sciences*, 87(7), 933–937.

[22] Ma, L., Wei, J., Han, G., Sun, X., & Yang, X. (2024). Seed Osmo priming with polyethylene glycol (PEG) enhances seed germination and seedling physiological traits of

Coronilla varia L. under water stress. *PLOS ONE*, 19(5), e0303145

[23] Kumaresan, M., Rajaselvam, M., Nadhiya Devi, K., & Vasanthkumar, S. S. (2023). Effect of chemical and bioregulators on growth and yield of African marigold (*Tagetes erecta* L.). *Ecology, Environment and Conservation*, 29(3), 1345–1352.

[24] Vessey, J. K. (2003). Plant growth promoting rhizobacteria as biofertilizers. *Plant and Soil*, 255(2), 571–586.

International Journal of Environment, Agriculture and Biotechnology
Vol-11, Issue-2; Mar-Apr, 2026
Peer-Reviewed International Journal
Journal Home Page Available: https://ijeab.com/
Journal DOI: 10.22161/ijeab

Irrigation Frequency and Leaf Whorl Position Jointly Regulate Axillary Bud Quality of *Hevea brasiliensis* 'Reken 628'

Wenping Li [1, 2], Huizhen Yang [1, 2], Xianhong Chen[1 *], Jun Wang[1]

[1] Rubber Research Institute, Chinese Academy of Tropical Agricultural Sciences, Danzhou, Hainan, China
[2] College of Tropical Crops, Yunnan Agricultural University, Pu'er, Yunnan, China
Email: chenxhongjane@163.com (X. Chen).
*Corresponding author

Received: 18 Mar 2026; Received in revised form: 16 Apr 2026; Accepted: 22 Apr 2026; Available online: 30 Apr 2026

Abstract**—*****To clarify the regulatory effects of irrigation frequency and leaf whorl position on axillary bud quality of rubber tree 'Reken 628', a two-factor split-plot experiment was conducted using 3-year-old single-stem bud sticks. Two irrigation frequencies (once daily and twice daily) and three leaf whorl positions (2nd, 3rd, 4th reverse leaf whorls) were set. Morphological and physiological indices were measured, followed by ANOVA, correlation analysis, TOPSIS and PCA. The results showed that irrigation frequency had significant effects on leaf water content and scale bud eye length, with a significant interaction between irrigation frequency and leaf whorl position. Leaf width was extremely significantly positively correlated with leaf water content, and leaf water content was extremely significantly negatively correlated with scale bud scar thickness. TOPSIS evaluation showed that the highest axillary bud quality was observed under twice daily irrigation + 2nd reverse leaf whorl, with a comprehensive index of 0.7785. Under the same leaf whorl, twice daily irrigation was significantly better than once daily irrigation. This study provides a technical basis for standardized cultivation of 'Reken 628' bud sticks.*

Keywords**—*****Hevea brasiliensis, irrigation frequency, leaf whorl, axillary bud quality, TOPSIS***

I. INTRODUCTION

Hevea brasiliensis is a major economic tree species in tropical China. Budding propagation is central to the large-scale deployment of improved rubber tree cultivars, and axillary bud quality directly determines budding survival rate and seedling vigor, thus representing a key factor governing the efficiency of improved variety breeding. 'Reken 628' is a high-yielding stress-tolerant, and widely adaptable rubber tree cultivar that has been increasingly planted in major production regions including Hainan and Yunnan[1]. This cultivar features a compact canopy and pronounced natural self-pruning, which improves understory light transmission and favors intercropping systems[2]. Establishing optimized cultivation techniques for high-quality bud sticks is therefore practically important.

Water is a key environmental factor regulating plant organ development. Irrigation frequency modulates axillary bud differentiation and morphogenesis by influencing plant water status, photosynthate translocation, and cell turgor. Leaf whorl position determines source-sink strength and nutrient supply to axillary buds, leading to substantial variation in axillary bud quality among positions. Current research on rubber tree axillary bud quality has focused on single factors such as bud type[3], rootstock[4], leaf management[5–6] , and light intensity[7] . However, the interactive effects of irrigation frequency and leaf whorl position on axillary bud quality in 'Reken 628' remain poorly understood, and systematic analyses based on comprehensive evaluation are lacking.

In this study, 3-year-old single-stem bud sticks of 'Reken 628' grafted onto GT1 seedling rootstocks were used to evaluate the effects of irrigation frequency and leaf whorl position. Morphological and physiological traits of stems, leaves, and buds were measured to clarify response patterns and identify the optimal treatment combination. The results provide a scientific basis for efficient propagation of improved rubber tree varieties.

II. MATERIAL AND METHODS

Experimental site The experiment was conducted at the Rubber Tree Seedling Budding Demonstration Base of the Rubber Research Institute, Chinese Academy of Tropical Agricultural Sciences, located in Danzhou City, Hainan Province (109°29′E, 19°30′N, altitude 116.9 m). The area has a tropical monsoon climate. During the experimental period, the annual average temperature ranged from 21 to 30 °C, the annual average precipitation was 1652.3 mm, and the annual average sunshine duration was 1734 h, which is suitable for rubber tree growth [8].

Experimental Materials Three-year-old single-stem bud sticks of 'Reken 628' on GT1 seedling rootstocks were used. GT1 rootstocks were sown in October 2021, and budding was performed in October 2022. After sequential cutting back and shaping, uniform plants with four leaf whorls were obtained in September 2024. Uniform water and fertilizer management and plant protection measures were applied throughout the experimental period.

Experimental Design A two-factor split-plot design was used, with irrigation frequency as the main plot and leaf whorl position as the subplot. Six treatments were arranged with three replications and four plants per replicate.

Irrigation frequency: A1 = once daily at 08:00; A2 = twice daily at 08:00 and 18:00; 2 L per plant per application.

Leaf whorl position: B1 = 2nd reverse leaf whorl (from the top); B2 = 3rd reverse leaf whorl (from the top); B3 = 4th reverse leaf whorl (from the top).

Soil water content: 60%–70% in A1 and 75%–85% in A2. No leaves were removed during the experiment, and the photoperiod was 12 h.

Table 1 Experiment design

Treatment	Irrigation frequency	Leaf whorl position	Soil water content	Irrigation volume
A1B1	once-daily	2^{nd} reverse leaf whorl (from the top)	60%–70%	2 L per time
A1B2	once-daily	3^{rd} reverse leaf whorl (from the top)	60%–70%	2 L per time
A1B3	once-daily	4^{th} reverse leaf whorl (from the top)	60%–70%	2 L per time
A2B1	twice-daily	2^{nd} reverse leaf whorl (from the top)	75%–85%	2 L per time
A2B2	twice-daily	3^{rd} reverse leaf whorl (from the top)	75%–85%	2 L per time
A2B3	twice-daily	4^{th} reverse leaf whorl (from the top)	75%–85%	2 L per time

Experimental Methods After the experiment, indicators of bud sticks in each treatment group were measured as follows:

Morphological indicators:Leaf length and leaf width were measured with a ruler (precision 0.1 cm); plant height was measured with a tape measure (precision 0.1 cm); leaf number was counted directly.Length, width and thickness of scale bud scars, length and width of scale bud eyes, length, width and thickness of petiole bud scars, and length and width of petiole bud eyes were measured with a vernier caliper (precision 0.01 mm).Number of scale buds and number of petiole buds were counted directly.Stem diameter was measured with a vernier caliper at 30 cm above the base of bud sticks (precision 0.01 mm).

Physiological indicators:Leaf water content, stem water content, scale bud water content and petiole bud water content were determined by the drying-weighing method. Fresh samples were weighed (fresh weight W1), dried to constant weight at 60 °C and weighed (dry weight W2).Water content = (W1-W2)/W1 × 100%.

Bud eye damage rate:Total number of bud eyes in each treatment was counted. Bud eyes with depression, discoloration or mechanical damage were recorded as damaged bud eyes.Damage rate = (number of damaged bud eyes / total number of bud eyes) × 100%.

Data processing and analysis ANOVA was performed using DPS 20.05; Spearman correlation analysis was conducted using Origin 2024; comprehensive evaluation was carried out using the entropy-weighted TOPSIS method and PCA.

III. RESULT AND ANALYSIS

Main and Interactive Effects

As shown in Figure 1a, the leaf water content of the A1B3 (mean 63.33%), A1B2 (mean 63%), A1B1 (mean 62.67%), and A2B1 (mean 62%) were significantly higher than that of the A2B3 (mean 55.67%) by13.76% (difference 7.66), 13.17% (difference 7.33), 12.57% (difference 7.00), and 11.37% (difference 6.33), respectively. No significant differences were observed among the other treatments.

As shown in Figure 1b, the scale bud eye length of the A1B1 (mean 2.97 mm) was significantly longer than that of A1B3 (mean 2.1967 mm) by35.20% (difference 0.7733) and significantly longer than that of the A2B3 treatment (mean 2.1667 mm) by 37.07% (difference 0.8033). Meanwhile, the scale bud eye lengths of the A2B1 treatment (mean 2.84 mm) and A2B2 treatment (mean 2.85 mm) were significantly longer than that of the A2B3 treatment by 31.07% (difference 0.6733) and 31.69% (difference 0.6833), respectively. No significant differences were detected among the other treatments.

Irrigation frequency significantly affected leaf water content and scale bud eye length, and a significant interaction between irrigation frequency and leaf whorl position was detected. Under twice daily irrigation, the 2nd and 3rd reverse leaf whorls exhibited significantly higher leaf water content and longer bud eyes than the 4th whorl. At the same leaf position, A2 was significantly superior to A1.

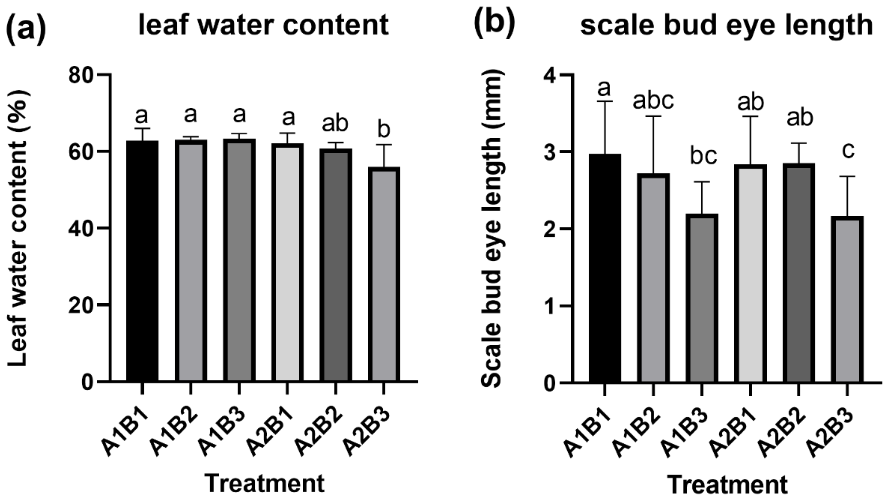

Fig.1 Effects of irrigation frequency and leaf whorl position on leaf water content and scale bud eye length in 'Reken 628' bud sticks

Note: Different lowercase letters indicate significant differences among treatments at $P < 0.05$; error bars represent standard deviation, n = 3. A1: once daily irrigation; A2: twice daily irrigation; B1: 2nd reverse leaf whorl; B2: 3rd reverse leaf whorl; B3: 4th reverse leaf whorl.

Trait Correlation Analysis

Figure 2 shows the correlations among various indices of stem, leaf, and axillary bud tissues of *Hevea brasiliensis* 'Reken 628' bud sticks under different watering frequencies (once daily, twice daily) and leaf whorl positions (2nd, 3rd, 4th canopies from the top).

Under the A1B1 treatment (Figure 2A), plant height was significantly positively correlated with leaf water content and highly significantly positively correlated with petiole bud scar width; it also showed highly significant positive correlations with leaf length, scale bud eye length, scale bud eye width, petiole bud eye length, and petiole bud eye width, respectively. Stem diameter was highly significantly negatively correlated with bud eye damage rate, and significantly positively correlated with leaf number, scale bud scar length, and petiole bud scar length, respectively. Leaf number was significantly positively correlated with petiole bud scar length and significantly negatively correlated with bud eye damage rate. Leaf length was significantly positively correlated with petiole bud scar width, and highly significantly positively correlated with leaf width, scale bud eye length, scale bud eye width, petiole bud eye length, and petiole bud eye width, respectively. Leaf width was significantly positively correlated with scale bud eye length, petiole bud eye length, and petiole bud eye width, respectively. Leaf water content was significantly positively correlated with scale bud eye length, scale bud eye width, and petiole bud eye width, respectively. Scale bud number was significantly positively correlated with scale bud scar length, scale bud eye length, scale bud eye width, petiole bud eye width, and petiole bud water content, respectively.

Scale bud scar length was significantly positively correlated with petiole bud water content and significantly negatively correlated with bud eye damage rate. Scale bud eye length was significantly positively correlated with petiole bud scar width, and highly significantly positively correlated with scale bud eye width, petiole bud eye length, and petiole bud eye width, respectively. Scale bud eye width was significantly positively correlated with petiole bud scar width, and highly significantly positively correlated with petiole bud eye length and petiole bud eye width, respectively. Scale bud water content was significantly positively correlated with petiole bud number. Petiole bud scar width was significantly positively correlated with petiole bud eye length and petiole bud eye width, respectively. Petiole bud eye length was highly significantly positively correlated with petiole bud eye width.

Under the A1B2 treatment (Figure 2B), plant height was significantly positively correlated with stem diameter, leaf water content, and scale bud number, respectively. Stem diameter was highly significantly positively correlated with leaf number and scale bud scar length, and also highly significantly positively correlated with petiole bud number.Leaf number was significantly positively correlated with petiole bud number. Leaf length was significantly positively correlated with leaf width.Leaf width was significantly positively correlated with leaf water content, scale bud number, and scale bud scar thickness, respectively, and highly significantly positively correlated with petiole bud scar width.Leaf water content was significantly positively correlated with scale bud number and petiole bud eye width, respectively.Scale bud number was significantly positively correlated with scale bud eye length and petiole bud scar width, respectively.Scale bud scar length was significantly positively correlated with scale bud water content and petiole bud water content, respectively, and highly significantly negatively correlated with bud eye damage rate.Scale bud scar width was extremely significantly positively correlated with scale bud eye width, highly significantly positively correlated with scale bud scar thickness, and significantly positively correlated with scale bud eye length, petiole bud scar width, petiole bud eye length, and petiole bud eye width, respectively.Scale bud scar thickness was highly significantly positively correlated with petiole bud scar width, and significantly positively correlated with scale bud eye width and petiole bud eye width, respectively.Scale bud eye length was extremely significantly positively correlated with petiole bud eye length, highly significantly positively correlated with scale bud eye width, and significantly positively correlated with petiole bud eye width.Scale bud eye width was highly significantly positively correlated with petiole bud scar width, and significantly positively correlated with petiole bud eye length.Scale bud water content was highly significantly positively correlated with petiole bud water content, and significantly negatively correlated with bud eye damage rate.Petiole bud scar length was significantly negatively correlated with bud eye damage rate.Petiole bud scar thickness was significantly positively correlated with petiole bud eye width.Petiole bud eye length was significantly positively correlated with petiole bud eye width.Petiole bud water content was significantly negatively correlated with bud eye damage rate.

Under the A1B3 treatment (Figure 2C), plant height was significantly negatively correlated with scale bud scar length and petiole bud scar length, respectively. Stem diameter was significantly positively correlated with scale bud water content. Leaf number was highly significantly positively correlated with leaf length and leaf width, respectively. Leaf length was extremely significantly positively correlated with leaf width. Leaf water content was extremely significantly positively correlated with petiole bud scar width, and significantly positively correlated with scale bud eye width and petiole bud eye width, respectively. Scale bud number was significantly negatively correlated with petiole bud scar length and petiole bud water content, respectively. Scale bud scar length was significantly positively correlated with scale bud scar width and petiole bud eye length, respectively. Scale bud scar width was significantly negatively correlated with petiole bud number, highly significantly positively correlated with petiole bud eye length, and significantly positively correlated with petiole bud scar width and petiole bud eye width, respectively. Scale bud scar thickness was highly significantly negatively correlated with scale bud water content. Scale bud eye length was significantly negatively correlated with petiole bud number. Scale bud eye width was significantly positively correlated with petiole bud eye width. Petiole bud number was significantly negatively correlated with petiole bud eye length, highly significantly negatively correlated with bud eye damage rate, and highly significantly positively correlated with petiole bud scar width and petiole bud eye width.

Under the A2B1 treatment (Figure 2D), plant height was significantly positively correlated with leaf number, scale bud scar thickness, petiole bud number, petiole bud scar length, petiole bud scar thickness and petiole bud eye length, respectively, and highly significantly positively correlated with stem diameter, scale bud scar thickness, scale bud eye length, petiole bud scar width and petiole bud eye width, respectively; stem diameter was significantly positively correlated with petiole bud scar width, petiole bud eye length and petiole bud eye width, respectively, highly significantly positively correlated with leaf number, leaf width, scale bud scar width, petiole bud number and petiole bud scar length, respectively, and extremely significantly positively correlated with scale bud scar thickness; stem water content was significantly positively correlated with leaf water content; leaf number was significantly positively correlated with scale bud scar thickness, petiole bud scar length, petiole bud scar width, petiole bud eye length and petiole bud eye width, respectively, highly significantly positively correlated with petiole bud number and petiole bud scar thickness, and extremely significantly positively correlated with leaf width; leaf length was significantly positively correlated with scale bud scar length, and highly significantly positively correlated with leaf width and scale bud eye width, respectively; leaf width was significantly positively correlated with petiole bud number; leaf water content was significantly negatively correlated with scale bud number; scale bud scar length was extremely significantly positively correlated with scale bud eye width and highly significantly positively correlated with petiole bud eye width; scale bud scar width was significantly positively correlated with scale bud eye length and petiole bud scar thickness, respectively, and highly significantly positively correlated with scale bud scar thickness, petiole bud number, petiole bud scar width, petiole bud eye length and petiole bud eye width, respectively; scale bud scar thickness was significantly positively correlated with scale bud eye length, highly significantly positively correlated with petiole bud scar length, petiole bud scar thickness and petiole bud eye length, respectively, and extremely significantly positively correlated with petiole bud number; scale bud eye length was significantly positively correlated with scale bud eye width, petiole bud number, petiole bud eye length and petiole bud eye width; scale bud eye width was significantly positively correlated with petiole bud eye width; scale bud water content was significantly positively correlated with petiole bud water content; petiole bud number was significantly positively correlated with petiole bud scar width and petiole bud eye width, highly significantly positively correlated with petiole bud scar thickness, and extremely significantly positively correlated with petiole bud scar length and petiole bud eye length, respectively; petiole bud scar length was significantly positively correlated with petiole bud scar width and petiole bud eye width, highly significantly positively correlated with petiole bud scar thickness, and extremely significantly positively correlated with petiole bud eye length; petiole bud scar width was significantly positively correlated with petiole bud eye length, and highly significantly positively correlated with petiole bud scar thickness and petiole bud eye width, respectively; petiole bud scar thickness was highly significantly positively correlated with petiole bud eye length; petiole bud eye length was highly significantly positively correlated with petiole bud eye width.

Under the A2B2 treatment (Figure 2E), plant height was significantly positively correlated with leaf length, leaf width, petiole bud scar length and petiole bud scar width, highly significantly positively correlated with scale bud eye length, scale bud eye width and petiole bud eye width, respectively, and extremely significantly positively correlated with scale bud scar length and petiole bud eye length; stem diameter was highly significantly positively correlated with leaf number and petiole bud scar thickness, and extremely significantly positively correlated with scale bud scar width and scale bud scar thickness; stem water content was significantly positively correlated with leaf length, leaf width, scale bud scar length and petiole bud scar width, respectively; leaf number was significantly positively correlated with petiole bud eye length, highly significantly positively correlated with scale bud scar thickness and petiole bud scar thickness, and extremely significantly positively correlated with scale bud scar width; leaf length was highly significantly positively correlated with leaf width and petiole bud scar width, and extremely significantly positively correlated with petiole bud scar length; leaf width was significantly positively correlated with petiole bud scar width and petiole bud scar thickness, and highly significantly positively correlated with petiole bud scar length; scale bud number was highly significantly positively correlated with scale bud water content; scale bud scar length was highly significantly positively correlated with scale bud eye width and petiole bud eye width, and extremely significantly positively correlated with scale bud eye length and petiole bud eye length; scale bud scar width was highly significantly positively correlated with petiole bud scar thickness, and extremely significantly positively correlated with scale bud scar thickness; scale bud scar thickness was extremely significantly positively correlated with petiole bud scar thickness; scale bud eye length was significantly positively correlated with scale bud eye width and petiole bud eye width, and highly significantly positively correlated with petiole bud eye length; scale bud eye width was extremely significantly positively correlated with petiole bud eye length and petiole bud eye width; petiole bud scar length was significantly positively correlated with petiole bud scar thickness, and highly significantly positively correlated with petiole bud scar width; petiole bud eye length was extremely significantly positively correlated with petiole bud eye width.

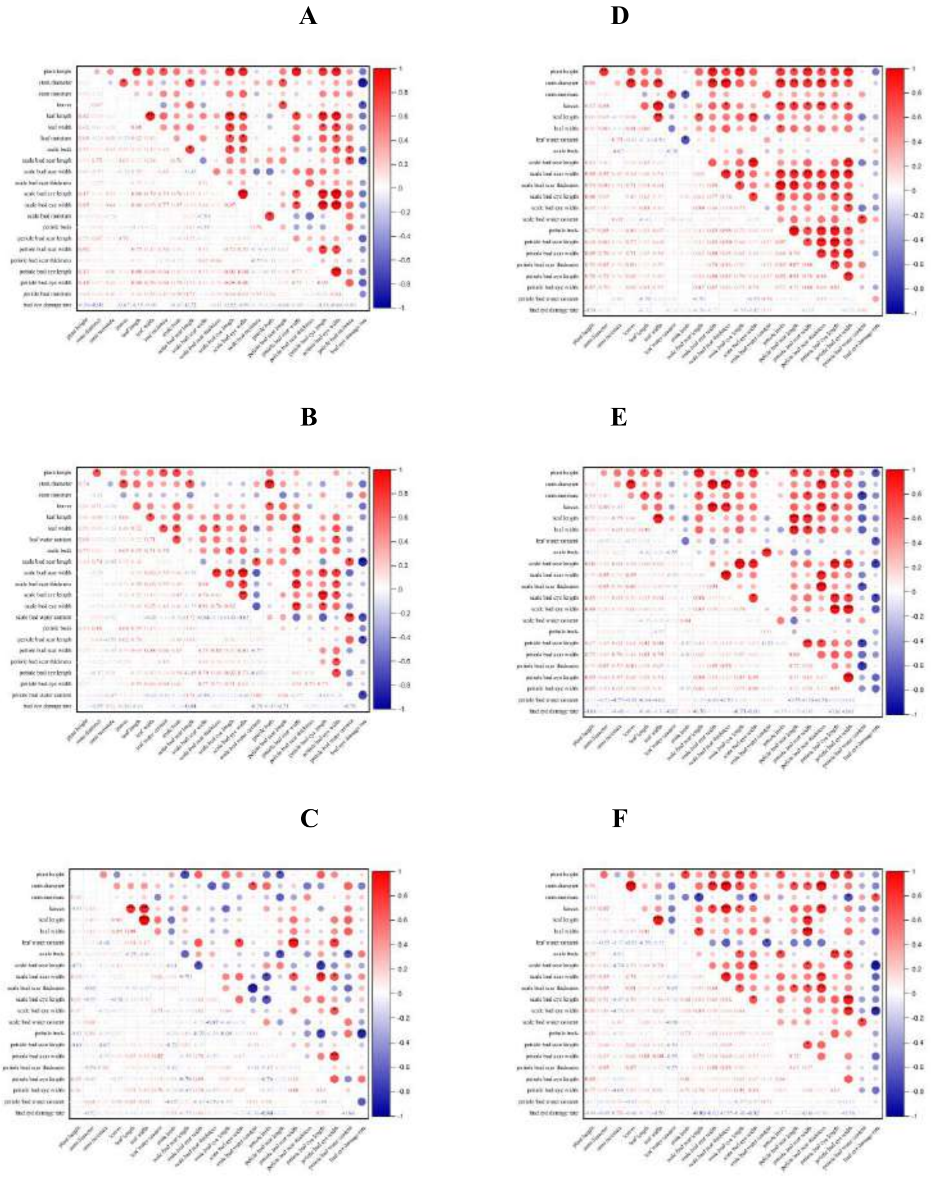

Fig.2 Correlation heatmap of measured traits across treatments

Note: A–C represent the correlation analysis among morphological indices of stems and leaves under A1B1, A1B2, and A1B3, respectively. D–F represent the correlation analysis among morphological indices of stems and leaves under A2B1, A2B2, andA2B3l, respectively. The size and color depth of the circles indicate the magnitude of the correlation coefficient and the significance level, respectively. Blue represents negative correlation and red represents positive correlation. The upper triangle shows significance markers, where *, **, and *** indicate statistically significant correlation at $p<0.05$, highly significant correlation at $p<0.01$, and extremely significant correlation at $p<0.001$, respectively. The lower triangle shows the values of correlation coefficients, where $|r|\geq0.7$ indicates strong correlation, $0.3\leq|r|<0.7$ indicates moderate correlation, and $|r|<0.3$ indicates weak correlation.

Under the A2B3 treatment (Figure 2F), plant height was significantly positively correlated with scale bud number, scale bud scar width, scale bud eye width, petiole bud number and petiole bud eye width, respectively, and highly significantly positively correlated with scale bud eye length and petiole bud eye length; stem diameter was significantly positively correlated with scale bud eye length, petiole bud scar length and petiole bud scar width, highly significantly positively correlated with scale bud scar width, and extremely significantly positively correlated with leaf number, scale bud scar thickness and petiole bud scar thickness, respectively; stem water content was significantly negatively correlated with scale bud scar length, scale bud eye width and petiole bud eye width, respectively, and significantly positively correlated with bud eye damage rate; leaf number was significantly positively correlated with scale bud scar width and scale bud eye length, highly significantly positively correlated with petiole bud scar thickness, and extremely significantly positively correlated with scale bud scar thickness; leaf length was highly significantly positively correlated with petiole bud scar width, and extremely significantly positively correlated with leaf width; leaf width was significantly positively correlated with scale bud scar length, and extremely significantly positively correlated with petiole bud scar width; leaf water content was significantly negatively correlated with scale bud water content; scale bud number was significantly positively correlated with scale bud eye length, petiole bud number and petiole bud eye width, and highly significantly positively correlated with petiole bud eye length; scale bud scar length was significantly positively correlated with petiole bud scar width and petiole bud eye width, highly significantly negatively correlated with bud eye damage rate, and highly significantly positively correlated with scale bud eye width; scale bud scar width was highly significantly positively correlated with scale bud scar thickness and petiole bud scar thickness; scale bud scar thickness was significantly positively correlated with scale bud eye length, petiole bud scar length and petiole bud scar width, respectively, and highly significantly positively correlated with petiole bud scar thickness; scale bud eye length was significantly positively correlated with scale bud eye width, and extremely significantly positively correlated with petiole bud eye width; scale bud eye width was highly significantly positively correlated with petiole bud eye width, and highly significantly negatively correlated with bud eye damage rate; scale bud water content was significantly positively correlated with petiole bud water content; petiole bud scar length was significantly positively correlated with petiole bud scar width.

Overall, watering frequency and leaf whorl position significantly affected the correlation pattern among indicators: most growth indices showed a synergistic enhancement relationship under A2B2 treatment; while under A1B4, plant height was negatively correlated with bud scar length, indicating that excessive leaf removal may inhibit longitudinal growth.

TOPSIS Comprehensive Evaluation

Raw measurement data were transformed by logarithm. Plant height, stem diameter, bud eye damage rate, scale bud scar thickness and petiole bud scar thickness were taken as negative indicators, while the weights of other indicators (leaf number, leaf water content, stem water content, leaf length, leaf width, scale bud scar length, scale bud scar width, scale bud eye length, scale bud eye width, scale bud number, scale bud water content, petiole bud scar length, petiole bud scar width, petiole bud eye length, petiole bud eye width, petiole bud number, petiole bud water content, etc.) were determined by the entropy weight method. The TOPSIS method was used for analysis, and the results are shown in Table 2.

When considering watering frequency, the axillary bud quality under twice-daily watering was superior to that under once-daily watering. When ignoring watering frequency and only considering leaf whorl position, the axillary bud quality at the 2nd leaf whorl was the best, followed by the 3rd leaf whorl, and the 4th leaf whorl was the lowest. Considering both watering frequency and leaf whorl position comprehensively, the axillary bud quality was optimal under A2B1, followed by A2B2, andA2B3. Under once-daily watering, the axillary bud quality at the 3rd leaf whorl was the best, followed by the 4th leaf whorl, and the 2nd leaf whorl was the lowest. The ranking of axillary bud quality was as follows: A2B1 (best), A2B2(second best), and the 3rd to 6th places were A2B3, A1B2, A1B3, and A1B1, respectively. From the perspective of application prospects: in the practice of bud selection for budding of *Hevea brasiliensis* 'Reken 628', the axillary bud quality at all leaf whorl positions under twice-daily watering was better than that under once-daily watering. However, on the premise of preferentially selecting axillary buds from the 2nd leaf whorl and then the 3rd leaf whorl, once-daily watering can still serve as a supplementary option to twice-daily watering, providing a feasible water management and leaf whorl position matching scheme for budding production.

Table 2 TOPSIS comprehensive analysis of morphological indices based on leaf, stem and axillary bud tissues

Treatment	**Comprehensive index (CI)**	**Rank**
A2B1	**0.7785**	**1**
A2B2	**0.3502**	**2**
A2B3	**0.3030**	**3**
A1B2	**0.2250**	**4**
A1B3	**0.2035**	**5**
A1B1	**0.1998**	**6**

Note: CI, approximation to the Optimal Vectors.

Principal Component Analysis

Principal component analysis (PCA) was performed on 22 morphological indices related to axillary bud quality of *Hevea brasiliensis* 'Reken 628' bud sticks, including traits related to leaves, stems and axillary buds (Figure 3). The eigenvalues of the first two principal components were 9.630 and 6.508, with variance contribution rates of 43.8% and 29.6%, respectively, and a cumulative contribution rate of 73.4%. This indicates that PC1 and PC2 can effectively summarize most of the information in the original data, and the index system achieves a satisfactory dimension reduction effect, allowing comprehensive evaluation of axillary bud quality under different watering frequency–leaf whorl position treatments.

Variance Explanation and Principal Component Extraction The eigenvalue of PC1 was 9.62965, which independently explained 43.8% of the variation in the original data, representing the core principal component reflecting axillary bud quality. The eigenvalue of PC2 was 6.50816, explaining 29.66% of the original data variation as the secondary principal component. Their cumulative contribution rate exceeded 70%, meeting the validity requirement for principal component analysis, so they can replace the original 22 indices for comprehensive evaluation.

Index Loading Distribution and Implications of Principal Components The main loading indices of PC1: indices with high positive loadings on PC1 included leaf width (LW, 0.29181), leaf number (L, 0.29929), scale bud eye length (SBEL, 0.29491), petiole bud scar length (LBSL, 0.28642), and petiole bud eye length (LBEL, 0.29163), all with loading values above 0.28. These indices showed strong positive correlations with PC1 and were core positive indicators for axillary bud quality and vegetative growth of bud sticks, reflecting plant vegetative organ vigor and axillary bud developmental potential. Indices with high negative loadings included stem diameter (SD, -0.2744) and scale bud scar thickness (SBST, -0.29823), which were predefined negative indicators (lower values expected) and negatively correlated with PC1, consistent with biological logic. Therefore, PC1 can be defined as the 'principal component of bud stick growth and axillary bud morphogenesis'. A higher PC1 score indicates better vegetative growth of bud sticks and superior morphological indices of axillary buds.

The main loading indices of PC2: indices with high positive loadings on PC2 included scale bud scar width (SBSW, 0.35976), scale bud eye width (SBEW, 0.37605), petiole bud number (LB, 0.29923), and leaf length (LL, 0.314), all with loading values above 0.29, mainly reflecting the spatial characteristics of bud eyes and axillary bud quantity. Indices with high negative loadings included scale bud scar length (SBSL, -0.32894), leaf water content (LM, -0.30789), and petiole bud scar thickness (LBST, -0.245), which showed inhibitory effects on PC2. Therefore, PC2 can be defined as the 'principal component of axillary bud morphological details and water physiology'. A higher PC2 score indicates superior morphological details of axillary buds, such as bud eye and bud scar width.

Sample Score Distribution and Grouping Characteristics The comprehensive performance of the six different watering frequency–foliage whorl position treatments showed clear separation in the PC1–PC2 plane (Figure 3):

A2B1 (twice daily watering + 2nd leaf whorl): located in the first quadrant (positive PC1, positive PC2), with the highest PC1 score (1.256), indicating outstanding performance in "favorable indices" such as leaf number, leaf width and bud eye length. Meanwhile, the positive PC2 score (0.2744) reflected superior traits such as bud eye width. This treatment showed the best overall status in vegetative growth, axillary bud morphogenesis and morphological details, representing the optimal comprehensive performance.

A2B2 (twice daily watering + 3rd leaf whorl): also located in the first quadrant with positive PC1 (0.523) and PC2 (1.082) scores, but lower PC1 than A2B1, indicating slightly weaker vegetative growth indices, while the higher PC2 may be related to larger bud eye width.

A2B3 (twice daily watering + 4th leaf whorl): located in the second quadrant (negative PC1, positive PC2). The negative PC1 indicated poorer vegetative growth indices, while the positive PC2 suggested retained advantages in traits such as bud eye width.

A1B1, A1B2, A1B3 (once daily watering treatments): distributed in the third and fourth quadrants with mostly negative PC1 and PC2 scores, showing overall poor morphological performance. In particular, A1B3 (PC1 = -1.114, PC2 = -0.995), located in the lower-left corner, had the lowest comprehensive scores across all indices.

Overall, the PC1 scores of treatments with twice daily watering (A2 series) were superior to those with once daily watering (A1 series). For leaf whorl positions, the order was 2nd whorl (B1) > 3rd whorl (B2) > 4th whorl (B3), consistent with the practical cultivation rule that axillary buds in the middle-upper leaf whorls of bud sticks exhibit better quality.

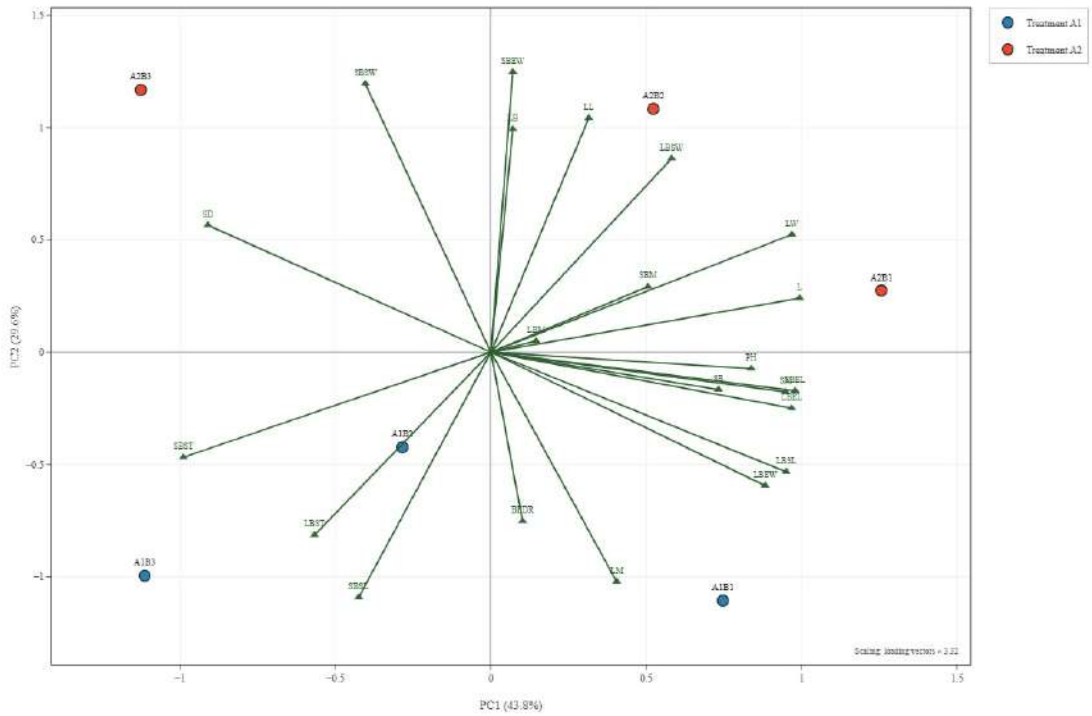

Fig.3. PCA biplot of treatments and traits. Scores (samples) are colored by treatment (A1: blue, A2: orange).

Note: Vectors (green arrows) represent loading values of 22 variables. The length and direction indicate contribution to PC1 and PC2. Variance explained: PC1 = 43.8% (eigenvalue 9.63), PC2 = 29.6% (eigenvalue 6.51), cumulative = 73.4%. Loadings scaling factor: 3.32 (relative arrow length).

IV. DISCUSSION AND CONCLUSION

DISCUSSION

Water supply status directly affects cell turgor, photosynthesis, and substance synthesis and transport in rubber tree bud sticks, thereby regulating stem and leaf growth as well as axillary bud development. In this experiment, the leaf water content of the 2nd and 3rd whorls under twice-daily watering was significantly higher than that of the 4th leaf whorl under the same watering frequency, indicating that appropriate water supply is more conducive to maintaining a relatively high water status in the middle-upper whorls, whereas excessive watering or relatively weak water metabolism capacity in lower canopies may occur, which is related to the physiological activity differences among different foliage canopies of rubber tree bud sticks. Under the tropical climate conditions in Danzhou, twice-daily watering can maintain a high and stable substrate water status, which is beneficial to sustaining cell turgor and photosynthate transport in bud sticks; in contrast, once-daily watering may cause water stress at noon and inhibit axillary bud differentiation. As an important morphological index of axillary bud development, scale bud eye length showed no significant difference between the 3rd leaf whorl under once-daily watering and the 2nd and 3rd whorls under twice-daily watering, suggesting that the regulatory effect of watering frequency on axillary bud morphogenesis is leaf-whorl-specific, and the middle-upper whorls present more stable responses to water changes, providing a specific positional reference for precise water regulation in rubber tree bud stick cultivation.

The significant correlations among various indices of bud sticks revealed the internal relationship between stem-leaf growth and axillary bud development. Leaf width was extremely significantly positively correlated with leaf water content, indicating that larger leaf morphology confers stronger water retention capacity and thus sufficient water supply for axillary bud development. Meanwhile, leaf water content was extremely significantly negatively correlated with scale bud scar thickness, and it is speculated that higher leaf water content may inhibit lignification of bud scar tissues, favoring axillary bud germination and growth. This conclusion is consistent with the response pattern of osmotic adjustment substances in different organs of rubber seedlings to water reported by Cheng *et al*. [9], confirming the consistent regulatory effect of water metabolism on organ morphogenesis in rubber tree seedlings. Stem water content was positively correlated with scale bud scar length and negatively correlated with scale bud scar width, reflecting the differential regulation of bud scar morphology by stem water metabolism; sufficient stem water can promote longitudinal growth of bud scars, providing more space for axillary bud development[10-11]. In addition, scale bud eye length was significantly positively correlated with both petiole bud scar length and petiole bud eye length, indicating coordinated morphological development of axillary buds, with mutual promotion between bud eye and bud scar growth. This is consistent with the findings of Jiang *et al*. [4] on the correlation between axillary bud quality and plant morphological indices in 'Reken 628', highlighting the morphological coordination characteristic of axillary bud development in this variety.

The comprehensive evaluation results using the TOPSIS method showed that A2B1 treatment was the optimal treatment for axillary bud quality. This is because twice-daily watering maintains stable water metabolism in bud sticks, and their synergistic effect promotes the formation of high-quality axillary buds. As a functional whorl in the middle-upper part of bud sticks, the 2nd leaf whorl has high physiological activity and strong nutrient supply capacity, so its axillary bud quality is significantly superior to that of the 3rd and 4th whorls. This is consistent with the apical dominance and nutrient distribution rules of rubber tree bud sticks, and also provides experimental support for the findings of Cha *et al*. [5–6] regarding the effects of leaf whorl position on axillary bud quality in umbrella-shaped 'Reken 628' bud sticks. The overall axillary bud quality under once-daily watering was inferior to that under twice-daily watering, indicating that appropriately increasing watering frequency is conducive to improving axillary bud quality during the cultivation of 'Reken 628' bud sticks. However, the axillary bud quality of the 3rd leaf whorl under once-daily watering remained relatively favorable and can serve as a supplement to the optimal treatment, providing a flexible scheme for bud selection under different water management conditions.

The comprehensive scores were calculated by weighting the scores of the two principal components in PCA according to variance (PC1 × 44.8% + PC2 × 30.3%) and ranked as follows: A2B1 (0.654) > A2B2 (0.560) > A1B1 (0.000) > A2B3 (-0.154) > A1B2 (-0.256) > A1B3 (-0.803). This order partially differs from the TOPSIS ranking (A2B1 > A2B2 > A2B3 > A1B2 > A1B3 > A1B1), mainly reflected in the swapped positions of A1B1 and A2B3. The PCA weighted score places greater emphasis on the weight of PC1 (vegetative growth), whereas TOPSIS objectively assigns weights to 22 indices via the entropy weight method, which may assign higher weights to bud eye morphological indices, resulting in a higher ranking for A2B3 (with a higher PC2 score) than A1B1 (with a higher PC1 score but extremely low PC2 score). This difference precisely reflects the different focuses of the two methods: PCA is a linear dimensionality-reduction technique, while TOPSIS is a multi-objective decision-making method. The latter is more consistent with the comprehensive trade-off between 'favorable indices' and 'negative indices' in actual production, indicating that the TOPSIS results are reliable and can be used to guide water management and leaf whorl matching strategies in bud selection for 'Reken 628' rubber tree budding.

This study only set two watering frequencies and focused solely on the three-year-old single-stem bud sticks of 'Reken 628', without covering different tree ages, seasons or soil types. In the future, multi-level gradient experiments should be carried out, combined with data on budding survival rate and seedling growth, to further verify the optimal water management scheme.

V. CONCLUSION

In this study, three-year-old single-stem bud sticks of *Hevea brasiliensis* 'Reken 628' were used as experimental materials to systematically investigate the effects of two watering frequencies (once daily and twice daily) combined with different leaf whorl positions on the morphology, physiology and axillary bud quality of bud sticks. Through analysis of variance, correlation analysis and comprehensive evaluation using the TOPSIS method, and PCA analysis, the core conclusions are as follows:

Watering frequency and leaf whorl position have a significant interactive effect on the axillary bud quality of 'Reken 628' rubber tree bud sticks. The 2nd and 3rd leaf whorls show more stable responses to water, while the 4th leaf whorl exhibits the poorest performance. Stem-leaf growth and axillary bud development of bud sticks are highly correlated, and leaf water content and leaf width are key indices affecting axillary bud morphogenesis. The A2B1 treatment yields the optimal axillary bud quality. Although the A1B3 overall axillary bud quality is lower than that of twice-daily watering treatments, it can be used as a suboptimal alternative in production scenarios with limited water resources or insufficient irrigation facilities. Appropriately increasing watering frequency and selecting axillary buds from middle-upper leaf whorls can significantly improve the quality of budding seedling propagation.

ACKNOWLEDGEMENTS

This work was supported by Hainan Provincial Natural Science Foundation of China(326MS0289), the earmarked fund for China Agriculture Research System (CARS-34-YZ4).

REFERENCES

[1] Yang YW, Xiong YL, Gao XJ, Yin YQ, Zhang FL(2026).Regional trial analysis of eight excellent rubber tree varieties in xishuangbanna. Tropical Agricultural Science and Technology, 4: 1-6.

[2] Wang XJ, Huang X, Zhang YY, Li WG, XF Zhang XF, XS Gao XS, Zhang HL(2025) Differences in understory light conditions among rubber plantations of different strains and their causes. Chinese Journal of Tropical Crops, 46(12): 100-111.

[3] Yang HZ, Li WP, Chen XH, Wang J (2026) Influence of axillary bud types on the branching angle of new shoots and the growth quality of bud sticks in rubber tree 'Reken 628'. International Journal of Environment, Agriculture and Biotechnology, 11(1), 108–122.

[4] Jiang XY, Gong XD, Ruan JL, Cha ZN, Chen XH, Jun W (2026) Effects of Cutting-Propagated Rootstocks on Axillary Bud Quality of *Hevea brasiliensis* 'Reken 628'. China Tropical Agriculture, 1: 70-79.

[5] Cha ZN, Ruan JL, Jiang XY, Gong XD, Chen XH , Wang J(2025) Rubber tree 'Reken 628' single-stem bud stick leaf-clipped treatment improves seedling axillary bud quality, International Journal of Innovative Science and Research,78(1): 1–13.

[6] Cha ZN, Ruan JL, Jiang XY, Gong XD, Chen XH, Wang J(2025) Effects of leaf reserved and clipped on axillary bud quality in umbrella-shaped *Hevea brasiliensis* 'Reken 628'bud-sticks. International Journal of Environment, Agriculture and Biotechnology 10(2):48–59.

[7] Ruan JL, Cha ZN , Gong XD, Jiang XY, Chen XH, Wang J(2024) Light intensity affects axillary bud quality of rubber mini-seedling budding CATAS73397, International Journal of Environment, Agriculture and Biotechnology, 9(6): 166–179.

[8] Chen XM, Li WG, Chen HL, Liu SJ, Zhang JH, Wu QL (2019) Establishment and application of climate suitability evaluation index for rubber tapping in Hainan Island: Taking Danzhou City as an example. Jiangsu Agricultural Sciences, 47(15): 278–281.

[9] Cheng YW, An F, Shi JR, Xie GS, Cai J (2022) Composition of osmotica in different organs of rubber seedlings and their contributions to osmotic potential. Journal of Tropical Biology, 13(1): 7–12.

[10] Adahé LNA., Kouadio VPG., Abrou EJN., Yao ON., Kossonou FSA, Tondoh JE, Yao CYA (2024) Plant species diversity in cocoa and rubber tree landscapes in Côte d'Ivoire. International Journal of Biological and Chemical Sciences, 17(6):2377-2395.

[11] Gao XS, Hu XX, Li T, Li WG, Huang X (2021). Research on characteristics of leaf anatomical structure and photosynthesis of 5 widely-used *Hevea brasiliensis* clones seedlings. Journal of Southwest Forestry University (Natural Science), 41(3): 31–36.

International Journal of Environment, Agriculture and Biotechnology
Vol-11, Issue-2; Mar-Apr, 2026
Peer-Reviewed International Journal
Journal Home Page Available: https://ijeab.com/
Journal DOI: 10.22161/ijeab

Women's Coping and Adaptation Strategies to the Effects of Climate Change: A Case of the Dodoma City Council, Tanzania

Lydia A. Mahela

Ph.D Candidate, Department of International Relations, Yonsei University Mirae Campus- Yonseidae-gil, Wonju-si, Gangwon-do, 26493, Republic of Korea
ORCID identifier: 0009-0006-6958-0973
Contact: mahelala@yonsei.ac.kr,

Received: 15 Mar 2026; Received in revised form: 17 Apr 2026; Accepted: 21 Apr 2026; Available online: 30 Apr 2026

***Abstract*— *As significant actors in the agricultural sector, women farmers have become increasingly active in adopting various strategies to mitigate the impacts of climate change in Dodoma. However, Dodoma is a semi-arid region; thus, its climate change adaptation strategies differ from those of other regions of Tanzania. The study focuses on the strategies they adopt to cope with climate change impacts in Dodoma. Using the content analysis of publicly available documents was conducted to evaluate the experiences, knowledge, and farming practices of women farmers, thereby helping identify factors that influence their adaptation choices. The study finds that access to resources, technologies, and extension services shaped the variation of women farmers' adaptation strategies. Women farmers use various adaptation strategies, such as crop rotation, genetically modified seeds, improved water management, soil health practices, diversification, and intercropping, to mitigate the impacts of climate change. The study findings have far-reaching implications. First, local governments in Dodoma need to implement targeted interventions to encourage widespread adoption among women farmers, thereby fostering agricultural sustainability and resilience. Second, financial institutions should introduce incentives to promote soft loans, enabling women farmers to access advanced agricultural inputs and invest in commercial farming.*

***Keywords*— Women farmers, Climate change impacts, Adaptation strategies, Agriculture, Dodoma.**

I. INTRODUCTION

"Climate change poses one of the most significant global challenges, disproportionately affecting vulnerable populations, particularly those reliant on agriculture in developing countries (Baez et al., 2010; IPCC, 2007). Its impacts, such as reduced crop yields and fluctuating weather patterns, severely threaten food security and livelihoods (Arif et al., 2020). Women farmers, who constitute a large percentage of the agricultural labor force in many regions, are particularly vulnerable due to existing gender inequalities that limit their access to resources and decision-making power (Reggers, 2019; Huyer et al., 2021). Consequently, understanding their adaptation strategies is crucial for building agricultural resilience.

Dodoma, a semi-arid region in Tanzania, is a key agricultural area highly susceptible to climate variability, where women farmers play a central role in food production (URT, 2000; Swai et al., 2012). While studies have highlighted the challenges faced by women farmers in adapting to climate change in Tanzania (e.g., Gwambene & Saria, 2024), a comprehensive understanding of the specific factors influencing women's adoption choices and the types of strategies they employ in the unique context of Dodoma remains underexplored. Existing literature often focuses on broader gender disparities or general adaptation practices but lacks a detailed analysis of the specific drivers and forms of adaptation among women farmers in this particular region.

This study aims to fill this critical gap by investigating the factors influencing women farmers' adoption of climate change adaptation strategies and the specific strategies they use to cope with climate change impacts in Dodoma City Council, Tanzania. The study findings will provide valuable insights for policymakers to develop targeted, gender-responsive interventions that foster agricultural sustainability and enhance women's resilience in climate-vulnerable regions.

1.1 Research Question

"Building on the identified gaps, this study aims to explore the adaptation strategies employed by women farmers in Dodoma City Council, Tanzania. Specifically, this research addresses the following questions:

1. What factors influence women farmers' decisions to adopt climate change adaptation strategies in Dodoma?
2. What specific adaptation strategies do women farmers adopt to cope with the impacts of climate change in Dodoma?

II. LITERATURE REVIEW

2.1 Climate Change Impact and Gender Vulnerability

Climate change is one of the most significant challenges of our time, predominantly negatively affecting countries, albeit to varying degrees and through different channels (Baez et al., 2010). Beyond the immediate human and material damage, climate change reduces yields of certain crops, impacting agricultural output and food security. According to Arif et al. (2020) and Musyimi (2020), fluctuations in temperature and precipitation patterns pose a significant threat to the livelihoods of women farmers, who rely on agriculture as their primary source of income. As a result, while nature itself does not discriminate, the effects of climate change are not gender-neutral, given the intersection of environmental and social inequities (Reggers, 2019; Huyer et al., 2021). Studies indicate that women, who comprise 54% to 81% of the agricultural labor force, face increased vulnerability due to existing gender inequality, particularly in Tanzanian societies, including Dodoma (Babugura, 2021; FAO, 2024; NBS, 2022).

Women are widely regarded as a marginalized group in climate change debates. Lacking resources, they are portrayed as victims of progress, while stoically bearing the burden of survival as subsistence food producers, ensuring household food security (Okali & Naess, 2013). Therefore, understanding gender roles and societal perceptions of gender is regarded as an essential asset for promoting socially inclusive and equitable outcomes from coordinated climate action (Cohen et al., 2016).

2.2 Women's Adaptive Capacity and Barriers

Since the mid-1980s, climate change has been a central focus of international environmental discussions. Climate change adaptation has emerged as a global priority (Chersich & Wright, 2019). The IPCC's assessments consistently highlight women's disproportionate vulnerability to the impacts of climate change and emphasize the need for gender-responsive adaptation. The IPCC's Sixth Assessment Report (AR6) references gender, equity, and justice more frequently than any previous report, underscoring the need to integrate diverse perspectives into adaptation planning. This recognition stems from the reality that women often face higher risks due to their roles, social structures, and economic vulnerabilities (IPCC 2007).

Consequently, the Paris Agreement (2015) also acknowledges that adaptation actions should be gender-responsive. It recognizes that climate change disproportionately affects women and other marginalized groups and that adaptation strategies must be designed to address these inequalities and promote gender equality. According to the IPCC (2007) report, climate change has a greater impact on developing nations and populations, and its effects and vulnerabilities differ for men and women. Consequently, UNFPA & WEDO 2009) observed that gender disparities in access to resources, divisions of labor, and decision-making authority hinder adaptation to climate change.

Gender roles and expectations shape climate change, influencing women's experiences and responses to risks and consequences. These vulnerabilities stem from unequal access to resources, limited decision-making authority, social norms, cultural traditions, and institutional constraints. Gender roles are crucial to climate change adaptation and mitigation because men and women in agriculture experience different effects (Prakash et al., 2022; Deji, 2020). Consequently, there is growing concern that women are more vulnerable to these impacts than men due to unequal gender relations, which tend to disadvantage women in access to and control over resources, social norms, cultural practices, and institutional constraints. Women who lead smallholder agricultural households in Sub-Saharan Africa are reportedly the poorest and most food insecure (Byela et al., 2015). As a result, they are likely to be highly susceptible to climatic changes. Therefore, to address the differential impacts of climate change, this study considers the vulnerabilities of different social groups, particularly women farmers in Dodoma.

2.3 Adaptation Strategies in Agriculture

Adaptation to climate change in agriculture appears to be influenced by farmers' perceptions of climate change (Bryant et al., 2000). In farming communities, men and women have distinct roles and responsibilities, leading them to experience climate change differently. Variations in climate change experience, along with existing gender inequality, often diminish women's adaptive capacity and affect their decisions about adaptation strategies (Mehar et al., 2016). This clearly indicates that, while perception shapes adaptation, it differs by gender.

Various agricultural management techniques are increasingly used to help adapt to climate change. These include the planting of drought-tolerant crops, early crop planting, crop diversification, and rainwater harvesting (Franklin et al., 2021; Atube et al., 2021; Gebre & Rahut, 2021; Shahbaz et al., 2022). Numerous studies are now available on the factors affecting the adoption of climate change adaptation strategies in various developing countries (see Brüssow et al., 2019; Shahbaz et al., 2022).

2.4 The Context of Dodoma, Tanzania

Dodoma is one of Tanzania's key food producers and is often called the country's food basket (URT, 2000). Women make up over 57% of the agricultural workforce in Dodoma but face institutional barriers and traditional gender norms that restrict their access to resources and decision-making power (Akram-Lodhi and Komba, 2018; Jones et al., 2023).

Pattnaik et al. (2017) posit that the role of women in agriculture in Dodoma is increasing, and male outmigration in the face of climate change is prompting more women to engage in the agricultural sector, a phenomenon described as the 'feminization of agrarian distress.' However, Gwambene and Saria's (2024) study on female smallholder farmers' resilience in adapting to climate change in the central regions of Tanzania, specifically in Dodoma, Singida, and Tabora, reveals that female smallholder farmers face significant challenges and risks from shifting rainfall patterns, temperature fluctuations, and extreme events such as floods and droughts. As a result, these farmers employ various adaptation techniques, including local knowledge and traditional practices, to mitigate their vulnerability to the impacts of climate change (Gwambene, 2020; Tilumanywa, 2021).

Notwithstanding, women's lack of land ownership under the patriarchal system results in a disproportionate distribution of women's farm outputs in Dodoma (Lawson et al., 2020; Ylipaa et al., 2019). Another notable barrier to women's climate change adaptive capacity in Dodoma is that men remain in charge of on- and off-the-field farm production and the sale of produce. These tendencies position women as the most vulnerable group in terms of the impact of climate change on the agricultural sector, which continues to affect their farming and livelihood activities, primarily due to their limited adaptive capacity in Dodoma (Atube et al., 2021; Kitole and Utouh, 2023). Based on the above, this study aims to identify climate adaptation strategies that Dodoma women farmers can adopt to mitigate the impact of climate change.

2.5 Research Gap

Drawing on the literature and the challenges women farmers face, this study seeks to address the research gap by analyzing the factors that influence the adoption of climate change adaptation strategies among vulnerable groups (women farmers) in developing countries. The study will further investigate the specific strategies that women farmers can use to cope with climate impacts in the Dodoma City Council, Tanzania.

2.6 Analytic framework

The study examines the relationship among women, climate change, and adaptation, with an emphasis on women's experiences, challenges, and resilience strategies. Principles derived from resilience theory include the intersection of gender and social norms, resilience and empowerment, and adaptive management. Resilience theory focuses on how individuals respond to and recover from adversity. Additionally, resilience theory aligns with feminist theory and the capability approach, both of which emphasize gendered power dynamics and the ability to adapt to changing circumstances (Remennick & Adi, 2023; MacArthur et al., 2022). As a result, this study highlights women's experiences with climate change in a direct, explicit manner.

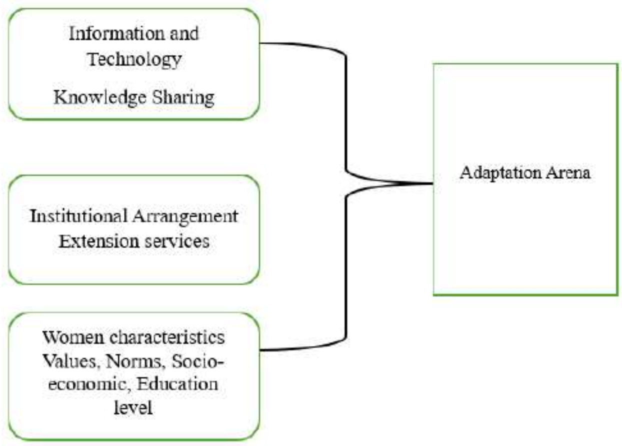

Fig. 1 Conceptual Framework

The conceptual framework shows that Information and Technology Knowledge sharing, institutional arrangements, extension services, and women's characteristics and socio-economic and educational levels influence the adaptation arena.

2.6.1 Information and Technology Knowledge Sharing

Information and knowledge sharing is an element in the adaptation context that influences the capacity to implement suitable responses to the climate change adaptation strategy. However, studies on how gender roles affect this element are lacking. Therefore, this aspect needs to be examined through a gender-sensitive lens. A critical gap in the literature this study seeks to address. According to Vogel and O'Brien (2006) and McOmber et al. (2013), climate information must be accurate, relevant, and accessible across genders to be beneficial to all. However, in Dodoma, the availability of adequate and appropriate climate information, knowledge, and data hinders climate adaptation efforts (GoK, 2014a).

In Dodoma, women's knowledge sharing about climate change relies heavily on traditional methods, which can limit access to up-to-date information and technology because of limited infrastructure, poverty, and illiteracy. While mobile phones offer a practical way to share new farming techniques and best practices, enhancing women's ICT self-efficacy is crucial for them to fully leverage these tools for effective knowledge management and adaptation to climate change impacts, such as drought and reduced agricultural yields.

Women farmers in Dodoma are increasingly adopting climate-smart agriculture (CSA) practices, especially in Mpunguzi, Mbalawala, and Hombolo. While CSA has the potential to mitigate climate change impacts, its benefits are not shared equally, as evidenced by a notable gender gap in adoption (Lana M et al., 2025). To ensure successful implementation and increase women's uptake of CSA, it is essential to promote equitable land access, develop inclusive training programs that account for women's time constraints, and increase the presence of female extension workers to improve information dissemination. Furthermore, enhancing access to credit, strengthening social networks through farmer groups, and improving transport infrastructure to reduce logistical challenges are vital steps to support broader CSA adoption (Swai, O., 2017; Awoke, M. D., et al., 2025; Lana, M., et al., 2025).

2.6.2 Institutional Arrangement with the extension services

Institutional arrangements play a crucial role in mitigating vulnerability. Local institutions, including state and civil society organizations, especially those that foster social capital through group-based strategies, can be highly beneficial for women and communities. They create opportunities for knowledge exchange, resource gathering, and strengthening resilience in the context of climate change adaptation strategies (Mueller et al., 2013; Ngigi et al., 2015).

Access to extension services can significantly improve agricultural productivity. This, in turn, helps achieve several Sustainable Development Goals (SDGs), including SDG 2—ending hunger, ensuring food security, and promoting sustainable agriculture. However, in Dodoma, women's access to extension services remains low. Therefore, expanding women farmers' access to these services will enhance their well-being by providing them with information on effective climate adaptation strategies in Dodoma (Davis, Babu, and Ragasa, 2020; Spielman et al., 2021).

Women farmers in Dodoma have lower literacy levels, which makes them less effective in climate change adaptation strategies than their male counterparts and puts them at a disadvantage in understanding its impacts (Amran & Abdul Fatah, 2020). Interactive and communicative learning methods are necessary to encourage hands-on learning, field experiments, and the development of critical thinking skills, while also highlighting women role models and trainers to support ongoing human capital development (McGuire et al., 2022).

2.6.3 Women's characteristics, values, norms, socioeconomic status, and education level

Women's adaptation to climate change is profoundly shaped by socioeconomic factors, education, gender norms, and individual values. These factors influence their access to resources, knowledge, decision-making authority, and preferred strategies. In Dodoma, women face disproportionate vulnerability to climate impacts; however, they are also strategic agents who can leverage social networks and traditional knowledge to enhance resilience, particularly when empowered to assume leadership roles and decision-making responsibilities (Bryan et al., 2024).

Social norms and values within a community, to a certain extent, influence the range of resources and skills that individuals can access, control, and manage to build adaptive capacities (Phan et al., 2019). Research on vulnerability and climate change adaptation frequently highlights the crucial role of gender, alongside ethnicity, culture, economy, age, disability, and social class, in shaping socialization and capacities (Balehey et al., 2018; Garcia et al., 2020).

In Dodoma, women's socioeconomic status, education, and prevailing social norms significantly shape their ability to adapt to climate change. Lower education and economic status limit access to resources and modern techniques, while traditional norms often constrain their decision-making power. Women tend to prioritize food, water, and firewood security through practices such as diversifying subsistence crops, whereas men usually focus on market-oriented, capital-intensive strategies. Targeted interventions are crucial, including land reforms, inclusive training, improved access to credit and extension services for women, and enhanced decision-making roles to strengthen adaptive capacity (Swai, O. W., 2017).

III. METHODOLOGY

3.1 Research Design

The study adopts a qualitative approach, using content analysis to examine the factors that influence women farmers' groups' adoption of climate change adaptation strategies in Dodoma.

3.2 Study Area

The study area of this paper is the Dodoma region in Tanzania, East Africa. Dodoma is situated at approximately 6°10′S latitude and 35°45′E longitude, at an elevation of around 1,200 meters above sea level. The area covers 2,769 square kilometers (URT 1961; NBS 2022). The climate features are wet and dry seasons, with the dry season dominating for most of the year. These climatic conditions, combined with water scarcity and soil degradation, pose significant challenges to agricultural activities. Despite these constraints, agriculture remains the primary economic activity, particularly in rural areas, where many women are farmers and bear the brunt of these impacts (Swai et al., 2012; URT, 2007).

Although women constitute the majority of the agricultural workforce in Dodoma, they face institutional barriers, traditional norms, and limited access to resources and decision-making power (Akram-Lodhi and Komba, 2018; Jones et al., 2023). These conditions make Dodoma a suitable study area for this scholarship.

3.3 Data Collection

To gain a deeper understanding of the factors influencing women farmers' groups' adoption of climate change adaptation strategies, the study collected data by analyzing publicly available documents. Specifically, government reports, NGO publications, academic studies, local agricultural extension materials, and policy documents on the strategies that vulnerable women farmers' groups adopt to address climate change were gathered and analyzed.

The criteria for document selection focused on publications and reports containing the terms climate change, vulnerable women, and agriculture, with emphasis on those related to Dodoma and on publication date. For the purpose of this paper, publication dates from 2019 to 2025 were considered.

3.4 Data Analysis

Content analysis was used in this study to analyze the gathered data. Content analysis is a research method that systematically examines and identifies patterns, themes, and meanings in qualitative data. To achieve this, the study limited its content search to adaptation strategies and the factors influencing women farmers' adaptation strategies, developing themes from the gathered data.

IV. RESULTS

4.1 Conceptual Framework Integration

The study was guided by the analytical framework during data collection and analysis. Themes were developed from the variables in the framework and used to analyze the gathered documents. Based on the themes, the documents were grouped under each heading, and their content was analyzed for consistency.

4.2 Factors Influencing Women Farmers Adaptation Choices

4.2.1 Access to Resources and Technologies

The content analysis revealed that women's access to land, financial capital (soft loans), and improved agricultural technologies significantly influenced their ability to adopt advanced adaptation strategies. Documents highlighted that patriarchal land ownership systems (Lawson et al., 2020) and limited financial inclusion (Mamkwe, E., 2020) are major barriers.

4.2.1.1 Information Sharing

The results of the content analysis indicated that information sharing is a vital factor influencing women farmers' adoption of climate change adaptation strategies. Using mobile phones, women farmers in Dodoma can adopt drought-tolerant crops as an agricultural adaptation strategy (URT, 2009).

4.2.2.2 Access to Extension Services

The results of the content analysis indicate that access to extension services significantly improves agricultural productivity and helps achieve Sustainable Development Goal 2 (SDG 2)—ending hunger, ensuring food security, and promoting sustainable agriculture. Furthermore, access to these services enhances the well-being of women farmers by providing information on effective climate adaptation strategies in Dodoma (Davis, Babu, and Ragasa, 2020; Spielman et al., 2021).

4.2.3 Institutional Arrangements

The results of the content analysis indicated that institutional arrangements play a crucial role in mitigating vulnerability. Thus, local institutions, including state and civil society organizations, especially those that foster social capital through group-based strategies, are highly beneficial for women and communities. They create opportunities for knowledge exchange, resource mobilization, and resilience strengthening in the context of climate change adaptation strategies (Mueller et al., 2013; Ngigi et al., 2015).

4.2.4 Socio-economic status

The content analysis indicated that women's adaptation to climate change is profoundly influenced by socioeconomic factors, educational attainment, gender norms, and individual values. These elements affect their access to resources, knowledge, decision-making authority, and preferred strategies. According to Bryan et al. (2024), when women are empowered to assume leadership roles and decision-making responsibilities, they can leverage social networks and traditional knowledge to enhance resilience and adopt appropriate strategies to mitigate climate change.

4.3 Specific Adaptation Strategies Adopted by Women Farmers

4.3.1 Crop Rotation and Use of Improved Varieties

The study finds that women farmers in Dodoma frequently adopted crop rotation and the use of fast-maturing, drought-tolerant maize seeds (e.g., Situka) as key strategies. The analysis shows that these choices were often driven by the need to secure the household food supply given erratic rainfall patterns (URT, 2009).

4.3.1.1 Improved water use and management

Analysis of documents indicated that the Dodoma City Council and the Ministry of Water and Agriculture have implemented various strategies to help women adapt to the impacts of climate change (URT, 2023), including water harvesting systems and water-saving technologies.

4.3.1.2 Soil Health and Management

The study shows that women farmers in Dodoma, in collaboration with the Tanzania Agriculture Research Institute (TARI), frequently identify and characterize soil properties and production systems that optimize the use of available moisture and minimize land degradation. In addition, they have developed plant nutrition recommendation packages tailored to selected soils, agro-climatic conditions, and social circumstances. This maintains and enhances analytical services for soils, water, and plant samples for various purposes, including land evaluation, soil fertility appraisals, and water management studies (TARI, 2016).

4.3.1.3 Diversification and Intercropping

The study indicates that many female farmers in Dodoma have adopted intercropping as a mitigation strategy, combining maize with other crops, such as groundnuts, beans, and sorghum, to enhance soil nutrients and thereby improve crop yields (URT 2024; Swao O 2020).

V. DISCUSSION

The study findings indicate that access to information and technology, knowledge sharing, institutional arrangements, extension services, and socio-economic status are key factors affecting women farmers' adaptation choices. The results above indicate that the resources and technology available affect women farmers' choices of adaptation strategies. Due to inadequate resources and technology, women tend to adopt traditional strategies.

In relation to information sharing, it was evident that it plays a key role in their choice of adaptation strategies. The more information women farmers have about climate change, the more they adopt effective strategies to mitigate it.

With regard to institutional arrangements, the results indicate that effective institutional arrangements will shape women farmers' choice of adaptation strategies. Therefore, it is vital for governments to put in place the right institutions to help support women farmers' choices.

In addition, extension services are vital in shaping women farmers' adaptation strategies. Women farmers' access to extension services will provide them with diverse options that will guide their choice of climate change adaptation strategies.

Results on socio-economic status indicate that empowering women to take leadership and decision-making roles in communities will provide them with opportunities to contribute to developing the best strategies for climate change adaptation.

VI. LIMITATIONS OF THE STUDY

The current study adopted a content analysis of public documents. These documents reflect individuals' views, which may be subject to bias. Another notable limitation is the study's scope. The study was limited to a specific area that has distinct characteristics from other geographic zones.

VII. FUTURE RESEARCH

Future studies should empirically test the relationships among the variables in the research framework. In addition, future studies should examine different geographic regions to capture diverse perspectives.

REFERENCES

[1] A.T.M Sanaul Haque, Lalit Kumar, Navjot Bhullar. 2023. Gendered perceptions of climate change and agricultural adaptation practices: a systematic review

[2] AWDF *2015 Climate Change and the Livelihoods of Women*: The AWDF and Grantees Approach.

[3] Bast .J. (2010). *Seven Theories of Climate Change*. The Heartland Institute 33pp

[4] Blakstad, M.M., Smith, E.R., 2020. Climate change worsens global inequity in maternal nutrition. Lancet 4, e547–e548. https://doi.org/10.1016/S2542-5196(20)30246-1.

[5] Boora, S., Kaur, B., Tyagiq, R., Bishnoi, D. K., k, M., and k, R. (2023). Extent of adoption of intercropping practices among farmers of Haryana. Indian Journal of Extension Education, 59(1),

[6] Brock, H., 2012. Climate Change: Drivers of Insecurity and the Global South. Retrieved from. https://www. files. ethz. ch/isn/138982/Competition.

[7] Elizabeth Bryan, Muzna Alvi, Sophia Huyer (2024). Addressing gender Inequalities and strengthening women's agency to create more climate-resilient and sustainable food systems.

[8] Food and Agriculture Organisation (FAO) (2007). People-centered climate change adaptation: Integrating gender issues, Policy Brief, Rome.

[9] Francis Mwaijande. (2025). Policy Agenda Setting for Blue Economy and Socio-Economic Development in Tanzania.

[10] International Union for Conservation of Nature (2007). Gender Aspects of Climate Change, Briefing paper, retrieved from http://www.iucn.org/en/news/archive/2007/03/7_gender_climate_change.pdf.

[11] International Union for Conservation of Nature (IUCN/UNDP/GGCA) (2009). Training Manual on Gender Climate Change http://data.iucn.org/dbtw-wpd/edocs/2009-012.pdf

[12] Kemboi, E., Muendo, K., and Kiprotich, C. (2020). Crop diversification analysis amongst smallholder farmers in Kenya (empirical evidence from Kamariny ward, Elgeyo Marakwet County). Cogent Food and Agriculture, 6(1)

[13] Kenfaoui, J., Lahlali, R., Laasli, S., Lahmamsi, H., Goura, K., Taoussi, M., Mennani, M., Fardi, M., Tahiri, A., Amiri, S., and Ghadraoui, L. E. (2024). Farmer's knowledge, perception, and practices in managing insect pests and diseases of grapevine in Morocco. International Journal of Pest Management

[14] Kalele, D. N., Ogara, W. O., Oludhe, C., and Onono, J. O. (2021). Climate change Impacts and relevance of smallholder farmers' response in arid and semi-arid lands in Kenya.

[15] Mahlet Degefu Awoke, Katharina Löhr, Katharina Löhr, Marcos Lana, Boris D. Soh Wenda, Kwabena Buabeng, Johannes Michael Hafner, Stefan Sieber (2024). Exploring gender dynamics in climate-smart agriculture adoption: a study in semi-arid Dodoma, Tanzania

[16] Mbwambo, J. S., Mwatawala, H. W., & Mngale, A. S. (2011). Farmers coping Strategies against climate change in Singida District, Tanzania.

[17] Mishra, P., 2017. Green human resource management: A framework for sustainable organizational development in an emerging economy. Int. J. Organ. Anal. 25 (5), 762–788.

[18] Ministry of Agriculture*: www.kilimo.go.tz*

[19] National Burea of Statistics Census Report 2022

[20] Nabikolo, D., Bashaasha, B., Mangheni, M. N., & Majaliwa, J. G. M. (2012). Determinants of climate change adaptation among male and female-headed farm households in Eastern Uganda

[21] Prof. Aurelia Ngirwa Kamuzora. 2023. Effects of Climate Change Adaptation Strategies on Maize Productivity among Smallholder Farmers in Dodoma, Tanzania

[22] UNDP (2010), *Asia-Pacific Human Development Report – Power, Voice and Rights: A Turning Point for Gender Equality in Asia and the Pacific*, Macmillan Publishers India, Pg 255

[23] UNFCCC. 2007. *Climate Change: Impacts, Vulnerabilities and Adaptations in Developing Countries*. Pg 68 United Nations Population Fund (UNFPA/WEDO) (2009). Climate Change Connections. Gender and Population

[24] Rodenberg, B. (2009). Climate Change Adaptation from a Gender Perspective. German Development Institute Es sind die Machtverhältnisse, die Frauen für denKlimawandel verwundbarer machen', Böll THEMA, Heft 2/2009,p. 14<http://www.boell.de/downloads/publikationen/BoellThema_2.2009_abRea der7kommentierbar.pdf> (10.12.2023)

[25] Sahu, G. T., Kaur, S., and Singh, G. (2019). Knowledge level of farmers and constraints faced in adoption of crop rotation system. Current Journal of Applied Science and Technology,

[26] Smith, K.R., Woodward, A., Campbell-Lendrum, D., Chadee, D.D., Honda, Y., Liu, ., et al., 2014. Human health: impacts, adaptation, and co-benefits. In: Field, C.B., et al. (Eds.), Climate Change 2014: Impacts, Adaptation, and Vulnerability. Part A: Global and Sectoral Aspects. Contribution of Working Group II to the Fifth Assessment Report of the Intergovernmental Panel on Climate Change. Cambridge University Press, Cambridge, UK and New York, NY, pp. 709–754.

[27] Swai, O. W., Mbwambo, J. S., & Magayane, F. T. (2019). Gender and adaptation practices to the effects of climate change in Bahi and Kondoa Districts Dodoma region, Tanzania. Journal of Sustainable Development, 5(12)

[28] Ulrich-Schad, J., De Jalón, S. G., Babin, N., Pape, A., and Prokopy, L. (2017). Measuring and understanding agricultural producers' adoption of http://www.wedo.org/category/act/climate-change-toolkit (09.12.2023)

[29] URT (2022). *Population and Housing Census. National Bureau of Statistics*. Ministry of Finance,

[30] URT (2013): *National Agriculture Policy.*

[31] United Republic of Tanzania. (2007). National Adaptation Programme of Action APA). Vice President's Office, Division of Environment, January 2007. 52pp.

[32] United Republic of Tanzania. (2023). Dodoma Region Socio-economic Profile. Government Printer Dar es Salaam Tanzania.

[33] UNDP (2023). *Bridging the gender gap: Empowering Women in the Agricultural Sector.*

[34] Velasco-Muñoz, J. F., Aznar-Sánchez, J. Á., López- Felices, B., and Balacco, G. (2022). Adopting sustainable water management practices in agriculture based on stakeholder preferences. Agricultural Economics (Zemědělská Ekonomika),

[35] Weiler, V., Udo, H.M.J., Viets, T., Crane, T.A., De Boer, I.J.M., 2014. Handling multi-functionality of livestock in a life cycle assessment: the case of smallholder dairying in Kenya. Curr. Opin. Environ. Sustain. 8, 29–38. https://doi.org/10.1016/j. cosust.2014.07.009.

[36] Women's Environment & Development Organization (WEDO) (2007). Changing the Climate: Why women's perspectives matter, New York, p. 3.

[37] Women's Environment and Development Organization (WEDO/ABANTU) for Development/Action Aid/ENDA (2008). Gender, Climate Change and Human Security: Lessons from Bangladesh, Ghana and Senegal<http://www.wedo.org/wp-content/uploads/hsn-study-final-may-20- 2008.pdf> (09.12.2023).

International Journal of Environment, Agriculture and Biotechnology
Vol-11, Issue-2; Mar-Apr, 2026
Peer-Reviewed International Journal
Journal Home Page Available: https://ijeab.com/
Journal DOI: 10.22161/ijeab

AI-Driven Integration of Multi-Omics Data for Gene Function Discovery and Prediction of Complex Crop Phenotypes

Binsy Karattuchali*, Mohammed Fazil Chalattilkalladithodi

*Corresponding author

Received: 16 Mar 2026; Received in revised form: 19 Apr 2026; Accepted: 23 Apr 2026; Available online: 30 Apr 2026

***Abstract*— *Recent advances in high-throughput genotyping, phenotyping, and multi-omics technologies have generated large, heterogeneous datasets spanning genomics, transcriptomics, proteomics, metabolomics, epigenomics, and phenomics across plant species. Conventional statistical and machine-learning approaches often struggle to integrate these modalities, limiting mechanistic insight and predictive accuracy for complex genotype-environment-phenotype relationships. Artificial intelligence (AI), particularly deep learning and graph-based architectures, provides powerful tools for multi-omics data fusion, regulatory network reconstruction, and prediction of polygenic, environmentally modulated traits. This review synthesizes current applications of AI-driven multi-omics integration in plant science, with a focus on gene function annotation, cellular network inference, and complex crop phenotype prediction. We examine key methodological frameworks including autoencoders, variational generative models, multimodal transformers, graph neural networks, and self-supervised foundation models, highlighting representative case studies in Arabidopsis and major crops such as rice, maize, wheat, and tomato. We critically assess challenges related to data quality, batch effects, domain shift, metadata standardization, model interpretability, and reproducibility, and outline future directions encompassing plant-specific foundation models, pan-omics integration, digital-twin cropping systems, and community-driven benchmarking.*

Keywords*— *Artificial intelligence, Multi-omics integration, Gene function prediction, Crop phenotypes, Graph neural networks, Reproducibility.

I. INTRODUCTION

Over the past decade, plant science has undergone rapid expansion in biological and agronomic data generation (Marks et al., 2023; Shiu & Lehti-Shiu, 2024). High-quality reference genomes and pangenomes for major crops are now complemented by large-scale resequencing, single-cell and spatial transcriptomics, chromatin accessibility profiling, proteomics, metabolomics, and high-throughput phenotyping using drones, robotics, and imaging platforms (Gill et al., 2022). Despite this data richness, integrating heterogeneous multi-omics datasets to achieve mechanistic insight and predictive accuracy remains a central challenge (Kajrolkar, 2025). Conventional analytical approaches fail to capture nonlinear dependencies, conditional interactions, and cross-modal relationships that underpin complex traits (Jamil et al., 2020), with limitations amplified by technical noise, missing values, batch effects, and strong tissue-, time-, and environment-specific variation typical of plant datasets (Jain et al., 2024).

AI provides a complementary framework for addressing these challenges. Deep learning architectures including autoencoders, GNNs, CNNs, recurrent networks, and transformers learn latent representations capturing nonlinear and hierarchical structure across multiple biological layers (Cembrowska-Lech et al., 2023). By integrating genomics through phenomics, these models enable inference of gene function, reconstruction of regulatory and metabolic networks, and prediction of complex phenotypes under diverse environmental conditions (Montesinos-Lopez et al., 2024; Xu et al., 2025).

This review provides an integrated overview of AI methodologies for multi-omics data fusion in plant science, summarizing key model architectures, representative applications, critical limitations, and future directions.

II. MULTI-OMICS DATA IN PLANT SYSTEMS: OPPORTUNITIES AND INTEGRATION CHALLENGES

The multi-omics paradigm reflects the hierarchical flow of biological information from DNA sequence variation to organism-level phenotypes (Mahmood et al., 2022). No single omics layer can fully explain complex traits such as yield, stress tolerance, or nutritional quality (Balotf et al., 2025). Genomics defines the static genetic blueprint; transcriptomics characterizes dynamic regulatory activity; proteomics reveals functional protein machinery; metabolomics captures biochemical endpoints; epigenomics identifies heritable regulatory modifications; and phenomics quantifies observable outcomes shaped by gene-environment interactions (Amin et al., 2025).

2.1 Omics Layers

Genomics constitutes the foundational layer of multi-omics integration. Chromosome-scale reference genomes are now available for major crops enabled by PacBio HiFi and Oxford Nanopore sequencing (Wang et al., 2023; Hufford et al., 2021). Pangenomes capture intraspecific diversity including structural variation and presence-absence variation absent from linear reference genomes; the maize pangenome comprises over 100,000 non-redundant genes and highlights extensive copy-number variation (Hufford et al., 2021; Jayakodi et al., 2024). However, genomic variation alone rarely explains phenotypic outcomes without functional context, underscoring the necessity of multi-omics integration.

Transcriptomics provides a dynamic view of gene expression. In rice, time-resolved transcriptome analyses during dehydration/rehydration and functional studies of OsCCA1 controlling ABA signaling revealed key transcriptional hubs governing osmotic adjustment (Park & Jeong, 2023; Wei et al., 2022). In maize, Stereo-seq spatial transcriptomics of the developing ear revealed spatially resolved regulatory networks (Y. Wang et al., 2024). Proteomics captures post-transcriptional and post-translational regulation; proximity-labeling techniques such as TurboID enable in vivo detection of transient interactions (Arora et al., 2020). Metabolomics in wheat linked flavonoid accumulation to specific loci via metabolite-based GWAS (J. Chen et al., 2020; D. Ma et al., 2022), although comprehensive metabolite annotation remains challenging (Mahieu & Patti, 2017; Nguyen et al., 2024). Epigenomic mechanisms including DNA methylation, histone modifications, and chromatin accessibility drive phenotypic plasticity; stress-responsive TE activation in maize and heat-induced 3D genome reorganization in Arabidopsis illustrate epigenomic variation as a key regulatory layer (Liang et al., 2021; L. Sun et al., 2020). High-throughput phenomics translates molecular variation into quantitative traits using RGB, hyperspectral, and 3D scanning platforms, with UAV-based imaging successfully predicting soybean yield (Herrero-Huerta et al., 2020).

2.2 Integration Challenges

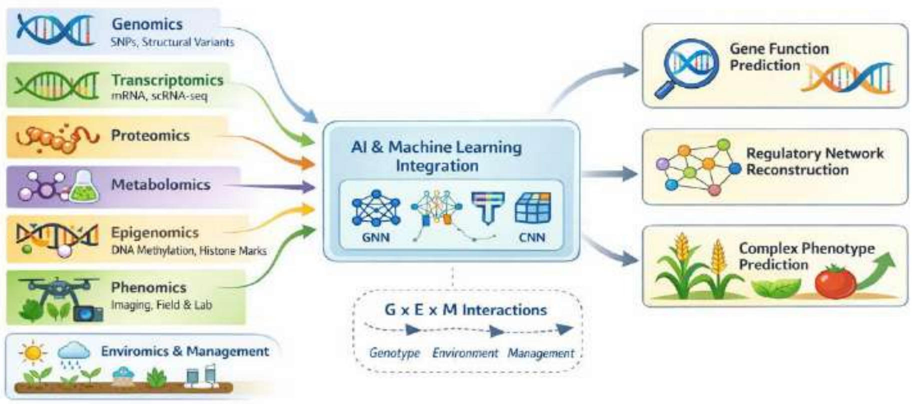

Fig.1. Conceptual overview of AI-driven multi-omics integration in plants.

Heterogeneous omics (genomics, transcriptomics, proteomics, metabolomics, epigenomics, phenomics) and environmental/management data are integrated using advanced AI frameworks (graph neural networks, CNNs, transformers, multimodal deep networks) to predict gene function, reconstruct regulatory networks, and forecast complex crop phenotypes. G×E×M interactions influence outputs, enabling climate-resilient crop design and precision breeding.

Integrating multi-omics datasets poses substantial technical challenges. Omics layers differ markedly in data structure, dimensionality, and preprocessing requirements, necessitating modality-specific normalization (Huang et al., 2017). Batch effects arising from differences in instrumentation frequently obscure biological signals (Leek et al., 2010). Missing data are pervasive because comprehensive profiling across all layers is rarely feasible (Flores et al., 2023). Nonlinear gene-environment interactions, epistasis, pleiotropy, and feedback regulation exceed the representational capacity of traditional linear models. Consequently, classical integration approaches such as PCA and canonical correlation analysis often fail to capture meaningful biological relationships, whereas emerging deep learning frameworks better model nonlinear, hierarchical interactions.

III. AI APPROACHES FOR MULTI-OMICS INTEGRATION

Effective integration of multi-omics data requires computational frameworks capable of jointly modeling high-dimensional, heterogeneous, and frequently incomplete datasets while capturing nonlinear, context-dependent interactions. Deep learning and AI methodologies have consistently outperformed traditional statistical and classical machine learning approaches in predictive accuracy, scalability, and biological relevance (Libbrecht & Noble, 2015; Reel et al., 2021).

3.1 Classical Machine Learning

Before deep learning, classical machine learning methods including random forests, SVMs, LASSO, elastic net, PLS regression, and Bayesian networks were widely applied to QTL mapping, genomic selection, and eQTL studies (Crossa et al., 2010; Rohart et al., 2017). These approaches offer useful interpretability but exhibit substantial limitations for large-scale, multi-omics integration: most assume linear or additive relationships, limiting their capacity to model epistatic interactions, nonlinear regulation, or G×E effects. They scale poorly to the extreme dimensionality of omics datasets (Libbrecht & Noble, 2015; Reel et al., 2021). Classical methods are now primarily used as benchmarking tools within hybrid pipelines.

3.2 Autoencoders and Variational Autoencoders

Autoencoders (AEs) compress diverse inputs into a low-dimensional latent bottleneck via an encoder-decoder architecture (Hinton & Salakhutdinov, 2006). In plants, denoising autoencoders applied to maize RNA-seq and LC-MS profiles under nitrogen limitation identified latent factors linked to nitrogen assimilation while mitigating batch effects (Kannan et al., 2025). Variational autoencoders (VAEs) model latent variables as probability distributions, optimizing the evidence lower bound (ELBO) to balance reconstruction accuracy against prior divergence (Kingma & Welling, 2013), enabling uncertainty quantification, generative sampling, and missing data imputation. Multimodal VAEs integrating SNPs, transcriptomes, and metabolomes in rice achieved approximately 25% higher accuracy than PCA or CCA baselines and imputed up to 30% missing metabolomic features (Zargar et al., 2022). Conditional VAEs integrating time-series scRNA-seq and metabolomics during Arabidopsis floral transition revealed coordinated changes in hormone signaling and secondary metabolism (Jeong et al., 2024).

3.3 Multimodal Deep Neural Networks

Multimodal deep neural networks (MDNNs) integrate heterogeneous data types via modality-specific subnetworks with flexible fusion strategies (Tabakhi et al., 2023). Early fusion concatenates features from all modalities; intermediate (hybrid) fusion combines modality-specific encoders through attention or tensor operations, preserving modality-specific structure while enabling nonlinear cross-modal interactions (Montesinos-Lopez et al., 2023); late fusion aggregates predictions from independently trained unimodal models via ensembling. MDNNs integrating genotypic information, remote-sensing imagery, and environmental variables have demonstrated improved prediction of agronomic traits compared with unimodal approaches (Shamsuddin et al., 2024), and advanced architectures incorporating cross-attention and gating units improve interpretability and dynamic modality weighting (Gong et al., 2023).

3.4 Transformers

Transformers use self-attention mechanisms to model long-range dependencies and contextual relationships, making them well-suited for sequence-based and heterogeneous omics data (Vaswani et al., 2017). Genomic transformers such as DNABERT predict regulatory elements and chromatin accessibility from k-mer tokenized sequences and have been applied to plant genomes for promoter and enhancer identification (Ji et al., 2021). Cross-attention mechanisms link genomic variants with transcriptomic or metabolomic profiles, and diverse data types including SNPs, gene expression tokens, and image patches can be unified into a single sequence for joint modeling (Rao et al., 2021). Vision transformers (ViT) outperform CNNs in feature extraction from high-resolution or hyperspectral plant imagery, and coupling ViT with transcriptomic data via cross-attention reveals spectral-transcriptomic correlations relevant to nutrient use efficiency and stress responses (Dosovitskiy et al., 2020). Practical limitations of large transformer models include high computational and memory demands, mitigated by model distillation and parameter-efficient fine-tuning (Zaheer et al., 2020).

3.5 Graph Neural Networks

GNNs learn representations on graph-structured data, propagating information across nodes (genes, proteins, metabolites) and edges (PPI, co-expression, metabolic reactions) to integrate heterogeneous multi-omics measurements (Kipf & Welling, 2016; Velickovic et al., 2017). Graph convolutional networks (GCNs) learn node representations by aggregating local neighborhood information; graph attention networks (GATs) assign condition-specific weights to edges, prioritizing regulatory interactions under stress. Heterogeneous GNNs model multiple node and edge types simultaneously, enabling joint learning of TF-gene, protein-protein, and metabolic interactions. In plants, integration of TF binding data, pathway annotations, and single-cell expression profiles has improved GRN reconstruction accuracy compared with classical approaches (Huynh-Thu et al., 2010). Intrinsic attention mechanisms and post-hoc tools such as GNNExplainer reveal influential subgraphs, enabling tracing of signal propagation through regulatory hierarchies (Ying et al., 2019).

3.6 Self-Supervised Learning and Foundation Models

Self-supervised learning (SSL) leverages unlabeled data to learn generalizable representations via surrogate tasks including masked-omics modeling, contrastive learning, and cross-modal prediction, addressing the scarcity of labeled multi-omics datasets in plant biology (LeCun et al., 2015; Liu et al., 2021). Foundation models such as protein language models trained on hundreds of millions of sequences generate embeddings predicting enzyme function and variant effects (Rives et al., 2021; Elnaggar et al., 2021). Vision transformers pretrained on field images enable robust trait extraction and transfer learning for phenotyping (Dosovitskiy et al., 2020). SSL and foundation models provide scalable, flexible frameworks to accelerate gene function discovery and crop trait prediction, particularly when combined with domain adaptation and interpretable fine-tuning.

IV. AI FOR GENE FUNCTION PREDICTION

In plant genomics, approximately 40-60% of genes in major crop genomes remain annotated as hypothetical or uncharacterized proteins (Michael & VanBuren, 2020). Conventional annotation strategies based on sequence similarity searches, domain identification, and co-expression network analyses perform poorly for lineage-specific or rapidly evolving plant genes, exhibiting high false-negative rates and failing to capture conditional regulation, epistatic interactions, or post-transcriptional control (Bolser et al., 2016). AI-driven frameworks can reduce annotation errors and improve predictive accuracy by approximately 20-30% in early benchmarking studies by integrating multi-omics data to uncover nonlinear biological patterns (Jumper et al., 2021).

4.1 Predicting Gene Function Using Integrated Omics

Deep learning-based multimodal frameworks learn shared latent representations from heterogeneous omics datasets including VAEs, multimodal transformers, GNNs, and multimodal autoencoders integrating genomic variation, transcriptomic profiles, epigenomic information, and proteomic measurements. In Arabidopsis, machine-learning frameworks combining genomic, transcriptomic, and methylomic data outperform genome-only models in predicting complex traits and identifying regulatory genes, with models achieving predictive accuracies exceeding 80% for gene expression based on flanking sequence inputs (P. Wang et al., 2024; Peleke et al., 2024). Transfer learning extends applicability to data-limited crops; cross-species learning strategies have improved regulatory network inference in poplar and maize (Mummadi et al., 2025). Multimodal deep learning frameworks effectively capture nonlinear and context-dependent regulatory effects including epistasis and environment-specific gene activity, and can impute missing omics layers such as predicting chromatin states from genotype and expression data.

4.2 Transcription Factor-Target Prediction

TF-target prediction requires integration of sequence-based binding potential with chromatin accessibility, epigenetic modifications, and condition-specific expression dynamics. Deep learning reframes TF-target inference as a heterogeneous graph learning problem: GNNs and GATs represent TFs, target genes, and regulatory elements as nodes, with edges encoding evidence from TF binding assays (DAP-seq, ChIP-seq), ATAC-seq accessibility, cis-motif occurrence, and histone modifications (Song et al., 2016). In Arabidopsis, large-scale DAP-seq datasets have provided a foundation for integrative regulatory network reconstruction, with subsequent studies showing that epigenomic context substantially refines TF-target predictions under stress conditions (Maher et al., 2017). Transformer-based architectures further advance TF-target prediction by modeling long-range dependencies, and integrative learning-based frameworks consistently outperform motif-only tools such as FIMO when evaluated against experimentally validated TF-target interactions (Fornes et al., 2019).

4.3 Enzyme Function Prediction and Case Studies

Plant enzymes frequently exhibit lineage-specific expansion, neo-functionalization, and relaxed substrate specificity, limiting homology-based annotation (Schlapfer et al., 2017). Protein language models (PLMs) such as ESM-1b and ProtBERT, pretrained on hundreds of millions of sequences, capture evolutionary constraints and functional motifs without explicit sequence alignment (Rives et al., 2021; Elnaggar et al., 2021). PLM-derived embeddings integrated with transcriptomic and metabolomic data enabled reconstruction of large portions of tomato flavonoid and phenylpropanoid biosynthetic pathways (Zhu et al., 2018). GNNs applied to curated metabolic graphs infer EC numbers and pathway positions; in maize, attention-based GNNs resolved isoform-level functions within oxylipin and jasmonate biosynthesis (Zhang et al., 2021). PLM- and GNN-based approaches outperform classical sequence similarity methods by approximately 30-50% for orphan plant enzymes. Key case studies illustrate these advances: in rice, transformer-based architectures prioritized CIPKs involved in osmotic stress adaptation, with CRISPR-Cas9 validation confirming altered proline accumulation and enhanced salt tolerance (Guo et al., 2024); in maize, graph attention networks identified previously uncharacterized lipid transfer proteins associated with kernel filling, confirmed by near-isogenic lines and field trials (Zhang et al., 2021); and in tomato, graph convolutional networks successfully reconstructed anthocyanin and flavonoid biosynthetic branches with enzymatic and regulatory roles validated by qRT-PCR and enzyme activity assays (Zhu et al., 2018).

5. AI for Reconstructing Cellular and Regulatory Networks

Cellular and regulatory networks including GRNs, PPI networks, metabolic pathways, and signaling cascades constitute the molecular circuitry governing plant development, homeostasis, and stress responses. Reconstructing these networks from high-dimensional omics data remains challenging due to nonlinear interactions, feedback regulation, and pervasive crosstalk (Zitnik et al., 2018). Conventional approaches such as WGCNA, ARACNE, and Bayesian networks primarily infer static or pairwise associations. AI approaches including GNNs, RNNs, VAEs, and transformers substantially improve network reconstruction by learning higher-order dependencies and context-specific regulatory logic (Zitnik et al., 2018).

5.1 Network Inference and Dynamic Modeling

GNNs operate directly on graph-structured data with multi-omics features incorporated as node or edge attributes, enabling context-aware regulatory inference (Kipf & Welling, 2016). Heterogeneous GNNs enhance inference by explicitly modeling multiple node and edge types, enabling simultaneous learning of TF-gene, protein-protein, and metabolic interactions. Integration of TF binding data, pathway annotations, and single-cell expression profiles has improved GRN reconstruction accuracy compared with classical approaches such as GENIE3 and Inferelator (Huynh-Thu et al., 2010). GNN-based models support modular network decomposition, facilitating rational prioritization of candidate regulators for genome editing.

Regulatory networks are inherently dynamic, undergoing extensive temporal and condition-dependent rewiring. RNNs including LSTM and GRU architectures infer delayed regulatory effects and nonlinear feedback loops from time-series transcriptomic and metabolomic data (Hochreiter & Schmidhuber, 1997). Neural ODEs model regulatory dynamics as continuous-time systems governed by learnable differential equations, and in plant biology have reconstructed developmental continua from scRNA-seq data, capturing cell-fate transitions and oscillatory modules involved in meristem maintenance and floral transition (Trapnell et al., 2014; R.T.Q. Chen et al., 2018). Pathway crosstalk such as JA-SA antagonism in immunity is modeled by multimodal transformers with multi-head attention, where distinct biological layers are integrated via cross-attention mechanisms (Vaswani et al., 2017). In Arabidopsis, integrative network analyses consistently identify NPR1 and AP2/ERF transcription factors as central hubs mediating JA-SA antagonism and multi-hormone crosstalk (J. Yang et al., 2019).

5.2 Single-Cell Network Reconstruction

Bulk omics analyses average signals across heterogeneous cell populations, obscuring cell-type-specific regulatory programs. ScRNA-seq and scATAC-seq combined with multi-omics integration have enabled reconstruction of cell-type-resolved GRNs at unprecedented resolution (Ryu et al., 2019). VAEs and graph-based models denoise dropout-prone single-cell data, infer developmental trajectories, and reconstruct TF-target interactions at the cell-cluster level. In Arabidopsis roots, large-scale scRNA-seq atlases revealed 149 expression modules along developmental trajectories, including regulators of quiescent center maintenance, metabolic specialization, and auxin-mediated gravitropism (Han et al., 2024). Integration of chromatin accessibility and transcriptomic data further revealed thousands of cell-type-specific regulatory elements (Dorrity et al., 2021). Comparable studies in rice root tips established transferable frameworks for GRN reconstruction in crops (Feng et al., 2022). These AI-driven single-cell network models support precision genome engineering and integration with spatial transcriptomics for three-dimensional regulatory mapping.

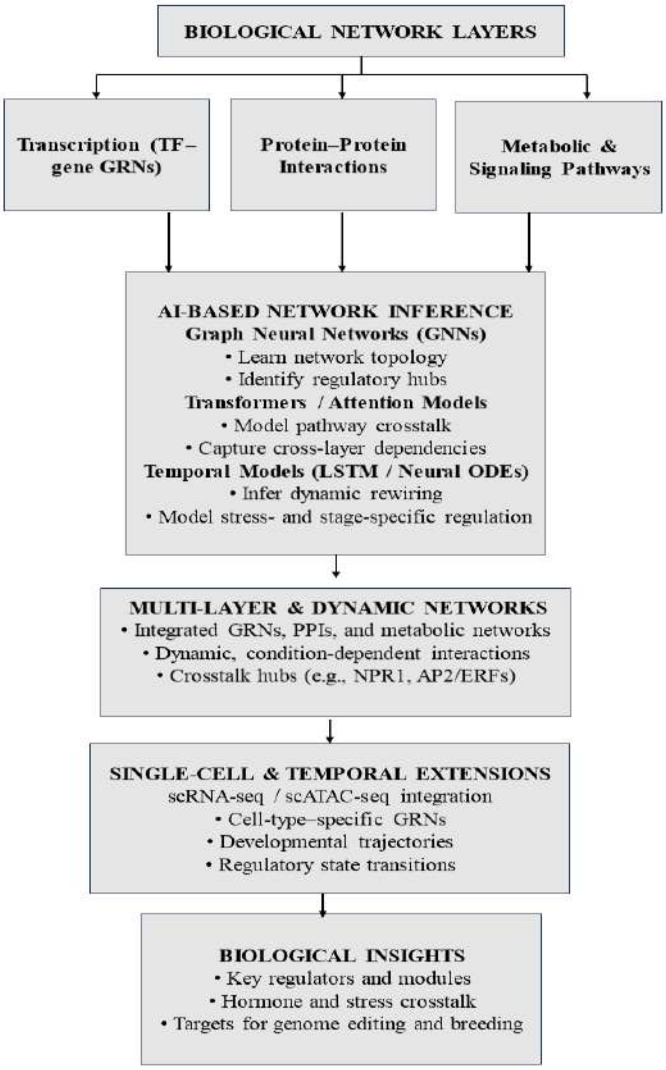

Fig.2. AI frameworks for regulatory network reconstruction and crosstalk modelling

The figure illustrates AI-based integration of transcriptional, protein–protein, and metabolic networks using graph neural networks, transformer models, and temporal learning approaches. These frameworks enable dynamic, cell-type–resolved reconstruction of regulatory networks and the identification of key crosstalk regulators relevant to plant development, stress responses, and crop improvement.

V. AI FOR PREDICTING COMPLEX CROP PHENOTYPES

Complex agronomic phenotypes including yield, phenological development, stress tolerance, nutritional quality, and resource-use efficiency are governed by highly polygenic architectures shaped by nonlinear G×E×M interactions. Conventional GS methods such as RR-BLUP and GBLUP predominantly assume additive genetic effects and linear responses, limiting their capacity to capture epistasis, pleiotropy, rare alleles, and environment-dependent phenotypic plasticity (Crossa et al., 2017). AI approaches including deep neural networks, kernel-based learning, and transformer architectures offer a powerful alternative by learning hierarchical and nonlinear representations from high-dimensional data.

6.1 Genotype-Phenotype and Multi-Omics Prediction

Deep learning enhances genomic prediction by automatically extracting multi-scale features capturing linkage disequilibrium, epistasis, and long-range genetic interactions. CNNs applied to SNP matrices enable detection of local haplotype patterns and non-additive effects beyond the capabilities of linear models (W. Ma et al., 2018; O.A. Montesinos-Lopez et al., 2021). Pretrained DNA language models such as DNABERT embed sequence variation into contextual representations, and attention-based models have consistently outperformed GBLUP across environments by modeling epistatic interactions, rare variants, and G×E effects in wheat and maize multi-environment trials (Ji et al., 2021; Crossa et al., 2019). MDNNs address the limitations of single-omics genomic selection by integrating multiple omics modalities through intermediate fusion architectures (Subramanian et al., 2020). In sorghum and maize, MDNNs integrating SNPs with transcriptomic and metabolomic profiles significantly improved predictions of drought tolerance, nitrogen-use efficiency, and biomass accumulation (Gu et al., 2025). In tomato, late-fusion ensemble models combining transcriptomic data with hyperspectral phenotyping achieved high classification accuracy for fruit quality traits including carotenoid content and firmness (Xiang et al., 2022). VAEs and generative models improve robustness by imputing missing omics layers, enabling stable phenotype prediction under partial data availability (Way & Greene, 2017).

6.2 Modeling G×E×M Interactions

AI-based models encode enviromics including weather, soil, and management variables as structured, time-resolved inputs. RNNs and LSTM architectures model seasonal and intra-seasonal environmental dynamics (Khaki & Wang, 2019), while transformer architectures integrate genomic markers with sequential environmental data and high-throughput phenotyping, capturing long-range temporal dependencies and context-specific genetic effects such as heat- or drought-induced shifts in QTL expression (O.A. Montesinos-Lopez et al., 2021). These frameworks support climate-resilient breeding by enabling in silico evaluation of genotype performance under future climate scenarios. Key examples include: multi-modal AI frameworks combining dense SNP markers, UAV-derived multispectral indices, and meteorological data substantially improving wheat yield predictions across multi-environment trials (Merrick et al., 2022); integrated transcriptomic-metabolomic models predicting tomato fruit quality traits including carotenoid, sugar, and organic acid content (Zhu et al., 2018; Xiang et al., 2022); and time-resolved multi-omics integration in rice distinguishing tolerant and susceptible genotypes under drought while identifying key dehydration-responsive transcription factor networks (V.H. Nguyen et al., 2023). AI-enabled G×E×M modeling shortens breeding cycles, improves early-generation selection accuracy, and facilitates climate-smart cultivar development.

VI. DATA QUALITY, REPRODUCIBILITY, AND STANDARDIZATION CHALLENGES

The successful translation of AI-driven multi-omics approaches into production environments is critically dependent on data quality, rigorous experimental design, and robust computational reproducibility. Plant omics datasets are frequently compromised by technical noise, batch effects, incomplete metadata, and platform heterogeneity, collectively inflating spurious correlations and restricting generalizability across laboratories, species, and environments.

7.1 Metadata, FAIR Principles, and Benchmarking

Reproducibility in omics research fundamentally depends on comprehensive and standardized metadata. A substantial fraction of publicly available plant omics datasets lack critical contextual information including growth conditions, stress intensity, sampling time points, and soil properties (Rajesh et al., 2021). The FAIR (Findable, Accessible, Interoperable, Reusable) data principles promote structured metadata annotated with community-recognized ontologies. In plant phenomics, the MIAPPE standard specifies more than 120 metadata fields; despite widespread endorsement, compliance remains below 30% in major repositories such as GEO (Rajesh et al., 2021). Frameworks such as ISA-Tab and the Plant Ontology support harmonized annotation across studies, though inconsistent terminology continues to confound meta-analyses (Dumschott et al., 2023). Emerging FAIR assessment tools including FAIRshake automate the evaluation of FAIR metrics and identify datasets unsuitable for AI model training (Cuellar et al., 2022). In contrast to computer vision and NLP, plant AI research lacks widely adopted benchmarks for multi-omics applications (Amin et al., 2025). Community-driven initiatives such as PlantGenie and OpenPlantML have proposed benchmark tasks encompassing GRN inference, yield prediction, and stress classification. A major limitation is the scarcity of held-out test datasets with experimentally validated ground truth, increasing the risk of overfitting. Federated benchmarking approaches, in which institutions share models or evaluation metrics without exchanging raw data, are emerging as a promising solution (Burankova et al., 2024).

7.2 Domain Shift and Explainability

AI models trained under controlled experimental conditions frequently exhibit degraded performance in heterogeneous field environments due to domain shift. Batch effects can exceed true biological signal (Leek et al., 2010), and correction methods such as ComBat, Harmony, and surrogate variable analysis are effective when batch variables are accurately annotated (Johnson et al., 2006; Korsunsky et al., 2019), but their effectiveness diminishes when metadata are incomplete or technical covariates are confounded with biological factors. Domain adaptation strategies including Domain Adversarial Neural Networks and VAEs have demonstrated improved transferability by aligning feature distributions across domains, with unsupervised domain adaptation enhancing plant disease recognition when transferring models from laboratory imagery to field conditions (Wu et al., 2023).

The increasing adoption of complex AI architectures has intensified concerns regarding model transparency, interpretability, and user trust (Tjoa & Guan, 2020). Attention-based architectures offer intrinsic interpretability by assigning weights to input features or graph nodes (Vaswani et al., 2017). Post-hoc explanation techniques such as SHAP and LIME decompose individual predictions into feature-level contributions (Lundberg & Lee, 2017); SHAP analyses of deep learning-based drought tolerance models in rice identified OsNAC transcription factor expression, proline accumulation, and ABA-related features as dominant contributors, consistent with well-characterized stress-response pathways (L. Xu et al., 2024). Pathway-centric explanations from GNNs enable higher-order interpretability by mapping predictions onto known biological pathways, and hybrid modeling strategies combining deep neural feature extractors with transparent downstream models further balance performance and interpretability (Molnar, 2022).

7.3 Ethical and Data-Sharing Issues

Large-scale proprietary breeding datasets are frequently siloed within private corporations, raising concerns regarding knowledge monopolization and unequal access to AI-driven innovation (Rotz et al., 2019). Open science infrastructures including CyVerse, PlantArrayNet, and ELIXIR Plants promote data sharing aligned with FAIR data principles (Goff et al., 2011). Federated learning enables collaborative model training across distributed datasets without direct exchange of raw data, preserving confidentiality while leveraging collective statistical power (Q. Li et al., 2021; T. Li et al., 2020). International ethical AI frameworks from the FAO and OECD emphasize transparency, accountability, inclusiveness, and sustainability in agricultural AI systems, calling for systematic bias audits to address the overrepresentation of temperate, high-input cropping systems in training datasets. Community-governed initiatives such as DivSeek International and IPPN play a pivotal role in establishing shared standards for metadata harmonization, interoperability, and benefit-sharing (Minervini et al., 2015).

Table 1. Quantitative Performance of AI-Based Multi-Omics Integration Methods in Representative Plant Studies

AI Approach	Data Modalities	Plant System / Trait	Quantitative Outcome	Benchmark Comparison	Key Advantage	Representative Studies
Classical ML (RF, LASSO, PLS)	SNPs; transcriptomics; metabolomics	Maize yield, drought tolerance	R2: 0.35-0.55	PCA/linear (R2 < 0.40)	Interpretability; feature selection	Crossa et al., 2010; Rohart et al., 2017
Autoencoders (AE)	Transcriptomics + metabolomics	Maize nitrogen stress	Variance: ~60-70%	PCA: ~40-50%	Noise reduction; batch correction	Du et al., 2021; Yu, 2022
VAE / cVAE	SNPs + RNA-seq + metabolomics	Rice drought resilience	Accuracy +20-25%; imputation ~30%	PCA/CCA	Generative modeling; imputation	Zargar et al., 2022
Multimodal DNNs	SNPs + UAV imagery + weather	Wheat yield prediction	RMSE reduction: 10-25%	Genomic selection	G×E modeling; cross-modal	Montesinos-Lopez et al., 2021
Attention-based MDNNs	Hyperspectral + RNA-seq	Disease classification (tomato)	Accuracy: 85-92%	Unimodal CNNs: 70-80%	Dynamic modality weighting	Li et al., 2023; Gong et al., 2023
Transformers (sequence)	DNA sequence	Regulatory element prediction	AUROC: 0.85-0.92	CNN: ~0.80	Long-range dependencies	Ji et al., 2021; Avsec et al., 2021

Multimodal transformers	Genomics + transcriptomics + images	Phenotype prediction	Accuracy +15-30%	CNN or RNN baselines	Cross-attention; unified tokenization	Rao et al., 2021
GNNs (gene function)	Co-expression + PPI + GWAS	Gene function (maize, rice)	Top-k prioritization +20-35%	Network propagation	Topology-aware learning	Zitnik et al., 2018; Pan et al., 2024
GNNs (phenotype)	Multi-omics graphs	Kernel weight; yield traits	R2: 0.55-0.70	Linear mixed models	Mechanistic interpretability	Zhang et al., 2021
Self-supervised (SSL)	Unlabeled omics data	Multiple crops	Downstream accuracy +10-40%	Training from scratch	Label efficiency; transferability	Rives et al., 2019; Liu et al., 2021
Foundation models	Protein sequences; images; omics	Enzyme function; phenotyping	Zero/few-shot comparable to supervised	Task-specific models	Cross-species generalization	Elnaggar et al., 2020

Abbreviations: AUROC, area under the receiver operating characteristic curve; RMSE, root mean square error; R2, coefficient of determination.

VII. FUTURE PERSPECTIVES

The convergence of AI and multi-omics is reshaping plant biology from a predominantly descriptive discipline into a predictive and hypothesis-generating science (Tardieu et al., 2017; Cooper & Messina, 2021). A major future direction lies in the development of large-scale, self-supervised foundation models trained on vast collections of unlabeled plant genomic, transcriptomic, and proteomic data. Analogous to protein and genomic language models demonstrating strong transferability, plant-focused foundation models are poised to enable cross-species generalization for gene function prediction and variant effect estimation even in data-scarce crops (Rives et al., 2021; Ji et al., 2021). Extending these models to multimodal embeddings jointly encoding genomics, epigenomics, transcriptomics, and phenomics will further support few-shot and zero-shot learning (Washburn et al., 2019).

Future AI systems will need to integrate increasingly diverse biological and environmental modalities including microbiome profiles, volatilomics, hyperspectral and thermal imaging, three-dimensional canopy architecture, root phenomics, and continuous soil and climate sensor data, requiring hierarchical multimodal architectures capable of modeling interactions across spatial, temporal, and organizational scales (Mataigne et al., 2022; Amin et al., 2025). Causal representation learning and hybrid mechanistic-data-driven models represent another critical frontier; incorporating causal inference frameworks and structured biological priors will improve interpretability, robustness, and decision relevance for breeding and agronomy (Y. Wang & Jordan, 2021). Generative AI models could substantially reduce the cost and duration of empirical field trials by simulating plausible molecular and phenotypic responses under future climate conditions (Hu et al., 2024). AI-enabled digital twins that simulate growth, development, and physiological responses across the life cycle by integrating neural ODEs with process-based crop models offer a promising platform for forecasting trait performance and guiding ideotype design (Hammer et al., 2019).

Progress in federated and privacy-preserving learning will be essential for scaling AI across institutional and national boundaries (T. Li et al., 2020; Warnat-Herresthal et al., 2021). The long-term success of AI in plant science will depend on sustained investment in FAIR-compliant data infrastructures, open benchmarks, and interdisciplinary training, with close collaboration among plant biologists, breeders, data scientists, and policymakers to ensure AI systems are interpretable, equitable, and aligned with global food security goals.

VIII. CONCLUSION

AI-driven multi-omics integration is transforming plant science by enabling predictive modeling and mechanistic insights that were previously unattainable. By capturing nonlinear interactions across genomics, transcriptomics, proteomics, metabolomics, epigenomics, and phenomics, AI approaches can infer gene function, reconstruct regulatory networks, and predict complex phenotypes emerging from G×E×M interactions. In crops such as rice, maize, wheat, and tomato, these approaches have accelerated gene discovery including annotation of thousands of orphan genes with high accuracy (>85%), revealed dynamic regulatory modules and crosstalk hubs, and enhanced genomic prediction for yield, stress tolerance, and quality traits (R2 gains of 15-30% over classical methods). Advanced architectures including GNNs, transformers, and foundation models enable scalable integration of heterogeneous multi-omics data while addressing G×E×M interactions critical for climate-resilient breeding.

However, challenges remain: data quality, batch effects, domain shift, metadata standardization, model interpretability, and ethical data sharing limit the reproducibility, transferability, and equitable application of AI models. Black-box architectures risk generating spurious causal inferences, while proprietary datasets and uneven global resources exacerbate inequities in crop improvement. Overcoming these limitations requires causal validation experiments, interpretable hybrid models, FAIR-compliant data infrastructures, and community-driven benchmarking. With these safeguards, AI-driven multi-omics integration can guide rational crop design, anticipate environmental responses, and accelerate breeding for resilient, high-yielding varieties, ultimately unlocking the molecular basis of complex traits to ensure food security in a rapidly changing environment while fostering equitable and reproducible plant science.

REFERENCES

[1] Allen, D. K., & Young, J. D. (2019). Tracing metabolic flux through time and space with isotope labeling experiments. Current Opinion in Biotechnology, 64, 92-100.

[2] Amin, A., Zaman, W., & Park, S. (2025). Harnessing Multi-Omics and Predictive modeling for Climate-Resilient crop breeding: from genomes to fields. Genes, 16(7), 809.

[3] Arora, D., Abel, N. B., Liu, C., et al. (2020). Establishment of Proximity-Dependent biotinylation approaches in different plant model systems. The Plant Cell, 32(11), 3388-3407.

[4] Avsec, Z., Agarwal, V., Visentin, D., et al. (2021). Effective gene expression prediction from sequence by integrating long-range interactions. Nature Methods, 18(10), 1196-1203.

[5] Balotf, S., Wilson, R., Hemmati, R., et al. (2025). Plant-pathogen interactions: making the case for multi-omics analysis of complex pathosystems. Stress Biology, 5(1), 66.

[6] Bolser, D. M., Staines, D. M., Perry, E., & Kersey, P. J. (2016). ENSEMBL Plants: integrating tools for visualizing, mining, and analyzing plant genomic data. Methods in Molecular Biology, 1533, 1-31.

[7] Burankova, Y., Klemm, J., Lohmann, J. J. G., et al. (2024). FedRBE: a decentralized privacy-preserving federated batch effect correction tool for omics data based on limma. arXiv. https://doi.org/10.48550/arxiv.2412.05894

[8] Cembrowska-Lech, D., Krzeminska, A., Miller, T., et al. (2023). An Integrated Multi-Omics and Artificial Intelligence framework for advance plant phenotyping in horticulture. Biology, 12(10), 1298.

[9] Chen, J., Hu, X., Shi, T., et al. (2020). Metabolite-based genome-wide association study enables dissection of the flavonoid decoration pathway of wheat kernels. Plant Biotechnology Journal, 18(8), 1722-1735.

[10] Chen, R. T. Q., Rubanova, Y., Bettencourt, J., & Duvenaud, D. (2018). Neural ordinary differential equations. Advances in Neural Information Processing Systems, 31, 6572-6583.

[11] Choudhury, S. D., Samal, A., & Awada, T. (2019). Leveraging image analysis for high-throughput plant phenotyping. Frontiers in Plant Science, 10, 508.

[12] Cooper, M., & Messina, C. D. (2021). Can we harness Enviromics to accelerate crop improvement by integrating breeding and agronomy? Frontiers in Plant Science, 12, 735143.

[13] Crossa, J., De Los Campos, G., Perez, P., et al. (2010). Prediction of genetic values of quantitative traits in plant breeding using pedigree and molecular markers. Genetics, 186(2), 713-724.

[14] Crossa, J., Martini, J. W., Gianola, D., et al. (2019). Deep kernel and deep learning for Genome-Based prediction of single traits in multienvironment breeding trials. Frontiers in Genetics, 10, 1168.

[15] Crossa, J., Perez-Rodriguez, P., Cuevas, J., et al. (2017). Genomic selection in plant breeding: Methods, models, and perspectives. Trends in Plant Science, 22(11), 961-975.

[16] Cuellar, L. K., Friedrich, A., Gabernet, G., et al. (2022). A data management infrastructure for the integration of imaging and omics data in life sciences. BMC Bioinformatics, 23(1), 61.

[17] Dorrity, M. W., Alexandre, C. M., Hamm, M. O., et al. (2021). The regulatory landscape of Arabidopsis thaliana roots at single-cell resolution. Nature Communications, 12(1), 3334.

[18] Dosovitskiy, A., Beyer, L., Kolesnikov, A., et al. (2020). An image is worth 16x16 words: Transformers for image recognition at scale. arXiv. https://doi.org/10.48550/arxiv.2010.11929

[19] Dumschott, K., Dorpholz, H., Laporte, M., et al. (2023). Ontologies for increasing the FAIRness of plant research data. arXiv. https://doi.org/10.48550/arxiv.2309.07129

[20] Elnaggar, A., Heinzinger, M., Dallago, C., et al. (2020). ProtTrans: towards cracking the language of life through self-supervised deep learning. arXiv. https://arxiv.org/abs/2007.06225

[21] Elnaggar, A., Heinzinger, M., Dallago, C., et al. (2021). ProtTrans: Toward understanding the language of life through self-supervised learning. IEEE Transactions on Pattern Analysis and Machine Intelligence, 44(10), 7112-7127.

[22] Feng, D., Liang, Z., Wang, Y., et al. (2022). Chromatin accessibility illuminates single-cell regulatory dynamics of rice root tips. BMC Biology, 20(1), 274.

[23] Flores, J. E., Claborne, D. M., Weller, Z. D., et al. (2023). Missing data in multi-omics integration: Recent advances

through artificial intelligence. Frontiers in Artificial Intelligence, 6, 1098308.

[24] Fornes, O., Castro-Mondragon, J. A., Khan, A., et al. (2019). JASPAR 2020: update of the open-access database of transcription factor binding profiles. Nucleic Acids Research, 48(D1), D87-D92.

[25] Gill, T., Gill, S. K., Saini, D. K., et al. (2022). A comprehensive review of high throughput phenotyping and machine learning for plant stress phenotyping. Phenomics, 2(3), 156-183.

[26] Goff, S. A., Vaughn, M., McKay, S., et al. (2011). The iPlant Collaborative: Cyberinfrastructure for plant biology. Frontiers in Plant Science, 2, 34.

[27] Gong, P., Cheng, L., Zhang, Z., et al. (2023). Multi-omics integration method based on attention deep learning network for biomedical data classification. Computer Methods and Programs in Biomedicine, 231, 107377.

[28] Gu, W., Feng, Y., Liu, C., et al. (2025). Transcriptomic and metabolomic unraveling of nitrogen use efficiency in sorghum. Plant Growth Regulation, 105(3), 687-706.

[29] Guo, Z., Wang, S., Zhang, F., et al. (2024). Common and specific genetic basis of metabolite-mediated drought responses in rice. Stress Biology, 4(1), 6.

[30] Hammer, G., Messina, C., Wu, A., & Cooper, M. (2019). Biological reality and parsimony in crop models. In Silico Plants, 1(1).

[31] Han, E., Geng, Z., Qin, Y., Wang, Y., & Ma, S. (2024). Single-cell network analysis reveals gene expression programs for Arabidopsis root development and metabolism. Plant Communications, 5(8), 100978.

[32] Hassan, A. H., Mokhtar, M. M., & Allali, A. E. (2024). Transposable elements: multifunctional players in the plant genome. Frontiers in Plant Science, 14, 1330127.

[33] Herrero-Huerta, M., Rodriguez-Gonzalvez, P., & Rainey, K. M. (2020). Yield prediction by machine learning from UAS-based multi-sensor data fusion in soybean. Plant Methods, 16(1), 78.

[34] Hinton, G. E., & Salakhutdinov, R. R. (2006). Reducing the dimensionality of data with neural networks. Science, 313(5786), 504-507.

[35] Hochreiter, S., & Schmidhuber, J. (1997). Long short-term memory. Neural Computation, 9(8), 1735-1780.

[36] Hu, T., Zhang, X., Khanal, S., et al. (2024). Climate change impacts on crop yields: A review of empirical findings, statistical crop models, and machine learning methods. Environmental Modelling and Software, 179, 106119.

[37] Huang, S., Chaudhary, K., & Garmire, L. X. (2017). More is better: recent progress in multi-omics data integration methods. Frontiers in Genetics, 8, 84.

[38] Hufford, M. B., Seetharam, A. S., Woodhouse, M. R., et al. (2021). De novo assembly, annotation, and comparative analysis of 26 diverse maize genomes. Science, 373(6555), 655-662.

[39] Humplík, J. F., Lazar, D., Husickova, A., & Spichal, L. (2015). Automated phenotyping of plant shoots using imaging methods for analysis of plant stress responses. Plant Methods, 11(1), 29.

[40] Huynh-Thu, V. A., Irrthum, A., Wehenkel, L., & Geurts, P. (2010). Inferring regulatory networks from expression data using tree-based methods. PLoS ONE, 5(9), e12776.

[41] Jain, A., Sarsaiya, S., Singh, R., et al. (2024). Omics approaches in understanding the benefits of plant-microbe interactions. Frontiers in Microbiology, 15, 1391059.

[42] Jamil, I. N., Remali, J., Azizan, K. A., et al. (2020). Systematic Multi-Omics Integration (MOI) approach in plant systems biology. Frontiers in Plant Science, 11, 944.

[43] Jayakodi, M., Lu, Q., Pidon, H., et al. (2024). Structural variation in the pangenome of wild and domesticated barley. Nature, 636(8043), 654-662.

[44] Jeong, Y., Ronen, J., Kopp, W., et al. (2024). scMaui: a widely applicable deep learning framework for single-cell multiomics integration in the presence of batch effects and missing data. BMC Bioinformatics, 25(1), 257.

[45] Ji, Y., Zhou, Z., Liu, H., & Davuluri, R. V. (2021). DNABERT: pre-trained bidirectional encoder representations from transformers model for DNA-language in genome. Bioinformatics, 37(15), 2112-2120.

[46] Johnson, W. E., Li, C., & Rabinovic, A. (2006). Adjusting batch effects in microarray expression data using empirical Bayes methods. Biostatistics, 8(1), 118-127.

[47] Jumper, J., Evans, R., Pritzel, A., et al. (2021). Highly accurate protein structure prediction with AlphaFold. Nature, 596(7873), 583-589.

[48] Kajrolkar, A. (2025). Integrating multi-omics data for plant stress response: Current advances and future directions. Premier Journal of Plant Biology. https://doi.org/10.70389/pjpb.100012

[49] Kannan, J., Palani, T., Selvakumar, D., et al. (2025). Computational approaches in multi-omics for crop improvement. Current Bioinformatics, 20.

[50] Khaki, S., & Wang, L. (2019). Crop yield prediction using deep neural networks. Frontiers in Plant Science, 10, 621.

[51] Kingma, D. P., & Welling, M. (2013). Auto-encoding variational Bayes. arXiv. https://doi.org/10.48550/arxiv.1312.6114

[52] Kipf, T. N., & Welling, M. (2016). Semi-supervised classification with graph convolutional networks. arXiv. https://arxiv.org/abs/1609.02907

[53] Korsunsky, I., Millard, N., Fan, J., et al. (2019). Fast, sensitive and accurate integration of single-cell data with Harmony. Nature Methods, 16(12), 1289-1296.

[54] Langfelder, P., & Horvath, S. (2008). WGCNA: an R package for weighted correlation network analysis. BMC Bioinformatics, 9(1), 559.

[55] LeCun, Y., Bengio, Y., & Hinton, G. (2015). Deep learning. Nature, 521(7553), 436-444.

[56] Leek, J. T., Scharpf, R. B., Bravo, H. C., et al. (2010). Tackling the widespread and critical impact of batch effects in high-throughput data. Nature Reviews Genetics, 11(10), 733-739.

[57] Leek, J. T., & Storey, J. D. (2007). Capturing heterogeneity in gene expression studies by surrogate variable analysis. PLoS Genetics, 3(9), e161.

[58] Li, Q., Wen, Z., Wu, Z., et al. (2021). A survey on federated learning systems. IEEE Transactions on Knowledge and Data Engineering, 35(4), 3347-3366.
[59] Li, T., Sahu, A. K., Talwalkar, A., & Smith, V. (2020). Federated learning: Challenges, methods, and future directions. IEEE Signal Processing Magazine, 37(3), 50-60.
[60] Li, Z., Tao, W., Liu, J., et al. (2023). Tomato leaf disease recognition via optimizing deep learning methods. Horticulturae, 9(9), 1034.
[61] Liang, Z., Anderson, S. N., Noshay, J. M., et al. (2021). Genetic and epigenetic variation in transposable element expression responses to abiotic stress in maize. Plant Physiology, 186(1), 420-433.
[62] Libbrecht, M. W., & Noble, W. S. (2015). Machine learning applications in genetics and genomics. Nature Reviews Genetics, 16(6), 321-332.
[63] Liu, X., Zhang, F., Hou, Z., et al. (2021). Self-supervised learning: generative or contrastive. IEEE Transactions on Knowledge and Data Engineering, 1.
[64] Lundberg, S. M., & Lee, S. (2017). A unified approach to interpreting model predictions. Advances in Neural Information Processing Systems, 30.
[65] Ma, C., Xin, M., Feldmann, K. A., & Wang, X. (2014). Machine learning-based differential network analysis in Arabidopsis. The Plant Cell, 26(2), 520-537.
[66] Ma, D., Xu, B., Feng, J., et al. (2022). Dynamic metabolomics and transcriptomics analyses for characterization of phenolic compounds in wheat grain. Frontiers in Nutrition, 9, 844337.
[67] Ma, W., Qiu, Z., Song, J., et al. (2018). A deep convolutional neural network approach for predicting phenotypes from genotypes. Planta, 248(5), 1307-1318.
[68] Maher, K. A., Bajic, M., Kajala, K., et al. (2017). Profiling of accessible chromatin regions across multiple plant species and cell types. The Plant Cell, 30(1), 15-36.
[69] Mahieu, N. G., & Patti, G. J. (2017). Systems-level annotation of a metabolomics data set reduces 25,000 features to fewer than 1,000 unique metabolites. Analytical Chemistry, 89(19), 10397-10406.
[70] Mahmood, U., Li, X., Fan, Y., et al. (2022). Multi-omics revolution to promote plant breeding efficiency. Frontiers in Plant Science, 13, 1062952.
[71] Marks, R. A., Amezquita, E. J., Percival, S., et al. (2023). A critical analysis of plant science literature reveals ongoing inequities. Proceedings of the National Academy of Sciences, 120(10), e2217564120.
[72] Mataigne, A., Vannier, N., Vandenkoornhuyse, P., & Hacquard, S. (2022). Multi-genome metabolic modeling predicts functional inter-dependencies in the Arabidopsis root microbiome. Microbiome, 10(1), 217.
[73] Merrick, L. F., Herr, A. W., Sandhu, K. S., Lozada, D. N., & Carter, A. H. (2022). Optimizing plant breeding programs for genomic selection. Agronomy, 12(3), 714.
[74] Michael, T. P., & VanBuren, R. (2020). Building near-complete plant genomes. Current Opinion in Plant Biology, 54, 26-33.
[75] Minervini, M., Scharr, H., & Tsaftaris, S. A. (2015). Image analysis: The new bottleneck in plant phenotyping. IEEE Signal Processing Magazine, 32(4), 126-131.
[76] Molnar, C. (2022). Interpretable Machine Learning. https://christophm.github.io/interpretable-ml-book/
[77] Montesinos-Lopez, A., Rivera, C., Pinto, F., et al. (2023). Multimodal deep learning methods enhance genomic prediction of wheat breeding. G3 Genes Genomes Genetics, 13(5).
[78] Montesinos-Lopez, O. A., Chavira-Flores, M., Kiasmiantini, et al. (2024). A review of multimodal deep learning methods for genomic-enabled prediction in plant breeding. Genetics. https://doi.org/10.1093/genetics/iyae161
[79] Montesinos-Lopez, O. A., Montesinos-Lopez, A., Perez-Rodriguez, P., et al. (2021). A review of deep learning applications for genomic selection. BMC Genomics, 22(1), 19.
[80] Muller, M., & Munne-Bosch, S. (2015). Ethylene response factors: a key regulatory hub in hormone and stress signaling. Plant Physiology, 169(1), 32-41.
[81] Mummadi, S. T., Islam, M. K., Busov, V., & Wei, H. (2025). Gene regulatory network prediction using machine learning, deep learning, and hybrid approaches. Forestry Research, 5(1), 0.
[82] Nguyen, Q., Nguyen, H., Oh, E. C., & Nguyen, T. (2024). Current approaches and outstanding challenges of functional annotation of metabolites. Briefings in Bioinformatics, 25(6).
[83] Nguyen, V. H., Morantte, R. I. Z., Lopena, V., et al. (2023). Multi-environment genomic selection in rice elite breeding lines. Rice, 16(1).
[84] Pan, Y., Ji, X., You, J., et al. (2024). CSGDN: Contrastive signed graph diffusion network for predicting crop gene-phenotype associations. arXiv. https://doi.org/10.48550/arxiv.2410.07511
[85] Park, S. Y., & Jeong, D. (2023). Comprehensive analysis of rice seedling transcriptome during dehydration and rehydration. International Journal of Molecular Sciences, 24(9), 8439.
[86] Peleke, F. F., Zumkeller, S. M., Gultas, M., Schmitt, A., & Szymanski, J. (2024). Deep learning the cis-regulatory code for gene expression in selected model plants. Nature Communications, 15(1), 3488.
[87] Rajesh, A., Chang, Y., Abedalthagafi, M. S., et al. (2021). Improving the completeness of public metadata accompanying omics studies. Genome Biology, 22(1), 106.
[88] Rao, R., Liu, J., Verkuil, R., et al. (2021). MSA Transformer. bioRxiv. https://doi.org/10.1101/2021.02.12.430858
[89] Reel, P. S., Reel, S., Pearson, E., Trucco, E., & Jefferson, E. (2021). Using machine learning approaches for multi-omics data analysis: A review. Biotechnology Advances, 49, 107739.
[90] Rives, A., Meier, J., Sercu, T., et al. (2019). Biological structure and function emerge from scaling unsupervised learning to 250 million protein sequences. bioRxiv. https://doi.org/10.1101/622803

[91] Rives, A., Meier, J., Sercu, T., et al. (2021). Biological structure and function emerge from scaling unsupervised learning to 250 million protein sequences. Proceedings of the National Academy of Sciences, 118(15).

[92] Rohart, F., Gautier, B., Singh, A., & Cao, K. L. (2017). mixOmics: An R package for omics feature selection and multiple data integration. PLoS Computational Biology, 13(11), e1005752.

[93] Rotz, S., Duncan, E., Small, M., et al. (2019). The politics of digital agricultural technologies: A preliminary review. Sociologia Ruralis, 59(2), 203-229.

[94] Ryu, K. H., Huang, L., Kang, H. M., & Schiefelbein, J. (2019). Single-cell RNA sequencing resolves molecular relationships among individual plant cells. Plant Physiology, 179(4), 1444-1456.

[95] Schlapfer, P., Zhang, P., Wang, C., et al. (2017). Genome-wide prediction of metabolic enzymes, pathways, and gene clusters in plants. Plant Physiology, 173(4), 2041-2059.

[96] Shamsuddin, D., Danilevicz, M. F., Al-Mamun, H. A., et al. (2024). Multimodal deep learning integration of image, weather, and phenotypic data under temporal effects for early prediction of maize yield. Remote Sensing, 16(21), 4043.

[97] Shiu, S., & Lehti-Shiu, M. D. (2024). Assessing the evolution of research topics in a biological field using plant science as an example. PLoS Biology, 22(5), e3002612.

[98] Song, L., Huang, S. C., Wise, A., et al. (2016). A transcription factor hierarchy defines an environmental stress response network. Science, 354(6312).

[99] Subramanian, I., Verma, S., Kumar, S., Jere, A., & Anamika, K. (2020). Multi-omics data integration, interpretation, and its application. Bioinformatics and Biology Insights, 14, 117793221989905.

[100] Sun, L., Jing, Y., Liu, X., et al. (2020). Heat stress-induced transposon activation correlates with 3D chromatin organization rearrangement in Arabidopsis. Nature Communications, 11(1), 1886.

[101] Sun, Y., Fan, X., Cao, D., et al. (2010). Integration of brassinosteroid signal transduction with the transcription network for plant growth regulation in Arabidopsis. Developmental Cell, 19(5), 765-777.

[102] Tabakhi, S., Suvon, M. N. I., Ahadian, P., & Lu, H. (2022). Multimodal learning for multi-omics: A survey. World Scientific Annual Review of Artificial Intelligence, 01.

[103] Tardieu, F., Cabrera-Bosquet, L., Pridmore, T., & Bennett, M. (2017). Plant phenomics, from sensors to knowledge. Current Biology, 27(15), R770-R783.

[104] Tjoa, E., & Guan, C. (2020). A survey on explainable artificial intelligence (XAI): Toward medical XAI. IEEE Transactions on Neural Networks and Learning Systems, 32(11), 4793-4813.

[105] Trapnell, C., Cacchiarelli, D., Grimsby, J., et al. (2014). The dynamics and regulators of cell fate decisions are revealed by pseudotemporal ordering of single cells. Nature Biotechnology, 32(4), 381-386.

[106] Van Bel, M., Diels, T., Vancaester, E., et al. (2017). PLAZA 4.0: an integrative resource for functional, evolutionary and comparative plant genomics. Nucleic Acids Research, 46(D1), D1190-D1196.

[107] Vaswani, A., Shazeer, N., Parmar, N., et al. (2017). Attention is all you need. Advances in Neural Information Processing Systems, 30.

[108] Velickovic, P., Cucurull, G., Casanova, A., et al. (2017). Graph attention networks. arXiv. https://arxiv.org/abs/1710.10903

[109] Wang, J., Yang, W., Zhang, S., et al. (2023). A pangenome analysis pipeline provides insights into functional gene identification in rice. Genome Biology, 24(1), 19.

[110] Wang, P., Lehti-Shiu, M. D., Lotreck, S., et al. (2024). Prediction of plant complex traits via integration of multi-omics data. Nature Communications, 15(1), 6856.

[111] Wang, Q., Wang, B., Liu, H., et al. (2022). Comparative proteomic analysis for revealing the advantage mechanisms of salt-tolerant tomato. PeerJ, 10, e12955.

[112] Wang, X., Singh, D., Marla, S., Morris, G., & Poland, J. (2018). Field-based high-throughput phenotyping of plant height in sorghum. Plant Methods, 14(1), 53.

[113] Wang, Y., & Jordan, M. I. (2021). Desiderata for representation learning: a causal perspective. arXiv. https://doi.org/10.48550/arxiv.2109.03795

[114] Wang, Y., Luo, Y., Guo, X., et al. (2024). A spatial transcriptome map of the developing maize ear. Nature Plants, 10(5), 815-827.

[115] Warnat-Herresthal, S., Schultze, H., Shastry, K. L., et al. (2021). Swarm learning for decentralized and confidential clinical machine learning. Nature, 594(7862), 265-270.

[116] Washburn, J. D., Mejia-Guerra, M. K., Ramstein, G., et al. (2019). Evolutionarily informed deep learning methods for predicting relative transcript abundance from DNA sequence. Proceedings of the National Academy of Sciences, 116(12), 5542-5549.

[117] Way, G. P., & Greene, C. S. (2017). Extracting a biologically relevant latent space from cancer transcriptomes with variational autoencoders. Pacific Symposium on Biocomputing, 23, 80-91.

[118] Wei, H., Xu, H., Su, C., Wang, X., & Wang, L. (2022). Rice CIRCADIAN CLOCK ASSOCIATED 1 transcriptionally regulates ABA signaling to confer multiple abiotic stress tolerance. Plant Physiology, 190(2), 1057-1073.

[119] Wu, X., Fan, X., Luo, P., et al. (2023). From laboratory to field: Unsupervised domain adaptation for plant disease recognition in the wild. Plant Phenomics, 5, 0038.

[120] Xiang, Y., Chen, Q., Su, Z., et al. (2022). Deep learning and hyperspectral images based tomato soluble solids content and firmness estimation. Frontiers in Plant Science, 13, 860656.

[121] Xu, F., Wu, T., Cheng, Q., Wang, X., & Yan, J. (2025). Foundation models in plant molecular biology: advances, challenges, and future directions. Frontiers in Plant Science, 16, 1611992.

[122] Xu, L., Ning, S., Xu, X., et al. (2024). Comparative analysis of machine learning models and explainable AI for agriculture drought prediction. Agricultural Water Management, 306, 109176.

[123] Yang, J., Duan, G., Li, C., et al. (2019). The crosstalks between jasmonic acid and other plant hormone signaling. Frontiers in Plant Science, 10, 1349.

[124] Yang, Y., Saand, M. A., Huang, L., et al. (2021). Applications of multi-omics technologies for crop improvement. Frontiers in Plant Science, 12, 563953.

[125] Ying, R., Bourgeois, D., You, J., Zitnik, M., & Leskovec, J. (2019). GNNExplainer: Generating explanations for graph neural networks. arXiv. https://doi.org/10.48550/arxiv.1903.03894

[126] Yu, T. (2022). AIME: Autoencoder-based integrative multi-omics data embedding that allows for confounder adjustments. PLoS Computational Biology, 18(1), e1009826.

[127] Zaheer, M., Guruganesh, G., Dubey, A., et al. (2020). Big Bird: Transformers for longer sequences. Advances in Neural Information Processing Systems, 33, 17283-17297.

[128] Zargar, S. M., Mir, R. A., Ebinezer, L. B., et al. (2022). Physiological and multi-omics approaches for explaining drought stress tolerance and supporting sustainable production of rice. Frontiers in Plant Science, 12, 803603.

[129] Zhang, F., Wu, J., Sade, N., et al. (2021). Genomic basis underlying the metabolome-mediated drought adaptation of maize. Genome Biology, 22(1), 260.

[130] Zhu, G., Wang, S., Huang, Z., et al. (2018). Rewiring of the fruit metabolome in tomato breeding. Cell, 172(1-2), 249-261.

[131] Zitnik, M., Agrawal, M., & Leskovec, J. (2018). Modeling polypharmacy side effects with graph convolutional networks. Bioinformatics, 34(13), i457-i466.

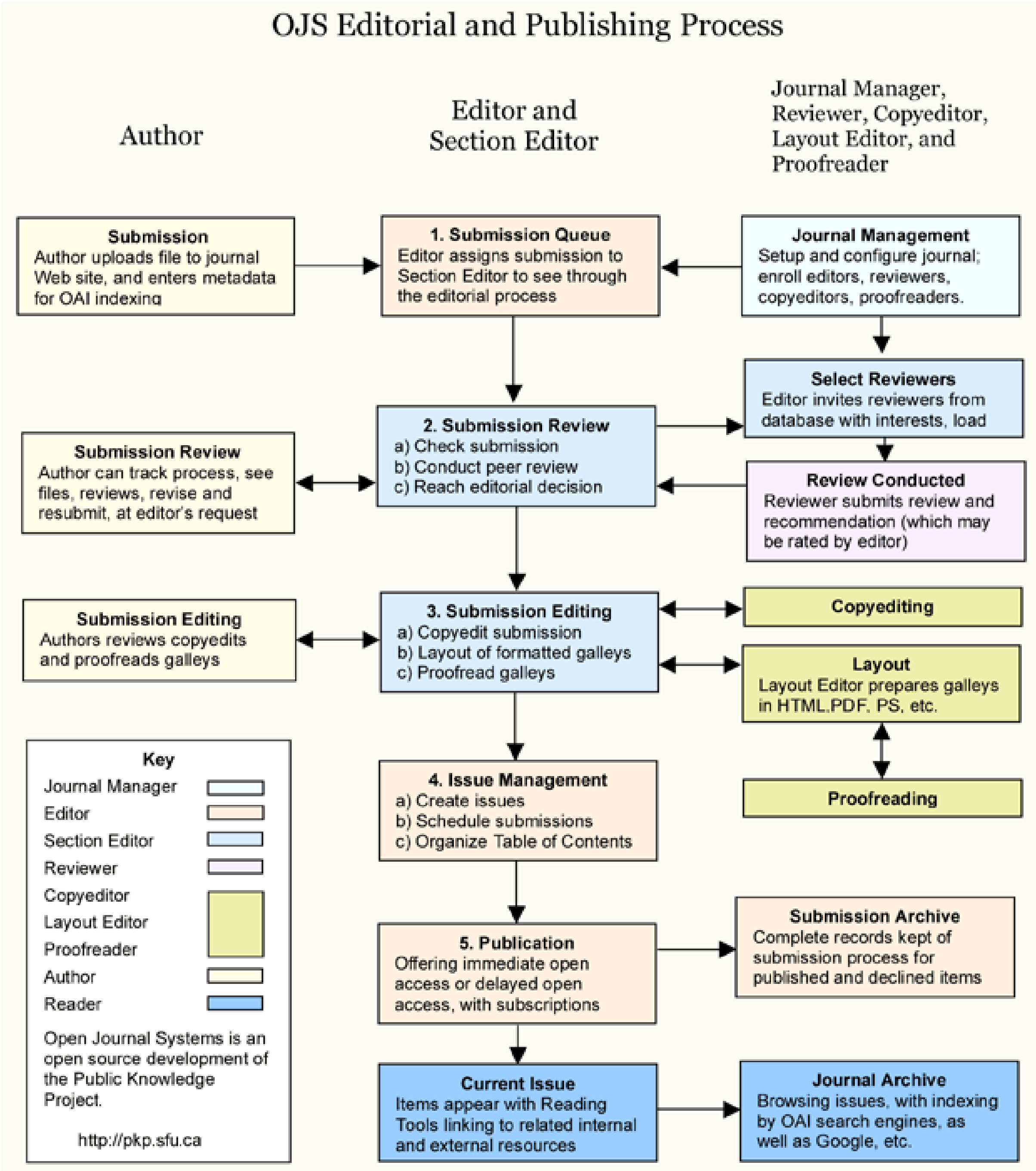

~OJS Workflow~

Important links:

Paper Submission Link:

OJS:

https://ijeab.com/ojs/index.php/ijeab/about/submissions

https://ijeab.com/submit-paper/

Editorial Team:

https://ijeab.com/editorial-board/

Peer Review Process:

https://ijeab.com/peer-review-process/

Publication Ethics:

https://ijeab.com/publication-policies-and-ethics/

Author Guidelines:

https://ijeab.com/author-guidelines/

Join Us a Reviewer:

https://ijeab.com/join-us/

Journal Indexed and Abstracted in:

- Qualis-CAPES -Brazil
- Normatiza (Under Review)
- Bielefeld Academic Search Engine(BASE)
- Aalborg University Library (Denmark)
- WorldCat: The World's Largest Library Catalog
- Semantic Scholar
- J-Gate
- Open J-Gate
- CORE-The world's largest collection of open access research papers
- JURN
- Microsoft Academic Search
- Google Scholar
- Kopernio - powered by Web of Science
- Pol-Index
- PBN(Polish Scholarly Bibliography)Nauka Polaska
- Scilit, MDPI AG (Basel, Switzerland)
- Tyndale University College & Seminary
- indiana Library WorldCat
- CrossRef DOI-10.22161/ijeab
- Neliti - Indonesia's Research Repository
- Journal TOC
- Dimensions.ai: Re-imagining discovery and access to research
- Citeseerx
- Massachusetts Institute of Technology (USA)
- Simpson University (USA)
- University of Louisville (USA)
- Biola University (USA)
- IE Library (Spain)
- Mount Saint Vincent University Library (Halifax, Nova Scotia Canada)
- University Of Arizona (USA)
- INDIANA UNIVERSITY-PURDUE UNIVERSITY INDIANAPOLIS (USA)
- Roderic Bowen Library and Archives (United Kingdom)
- University Library of Skövde (Sweden)
- Indiana University East (campuslibrary (USA))
- Tilburg University (The Netherlands)
- Williams College (USA)
- University of Connecticut (USA)
- Brandeis University (USA)
- Tufts University (USA)
- Boston University (USA)
- McGill University (Canada)
- Northeastern University (USA)
- BibSonomy-The blue social bookmark and publication sharing system
- Slide Share
- Academia
- Archive
- Scribd
- SJIF-InnoSpace
- ISSUU
- Research Bib
- DRJI
- journal-repository

Platform & workflow by OJS / PKP

Infogain Publication
International Journal of English, Literature and Social Science (IJELS)